The Notch pathway as a biomarker in pancreatic ductal adenocarcinoma and its potential therapeutic modulation

Submitted for the degree of Doctor of Philosophy

at the University of Leicester

by

Mr Christopher D. Mann

M.B.Ch.B. (Hons) B.Sc. (Hons) M.R.C.S.(Eng)

Department of Cancer Studies and Molecular Medicine

University of Leicester

November 2011

ABSTRACT

The Notch pathway as a biomarker in pancreatic ductal adenocarcinoma and its potential therapeutic modulation

Christopher D. Mann

Pancreatic ductal adenocarcinoma (PDAC) is the 5th commonest cause of cancer related deaths in the UK and has a poor prognosis with 1-year survival of only 10%. Improved understanding of pancreatic carcinogenesis would allow identification of biomarkers to predict disease progression, prognosis, and allow targeting of novel therapeutics.

The Notch pathway involves a group of transmembrane receptors, important in tissue development, which re-activate in a number of malignancies. Preliminary evidence suggests this occurs in PDAC. The aim of this study was to examine Notch pathway components as potential diagnostic and prognostic markers in PDAC, as well as a therapeutic target.

Nuclear Notch-1, -3, -4 and their targets HES-1 and HEY-1 were up-regulated in a series of 42 resected PDAC compared to normal pancreas. Further up-regulation was seen when in advanced tumours. Nuclear Notch-3 and its target HEY-1 were associated with shortened survival following resection, with HEY-1 maintaining prognostic significance on multivariate analysis.

Notch-1 siRNA knockdown resulted in reduction in viability, G_1 arrest and induction of apoptosis, with Notch-3 knockdown resulting in reduction in viability, G_2/M arrest and induction of apoptosis. Treatment with the gamma secretase inhibitor (GSI)-I resulted in greater inhibition than seen with combined Notch-1/3 knockdown. These effects however, were not confirmed in a murine xenograft model of PDAC using an alternative GSI, MRK-003. These findings may relate to poor pharmacological activity or reduced bioavailability of this particular agent in the mouse model.

Using immunoprecipitation and mass spectrometry, a method was developed to detect a fragment of the Notch receptor in plasma of patients with PDAC. Although Notch-1 could not be detected, Notch-3 was detected in both controls and patients with PDAC, although at higher levels in the later. This may suggest a role as diagnostic biomarker.

ACKNOWLEDGEMENTS

I would like to thank my supervisors Professor Maggie Manson, Professor William Steward and Mr David Berry for their support throughout this project and critical revision of this thesis. I would also like to thank Dr Lynne Howells and Dr Stewart Sale for their assistance with the xenograft model. Thank you also to Dr Don Jones Jr and Dr Frieda Teichert for their help with the mass spectrometry.

I would also like to thank all those at the Biocentre for all their support and excellent company during my time in research. Thank you also to Dr Kevin West for his assistance with the histological aspects of the study, and to Dr Karen Kulbecki for her assistance in cutting the sections for immunohistochemistry.

Thank you to my parents, brother, and friends for their encouragement and support, and just generally putting up with me through the highs and lows of research!

Lastly I would like to sincerely thank the Royal College of Surgeons of England through their support of this work through the Sir Samuel Scott of Yews Trust Research Fellowship.

CONTENTS

FIGURES

Chapter 1

Chapter 2

Chapter 3

Chapter 5

Chapter 6

TABLES

Chapter 2

Chapter 3

ABBREVIATIONS

Aβ	Amyloid-β-like
ADAM	A disintegrin and metalloproteinase
AJCC	American Joint Committee on Cancer
APP	Amyloid precursor protein
ATP	Adenosine triphosphate
bHLH	Basic helix-loop-helix
BRCA	Breast cancer susceptibility gene
BSA	Bovine serum albumin
CA 19.9	Carbohydrate antigen 19.9
CADASIL	Cerebral autosomal dominant arteriopathy with subcortical infarcts and leukoencephalopathy
CBF-1	C promotor binding factor 1
CDK	Cyclin-dependent kinase
CEA	Carcinoembryonic antigen
CI	Confidence interval
CoA	Co-activators
CoR	Co-repressors
CSL	CBF1, Suppressor of Hairless or Lag-1
CT	Computerised tomography
CTBP1	C-terminal binding protein 1
DAB	3,3-diaminobenzidine
dFdCTP	Gemcitabine triphosphate
DFS	Disease-free survival
DMP	Dimethyl pimelimidate

DMSO	Dimethylsulfoxide
EDTA	Ethylenediaminetetraacetic acid
EGF	Epidermal growth factor
EGFR	Epidermal growth factor receptor
ELISA	Enzyme-linked immunosorbent assay
FACS	Fluorescence-activated cell sorting
FAMMM	Familial atypical mole multiple melanoma
FCS	Foetal calf serum
FGFR	Fibroblast growth factor receptor
G_0	Gap 0 phase
G_1	Gap 1 phase
G_2	Gap 2 phase
GSI	Gamma secretase inhibitor
HCC	Hepatocellular carcinoma
HDAC	Histone deacetylase
HES	Hairy/Enhancer of Split family
HEY	HES-related repressor protein
HNPCC	Hereditary nonpolyposis colorectal cancer
HPV	Human papilloma virus
HRP	Horseradish peroxidise
IARC	International Agency for Research on Cancer
ICN (NICD)	Intracellular Notch domain (active Notch)
IMS	Industrial methylated spirits
IOUS	Intraoperative ultrasound
JAK	Janus kinase

JNK	c-Jun N-terminal kinase
Kras	Kirsten Ras
KW	Kruskal-Wallis test
LFNG	Lunatic Fringe
LNR	Lin 12/Notch repeats
LREC	Leicestershire Research Ethics Committee
M	Mitosis
MALDI	Matrix-assisted laser desorption ionisation
MAML	Mastermind-like
MAPK	Mitogen-activated protein kinase
MDCT	Multidetector computerised tomography
MFNG	Manic Fringe
MINT	Msx2-interacting nuclear target protein
MMP	Matrix metalloproteinase
MMTV	Mouse mammary tumour virus
mRNA	Messenger RNA
miRNA	MicroRNA
MS	Mass Spectrometry
MUC	Mucin
MW	Mann-Whitney U test
Nβ21	Notch amyloid-β-like fragment (21 amino-acids in length)
Nβ25	Notch amyloid-β-like fragment (25 amino-acids in length)
NCOR	Nuclear co-repressor
NF-κB	Nuclear factor κB
NICE	National Institute of Clinical Excellence

NLR	Neutrophil-lymphocyte ratio
NLS	Nuclear localisation signals
NRARP	Notch regulated ankyrin repeat protein
OS	Overall survival
PanIN	Pancreatic intraepithelial neoplasia
PBS	Phosphate buffered saline
PBX1	Pre-B-cell leukaemia transcription factor 1
PCAF	p300/CBP-associated factor
PDGFR	Platelet-derived growth factor receptor
PEST	Polypeptide enriched in proline, glutamate, serine, and threonine residues
PI	Propidium iodide
PI3K	Phosphoinositide-3-kinase
PRSS1	Protease serine 1
R_0	Negative resection margins
R_1	Involved resection margins
RFNG	Radical Fringe
RT-PCR	Reverse transcriptase polymerase chain reaction
S	Synthesis phase
SCID	Severe combined immunodeficiency
SDS	Sodium dodecyl sulphate
SEER	Surveillance epidemiology and end results
siRNA	Small interfering RNA
SKP	S phase kinase-associated protein
STAT	Signal transducer and activator of transcription

TACE	Tumour necrosis factor-α converting enzyme
T-ALL	T-cell acute lymphoblastic leukaemia
TAD	Transactivation domain
TBS	Tris-buffered saline
TCF	T-cell factor
TCR	T-cell receptor
TGFβ	Transforming growth factor-β
TNFα	Tumour necrosis factor-α
VEGF	Vascular endothelial growth factor

CHAPTER 1

INTRODUCTION

1.1 PANCREATIC CANCER

Pancreatic cancer is an aggressive malignancy, with insidious onset, delayed presentation and poor prognosis. Pancreatic neoplasia covers a broad spectrum of pathologies, including those which arise from cells of exocrine and endocrine function. Exocrine tumours are the most prevalent, of which ductal adenocarcinoma account for approximately 95%. Rarer types of exocrine tumours include acinar cell carcinoma, adenosquamous carcinoma, squamous carcinoma, colloid carcinoma, and signet ring carcinoma. Endocrine tumours, including insulinoma and glucagonoma, account for 1% of all pancreatic tumours and are usually benign. This thesis focuses on pancreatic ductal adenocarcinoma.

Despite improvements in surgery, chemotherapy and radiotherapy, it has one of the worst prognoses of all gastrointestinal malignancies, with a 1-year survival rate of only 10%, attributed to its tendency for aggressive local spread, early metastasis and late presentation. Surgical resection remains the only potential curative measure, however less than 10% of tumours are amenable. Despite resection with curative intent, overall survival approximates to only 5-12% at 5 years (Jemal *et al*, 2002; Garcea *et al*, 2008). This dismal picture is compounded by a poor response to current chemotherapeutic agents. Our knowledge of the processes involved in pancreatic carcinogenesis is still far from complete. Improved understanding of the pathways involved would allow identification of biomarkers to predict disease progression and prognosis and to allow targeting of novel therapeutics.

1.1.1 Epidemiology

Pancreatic carcinoma is the fifth commonest cause of cancer-related deaths in the United Kingdom. However it is only the 10th most commonly diagnosed cancer, accounting for approximately 3% of all cancer. Overall the incidence of pancreatic carcinoma has remained relatively constant, although there has been a reduction in males, probably due to the decline in smoking prevalence (Figure 1.1a, Cancer Research UK, 2007). In 2007, there were 7684 newly diagnosed cases of pancreatic cancer in the UK; an incidence of 12.5 per 100,000 in men and 12.7 per 100,000 in women (Cancer Statistics, Cancer Research UK, 2007). This confers a lifetime risk of 1 in 86 for both men and women, although this may be somewhat biased by the relative longevity of females. Incidence increases with age, with approximately 75% of cases occurring in patients over 65 years of age (Figure 1.1b). The recent American SEER report (Surveillance Epidemiology and End Results, National Cancer Institute, 2011) found a higher incidence in the black compared to the white population (age-adjusted incidence 16.67 compared to 11.34 per 100,000 person-years) between 1975-2008, with lower rates in Hispanic and Asian populations.

a)

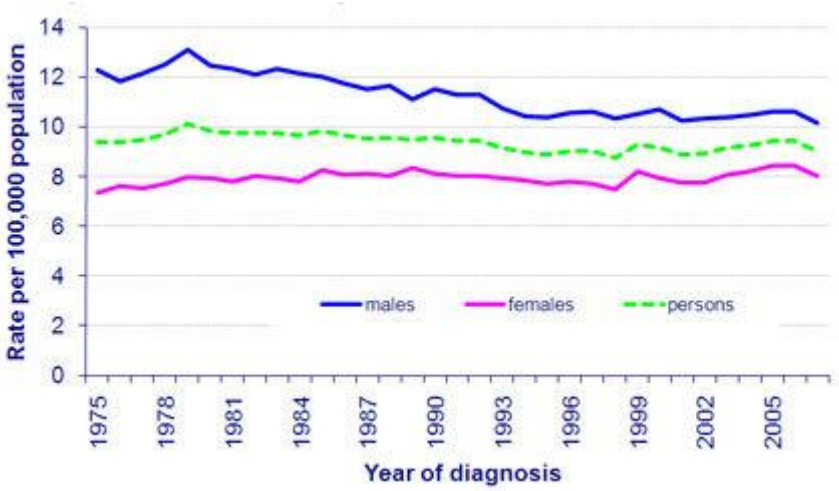

b)

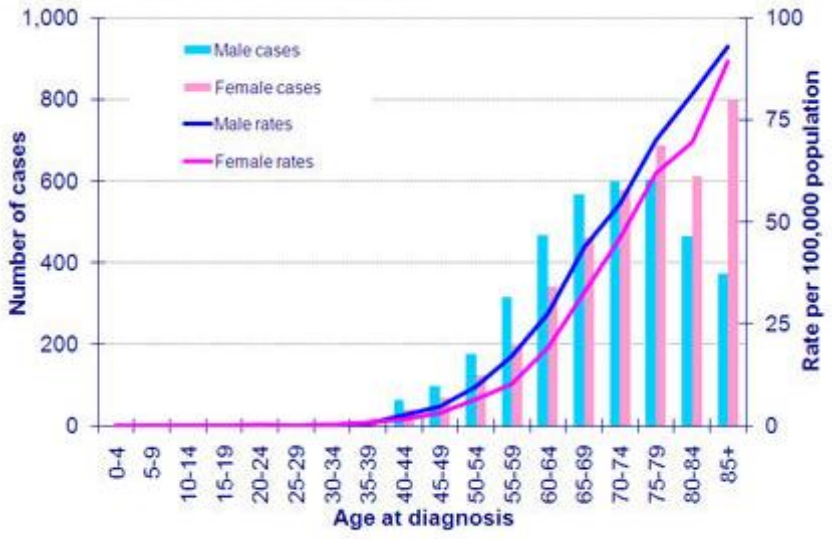

Figure 1.1 – Incidence of Pancreatic cancer in the United Kingdom
a) Overall age-standardised incidence rates of pancreatic cancer.
b) Number of new cases and age-specific incidence rates
(from Cancer Statistics, Cancer Research UK.)

1.1.2 Aetiology

1.1.2.1 Genetic

Inherited mutations may account for 2-10% of all pancreatic carcinomas (Tersmette *et al*, 2001; Bartsch *et al*, 2004; Jacobs *et al*, 2010). Individuals with one, two, or three first degree relatives (parent, child, or sibling) with a history of pancreatic cancer demonstrate risk increases that are approximately 6-, 18-, and 57-fold above baseline, respectively. There exist several known familial conditions which encompass pancreatic cancer as part of their spectra, although these account for only a minority of the familial cases. These include Peutz-Jeghers (Latchford *et al*, 2006); familial atypical mole-multiple melanoma (FAMMM)/Melanoma-pancreatic cancer syndrome, due to a mutation in the *CDKN2A/p16* gene (Goldstein *et al*, 1995); BRCA2 mutation (Ozcelik *et al*, 1997); and hereditary non-polyposis colorectal cancer (HNPCC; Kastrinos *et al*, 2009). In addition, familial pancreatic cancer can be associated with hereditary pancreatitis, an autosomal dominant disease caused in 70% of the cases by a mutation in cationic trypsinogen (protease serine 1; *PRSS1;* Whitcomb *et al*, 1996). Mutated *PRSS1* is resistant to inactivation, leading to pancreatic autodigestion, with affected individuals having a 50-fold increased risk of developing pancreatic cancer with a lifetime risk of nearly 40% (Lowenfels *et al*, 1997).

1.1.2.2 Environmental

The International Agency for Research on Cancer (IARC) has classified tobacco as a proven carcinogen for cancer of the pancreas (IARC Monograph: Tobacco Smoke and

involuntary Smoking, World Health Organisation). Smoking carries a 75% increased risk of developing pancreatic cancer compared with non-smokers, which persists for 10 years after smoking is ceased (Iodice *et al*, 2008). Although several large case-control studies have been performed investigating the effects of alcohol on risk of pancreatic carcinoma, its impact remains controversial; one found heavy alcohol consumption to be associated with an increased risk of the malignancy, even when stratifying by smoking status and history of chronic pancreatitis (Lucenteforte *et al*, 2011), however another study found only a small increased risk in male heavy drinkers (Michaud *et al*, 2010). A high dietary fat intake has been associated with increased risk, particularly saturated animal fat (Thiebaut *et al*, 2009), as has a high body mass index (Jiao *et al*, 2010). Occupational exposure to several chemicals has also been associated with increased risk of pancreatic cancer, including chlorinated hydrocarbon solvents, asbestos, synthetic polymer dust, ionising radiation, pesticides, diesel and gasoline engine exhaust fumes (Santibanez *et al*, 2010).

1.1.2.3 Past medical history

A past history of chronic pancreatitis has been shown to increase the risk of developing pancreatic adenocarcinoma with relative risks reported of up to 13.3, however over a 20 year period, only 5% of patients with chronic pancreatitis will develop pancreatic carcinoma (Raimondi *et al*, 2010; Greer and Whitcomb, 2009; Dite *et al*, 2010). Similarly, type II diabetes mellitus is associated with pancreatic cancer with an odds ratio of 1.82 on meta-analysis, with a greater risk in those patients with the disease for ≥5 years (Huxley *et al*, 2005).

1.1.3 Pathology

Macroscopically, most infiltrating ductal adenocarcinomas produce a firm sclerotic mass with poorly defined edges and yellow-white in colour. Upon palpation, this tumour can be difficult to differentiate from the mass produced in chronic pancreatitis. Microscopically, the tumour consists of infiltrating gland-forming neoplastic epithelium with an intense desmoplastic reaction (Figure 1.2a,b). Due to this, only a minority of cells in the mass are actually tumour cells. Vascular and perineural invasion are often present. The majority of pancreatic cancers express immunohistochemically detectable cytokeratin (cytokeratins 7, 8, 13, 18, and 19), carcinoembryonic antigen, carbohydrate antigen 19–9 (CA19–9), B72.3 (TAG-72), CA 125, and DUPAN 2. Most pancreatic cancers also express a number of mucins, including MUC1, MUC3, MUC4, and MUC5AC (Maitra and Hruban, 2008).

Pancreatic cancer is associated with several different genetic mutations, both somatic and inherited. Those involved specifically with pancreatic adenocarcinoma include *K-RAS2, p16/CDKN2A, TP53,* and *DPC4/SMAD4*. Mutations in the *K-RAS* gene occur in >90% of cases (Almoguera *et al*, 1988). The activating mutation of *KRAS2* is associated with several downstream effector pathways, including the phosphoinositide-3-kinase (PI3K) and RAF-mitogen-activated protein kinase (RAF-MAPK) pathways. *P16/CDKN2A*, *TP53*, and *DPC4/SMAD4* are tumour suppressor genes; inactivating mutations in the p16 gene occur in 95% of pancreatic cancers (Schutte *et al,* 1997) and p53 in 50% (Pellegata *et al*, 1994).

An important stage in the development of pancreatic adenocarcinoma is the occurrence of histologically distinct precursor lesions known as pancreatic intraepithelial neoplasia (PanIN) (Hruban *et al*, 2004). PanINs are microscopic lesions in the smaller pancreatic ducts, and consist of mucin-secreting epithelial cells. Progression begins with a flat duct lesion without atypia (PanIN-1A), developing into a papillary duct lesion without atypia (PanIN-1B), then with atypia (PanIN-2), and finally into carcinoma *in situ* (PanIN-3) (Figure 1.2c). Molecular analysis of PanINs demonstrates that they harbour many of the same genetic mutations as are found in invasive pancreatic carcinoma (Maitra *et al*, 2006). Activating point mutations in codon 12 of the *K-ras2* gene typically occur in early low-grade PanIN lesions (PanIN-1), whereas inactivating mutations in the *p16/CDKN2A* gene occur in intermediate lesions (PanIN-2), and inactivating mutations in *SMAD4*, *TP53*, and *BRCA2* occur in late lesions (PanIN-3). Telomere shortening is also an early event, occurring in PanIN-1 lesions, and telomere shortening may contribute to the accumulation of chromosomal abnormalities in PanINs (van Heek *et al*, 2002).

a) **b)**

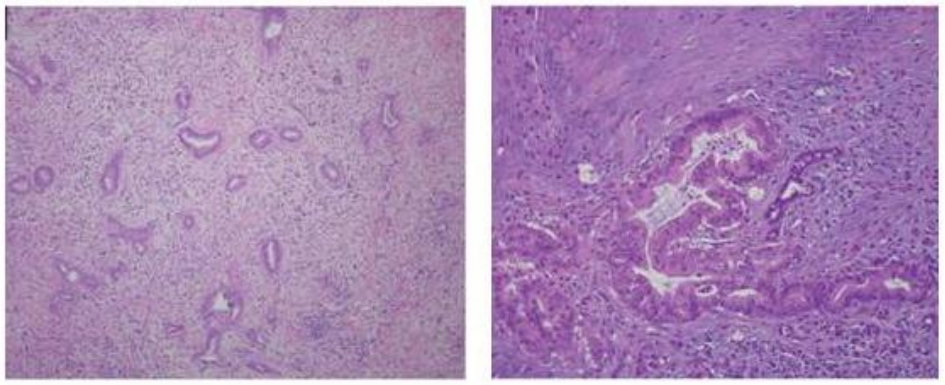

c)

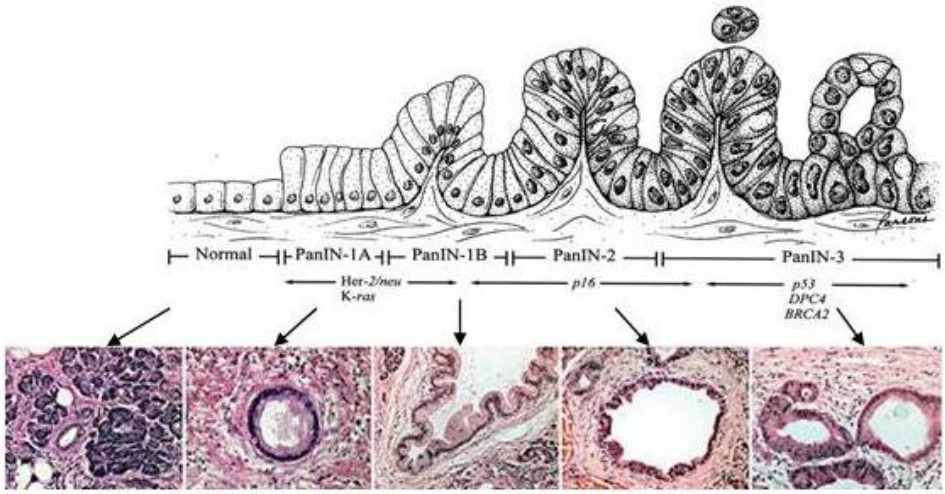

Figure 1.2 – Pancreatic carcinoma and pancreatic intraepithelial neoplasia (PanIN).
Pancreatic carcinoma under a) low and b) high power magnification.
c) Histological-genetic progression model for pancreatic carcinoma (adapted from Wilentz *et al*, 2000).

1.1.4 Diagnosis

Patients often suffer vague and non-specific symptoms, however only present when alarm symptoms such as obstructive jaundice occur, due to a head of pancreas tumour obstructing the distal common bile duct. This is often associated with anorexia and loss of weight. Patients may also describe epigastric pain radiating into the back, due to involvement of visceral afferent nerves or induced pancreatitis.

Due to the vague initial symptoms, patients often present late with advanced metastatic disease. Metastatic spread occurs to local lymph nodes, distant lymph nodes (both intra- and extra-abdominal), liver, lungs and peritoneum. Diagnosis is challenging, often with a time lapse before an abnormality is detected, usually on ultrasound, which triggers further investigation. A number of serum tumour markers have been investigated to aid diagnosis, including CEA, CAM17.1, HSP27, DU-PAN2 and MIC-1, however either availability or relative insensitivity limits their application (Bunger *et al*, 2011). CA 19-9 is a glycoprotein which is commonly used to aid the diagnosis of pancreatic carcinoma. In addition, elevated levels have been associated with resectability at both staging laparoscopy (Maithel *et al*, 2008) and laparotomy (Ong *et al*, 2008), as well as response to chemotherapy (Hess *et al*, 2008), and survival following resection (Ferrone *et al*, 2006). CA 19-9 may, however, be raised in a number of benign conditions, including acute and chronic pancreatitis, liver cirrhosis, obstructive jaundice, cholangitis, as well as a number of other malignancies (67% of cholangiocarcinomas; 41% gastric; 34% colorectal; 49% HCC) (Duffy *et al*, 2010). CA 19-9 is not expressed in patients who are Lewis antigen A^-B^- as the molecule on which the CA 19-9 epitope is found is a sialylated Lewis A blood

group antigen (Takasaki *et al*, 1988). This genotype accounts for approximately 5-10% of the Caucasian population. Combining all studies from the literature and using a cut-off of 37 U/ml, CA 19-9 has been found to have an overall mean sensitivity of 81% and specificity of 90% for pancreatic cancer. Increasing the cut-off to 100 U/ml improved specificity to 98% but reduced sensitivity to 68% (Duffy *et al*, 2010). In addition, CA 19-9 particularly lacks sensitivity for early or small sized tumours, and poorly differentiated tumours produce lower levels than moderately or well-differentiated cancers. As of yet, no effective screening test exists.

1.1.5 Management

Following referral, all patients with suspected pancreatic malignancy are entered into a standard management algorithm in our centre following discussion at our Multidisciplinary team meeting (Figure 1.4). All patients undergo a contrast-enhanced multidetector helical CT scan of the thorax and abdomen in order to identify and stage the primary tumour, particularly with respect to vascular involvement, and to screen for metastatic disease (Figure 1.3). Those patients deemed suitable for pancreatic resection, based upon CT results, functional status and anaesthetic assessment, proceed to staging laparoscopy and intra-operative ultrasound (IOUS). This allows assessment of peritoneal disease, hepatic metastases and lymph node metastases below the resolution of CT scanning. If no contraindication to attempted resection is found, the patient then proceeds to exploratory laparotomy and intra-operative frozen section biopsies. Criteria to abandon resection include extra-pancreatic spread, extra-pancreatic lymph node involvement on frozen section, and vascular involvement (involvement of either the superior mesenteric artery

involvement or >2cm of the superior mesenteric vein). Patients with resectable pancreatic head tumours undergo a pancreaticoduodenectomy (either standard or pylorus-preserving) with an isolated Roux-en-Y pancreaticojejunostomy. Those with pancreatic tail tumours undergo distal pancreatectomy. Patients with positive intra-operative pancreatic resection margins on two occasions proceed to a total pancreatectomy. Where curative resection is not deemed feasible, patients undergo a combined hepaticojejunostomy-en-Y and gastrojejunostomy for palliation (Biliary bypass). Following surgery, patients are considered for adjuvant chemotherapy.

Patients not suitable for resection are considered for chemotherapy +/- radiotherapy, following tissue diagnosis confirming pancreatic adenocarcinoma (ultrasound-guided pancreatic biopsy/liver metastasis biopsy or biopsy from laparoscopy). More recently those patients with locally-advanced disease are considered for chemoradiotherapy to downstage the disease prior to resection as part of the SCALOP trial, however such patients were not included in this study. Those patients considered too unfit for this are treated in a palliative manner. NICE recommends the use of Gemcitabine as the first line chemotherapeutic agent in pancreatic carcinoma. It works as a nucleoside analogue, incorporating itself into cellular DNA, and inhibiting DNA synthesis. Following uptake into the cell, Gemcitabine undergoes several phosphorylations to form active metabolites. Gemcitabine triphosphate (dFdCTP) is incorporated into the DNA by DNA polymerase. This results in chain termination, but as the metabolite is not at a terminal position on the chain, it cannot be detected for DNA repair, a phenomenon known as “masked chain termination”. In addition, the drug also inhibits the production of deoxyribonucleotides, which are essential for DNA synthesis, and can inhibit enzymes involved in its own inactivation. In this way, the drug is able to

"self-potentiate", exerting its effect through several different mechanisms (Figure 1.5) (Ueno *et al*, 2007).

1.1.6 Outcome

Surgical resection offers the only chance of long-term survival; however resection is possible in only 10-20% of patients (Li *et al*, 2004). Even following surgery with curative intent, the median survival in the literature is only 15.8 months with 5-year survival of 12% (Garcea *et al*, 2008), although this may approach 40-50% in patients with favourable prognostic factors (i.e. small tumour size, negative lymph nodes; Garcea *et al*, 2007). The use of Gemcitabine chemotherapy has been shown to improve survival in patients with unresectable disease, achieving 1-year survival rates of 18% (Burris *et al*, 1997).

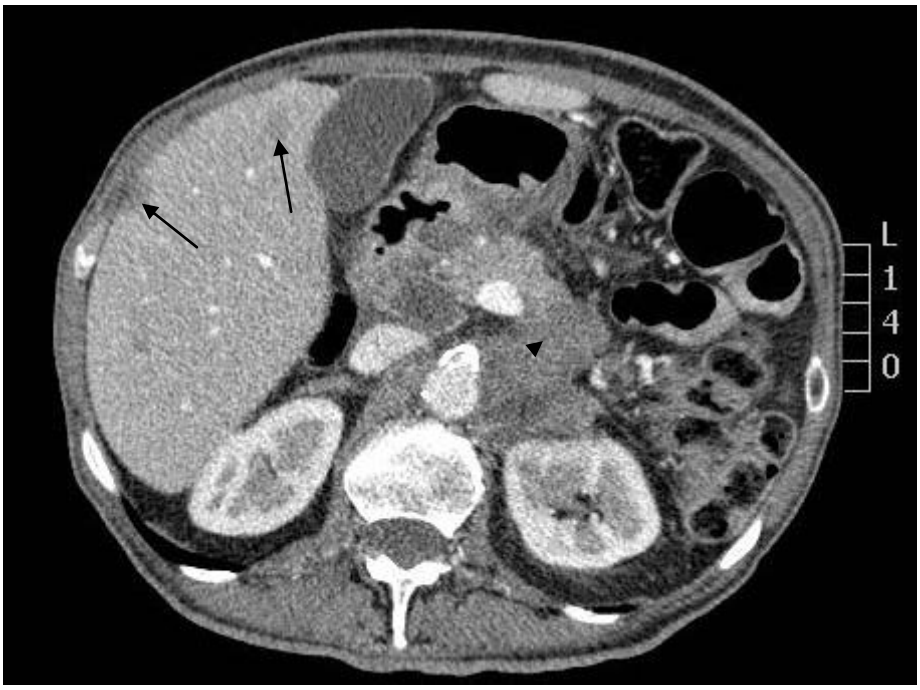

Figure 1.3 – CT scan of a patient with advanced pancreatic adenocarcinoma
Arrow head, pancreatic body primary tumour; arrow, liver metastases.

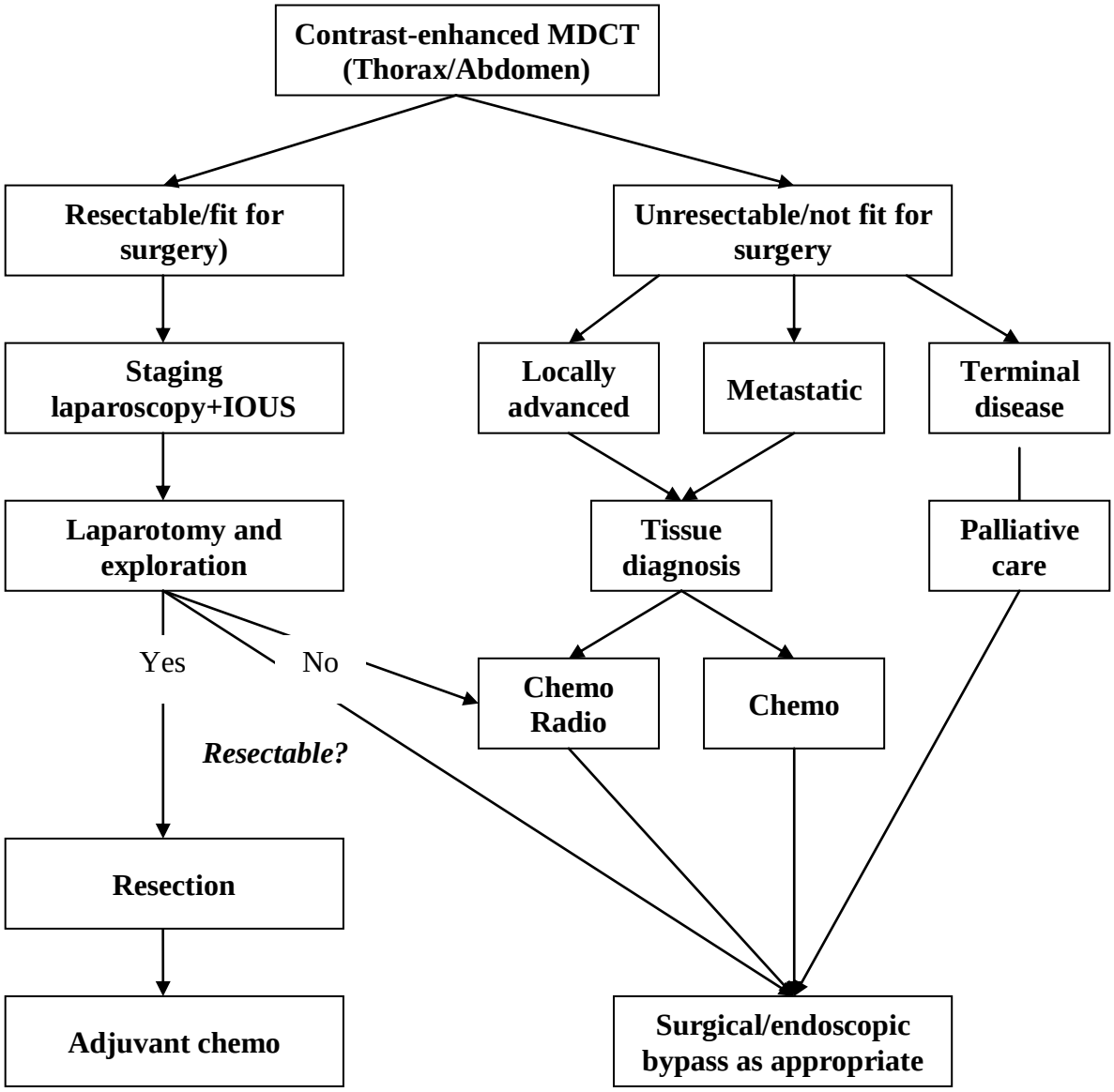

Figure 1.4 – Management algorithm for patients with pancreatic carcinoma at the University Hospitals of Leicester.
IOUS, intraoperative ultrasound; MDCT, multidetector computerised tomography.

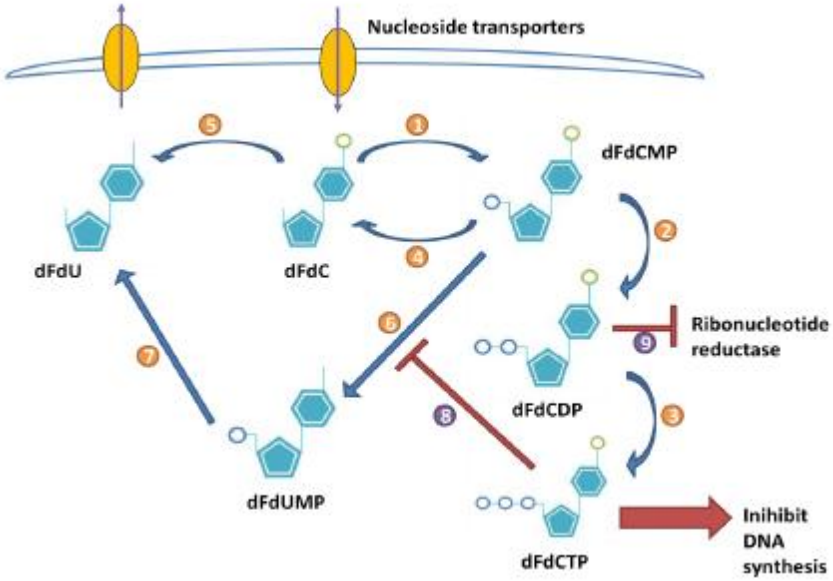

Figure 1.5 – Mechanisms and metabolism of gemcitabine (adapted from Ueno *et al*, 2007). Gemcitabine (dFdC) sequentially phosphorylated through 1) mono- (dFdCMP), 2) di- (dFdCDP) to 3) gemcitabine triphosphate (dFdCTP) which is incorporated into DNA by DNA polymerase; 4) phosphorylated metabolites are then reduced to unphosphorylated form and 5) gemcitabine is inactivated to 2'-deoxy-2', 2'difluorouridine (dFdU); 6) conversion to 2'-deoxy-2',2'difluoruridine monophosphate (dFdUMP); 7) inactive dFdUMP converted to dFdU for efflux; 8) inhibition of inactivation of dFdCMP by dFdCTP; 9) inhibition of deoxyribonucleotide synthesis by dFdCDP.

1.2 CELL SIGNALING PATHWAYS IN CARCINOGENESIS

Cells are continuously under the influence of intracellular signalling pathways. These signals drive gene transcription, the products of which determine the fate of the cell – whether it proliferates, senescenes, or dies. In healthy cells, the signals that drive proliferation and arrest are in precise balance. Dysregulation of these pathways to favour proliferation predisposes to cancerous change. The development of a cancer occurs in three stages:

1. Initiation – mutation of a single cell
2. Promotion – proliferation of the mutant cell
3. Progression – additional mutations form

Abnormal signalling in one pathway may produce initiation of a cancer; however defects in multiple pathways are likely to be needed for cancer progression. Dysregulation of the signalling pathways must effect several alterations in order for a cell to become malignant (Hanahan and Weinberg, 2011):

- Insensitivity to growth-inhibitory signals
- Self-sufficiency in growth signals
- Evasion of apoptosis
- Limitless potential to divide, avoiding terminal differentiation and senescence
- Initiation of angiogenesis
- Ability to invade and metastasise

Changes in several intracellular signalling pathways are known to occur during carcinogenesis. Changes in concentration, conformation or cellular location of intracellular molecules can affect signalling pathways, and lead to cancerous change. Several intracellular signalling pathways have been identified as having a possible role in pancreatic cancer, including the Wnt pathway and its target genes c-myc, cyclin D1 and MMP-7, the PI3K/Akt and JAK/STAT pathways. Identifying the responsible molecules and defining these sequences of events is important for understanding the disease process and may uncover novel targets for future therapies, and identify biomarkers, which may be useful alongside histological information in diagnosis or in predicting survival. One signalling pathway that has generated recent interest is the Notch pathway.

1.3 THE NOTCH SIGNALING PATHWAY

The Notch signalling pathway was first identified in 1917 when certain strains of *Drosophilia* characterised by notches at their wingblades were noted (Morgan *et al*, 1917). These notches were found to be caused by a gene insufficiency, which was subsequently cloned and identified as encoding a transmembrane receptor, designated Notch (Wharton *et al*, 1985). Notch orthologues have since been characterised in mammals and the interest in this pathway as an essential component of cellular signalling has increased. In addition, with the discovery that the Notch-1 receptor gene was involved in a chromosomal translocation in a group of patients with T cell acute lymphoblastic leukaemia (Ellisen *et al*, 1991), interest has flourished regarding the role of Notch dysreguation in carcinogenesis.

1.3.1 Notch receptors

The mammalian Notch receptor family consists of four transmembrane receptors, designated Notch-1, -2, -3, and -4. Notch proteins are synthesised as ~300-350 kDa proteins consisting of extracellular, transmembrane and intracellular domains (Figure 1.6). During maturation, the unprocessed Notch is transported to the trans-Golgi network where it is cleaved at a site just outside the transmembrane domain, referred to as the S1 cleavage site, by a furin-like protease (Logeat *et al*, 1998). This generates two distinct fragments, one consisting of the majority of the extracellular domain, the other of the intracellular and transmembrane domains and the remainder of the extracellular domain (Blaumueller *et al*, 1997). These two subunits associate non-covalently and are transported to and incorporated in the plasma membrane resulting in cell-surface expression of a mature heterodimeric type I transmembrane receptor (Rand *et al*, 2000). The extracellular domain contains numerous epidermal growth factor (EGF)-like repeats (36 in Notch-1 and Notch-2; 34 in Notch-3, and 29 in Notch-4) responsible for ligand binding, followed by a regulatory domain which maintains the unbound receptor in a resting state (Vardar *et al*, 2003). This region includes three Notch family specific Lin12/Notch repeats (LNRs) near the C-terminus of the extracellular domain and a heterodimerisation domain. The intracellular domain contains two protein–protein interaction domains (RAM domain and ankyrin repeats), two nuclear localisation signals (NLS), a transactivation domain (TAD), and a C-terminal PEST (polypeptide enriched in proline, glutamate, serine, and threonine residues) sequence involved in Notch protein degradation (Gupta-Rossi *et al*, 2001).

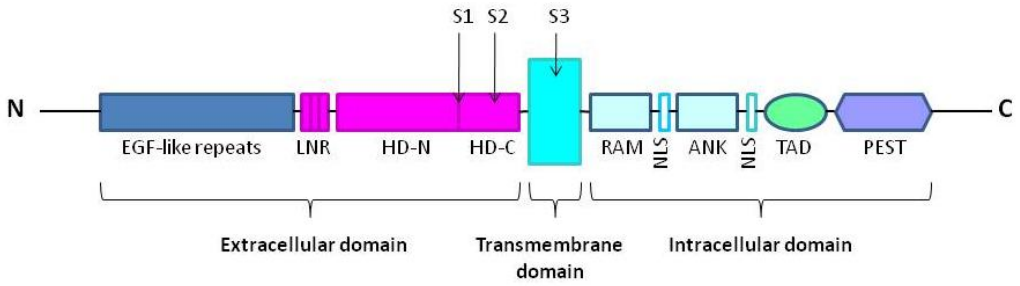

Figure 1.6 – Schematic organisation of the Notch receptor
EGF, epidermal growth factor; LNR, Lin12/Notch; HD-N/-C, heterodimerisation domain N- and C-terminus; NLS, nuclear localisation signal; ANK, Ankyrin repeat domain; TAD, transactivation domain; PEST, a region rich in proline, glutamine, serine and threonine residues. The cleavage sites for furin-like proteases (S1), ADAM-type metalloproteases (S2), and gamma secretase (S3) are shown (adapted from Nefedova and Gabrilovich, 2008)

1.3.2 Notch receptor activation

In the absence of ligand binding, Notch receptors are inactive. Binding of a ligand to the 11th and 12th EGF-like repeats induces a conformational change in the Notch extracellular domain and a series of proteolytic cleavages occurs. A S2 cleavage site within the Notch extracellular domain is exposed (Mumm *et al*, 2000). This is cleaved by the ADAM family (A Disintegrin and Metalloprotease) Tumour Necrosis factor-α Converting Enzyme (TACE - S2 cleavage) (Brou *et al*, 2000). This precipitates an additional proteolytic cleavage at a conserved S3 cleavage site within the transmembrane domain (S3 cleavage – between Gly1743 and Val1744 (Schroeter *et al*, 1998)) that requires presenilin-dependent protease activity (De Stooper *et al*, 1999; Struhl and Greenwald, 1999; Ye *et al*, 1999; Huppert *et al*, 2000; Okochi *et al*, 2002). The S3 cleavage is mediated by the γ-secretase complex comprising presenilin, nicastrin, Pen-2 and Aph-1 (Edbauer *et al*, 2003). Gamma-secretase has been found to have other cellular substrates, including the β-amyloid precursor protein, abnormal processing of which has been implicated in Alzheimer's disease

(Siemers *et al*, 2006). The S3 cleavage results in the release of the Notch intracellular domain (ICN) that subsequently translocates to the nucleus to effect Notch signalling (Shroeter *et al*, 1998; Struhl and Adachi, 1998; Figure 1.7).

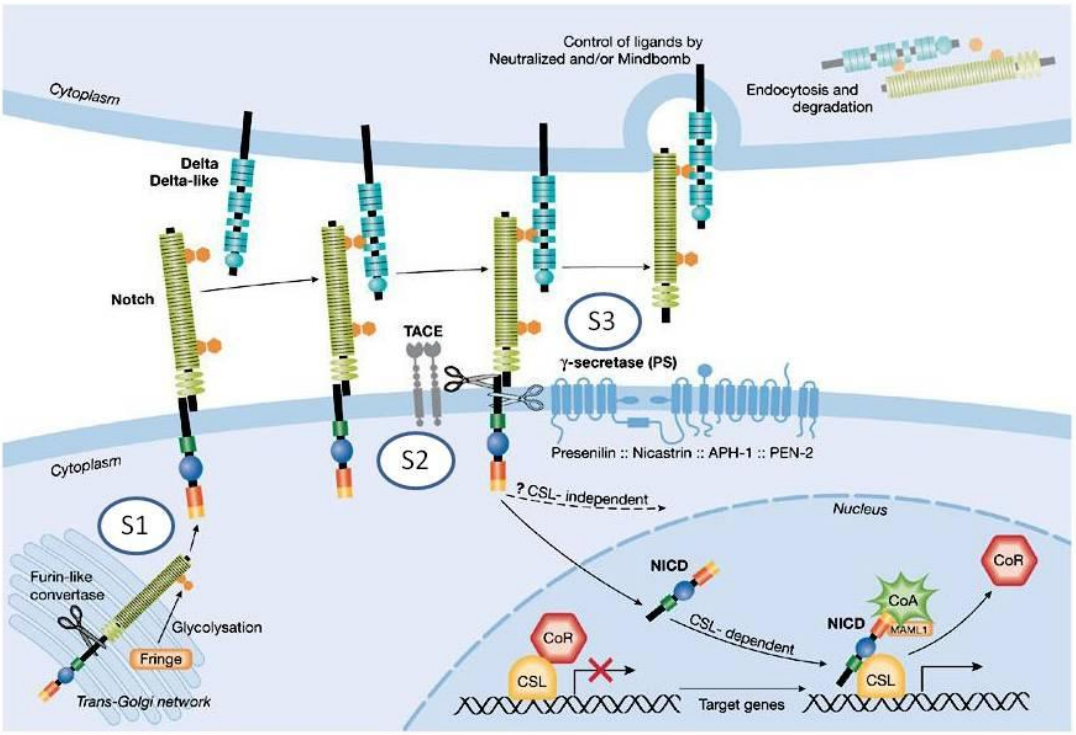

Figure 1.7 – Overview of the Notch pathway
Notch receptors are expressed as heterodimers at the cell surface following cleavage in the Golgi by a furin-like convertase (S1). Ligand binding results in Notch activation following two proteolytic cleavages, the first by the metalloprotease TACE (Tumour necrosis factor α converting enzyme) (S2) and the second by the γ-secretase activity of the multi-protein complex of presenilins (PS), which includes Nicastrin, APH-1 and PEN-2 (S3). The liberated intracellular Notch (NICD) translocates into the nucleus and binds to the transcription factor CSL (CBF1 in humans, Suppressor of Hairless in *Drosophila* and LAG in *C. elegans*), leading to transcriptional activation by displacement of co-repressors (CoR) and simultaneous recruitment of co-activators (CoA), including mastermind-like proteins (MAML1). Adapted from Radtke *et al*, 2005.

1.3.3 Notch ligands

At least two families of Notch ligand have been identified in mammals, designated Jagged (or Serrate 1 and 2) and Delta-like (1, 3 and 4). The ligands are also type I transmembrane proteins and binding occurs between adjacent cells. Little is known about the factors that regulate Notch ligand expression. It is however known that factors other than ligand expression regulate the strength of the Notch signal.

Endocytosis and lysosomal destruction of cell surface receptors is a well-known mechanism of receptor desensitisation. The activity of Notch ligands may be affected by the rate of internalisation and degradation. Neuralized and Mind Bomb are genes that encode E3 ubiquitin ligases (Lai et al, 2001; De Blandre *et al*, 2001; Yeh *et al*, 2001; Itoh *et al*, 2003; Pavlopoulos *et al*, 2001). These ligases transfer ubiquitin to a protein substrate, targeting it either for degradation, or in this case, for endocytosis (Bonifacino and Weissman, 1998). Neutralized and Mind Bomb therefore promote the internalisation by endocytosis, and degradation of Delta (Lai *et al*, 2001; Itoh *et al*, 2003; Pavlopoulos *et al*, 2001). Paradoxically, such internalisation may up-regulate Notch receptor activity (Itoh *et al*, 2003; Pavlopoulos *et al*, 2001; Parks *et al*, 2000). Several other findings support this hypothesis; dynamin-dependent endocytosis is required for Notch activation (Seugnet *et al*, 1997); and endocytosis-defective Delta proteins have reduced signalling capacity (Parks *et al*, 2000). Delta endocytosis promotes the release of the extracellular domain of Notch on a neighbouring cell (Parks *et al*, 2000), and one theory is that this may facilitate access of the ADAM family protease TACE and the subsequent proteolytic cleavages by the γ-secretase complex that culminate in the release of ICN.

Notch may also be influenced by receptor glycosylation (Haines and Irvine, 2003). An initial fucosylation of serine or threonine residues on the EGF-like repeats of the extracellular domain by O-fucosyltransferase-1 during post-translational modification has been shown to be necessary for Notch-ligand interaction and Notch activation (Sasamura *et al*, 2003; Okajima *et al*, 2003; Wang *et al*, 2001a). A group of genes designated Fringe have been identified to encode proteins with fucose-specific β-1,3 N-acetylglucosaminyltransferase activity (Moloney *et al*, 2000). These have been found to cause marked elongation of O-linked fucose residues on the extracellular EGF-like repeats of Notch. The glycosylation has been found to inhibit Jagged-1-mediated signalling and potentiate Delta-1-mediated signalling through Notch-1 (Hicks *et al*, 2000). In particular, fucosylation of the 12^{th} EGF repeat of the extracellular domain by Fringe has been shown to inhibit Jagged-Notch signalling (Lei *et al*, 2003). In contrast, the signalling mediated by both Delta-1 and Jagged-1 has been found to be potentiated by Fringe glycosylation of Notch-2 (Hicks *et al*, 2000).

Proteolytic cleavage of Delta by certain proteases (ADAM family Kuzbanian) can cause an extracellular fragment to be released into the extracellular fluid. These soluble ligands have been found to promote Notch signalling in some contexts (Qi *et al*, 1999) and inhibit it in others (Small *et al*, 2001; Mishra-Gorur *et al*, 2002). In addition, Notch ligands may undergo intracellular cleavage by a γ-secretase complex, similar to Notch, releasing an intracellular C-terminal domain. There is some evidence to suggest that this may translocate to the nucleus and effect transcription

(Bland *et al*, 2003), modulated in a reciprocated antagonistic manner by ICN (LaVoie and Selkoe, 2003).

It is also known that the EGF-repeats on the extracellular domains of both Notch and its ligands bind calcium ions, and depletion in extracellular Ca^{2+} induces a potent ligand-independent activation of Notch, possibly by altering the conformation of the extracellular domain (Rand et al, 2000).

1.3.4 Target gene transcription

In the absence of nuclear ICN, Notch target gene expression is repressed by the ubiquitously expressed C promotor binding factor 1 (CBF-1). This represses transcription by interactions with a co-repressor complex including histone deacetylase-1 and -2, CIR, and SKIP (Kao *et al*, 1998; Hsieh *et al*, 1999; Zhou *et al*, 2000; Jarriault *et al*, 1995; Mumm and Kopan, 2000). CBF-1 is also known as RBP-Jκ (recombination signal binding protein Jκ) or CSL (CBF1, Suppressor of Hairless or Lag-1) (Jarriault *et al*, 1995). Nuclear localisation of intracellular Notch has been shown to be essential for its activity (Jeffries and Capobianco, 2000). When Notch is activated, ICN translocates to the nucleus and binds to CSL, displacing the corepressor complex (Jarriault *et al*, 1995; Fortini and Artavanis-Tsakonas, 1994; Christensen *et al*, 1996; Kidd *et al*, 1998; Figure 1.7). This converts it from a transcriptional repressor into an activator (Mumm and Kopan, 2000). Binding of ICN to CSL has been shown to be inhibited by the protein MINT (Msx2-interacting nuclear target protein), which has been found to be expressed in a variety of tissues

(Kuroda *et al*, 2003). Transcription co-activators of the mastermind-like family (MAML) have been shown to be required for Notch-mediated transcriptional activation (Wu and Griffin, 2004; Wu *et al*, 2000; Fryer *et al*, 2002). They form a ternary complex with CSL-ICN by directly interacting with ICN. The ICN-MAML-CSL complexes associate with DNA containing CSL-binding sequences (Nam *et al*, 2003). MAML then recruits additional factors including histone acetyltransferase p300 and PCAF providing an additional stimulus for transcription of genes harbouring CBF-1-binding sites (Wu *et al*, 2000; Fryer *et al*, 2002; Nam *et al*, 2003; Yamamoto *et al*, 2001; Wallberg *et al*, 2002; Jeffries *et al*, 2002). This acetylates histones thereby altering the structure of chromatin, making it more amenable to active transcription. The CSL-ICN-MAML complex thus acts as a potent transcriptional activator of Notch target genes (Wu *et al*, 2000, 2002; Fryer *et al*, 2002, 2004).

There are three mammalian MAML genes, but only a single CSL gene. Any combination of Notch-1-4 and MAML-1-3 can form complexes with CSL and thus activate transcription (Wu *et al*, 2002), however any significance of different combinations has yet to be determined. In addition to the ISN-MAML-CSL complex mediated signalling, there is also some evidence that a CSL-independent pathway exists (Bush *et al*, 2001; Nofziger *et al*, 1999). F3/Contactin, a non-delta/non-jagged molecule, has been shown to be a functional ligand for Notch that mediates its effects via a CSL-independent pathway (Hu *et al*, 2003; Cui *et al*, 2004). It has also been shown that binding of ICN to a different coactivator, Deltex, excludes binding to CSL, and therefore the ICN-Deltex complex may target transcription of a distinct set

of genes in response to activation (Yamamoto *et al*, 2001; Fortini *et al*, 2009). The importance of these findings remains to be defined.

The transcription factors of the Hairy/Enhancer of Split family (HES) and the HES-related repressor protein (HERP, also known as HEY) (Iso *et al*, 2003) are amongst the well-recognised targets genes of Notch signalling. They belong to the basic helix-loop-helix (bHLH) family of proteins. Both of these families bind specific sequences in the promotor regions of target genes and act as transcriptional repressors through recruitment of co-repressors including the Groucho/TLE protein (Barolo *et al*, 2002). Despite this, there is some evidence that specific signalling can modulate HES-1, switching its effects towards transcriptional activation (Ju *et al*, 2004). NRARP (Notch regulated ankyrin repeat protein) is a protein whose transcription has also been identified to be activated by Notch signalling. NRARP has been found to block downstream of Notch by forming an inhibitor complex with ICN-CSL, thus functioning as a negative-feedback regulator (Krebs *et al*, 2001; Yun and Bevan, 2003; Lamar *et al*, 2001).

The Notch pathway however, is more complicated than the basic outline described above. Its effects are dependent on context and its activation can result in a number of possible effects, either inducing or inhibiting cell proliferation. It can be modulated by proteins other than the aforementioned ligands and can diverge from the 'classical' pathway mentioned above, for example through a CSL-independent route. Although Notch signals primarily through HES, HEY and related genes, little is known about which of these genes are responsible for the phenotypic effects of

Notch; HES-1 and HES-5 appear to mediate the effects of Notch in inhibiting neuronal development (Ohtsuka *et al*, 1999); HES-1 appears to be important in delaying pancreatic epithelial precursor differentiation (Jensen *et al*, 2000) and in biliary organogenesis (Sumazaki *et al*, 2004); HEY-1 and HEY-2 in embryonic vascular development (Fischer *et al*, 2004); and HEY-2 in cardiac development (Sakata *et al*, 2002; Donovan *et al*, 2002; Gessler *et al*, 2002). There is also extensive crosstalk with other signalling pathways involved in cell cycle control and regulators of apoptosis, including p21, cyclin D1, Ras/MAPK, JAK/STAT, PI3K/Akt and NF-κB (Cheng et al, 2001; Iso et al, 2003).

1.3.5 Degradation of Notch

Intracellular Notch is expressed at very low levels in signalling cells, suggesting that it undergoes rapid degradation (Wu *et al*, 2001). Although not yet fully defined, several mechanisms have been purported for the rapid clearance on ICN. Numb is a well recognised Notch antagonist that has been shown to influence cells fate in *Drosophila* by negatively regulating the Notch pathway (Spana and Doe, 1996; Zhong *et al*, 1996; Frise *et al*, 1996; Guo *et al*, 1996). Numb homologues have been identified in mammals (Zhong *et al*, 1996; Verdi *et al*, 1996). Numb has been purported to inhibit Notch by preventing nuclear translocation of the co-activator Suppressor of Hairless (Su(H)) (Frise *et al*, 1996). Other studies suggest that Numb interaction with ICN prevents its nuclear localisation by binding to the PEST sequence (Wakamatsu *et al*, 1999). There is evidence suggesting a role of ubiquitin/proteosome degradation in Notch. Ubiquitin is a 76-amino acid polypeptide that is covalently linked to substrates in a multistep process. This involves a

ubiquitin-activating enzyme (E1), a ubiquitin-conjugating enzyme (E2), and ubiquitin ligase (E3), which recognises the substrate and catalyses the transfer of ubiquitin on to it. Ubiquitins have been recognised as targeting proteins for degradation. Numb expression has been shown to promote the ubiquitination of membrane-bound Notch-1 and the degradation of the intracellular domain following receptor activation. The E3 ubiquitin ligase designated Itch has been shown to ubiquitinate membrane-bound Notch-1 *in vitro* and *in vivo*. Numb interacts with Itch resulting in enhanced Notch-1 ubiquitination and down-regulation of the Notch-1-dependent signal transduction. SEL-10, an F-box protein of the CDC4 family that is structurally similar to E3 ubiquitin ligases, negatively regulates Notch by binding to the C-terminus of ICN and targeting it for ubiquitin-mediated protein degradation (Wu *et al*, 2001; Hubbard *et al*, 1997; Oberg *et al*, 2001). E3 ubiquitin ligases that target membrane-bound Notch have also been described. The Cbl E3 ligase has been reported to result in ubiquitinisation and lysosomal degradation of membrane-bound Notch-1 (Dievart *et al*, 1999), as has Itch (Qiu *et al*, 2000).

Mammalian Numb has been shown to localise to endocytic vesicles and to bind to the endocytic protein α-Adaptin, which is a subunit of AP-2 complex (Santolini *et al*, 2000; Berdnik *et al*, 2002). AP-2 is a major component of clarithrin-coated pits that acts as an adapter between the intracellular domain of transmembrane receptors destined for endocytosis and the endocytic machinery. Recruitment of AP-2 to the plasma membrane promotes polymerisation of the clathrin, forming coated pits and internalisation of the targeted receptors. It has been suggested that α-Adaptin serves a regulatory function in promoting endocytosis. The interaction of Numb with α-

Adaptin suggests that Numb may be responsible for targeting membrane-bound Notch for endocytosis (Berdnik *et al*, 2002).

There may also be a link between phosphorylation of ICN and its degradation. Evidence exists that transcriptional activators are frequently targeted for removal by the transcriptional machinery itself (Chi *et al*, 2001; Vandel and Kourzarides, 1999). CBP/p300 recruitment appears to connect p53 transcription activation to ubiquitin-mediated proteolysis via complexing with MDM2 (Zhu *et al*, 2001; Grossman *et al*, 1998). MAML (specifically the C-terminal domain) strongly promotes hyperphosphorylation and proteolytic turnover of ICN in the presence of CBF1 (Fryer *et al*, 2002). The TAD2 (transactivation domain) region of MAML has been shown to be required to promote this phosphorylation, however it possesses no intrinsic protein kinase activity of its own. It may therefore be the case that MAML may target ICN for phosphorylation by an additional factor, for example a cyclin-dependent kinase, or that a protein kinase may directly associate with MAML, however more research is needed. The hyperphosphorylated nuclear ICN may be recognised through a C-terminal PEST motif by SEL-10 and targeted for ubiquitin-mediated proteolytic degradation (Wu *et al*, 2001; Hubbard *et al*, 1997; Oberg *et al*, 2001). In addition, NRARP binds to the MAML-ICN-CSL complex and directly promotes Notch proteolysis (Krebs *et al*, 2001; Lamar *et al*, 2001).

1.3.6 Notch in normal tissue development

As with other oncogenic signalling pathways, the Notch pathway has been shown to play an important role in embryogenesis and the development of a variety of tissues. Notch signals function in the developing tissues of multicellular animals to ensure that multipotent progenitor cells give rise to specific numbers of daughter cells of the correct differentiation in the proper position. Notch was originally shown to be involved in regulating cell fate determination, proliferation and differentiation in *D. melanogaster* and *Caenorhabditis elegans*. Activation in this context depends either on inductive signals or negative feedback loops that establish special or temporal differences in the magnitude of Notch signalling. Notch is normally downregulated in mature tissues, although in some, such as haemopoetic cells, Notch remains active. In others, Notch may be reactivated during regeneration (Raya *et al*, 2003) or metaplasia (Miyamoto *et al*, 2003) following response to injury. The response to Notch activation is dependent upon dose, cell type and context; it can inhibit cellular differentiation, although it can also induce a secondary fate selection, cause cell proliferation or arrest, or induce cell survival or apoptosis.

Notch was originally described as a mechanism for the inhibition of cell differentiation and was believed to maintain the cells in an undifferentiated state, allowing cells to respond to inductive cues at appropriate times to facilitate cellular diversification (Artavanis-Tsakonas *et al*, 1995). Notch signalling has been shown to inhibit myogenesis (Luo *et al*, 2005), neurogenesis (Baker, 2000), granulocyte differentiation (Milner *et al*, 1996) and T cell development (Mailard *et al*, 2005). Notch however, has also been shown to steer cells toward alternative differentiation,

an example of this being gliogenesis (Wang and Barres, 2000). Notch signalling can therefore prevent or promote cellular differentiation depending upon cell lineage.

The ability to regulate the differentiation fate of individual cells means that Notch signalling is involved in the development of numerous tissues in multicellular organisms. Notch receptors and ligands have been shown to be widely expressed during mammalian organogenesis (Artavanis-Tsakonas *et al*, 1999) and have been found to play a role in the development of tissues derived from all three primative germ cell layers: endoderm (e.g. pancreas (Lammert *et al*, 2000), mesoderm (e.g. haemopoetic system (Milner and Bigas, 1999), mammary gland (Callahan and Egan, 2004), vasculature (Karsan, 2005)), and ectoderm (e.g. nervous system (Yoon and Gaiano, 2005)). Notch signalling also controls foetal and postnatal tissue development, as well as development and maturation of adult tissues (Artavanis-Tsakonas *et al*, 1999). Tight control of Notch signalling is vital to the proper development of most tissues. In haemopoietic progenitor cells, absence of Notch prevents differentiation and is associated with reduced transcriptional activity of NF-κB (Cheng *et al*, 2001). Presence of Notch in small intestinal epithelium maintains it in an undifferentiated state; Notch inhibition results in differentiation of proliferative cells into post-mitotic goblet cells (van Es *et al*, 2005; Fre *et al*, 2009). In developing pancreatic tissue, Notch over-expression has been shown to prevent both endocrine and exocrine differentiation, preventing cells from leaving an undifferentiated state (Murtaugh *et al*, 2003).

1.3.7 The role of Notch signalling in malignancy

Tumour development can involve reactivation of pathways normally down-regulated when normal development is complete. Aberrant activation of Notch would therefore favour tumour formation, and recent research suggests that the Notch pathway may play a part in the carcinogenesis of several solid and haematological malignancies. The role of Notch in development suggests that its reactivation in tumours may act to maintain cancerous cells in an undifferentiated state and therefore would be a potential therapeutic target.

1.3.7.1 Haematological malignancy

The role of Notch in haematopoiesis is well-established (Milner and Bigas, 1999). It has been shown to be important in maintaining a pool of undifferentiated haemopoietic stem cells and is downregulated as they differentiate (Duncan *et al*, 2005). Inhibition of Notch signalling enhances haemopoietic stem cell differentiation *in vitro* and *in vivo*. In addition to this, Notch is involved in maintaining an uncommitted pool of lymphoid, myeloid and erythroid precursors. Notch has also been shown to be involved in regulating the development and differentiation of T-cells, B-cells, monocytes, macrophages, dendritic cells, osteoclasts and natural killer cells (Sambandam *et al*, 2005; He and Pear, 2003; Ohishi *et al*, 2000; Masuya *et al*, 2002; Cheng *et al*, 2003; Yamada *et al*, 2003; de Hart *et al*, 2005). Dysregulation of the precise expression of Notch signalling proteins can lead to the development of haematological malignancies.

T-cell acute lymphoblastic leukaemia (T-ALL) is an aggressive cancer that preferentially affects children and adolescents. It is commonly associated with acquired chromososomal translocations and other genetic or epigenetic abnormalities, which lead to aberrant expression of a select group of transcription factors. The first link between Notch signalling and human malignancies was uncovered when a chromosomal translocation t(7;9)(q34:34.3) associated with human T-ALL was shown to produce a truncated Notch-1, lacking the extracellular domain (Ellisen *et al*, 1991). The translocation leads to the juxtaposition of the C-terminal domain of Notch-1 on chromosome 9 with the T cell receptor-β (TCR-β) locus on chromosome 7. This results in the expression of a constitutively active Notch-1 (translocation-associated Notch-1 – TAN1), with the N-terminus lying near the transmembrane domain, in a TCR-β regulated manner. Thus the activity of ICN-1 is devoid of normal Notch regulation and ligand stimulation. Notch-1 signalling is a potent inducer of T-ALL in the mouse (Pear *et al*, 1996; Hoemann *et al*, 2000; Feldman *et al*, 2000) – irradiated mice transplanted with bone marrow cells transduced with intracellular Notch-1 (ICN-1) develop T-ALL with 100% penetrance (Aster *et al*, 2000). Less than 1% of human T-ALL however, exhibit the t(7;9) translocation (Ma *et al*, 1999), although mutations activating Notch-1 independent of this translocation are seen in greater than 50% of human T-ALL (Weng *et al*, 2004) in both adult and paediatric cases (Weng *et al*, 2004; Lee *et al*, 2005). Notch-1 dysregulation therefore plays an important role in the human T-cell carcinogenesis. The oncogenic effect of the dysregulated ICN is linked to the function of Notch during normal T-cell differentiation. Activating mutation of Notch-2 and Notch- 3 have also been shown to induce T-ALL (Rohn *et al*, 1996; Bellavia *et al*, 2000), suggesting that the different Notch family members affect the same target genes, although the target genes remain

undefined. Over-expression of HES-1 does not cause T-ALL, suggesting that other target genes are more important. Inactivating ICN and CSL using dominant negative forms of MAML results in cell cycle arrest and apoptosis of T-ALL cells, showing that the ICN-CSL-MAML complex is necessary for their survival.

The role of Notch in the pathogenesis of B-cell malignancies is less clear. Notch-1 and HES-1 mRNA expression is significantly lower in B-cell precursor acute lympoblastic leukaemia than in T-ALL (Chiaramonte *et al*, 2005) and Notch deficiency causes preferential development of B-cells over T-cells (Radtke *et al*, 1999). The majority of B lymphoma cell lines display well-regulated Notch signalling (Chiaramonte *et al*, 2003). B-cell derived Hodgkin's lymphoma cells however, exhibit overexpression of Notch-1 and the ligand Jagged-1 (Jundt *et al*, 2002). Notch-2 overexpression has also been reported in patients with B-cell chronic lymphocytic leukaemia, associated with increased B-cell survival (Hubmann *et al*, 2002). Oncogenic viruses have also been shown to utilise the Notch pathway to induce B cell immortalisation (He and Pear, 2003). From this information, it seems that Notch may have an oncogenic role in some, but not all B-cell malignancies.

Notch may also be involved in the pathogenesis of other haematological malignancies. Multiple myeloma in humans has been shown to over-express Notch-1 and 2, as well as the ligands Jagged- 1 and -2 (Houde *et al*, 2004; Jundt *et al*, 2004). Notch-1 protein and Jagged-1 protein and mRNA have also been found to be over-expressed in acute myeloid leukaemia (Chiaramonte *et al*, 2005; Todha and Nara, 2001). Over-expression of the Notch pathway may promote the development of acute

myeloid leukaemia by inducing excessive renewal of cells and preventing differentiation (Chiaramonte *et al*, 2005), however a more recent study has found that ligand-mediated Notch activation actually promotes cellular differentiation in this group of cells (Todha *et al*, 2005).

1.3.7.2 Solid Tumours

The discovery of Notch over-expression in haematological malignancies has lead to investigation of the potential role of Notch in other malignancies. Abnormal Notch receptor protein expression has been reported in several human tumours. Increased Notch-1 expression has been demonstrated in colorectal, skin, cervical (Gray *et al*, 1999; Zagouras *et al*, 1995), lung and brain (Cuevas *et al*, 2005; Purow *et al*, 2005) malignancies. Over-expression of Notch-2 mRNA has been observed in medulloblastomas and primitive neuroectodermal tumours. Notch-2 is normally expressed in cerebellar progenitor cells, suggesting a role supporting growth and transformation. Patients with tumours expressing high levels of Notch-2 or HES-1 showed reduced survival, although this did not reach statistical significance (Fan *et al*, 2004). Notch-2 protein has been found to be over-expressed in colorectal, cervical (Gray *et al*, 1999; Zagouras *et al*, 1995), meningioma (Cuevas *et al*, 1995) and skin cancers. Notch-3 mRNA expression has been found to be up-regulated in renal cell carcinoma (Rae *et al*, 2000). Notch-3 and Notch-4 proteins have been found to be over-expressed in malignant melanoma (Massi *et al*, 2006). Notch-4 mRNA has also been identified in breast cancer (Callahan and Egan, 2004).

Notch ligands have also been investigated in solid malignancies. Jagged-1 protein has been found to be over-expressed in prostatic (Santagata *et al*, 2004), cervical (Gray *et al*, 1999) and brain cancers (Cuevas *et al*, 1995; Purow *et al*, 2005). In addition, Jagged-2 and Delta-1 mRNA has been found to be over-expressed in cervical cancers (Gray *et al*, 1999). Delta-1 mRNA and protein were found to be over-expressed in gliomas (Purow *et al*, 2005). Elevated Delta-1 levels were found in patients with neuroblastomas and this served as a strong predictive factor of poor prognosis (Wei *et al*, 2004).

Using the mouse mammary tumour virus (MMTV), Gallahan and Callahan showed that MMTV was frequently integrated into the int-3 locus in mice developing tumours (Gallahan and Callahan, 1997). This was subsequently discovered to be analogous to Notch-4. The viral insertion resulted in the expression of the transmembrane and intracellular domains of the receptor i.e. the constitutively active form. Similarly, integration of intracisternal A particle (a defective murine retrovirus which undergoes transposition and acts as a mutagen) into the Notch-4 locus also results in expression of constitutively active Notch-4 (Kordon *et al*, 1995). Constitutively active Notch-4 has been shown to have oncogenic properties in mammary epithelial cells *in vitro* and *in vivo* (Smith *et al*, 1995; Soriano *et al*, 2000). Over-expression of constitutively active Notch-4 induces transformation of normal human breast epithelial cells *in vitro* (Imatani and Callahan, 2000). The oncogenic effects can be attributed to blocking differentiation of mammary epithelial cells. Several human breast cancer cell lines have been shown to over-express Notch-4 mRNA and two of these express mRNA encoding the truncated form of Notch-4. Notch-1 may also have a role in mammary tumorigenesis. Expression of either activated Notch-1 or Notch-4 has been shown to

induce malignant transformation of mammary epithelial cells *in vitro* (Soriano *et al*, 2000). In addition, c-ErbB2 transgenic mice infected with MMTV developed mammary tumours associated with integration of MMTV into the Notch-1 gene and expression of the constitutively active form (Dievart *et al*, 1999). A correlation between Ras and Notch-1 over-expression has been found in human breast cancer; Notch-1 levels were also higher than surrounding normal mammary tissue (Weijzen *et al*, 2002). Human breast cancer specimens have also been found to express Notch-1-4 mRNA (Callahan and Egan, 2004). Over-expression of Notch-1 protein has also been correlated with reduced tumour differentiation and reduced patient survival, however the opposite was found for Notch-2 (Parr *et al*, 2004). In addition, reduced expression of Numb was found in 50% of human breast cancer samples and levels were inversely correlated with tumour differentiation (Pece *et al*, 2004).

1.3.8 Notch in pancreatic cancer

Notch receptors and ligands have been shown to be widely expressed in the developing pancreas (Lammert *et al*, 2000). Notch appears to prevent cellular differentiation and maintain a population of undifferentiated precursor cells (Apelqvist *et al*, 1999) – mice lacking HES-1 display severe pancreatic hypoplasia caused by depletion of pancreatic epithelial precursors (Jensen *et al*, 2000). In pancreatic carcinogenesis, Notch signalling has been shown to mediate the tumour-initiating effects of transforming growth factor (TGF)-α by expanding a population of undifferentiated precursor cells (Miyamoto *et al*, 2003). Miyamoto *et al* (2003) demonstrated over-expression of Notch-2, -3 and -4 RNA, as well as RNA of ligands Delta-1 and Jagged-1 and -2; Presenilin-1; and RNA of target genes HES-1, HES-4,

and HEY-1, in human pancreatic cancer specimens compared to normal pancreatic tissue. The Notch inhibitor, Sel-1 RNA was found to be down-regulated. RT-PCR of human specimens revealed similar findings; 90% of tumours expressed at least one Notch target gene at >2-fold normal level; 40% expressed at >3-fold normal. In addition, HES-1 was found to be over-expressed in 6 out of 10 pancreatic cell lines. Immunohistochemistry of resected pancreatic cancer specimens demonstrated frequent up-regulation of Notch-1-4 and Jagged-1 and -2 in pancreatic cancer as well as PanIN lesions, with 62% of specimens showing moderate to high levels of at least one Notch protein (Miyamoto *et al*, 2003). Expression of different family members tended to be concordant within an individual specimen. HES-1 expression was infrequent in normal ductal epithelium, but was significantly increased in metaplastic ductal epithelium, PanIN and invasive pancreatic cancer. The presence of these changes in pancreatic intraepithelial neoplasia suggests that they occur early in the carcinogenic process.

Buchler *et al* (2005) demonstrated an up-regulation of Notch-2 mRNA in six pancreatic cancer cell lines that was particularly high in the undifferentiated cell lines. The Jagged ligands were also expressed in all cell lines. The other Notch receptors and ligands were variably expressed. RT-PCR of resected human specimens demonstrated up-regulation of Notch-3 and -4, Jagged-2 and Delta-1 mRNA in pancreatic cancer samples compared to normal tissue. Immunohistochemistry showed strong expression of Notch receptors in resected pancreatic cancer specimen. Notch-1 was particularly over-expressed in the nerves; Notch-2 and -3 were particularly expressed in vascular smooth muscle; and Notch-4 in vascular endothelium. Jagged-1 showed particularly high expression at sights of invasion into nerves and surrounding

tissue. Transfection of pancreatic cancer cells with ICN-1 and Jagged-1 resulted in an increased production of VEGF, and Jagged-1 significantly increased tumour cell invasion. These findings suggest a role for Notch in pancreatic cancer invasion and angiogenesis.

Wang *et al* (2006, a-d) demonstrated high levels of Notch-1 mRNA and protein expression in three pancreatic cancer cell lines. Down-regulation of Notch-1 using siRNA caused growth inhibition in the cell lines, which was confirmed to be due to induction of apoptosis. Similarly, transfection of the cells with ICN-1 cDNA increased Notch-1 expression and resulted in a significant promotion of cell growth. Knockdown of Notch-1 was associated with $G_{0/1}$ cell cycle arrest. A subsequent study by the same group showed that knockdown of Notch-1 using siRNA resulted in inhibited tumour cell invasion, where as transfection with ICN-1 cDNA increased invasion (Wang *et al*, 2006b). It was postulated that this was due to inactivation of NF-kB.

Although few studies have been performed, they indicate that the Notch pathway is up-regulated in pancreatic cancer and that it may play a role in pancreatic cancer cell growth, invasion and angiogenesis.

1.3.9 Oncogenic Notch signalling

Several mechanisms have been purported for the apparent oncogenic properties of Notch. These include inhibition of apoptosis, induction of proliferation and epithelial-mesenchymal transition.

1.3.9.1 Inhibition of Apoptosis

Anti-apoptotic effects of activated Notch proteins have been linked to the induction of bcl-2 (Mackensie *et al*, 2004) and increased signalling through the PI3K (Nair *et al*, 2003) and NF-kB (Oswald *et al*, 1998) pathways. Jagged-1 has also been shown to activate NF-kB signalling, itself inducing Jagged-1 transcription in a positive feedback loop (Nickoloff *et al*, 2002). ICN has also been shown to protect against apoptosis by inhibiting c-Jun N-terminal kinase (JNK) activation by physically interacting with and inhibiting JNK-interacting protein 1 (Mackensie *et al*, 2004; Kim *et al*, 2005).

1.3.9.2 Induction of Proliferation

Activated Notch-1 has been shown to promote cell cycle entry of kidney epithelial cells by enhancing CDK2 and Cyclin D1 activity (Ronchini and Capobianco, 2001). HES-1 has also been shown to promote cell cycle entry by repressing the transcription of the cyclin-dependent kinase inhibitor $p27^{Kip1}$ (Murata *et al*, 2005). ICN-1 induces expression of the S phase kinase-associated protein 2 (SKP2), a subunit of the ubiquitin-ligase complex SCF^{SKP2} that enhances proteosome degradation of $p27^{Kip1}$ and $p21^{Cip1}$ (Sarmento *et al*, 2005).

TGF-β functions as a tumour suppressor and inhibits the growth of the majority of epithelial cell types. ICN-1 suppresses these effects by sequestering the transcriptional coactivator p300 from Smad3, which is a down-stream molecule in the TGF-β signalling pathway (Masuda *et al*, 2005). ICN-4 may also bind to and inhibit Smad2-4 in breast cancer cells (Sun *et al*, 2005). Activated Notch therefore renders cells resistant to the growth inhibition of TGF-β.

Notch may also activate the Ras pathway. Tumours forming in ICN-4 transgenic mice exhibit activated PI3K and ERK signalling, downstream signals of the Ras pathway (Fitzgerald *et al*, 2000). Over-expression of activated Ras has been shown to increase Notch-1, -4 and Delta-1 protein expression in human fibroblasts and kidney epithelial cells and maintenance of the Ras-induced neoplastic phenotype has been shown to require sustained Notch activation (Weijzen *et al*, 2002). Notch may therefore act as a target of Ras and also activate it as part of a positive feedback loop.

1.3.10 Tumour Suppressive effects of Notch

There is however, some evidence that Notch maybe tumour suppressive in certain situations. A tumour suppressive role for Notch has been postulated in the cervix (Talora *et al*, 2002), prostate (Shou *et al*, 2001), brain (Fan *et al*, 2004) and skin (Nicolas *et al*, 2003). Notch-1 inactivation causes epidermal hyper-proliferation and subsequent tumour formation in mice (Nicolas *et al*, 2003). Notch-1 is also inactive in human basal cell carcinomas, however, is active in the normal human epidermis,

where it promotes keratinocyte differentiation (Thelu *et al*, 2002). In human cervical cancer, Notch-1 is initially over-expressed in the early stages of the disease, however is down-regulated in the later stages. It also causes growth-inhibition of HPV-positive cervical carcinoma cells (Talora *et al*, 2002). In human breast cancer, Notch-2 is elevated in well-differentiated tumours when compared to poorly-differentiated specimens and associated with improved prognosis. Notch-1 however is over-expressed in poorly-differentiated tumours and associated with a poorer prognosis (Parr *et al*, 2004).

The mechanisms for the tumour suppressive effects are poorly defined. Notch-1 and Notch-2 have been shown to up-regulate p21Cip1 and p27Kip1 causing cell cycle arrest (Sriurangpong *et al*, 2001; Rangarajan *et al*, 2001). Inhibition of Notch-1 in mice resulted in reduced p21Cip1 expression and the formation of skin tumours (Nicolas *et al*, 2003). In addition, ICN-1 in mouse keratinocytes reduces β-catenin, implicating β-catenin-mediated Wnt signalling in the tumour suppression.

1.3.11 Potential therapeutic modulation of Notch

As highlighted above, the evidence strongly indicates that Notch may be frequently deregulated in cancer and therefore inhibition of Notch may be a novel therapeutic strategy. A number of genetic and pharmacological strategies are available to block or silence Notch signalling. Specific strategies include antisense (Weijzen *et al*, 2002; Shelly *et al*, 1999), RNA interference (Purow *et al*, 2005) and monoclonal antibodies (Yasutomo *et al*, 2000). Non-selective strategies include soluble receptor decoys that

sequester Notch ligands (Nickoloff *et al*, 2003), and γ-secretase inhibitors (Weijzen *et al*, 2002; Curry *et al*, 2005). These agents target all Notch receptors non-selectively. Obviously an effective therapeutic agent would need to effectively inhibit Notch without unacceptable toxicity. Theoretically, non-selective inhibitors are likely to have a great range of side effects, but as tumours often express more than one Notch receptor, are perhaps a more practical approach.

1.3.11.1 Gamma-secretase inhibitors

Gamma-secretase inhibitors target the enzyme that is responsible for the S3 cleavage that liberates ICN. These agents were initially developed in an attempt to benefit patients with Alzheimer's disease (Siemers *et al*, 2006, 2007). β-amyloid precursors proteins are type I integral membrane proteins that are cleaved by first β-, then γ-secretase/presenilin to produce β-amyloid peptides which subsequently form the plaques found in patients' with Alzheimer's disease. Mutations in the presenilin component of gamma secretase cause familial early-onset Alzheimer's disease with increased processing of APP by γ-secretase. Recent drug trials investigating the use in Alzheimer's disease have shown gamma-secretase inhibitors to be safe in humans, and trials are starting in patients with advanced breast carcinoma and T-ALL. Many gamma-secretase inhibitors have been shown to inhibit Notch processing. They are however, non-specific, as several other proteins also interact with gamma secretase/presenilin (Lewis *et al*, 2003). Gamma-secretase inhibitors have been found to inhibit both Notch and APP cleavage with equal potency (de Strooper *et al*, 1999). Gamma-secretase inhibitors effectively down-regulated HES-1 protein expression in BXPC-3 human pancreatic cancer cells and significantly reduced both HES-1 and

HEY-1 expression following treatment of mouse pancreas explant cultures with TGF-α (Miyamoto *et al*, 2003). It also effectively prevented TGF-α-induced acinar-to-ductal metaplasia. In all experiments, the IC_{50} for down-regulation of HES-1 expression was 30μM. Levels of the Notch receptor proteins were not directly analysed themselves. The reported IC_{50} in this study is significantly higher than the IC_{50} of 18nM that was found to inhibit Notch-1 activation after 5-hour incubation with a human kidney cell line (Lewis *et al*, 2003). Gamma-secretase inhibitors have been shown to reduce activation of Notch-1, -2 and -4 and to induce G_2/M arrest followed by apoptosis in Kaposi's sarcoma cell lines. They also caused significant growth inhibition or tumour regression after injection into established Kaposi's sarcomas in mice (Curry *et al*, 2005). Treatment with γ-secretase inhibitors also inhibited cell growth in Ras-transformed fibroblasts (Weizjen *et al*, 2002).

1.3.11.2 Specific Notch inhibition

As mentioned previously, γ-secretase inhibitors are not specific to the Notch pathway. Specificity is particularly important when investigating the effects of proteins/receptors in isolation. Transfection with antisense mRNA is a specific approach to reducing protein expression. Transfection of Notch-1-expressing, Ras-transformed fibroblasts with antisense Notch-1 led to reduced cellular proliferation (Weijzen *et al*, 2002). In addition, immunodeficient SCID mice were inoculated with Ras-transformed fibroblast either transfected with antisense Notch-1, or not. Those inoculated with the transfected cells showed significantly delayed and reduced tumour formation that the other group. Transfection of cervical carcinoma with antisense Notch1 has been shown to increase cell death. Transfection of human lung cancer

cell lines with a dominant negative Notch-3 receptor dramatically reduced growth rate, increased growth factor dependence and increased apoptosis (Haruki *et al*, 2004).

Protein knockout using siRNA (small interfering RNA) utilises small (21-23) nucleotide fragments of RNA that when transfected into cells, target specific mRNA and result in its cleavage. Transfection with siRNA against Notch-1 in glioma cell lines resulted in a significant reduction of Notch-1 protein and of CBF-1 activity. Notch-1 siRNA resulted in reduced cellular proliferation and a significant increase in apoptosis, as well as induction of G_2M arrest in the survivors (Purow *et al*, 2005). In the same cell lines, use of siRNA against Delta-1 and Jagged-1 similarly resulted in reduced cellular proliferation and increased apoptosis. Pre-treatment of glioma cells with Notch-1 or Delta-1 siRNA significantly prolonged survival in a murine orthotopic brain tumour model. Transfection of a pancreatic cancer cell lines with Notch-1 siRNA has been shown to effectively knocked-down Notch-1 (Wang *et al*, 2006a, b). Transfection resulted in growth inhibition of the cell lines and induction of apoptosis. In another study, transfection with Notch-1 siRNA resulted in pancreatic cancer cells showing a reduced propensity for invasion (Wang *et al*, 2006b, d).

1.4 AIM AND OBJECTIVES

1.4.1 Aim

This aim of this study is to further understand the role of the Notch pathway in pancreatic carcinogenesis and its potential as a biomarker and therapeutic target.

1.4.2 Objectives

1 To examine the expression of the Notch receptors and target proteins in pancreatic adenocarcinoma *in vitro* and *in vivo.*

2 To determine the correlations of the Notch pathway constituents with disease progression, clinicopathological parameters and prognosis following resection.

3 To examine the potential therapeutic application of Notch pathway inhibition *in vitro* and *in vivo* and the mechanisms involved.

4 To explore the potential of the Notch receptors as a biomarker in pancreatic adenocarcinoma.

CHAPTER 2

MATERIALS AND METHODS

2.1 CLINICAL MATERIALS

Part of this project involved work on human pancreatic tissue, collected from the Department of Pathology archives at the Leicester General Hospital. Ethics committee approval for the use of this tissue was obtained (LREC number 7176; Appendix). Similarly, ethical committee approval was obtained for the use of serum from control subjects and patients with advanced pancreatic adenocarcinoma for proteomics work (also LREC number 7176).

2.1.1 Patient recruitment for immunohistochemical studies

Patients included in the study were those treated for resectable pancreatic adenocarcinoma between October 2000 and May 2007 and those treated for non-resectable pancreatic adenocarcinoma between January 2003 and January 2007 at the Leicester General Hospital, University Hospitals of Leicester. These timeframes were chosen in order to provide adequate follow-up information. Patients were identified from the Leicester Hepatopancreaticobiliary Multidisciplinary team database. Case notes were reviewed by a single observer (CDM) to confirm suitability for inclusion. Inclusion and exclusion criteria for the study are summarised below.

Inclusion criteria:

- Surgical resection of pancreatic adenocarcinoma (resected group) or unresectable pancreatic adenocarcinoma (unresectable group)
- Tissue available for immunohistochemistry
- Access to accurate follow-up information

Exclusion criteria:

- Tumour types other than primary pancreatic ductal adenocarcinoma (e.g. distal cholangiocarcinomas, periampullary tumours, neuroendocrine tumours)
- History of previous neoplasia
- Pre-operative/pre-biopsy chemoradiotherapy
- Perioperative mortality

From information obtained from the medical notes and computerised hospital records a database was compiled detailing patient demographics and clinicopathological factors including:

- Age and gender
- Pre-operative blood test results including serum CA19.9
- Operation type
- Histopathological factors (including tumour size, differentiation, lymph node involvement, perineural infiltration, microvascular invasion, and resection margin status)
- Survival data (updated as of 1st January 2011)

For patients 'out-of-area', follow-up data including death and cause of death was obtained by contacting other hospitals and the patient's General Practitioner.

Following identification of suitable patients, slides used for the original histological assessment were obtained from the Leicester General Hospital pathology archive. These slides were reviewed by an experienced Consultant Gastrointestinal Histopathologist in order to select appropriate blocks. Selected blocks were then removed from the pathology archives and sections cut for immunohistochemical assessment.

2.1.2 Patient recruitment for serum proteomics studies

Patients included in this study were those with unresectable pancreatic ductal adenocarcinoma (based upon either locally-advanced or metastatic disease) due to start gemcitabine-based chemotherapy between May 2009 and June 2009 at the Department of Oncology, Leicester Royal Infirmary, University Hospitals of Leicester. Patients were identified from the Leicester Hepatopancreaticobiliary Multidisciplinary team database. Case notes were reviewed by a single observer (CDM) to confirm suitability for inclusion. Inclusion and exclusion criteria for the study are summarised below.

Inclusion criteria:

- Histologically confirmed unresectable pancreatic ductal adenocarcinoma (locally-advanced or metastatic disease)
- Due to start Gemcitabine-based chemotherapy
- Patients must be able to give written consent

Exclusion criteria:

- Tumour types other than primary pancreatic ductal adenocarcinoma (e.g. distal cholangiocarcinomas, periampullary tumours, neuroendocrine tumours)
- History of previous neoplasia
- Patients unwilling or unable to comply with the protocol or give written consent

2.2 LABORATORY MATERIALS

2.2.1 Materials for *in vitro* experimentation

Unless otherwise stated, all chemicals were purchased from Sigma-Aldrich Company Limited (Poole, Dorset, UK), and solvents from Fisher Scientific (Loughborough, Leicestershire, UK). Materials from other suppliers included:

Acrylamide (30% acrylamide: bis acrylamide)	Anachem
Annexin V kit	Bender Medsystems
ATP-lite luminescence assay system	Perkin-Elmer
BioRad protein assay reagent	Bio-Rad
Caspase-Glo 3/7	Promega
Curcumin	Cayman Chemicals
Dulbecco's Modified Eagle Medium	Gibco BRL
ECL detection kit	Amersham

ECL-hyperfilm	Amersham
Foetal calf serum	Gibco BRL
Gamma secretase inhibitor I	Calbiochem
Gamma secretase inhibitor X	Calbiochem
Gemcitabine (Gemzar)	Eli Lilly
GeneChip® IVT Express Kit	Affymetrix
Hybond nitrocellulose	Amersham
Isoton II	Beckman Coulter
Lipofectamine 2000	Invitrogen
Marvel (dried milk powder)	Premier Brands
MRK-003	Merck U.K.
Neo-FX	Ambion
Opti-MEM tissue culture medium	Invitrogen
Protein molecular weight markers	Fermentas Life Sciences
Restore Western Blot Stripping Buffer	Thermo Scientific
RNeasy kit	Qiagen
Trypsin/EDTA	Gibco BRL

2.2.2 Materials for immunohistochemistry

Superfrost Plus™ slides	Menzel-Glazer
Glass cover slips	Menzel-Glazer
Haematoxylin-plus	Vector Laboratories
DPX mountant	Sigma
Envision+ detection kit	Dakocytomation

2.2.3 Materials for proteomics

The Notch-1 peptide was synthesised by Pepceuticals Limited (Nottingham, UK) and the Notch-3 peptide by Davids Biotechnologie (Regensburg, Germany). Antibodies against Notch-1 and Notch-3 were synthesised by Davids Biotechnologie. Oasis® HLB cartridges were obtained from Waters Ltd, Protein G Dynabeads from Invitrogen, and Microcon® YM-5 centrifugal filter devices from Millipore Ltd.

2.2.4 Antibodies

Details of primary antibodies used for immunohistochemistry and/or *in vitro* experimentation are shown in table 2.1. Horseradish peroxidase (HRP)-conjugated secondary antibodies were purchased from Sigma.

Table 2.1 – Primary antibodies used for *in vitro* and immunohistochemistry experiments

Antibody against	Species	Clone	Isotype	Epitope	Supplier
Actin	Goat	Monoclonal	IgG_1	C-terminus (350-375)	Santa-Cruz
Anti-Ki67	Mouse	Monoclonal (MIB-1)	IgG_1		Dako
HES-1	Rabbit	Monoclonal	IgG_{2b}	C-terminus (237-261)	Santa-Cruz
HEY-1	Rabbit	Polyclonal	IgG	C-terminus (207-261)	Abcam
Notch-1	Rabbit	Polyclonal	IgG	C-terminus	Santa-Cruz
Notch-3	Rabbit	Polyclonal	IgG	C-terminus (2107-2240)	Santa-Cruz
Notch-4	Rabbit	Polyclonal	IgG	C-terminus (1779-2003)	Santa-Cruz

2.2.5 Small interfering RNAs (siRNA)

siRNAs were used against Notch-1, Notch-3 and Notch-4. Several siRNAs were experimented with for each Notch protein, with the siRNA producing superior knockdown used for the final experiments. siRNAs were obtained from Santa Cruz, Qiagen and Ambion. The final siRNAs were s9634 for Notch-1 from Ambion, sc-37135 from Santa Cruz for Notch-3, and HS_NOTCH4_5 for Notch-4 from Qiagen. Transfection efficiency was optimised using a fluorescein-conjugated scrambled control siRNA. Chemical transfection using Lipofectamine 2000 (Invitrogen) and NeoFX (Ambion) was experimented with, as well as Amaxa nucleofection. Amaxa nucleofection resulted in a significant loss of cell viability and was therefore abandoned. Lipofectamine 2000 resulted in the greatest transfection efficiency in all cell lines and was therefore used for all experiments.

2.2.6 Suppliers' addresses

Abcam Inc, Cambridge, UK

Affymetrix UK, High Wycombe, UK

Agilent Technologies, South Queensferry, West Lothian, U.K.

Ambion Applied Biosystems, Warrington, U.K.

Amersham Pharmacia Biotech, Buckinghamshire, U.K.

Anachem, Bedfordshire, UK

ATCC, Manassas, VA, USA.

BDH, Darmsadt, Germany

Beckman Coulter UK Ltd, High Wycombe, UK

Bender Medsystems, Vienna, Austria

Bio-Rad, Hertfordshire, UK

Calbiochem, Nottingham, UK

Cayman Chemicals, Michigan, USA

Cell Signalling Technology, Hertfordshire, UK

Dako, Glostrup, Denmark

DakoCytomation, California, USA

Davids Biotechnologie, Regensburg, Germany

Eli Lilly, Basingstoke, UK.

Fermentas UK, York, UK

Fisher Scientific, Loughborough, Leicestershire, UK

Gibco-BRL (Invitrogen Life Technologies), Paisley, UK

Harlan Laboratories UK. Ltd., Bicester, UK

Invitrogen, Paisley, UK

Menzel-Glazer, via Fisher Scientific, Loughborough, Leicestershire, UK

Millipore Limited, Watford, UK

Pepceuticals Limited, Biocity, Nottingham, UK

Perkin-Elmer, Cambridge, UK

Premier Brands, Wirral, UK

Promega, Southampton, UK

Qiagen, West Sussex, UK

Santa Cruz Biotechnology, California, USA

Sigma-Aldrich Company Limited, Poole, Dorset, UK

Vector Laboratories, California, USA

Waters Limited, Thermo Electron, Elstree, UK

2.3 SOLUTIONS AND BUFFERS

2.3.1 Solutions and buffers for immunohistochemistry

Citric acid antigen retrieval buffer (x20) stock *200mM pH6*

Citric acid monohydrate 42g

Sodium hydroxide pellets

The citric acid was dissolved in distilled water and the pH adjusted using a calibrated pH meter (Hanna Instruments) to 6.0 using NaOH pellets. The volume was made up to 1L using distilled water. The solution was stored at 4°C and diluted 1:20 before use.

Tris-EDTA antigen retrieval buffer *10mM Tris base, 1mM EDTA, pH9*

Tris base 1.21g

EDTA 0.37g

Tween-20 0.5ml

The Tris base and EDTA were dissolved in distilled water and the pH adjusted to 9.0. The volume was made up to 1L using distilled water and the solution stored at 4°C if not used immediately.

Tris-buffered saline (TBS) (10x) wash buffer *500mM Tris base, 1.5M NaCl*

Tris base 60.5g

Sodium chloride 87.6g

The Tris base and sodium chloride were dissolved in distilled water and the pH adjusted to 9.0 using concentrated HCl. The volume was made up to 1L using

distilled water. The solution was stored at room temperature and diluted 1:10 prior to use.

Tris-HCl buffer for dilution of primary antibody *50mM pH7.2-7.6*

0.785g Tris-HCl added to 100ml distilled water and 1% BSA added immediately prior to use.

Envision$^+$ detection system

1. Peroxidase blocking solution

   0.03% hydrogen peroxide

2. Secondary antibody

   Peroxidase-labelled polymer conjugated to goat anti-rabbit immunoglobulin, in Tris-HCl buffer

3. Detection

   One drop of 3,3-diaminobenzidine (DAB) chromogen added to 1ml substrate buffer, containing hydrogen peroxide, immediately before use

2.3.2 Solutions and buffers for *in vitro* experimentation

Annexin buffer

10mM HEPES (pH 7.4)

150mM NaCl

5mM $MgCl_2$

1.8mM $CaCl_2$

The above solution was made up to 500ml in distilled water and stored at room temperature.

Blocking buffer 1

5% dried non-fat milk diluted in PBST (e.g. 2g milk in 40ml PBST)

Blocking buffer 2

5% BSA diluted in PBST

Cell lysis buffer (10x stock)

200mM Tris (pH 7.5)

1.5M NaCl

10mM EDTA

10mM EGTA

10% Triton X-100

25mM sodium pyrophosphate

10mM β-glycerolphosphate

10mM sodium orthovanadate

The above solution was made up to 500ml with dH_2O, and stored at 4°C. It was diluted to 1x before use and 1% protease inhibitors were added.

PBS-Tween (PBST)

0.1% Tween-20 (1ml Tween-20 added to 1L PBS)

Polyacrylamide denaturing running gel (10ml)

Volumes of water and acrylamide varied according to the percentage gel cast. The following remained the same: 2.5ml 1.5M Tris (pH 8.8), 100µl 10% SDS.

- 8% - 4.6ml water, 2.7ml 30% acrylamide
- 10% - 4ml water, 3.3ml 30% acrylamide
- 12% - 3.3ml water, 4ml 30% acrylamide
- 15% - 2.3ml water, 5ml 30% acrylamide

Polymerisation was initiated upon addition of 100µl ammonium persulphate and 10µl TEMED.

Polyacrylamide denaturing stacking gel (10ml)

6.8ml dH_2O

1.7ml 30% acrylamide

1.25ml 1M Tris (pH 6.8)

100µl 10% SDS

Polymerisation was initiated upon addition of 100µl ammonium persulphate and 10µl TEMED.

SDS loading buffer (3x stock)

187.5mM Tris-HCl (pH 6.8)

6% SDS (8ml)

30% glycerol (4ml)

0.03% w/v bromophenol blue

The stock solution was stored at room temperature. It was diluted to 1x immediately prior to use and 150mM dithiothreitol (DTT) added to the buffer.

Tris-EDTA buffer

10mM Tris HCl (pH 8.0), 1mM EDTA made up to an appropriate volume in distilled water and stored at room temperature.

TBS-Tween (TBST)

20mM Tris (pH 7.5)

150mM sodium chloride

0.1% Tween-20

The stock was made up to the appropriate volume in distilled water and stored at room temperature.

Western running buffer (10x)

25mM Tris

250mM glycine

0.1% SDS

The 10x stock was pH 8.3 and made up to 1L in distilled water and stored at room temperature. This was diluted to a 1x working solution prior to use.

Western stripping buffer

62mM Tris

2% SDS

The stock was made up in 500ml distilled water and stored at room temperature. Immediately prior to use, 0.8% v/v 2-mercaptoethanol was added.

Western transfer buffer

48mM Tris

37mM glycine

20% methanol

10% SDS

The stock was made up to a volume of 10L in distilled water and pH adjusted to 8.3.

It was stored at room temperature.

2.3.3 Solutions and buffers for microarray analysis

Antibody Solution Mix (600µl)

(Final 1x concentration: 1x Stain buffer, 2mg/ml BSA, 0.1mg/ml Goat IgG stock)

3µg/ml biotinylated antibody)

300µl 2x Stain buffer

24µl of 50mg/ml BSA

6µl of 10mg/ml goat IgG stock

3.6µl of 0.5mg/ml biotinylated antibody

266.4µl RNase-free dH_2O

Hybridisation buffer (2x stock)

(Final 1x concentration is 100mM MES, 1M $[Na^+]$, 20mM EDTA, 0.01% Tween-20)

8.3ml 12x MES stock buffer

17.7ml of 5M NaCl

4.0ml of 0.5M EDTA

0.1ml of 10% Tween-20

19.9ml RNase-free dH_20

Store 2-8°C in the dark and diluted to 1x prior to use.

2-(N-morpholino)ethanesulfonic acid (MES) stock buffer (20x)

(1.22M MES, 0.89M [Na^+])

64.61g MES hydrate

193.3g MES sodium salt

800ml RNase-free molecular biology grade dH_20

The above solution was mixed and adjusted to 1000ml. The pH was adjusted to between 6.5-6.7, and it was filtered through a 0.2µm filter. The solution was stored at 2-8°C in the dark and diluted to 1x prior to use.

RNase-free water

1ml of diethyl pyrocarbonate (DEPC) was added to 1L of dH_2O, mixed, and incubated at 37°C overnight. This was then autoclaved for 15 minutes to inactivate the DEPC.

SAPE (Streptavidin Phycoerythrin) Stain Solution

(Final 1x concentration: 1x Stain buffer, 2mg/ml BSA, 10µg/ml SAPE)

600µl 2x Stain buffer

48µl of 50mg/ml BSA

12µ of 1mg/ml Streptavidin Phycoerythrin (SAPE)

540µl RNase-free dH_2O

The above solution was made up and stored at 4°C foil wrapped in the dark.

SSPE Buffer (20x)

175.3g NaCl

27.6g NaH_2PO_4

9.4g EDTA

RNase-free dH_20

The above solution was made up to 1L and the pH adjusted to 7.4 using NaOH. It was autoclave for 20 minutes and diluted to 1x with RNase-free dH_2O prior to use.

Stain Buffer (2x)

(Final 1x concentration: 100mM MES, 1M [Na^+], 0.05% Tween-20)

41.7ml of 12x MES stock buffer

92.5ml of 5M NaCl

2.5ml of 10% Tween-20

113.3ml RNase-free dH_2O

The above solution was made up, filtered through a 0.2µm filter and stored at 2-8°C in the dark. It was made up to 1x with RNase-free dH_2O prior to use.

Wash Buffer A: Non-Stringent Wash Buffer

(6x SSPE, 0.01% Tween-20)

300ml of 20x SSPE

1.0ml of 10% Tween-20

699ml RNase-free dH_2O

The above solution was made up to 1L and filtered through a 0.2µm filter.

Wash Buffer B: Stringent Wash Buffer

(100mM MES, 0.1M [Na^+], 0.01% Tween-20)

83.3ml of 12x MES stock buffer

5.2ml of 5M NaCl

1.0ml of 10% Tween-20

910.5ml RNase-free dH_2O

The above solution was made up to 1L and filtered through a 0.2µm filter. It was stored at 2-8°C in the dark.

2.4 METHODS – IMMUNOHISTOCHEMISTRY

2.4.1 The EnVision^{+} immunohistochemistry technique

The technique employed for the current study was the EnVision^{+} system-HRP (DAB) kit, manufactured by DAKO, which has been previously found to compare favourably with other detection methods (Sabattini *et al.*, 1998). The system is biotin-independent, resulting in minimal background staining and permitting accurate detection of antigen presence and localisation. The secondary antibody is conjugated with a dextran backbone which is bound to HRP or alkaline phosphatase (AP) molecules (HRP in this case). Each dextran holds up to 20 secondary antibodies and 100 enzyme molecules, which therefore leads to marked signal amplification. This result in it being extremely sensitive, enabling shorter incubation times and lower concentrations of primary antibodies compared to the ABC technique (Sabattini *et al.*, 1998) (Figure 2.1). The HRP forms a complex with its substrate, hydrogen peroxide, which reacts with an electron-donating chromogen, in this case 3, 3'-diaminobenzidine (DAB), to produce a coloured end-product at the site of the antigen of interest.

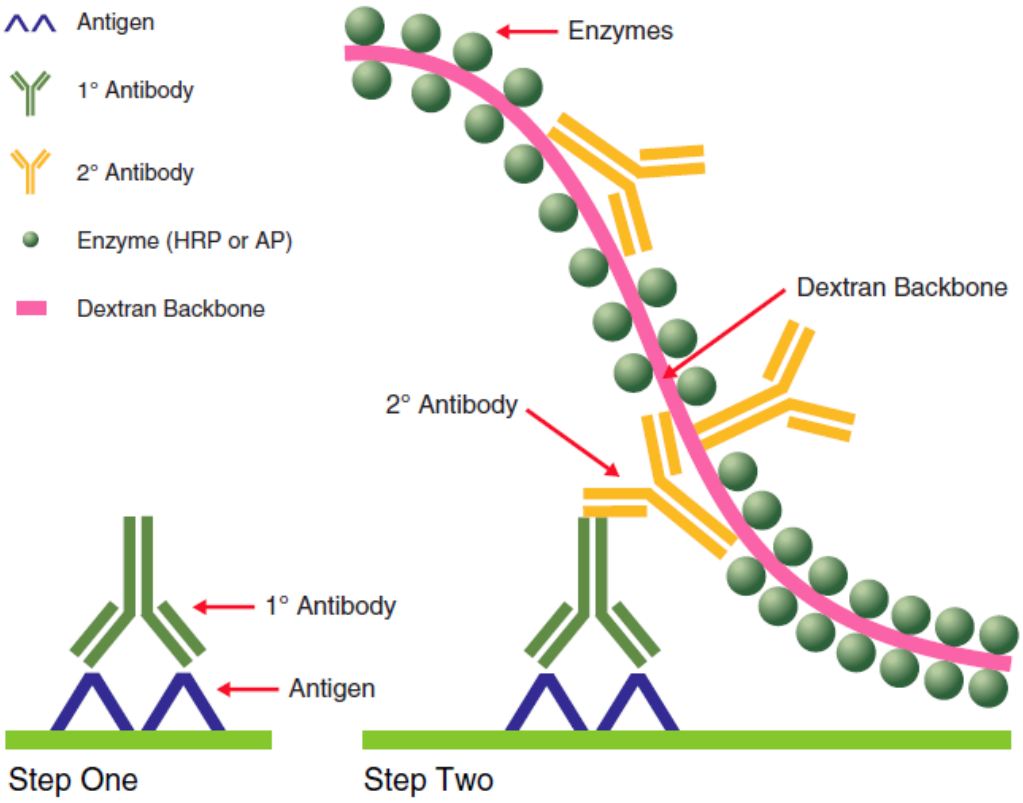

Figure 2.1 – Envision two-step polymer method

2.4.2 Preparation of tissue slides

Processing of embedded tissues was performed by Karen Kulbecki (Department of Cancer Studies and Molecular Medicine). Five µm sections of formalin-fixed, paraffin-embedded tissue blocks were cut on to Superfrost plus™ microscope slides using a Shandon Citadel 2000 processor. The first section from each block was stained with haematoxylin and eosin in order to identify different areas of histology. Subsequent sections were cut on to numbered slides so that serial sections from each block could be compared for different stains.

Haematoxylin and eosin staining was performed using a Shandon Varistaine 24-4 Staining machine (Shandon Inc, Pittsburgh, Pennsylvania, USA). Slides were initially put through two changes of xylene for 3 minutes each, then two changes of 100% IMS, one of 70% IMS, and one of dH_2O, for 1 minute each. Slides were stained with haematoxylin for 1.5 minutes, then rinsed in water for 1 minute. They were put into 1% acid water for 15 seconds then washed three times in water. Eosin staining was carried out for 3 minutes, followed by a 2 minute wash in water. Slides were then put back through 70% IMS, followed by 4 changes of 100% IMS and 2 changes of xylene.

2.4.3 EnVision+ Immunohistochemistry protocol

Each individual antibody was separately optimised prior to use of experimental tissue (see section 2.4.4). The general method is outlined below.

All reagents were equilibrated at room temperature prior to use. Slides were labelled, then deparaffinised in two changes of xylene for 5 minutes each. Slides were then rehydrated through two washes of 100% IMS, followed by one of 95% IMS for 5 minutes each. The slides were then washed in tap water for 5 minutes, followed by dH_2O for 5 minutes.

2.4.3.1 Antigen retrieval

1500ml Tris-EDTA antigen retrieval buffer was made up (per rack of slides). This was preheated until boiling for 15 minutes at 100% power in the microwave. The slides were then placed in the buffer bath and heated for 11 minutes at 100% power (900W), followed by 21 minutes at 40% power (360W). The slides were then cooled

for 30 minutes by placing the water bath under a cold running tap. The slides were then washed for 5 minutes in tap water, followed by 5 minutes in a TBS bath.

2.4.3.2 Peroxidase block

Following antigen retrieval, excess liquid was wiped from around the tissue sections, and one-two drops of the supplied peroxidase blocking solution (0.03% hydrogen peroxide containing sodium azide) placed over the tissue on each slide. The slides were then incubated for 10 minutes at room temperature. This is to quench any endogenous peroxidase activity. The slides were then rinsed with TBS, followed by washing in a TBS bath for 5 minutes.

2.4.3.3 Primary antibody

The appropriately diluted primary antibody was made up in 0.05M Tris-HCl buffer to which 1% BSA was added before use. Excess liquid was wiped from around the tissue sections, and the slides incubated with 150-200µl of the primary antibody dilution in a humidified chamber. Optimised antibody concentrations, incubation times and incubation conditions are shown in table 2.2. A negative control was included in each run to exclude non-specific staining, consisting of a section incubated with a non-specific immunoglobulin of the same class as the test antibody, diluted to the same concentration in Tris-HCl buffer. A section of known positive control tissue was also included in each run to ensure consistency between experiments. Following incubation, the slides were rinsed in TBS, and then underwent two 5 minutes washes in TBS baths.

Table 2.2 – Optimised conditions for immunohistochemistry

Antibody	Dilution	Incubation duration	Positive control tissue
Notch-1	1:1000	4°C overnight	Human epidermis
Notch-3	1:500	RT 1 hour	Mouse kidney
Notch-4	1:500	4°C overnight	Human kidney
HES-1	1:500	4°C overnight	Human liver
HEY-1	1:1000	4°C overnight	Human lung

Tris-EDTA buffer used for antigen retrieval in all cases; RT, room temperature.

2.4.3.4 Peroxidase-labelled polymer

Excess liquid was wiped from around the tissue sections, and the slides incubated with one-two drops of the supplied peroxidise-labelled polymer, consisting of a HRP-labelled polymer coupled to immunoglobulins raised against the appropriate species of the primary antibody. This was incubated for 40 minutes at room temperature in a humidified chamber. Following incubation, the slides were rinsed in TBS, and then underwent two 5 minutes washes in TBS baths.

2.4.3.5 Substrate-chromogen

One drop of DAB+ chromogen solution was added to 1ml of DAB+ substrate buffer (hydrogen peroxide). Excess liquid was wiped from around the tissue sections, and the slides incubated with several drops for 10 minutes at room temperature. Following incubation, the slides were rinsed in dH_2O, and then underwent three 5 minutes washes in dH_2O baths.

2.4.3.6 Haematoxylin counterstaining

The slides were then rinsed in tap water, then counterstained with vector haematoxylin QS for 5 seconds, and then rinsed again in tap water.

2.4.3.7 Mounting slides

The slides were then graded back through IMS (95%, 99%, 99%) and two changes of xylene for 5 minutes each. Slides were then wet-mounted using DPX mountant under glass cover slips.

2.4.4 Optimisation of Immunohistochemistry

Formalin tissue fixation may mask antigenic sites by crosslinking proteins. This is particularly likely with monoclonal antibodies as there is less chance of masking all epitopes that may be recognised by polyclonal antibodies. In the 1990s, it was shown that the formalin-induced cross-linkages between proteins could be broken down by heat treatment, and that many antibodies could be successfully used in formalin-fixed specimens (Shi *et al.*, 1991).

In order to assess the optimal staining conditions for each antibody and to subsequently confirm reproducibility between experiments, suitable positive control tissues were used. In this study, initially staining in the absence of antigen-retrieval was attempted for all antibodies, but as expected produced little or no staining. Although various forms of antigen retrieval have been reported in the literature (including the Hydrochloric acid and Formic acid methods), heat-mediated antigen retrieval by microwaving was chosen for all antibodies after review of the literature.

Several buffers have been utilised in the literature for heat-mediated antigen retrieval, including citrate, citrate-EDTA, TBS, Tris and Tris-EDTA. Initially both citrate and Tris-EDTA buffers were compared, however Tris-EDTA produced superior or equal results for all antibodies, therefore was utilised for the experimental tissue. Similarly,

alterations of heating time in the Tris-EDTA buffer were compared, as were primary antibody dilutions (using serial dilutions) and incubation conditions (1 hour at room temperature compared to 4°C for 20 hours), to produce the best possible staining. For all antibodies, heating in Tris-EDTA buffer at 900W for 11 minutes, followed by 21 minutes at 360W produced optimum retrieval. All slides were allowed to cool for 30 minutes by placing in a water bath under a cold running tap.

2.4.5 Scoring of immunohistochemistry

An Axioskop 2 plus microscope was used for slide interpretation (Carl Zeiss Ltd, Hertfordshire, UK). The scoring system had been previously devised in the department under the guidance of a Consultant Histopathologist, and used in publication (Doucas *et al.*, 2008). Staining was assessed in both tumour tissue and in the ductal epithelium of normal surrounding pancreas. Slides were initially examined under 100x magnification to identify areas of staining and then 10 separate areas of tumour tissue/ductal epithelial cells were examined at a higher power (40x) to identify cellular localisation (cytoplasmic, nuclear). Cytoplasmic staining was assessed semiquantitatively, with scores in 10% increments according to the percentage of tumour cells/ductal epithelial cells stained. Nuclear staining was assessed as positive if ≥10% of tumour/ductal epithelial cell nuclei stained positive and negative if <10% stained. Staining in tumour samples was only assessed in tumour cells – surrounding fibrous and inflammatory tissue was excluded from the scoring. Staining intensity was not used as a score as this has been shown to lack reproducibility (Zlobec *et al.*, 2007). Slides were graded independently by two observers blinded to the clinical data. In cases where discrepancy in the scoring occurred (>10%), slides were re-reviewed by both observers simultaneously and a final score agreed.

2.4.6 Ki67 staining

Ki67 staining was performed on formalin-fixed sections of xenograft tumour embedded in paraffin wax, prior to sectioning and mounting on Superfrost Plus™ slides (as above). The protocol was identical to that of the standard immunohistochemistry, with antigen retrieval via microwaving in a Tris-EDTA buffer. Sections were incubated with the anti-Ki67 antibody at 1:100 in 0.05M Tris-HCl buffer/1% BSA for 3 hours at room temperature. The remainder of the protocol was identical to above. Sections were visualised at 400x magnification using a Axioskop2 plus microscope and camera system. Scoring of positive cells was undertaken on 10 random fields of tumour tissue from each slide by two independent observers and expressed as a percentage of positively stained cells.

2.5 METHODS – *IN VITRO* EXPERIMENTS

2.5.1 Cell lines

All pancreatic adenocarcinoma cell lines were purchased from American Tissue Culture Collection (ATCC), Manassas, VA, USA:

- ASPC-1 Human. Tumour derived from ascites of patient with pancreatic adenocarcinoma. Moderate to poor differentiation (Chen *et al.*, 1982).
- BxPC-3 Human. Tumour derived from biopsy of the patient with adenocarcinoma of the body of the pancreas. Moderate to poor differentiation (Tan *et al.*, 1986).
- MIA PaCa-2 Human, tumour derived from metastatic pancreatic adenocarcinoma. Undifferentiated (Yunis *et al.*, 1977).
- PANC-1 Human. Tumour derived from primary human pancreatic adenocarcinoma (Lieber *et al.*, 1975).

ASPC-1, MiaPaCa-2 and PANC-1 have K-ras point mutations, whilst BxPC-3 possesses wild-type k-ras (Aoki *et al.*, 1997). ASPC-1 and BxPC-3 cells are known to display a more aggressive phenotype and metastasise earlier than PANC-1 and Mia PaCa-2 cells (Kulik *et al*, 1997). All cell culture was undertaken in a class II laminar flow cabinet. Cell lines tested negative for mycoplasma infection.

2.5.1.1 Maintenance of cell lines

ASPC-1 and BxPC-3 cells were maintained in RPMI-1640 cell culture medium containing 3mM L-glutamine and 2g/l glucose, supplemented with 10% FCS.

MiaPaCa-2 and PANC-1 cells were maintained in DMEM cell culture medium containing L-glutamine (4mM), sodium pyruvate (110mg/l) and 4.5g/l glucose, supplemented with 10% FCS.

All cell lines were maintained in a Sanyo incubator at 37°C, 5% CO_2 and 100% humidity, with media changes every 2-3 days.

2.5.1.2 Passaging of cell lines

Cells were routinely passaged when approximately 70% confluence had been reached. Following resurrection from storage, cells were not subcultured more than thirty times. Cells were gently washed twice in PBS (37°C) to remove all medium, and 5ml of 1x T/E added. The cells were incubated at 37°C for approximately 5 minutes, or until all the cells had just lifted off, whereupon the T/E was neutralised with the addition of 5ml of medium containing 10% FCS. Cells were pelleted at 200xg for 3 minutes and resuspended in 10ml medium containing 10% FCS. 2ml of cell suspension was then added to a fresh T125 flask containing 30ml of medium with 10% FCS. Cells were not re-passaged within 2 days of subculturing.

2.5.1.3 Freezing cell lines

All cell lines were frozen in 95% culture medium and 5% DMSO. Cells were trypsinised and, once detached, 3ml medium was added and mixed with an automatic

pipette. The cell suspension was then transferred to a universal container and centrifuged at 1200rpm for 5 minutes. Following this, the supernatant was discarded. Cells were then re-suspended in 2ml of freezing solution, vortexed and transferred into labelled containers suitable for freezing (1ml each container). The cells were frozen at -20°C for 3-5 hours, before being transferred into the -80°C freezer overnight. They were then stored in liquid nitrogen for long-term storage.

2.5.1.4 Reviving frozen cell lines

The cells were removed from liquid nitrogen storage and placed in a 37°C water bath. Immediately on defrosting, the cell suspension was then transferred to a medium flask with 15ml of culture medium containing FCS. The cells were left overnight, then observed under a microscope to ensure adhesion to the flask. The culture medium was then replaced with fresh medium, and the cells grown as described above.

2.5.1.5 Plating and treatment of cells

For experiments looking at basal expression of biomarkers, cells were plated on to 10cm plates and grown in standard culture medium as before. Plates were incubated at 37°C and harvested at the appropriate time point/cell density as described below.

For experiments requiring treatment of cells, cells were seeded at the required density in the appropriate size plates/wells and allowed to recover and attach overnight prior to treatment. The medium was then aspirated and replaced with medium containing the appropriate concentration of the treatment agent. Stock solutions of GSI-X, GSI-I, curcumin and gemcitabine were made up in DMSO immediately prior to use, such that all samples contained an equivalent volume of DMSO that did not exceed 0.1%.

All experiments included an untreated control and an equivalent percentage DMSO control.

2.5.2 Preparation of cell lysates

2.5.2.1 Whole cell lysate preparation

Following appropriate incubation times, the plates were placed on ice, the medium removed and cells washed twice with ice cold PBS. All residual liquid was removed and 200µl of cell lysis buffer added. Following 10 minutes of incubation on ice, the plates were thoroughly scraped and the lysate collected into a labelled eppendorf. This was incubated on ice for a further 15 minutes. Following this lysates were centrifuged at 4°C at 13000xg for 5 minutes, the supernatant preserved and either used immediately or frozen and stored at -20°C for later use.

2.5.2.2 Bio-Rad protein assay

Prior to use, protein concentration of cell lyses was determined to ensure that equal protein loading on gels could be achieved within each set of experiments.

Bio-Rad protein reagent was diluted 1:5 in distilled H_2O. 5µl of cell lysate was added to 1ml of this, vortexed, and the absorbance at 595nm determined using a Perkin Elmer λ2 UV/VIS spectrophotometer. Protein concentrations of samples were determined from a standard curve prepared in a similar manner using known concentrations of bovine serum albumin (BSA) and Microsoft excel software. Thereby, the volume of sample needed to give 30µg of protein could be calculated.

2.5.3 Western blotting

This was based on the method described by Shapiro and Maizel (1969).
Samples of known protein concentration (typically containing 30µg of protein) were combined with SDS loading buffer (unless otherwise stated) to give a final 1x concentration of SDS. They were then boiled for 5 minutes prior to loading onto a polyacrylamide gel consisting of a 5% stacking gel and 8, 10, 12 or 15% denaturing running gel, dependent upon the molecular weight of the protein of interest. Five µl of molecular weight protein ladder was also loaded. The samples were electrophoresed in 1x western running buffer at 120V for approximately 1 hour using the Bio-Rad vertical gel western system before transfer.

The proteins were transferred from the gel in western transfer buffer, using a Bio-Rad wet blotting system onto hybond-N nitrocellulose membrane at 100V for 2 hours, 4°C, or at 30V overnight at room temperature. Once transferred, the membrane was washed in PBST and blocked using 5% non fat milk in PBST or 5% BSA in PBST for 2 hours at room temperature. The membrane was then washed in PBST and the primary antibody added for 2 hours at room temperature, or overnight at 4°C. The primary antibody was diluted in either 5% non fat milk in PBST or 5% BSA in PBST. Following 5 x 5 minute washes in PBST, the appropriate secondary antibody was added for 1 hour at room temperature, diluted to 1:2000 in either 5% non fat milk in PBST or 5% BSA in PBST. The membrane was then washed again for 5 x 5 minutes in PBST.

Proteins were then visualised via chemiluminescence. The membrane was developed in ECL reagent for 1 minute. Excess liquid was drained, before the blot was wrapped

in Saran wrap and placed protein side up into an autoradiographic cassette. The membrane was exposed to ECL-hyperfilm and the blot developed in the dark using an X-ograph automated developer. Initial exposure time was 2 minutes, and if necessary this was repeated with longer or shorter exposure times.

The density of all bands was in the linear range of the film as determined via a standard curve. Pixel density was as determined using the Quantity One analysis software (BioRad).

2.5.3.1 Stripping and re-probing with actin

This was performed to demonstrate even protein loading. To re-probe blots with a loading control, membranes were washed for 5 minutes in PBST x2, and then placed in 50ml stripping buffer at 60°C in a shaking water bath for 45 minutes. The membranes were then washed x2 in PBST. The blots were then placed in blocking buffer for 2 hours at room temperature, or overnight at 4°C. The blot was covered with actin primary antibody, dilute to 1:1000 in blocking solution, and incubated for 2 hours at room temperature. Five x 5 minute washes were PBST were carried out, followed by a 1 hour incubation with the appropriate secondary antibody (anti-goat), diluted to 1:2000 in blocking solution. Five x 5 minute washes with PBST were performed, following which the membrane was developed as before.

2.5.3.2 Antibody conditions

All membranes were blocked in 5% milk in PBST, with primary antibodies diluted in 5% powdered BSA in PBST, and secondary antibodies diluted to 1:2000 in 5% milk in PBST. Primary antibody dilutions are shown in table 2.3.

Table 2.3 – Primary antibodies: conditions for Western blotting

1° Antibody	2° Antibody	Dilution	Protein Molecular Weight (kDa)
Notch-1	Rabbit	1:1000	110
Notch-3	Rabbit	1:500	120
Notch-4	Rabbit	1:500	60
HES-1	Rabbit	1:1000	34
HEY-1	Rabbit	1:2000	34

2.5.4 Transfection with siRNA

Cells were routinely passaged, then $1x10^6$ cells were plated on to 10cm plates in 10ml of medium containing FCS, and left to adhere overnight. Following cell adherence, medium was replaced with 7ml of fresh medium containing FCS. In RNase-free conditions, 30µl of Lipofectamine 2000 was added to 1500µl of Opti-MEM tissue culture medium (FCS-free). Five µl of siRNA was added to 1500µl of Opti-MEM tissue culture medium (FCS-free). These were both incubated for 5 minutes at room temperature, before adding the Lipofectamine-Opti-MEM mixture to the siRNA-Opti-MEM and gently mixing. This was then incubated for 20 minutes at room temperature to allow the transfection complexes to form. Following this, the transfection complexes were gently dropped on to the 10cm plates and mixed by gently swilling the plates, before incubating them for 24 hours in normal culture conditions. The medium was changed at 24 hours following transfection and replaced with tissue culture medium containing FCS appropriate to the cell line. Control cells were transfected in the same manner with control siRNA (scrambled sequence). Cells were then lysed/analysed at the desired time points.

All transfection experiments included an untreated control, a lipofectamine only sample, a sample transfected with control siRNA, and an experimental sample transfected with the desired siRNA. Western blots were included in all experiments to confirm siRNA knockdown.

Volumes of reagents were altered accordingly for experiments performed in plates smaller than 10cm (Table 2.4).

Table 2.4 – Volumes of reagents for transfection experiments

		10cm	**6-well**	**12-well**	**96-well**
Cell number		$1x10^6$	$1.7x10^5$	$6.7x10^4$	$5x10^3$
Medium		12ml	2ml	0.8ml	100µl
siRNA mix	OptiMEM	1500µl	250µl	100µl	25µl
	siRNA	600pmol	100pmol	40pmol	5pmol
Lipofectamine	OptiMEM	1500µl	250µl	100µl	25µl
mix	Lipo	30µl	5µl	2.0µl	0.25µl

2.5.6 Assessment of cell proliferation

2.5.6.1 Cell proliferation

Cells were seeded on 6-well plates at a density of 5,000 cells/well and allowed to adhere overnight, before being treated. To estimate the effect on proliferation of each cell line, each experiment consisted of an untreated control and a DMSO control, as well as cells treated with the agents under investigation.

Cells were then harvested at desired time points by trypsination, and 1.0ml of a single cell suspension was diluted with 9.0ml of Isoton buffer. Cells were counted using a ZM particle counter (Beckman Coulter, High Wycombe, UK). Experiments were performed in duplicate on three separate occasions to construct growth curves.

2.5.6.2 Cell recoverability following treatment with GSI-I

Cells were seeded at a density of 5,000 per well on 6-well plates and allowed to adhere overnight before treatment with GSI-I for 24 hours. The cells were then maintained in treated medium, or washed and replenished with fresh untreated medium and cultured for 120 hours. Following this, they were harvested and counted as for the growth curves.

2.5.6.3 Cell cycle analysis

This was based on the method described by Omerod (1990).

Flow cytometry of propidium iodide (PI) stained cells gives a measure of the number of cells within each phase of the cell cycle. Propidium iodide intercalates with DNA, and the fluorescent staining of cells is therefore directly proportional to the total amount of DNA present, which will double during S phase.

Cells were plated onto 6-wells plates at $2x10^5$ cells/well, left to adhere, before being left in FCS-free medium overnight to synchronise. They were then treated with appropriate concentrations of agents for varying periods, or transfected with siRNA. Adherent cells were washed in PBS x2, and then trypsinised. The trypsin was neutralised by addition of culture medium containing 10% FCS. The suspension was pelleted, the medium discarded, and washed x2 in PBS. The cells were then

resuspended in 200µl PBS. Cells were fixed by addition of 2ml ice cold 70% ethanol whilst vortexing vigorously and incubated at 4°C for a minimum of 2 hours. The fixed cells could be stored at 4°C for up to 1 week prior to analysis. Cells were pelleted by centrifugation at 600xg for 10 minutes and resuspended in 800µl PBS, whereupon RNase and PI were added to final concentrations of 10µg/ml and 5µg/ml respectively. The cells were incubated at 4°C overnight before analysis of DNA content was carried out using the Becton Dickinson FACscan apparatus and Cell Quest software. Subsequent data analysis was performed using Modfit LT software.

2.5.7 Assessment of cell viability and apoptosis

2.5.7.1 ATP quantification

ATP quantification was performed using the ATP-lite luminescence assay. ATP can be used as a marker for cell viability because it is present in all metabolically active cells and the concentrations declines very rapidly when the cells undergo apoptosis or necrosis. The assay is based upon the production of light caused by the reaction of ATP with D-luciferin and luciferase:

$$\text{ATP + D-luciferin} \xrightarrow[Mg^{2+}]{\text{LUCIFERASE}} \text{Oxyluciferin + AMP + } PP_i + CO_2 + \text{Light}$$

Emitted light is proportional to ATP concentration within certain limits.

Cells were seeded at 5,000 or 10,000 per well on 96-well plates (white ViewPlate, Perkin-Elmer) and left to adhere overnight, prior to treatment. Each well contained a

total volume of 100µl during treatment. The assay was performed following the desired treatment period.

All reagents were allowed to equilibrate to room temperature prior to use. Five ml of substrate buffer solution was added to 1 vial of lyophilised substrate solution (D-luciferin and luciferase) and gently agitated until homogenous. Fifty µl of mammalian cell lysis solution was added to each well, followed by 50µl of substrate solution. Plates then underwent dark-adaption on a plate shaker for 10 minutes before luminescence was read on a Fluostar Optima (BMG Labtech, Offenberg, Germany). Luminescence was proportional to ATP levels and expressed as fold change from DMSO controls. All values were normalised to a blank control (DMSO treated medium and ATP reagents).

2.5.7.2 Annexin V/PI staining for apoptosis and cell death

This was based on the method described by Vermes *et al*. (1995).

This protocol allows determination of live, apoptotic and necrotic populations of cells using PI and an annexin V FITC conjugate. Live cells that have not been committed to the apoptotic process take up neither annexin V nor PI. When cells begin to apoptose, they undergo cell membrane perturbations that result in the inner leaflet, which is rich in phosphatidylserine, flipping to the outside of the membrane. Annexin V staining allows apoptotic and necrotic cells to be distinguished from live cells due to its ability to bind to phosphatidylserine. Necrotic cells are distinguished from apoptotic cells via PI uptake into the nucleus.

Cells were plated onto 6-well plates at $8x10^4$ cells/well, left to adhere overnight, and then treated.

Following treatment, culture medium containing floating cells was reserved, whilst adherent cells were washed in PBS x2, then trypsinised for as brief a time as possible. Trypsin was then neutralised with medium containing 10% FCS and combined with the floating cell fraction. The cells were pelleted for 5 minutes at 350xg at 4°C, and resuspended in 4ml of fresh medium containing 10% FCS. The cells were incubated at 37°C for 30 minutes. The cells were then pelleted for 5 minutes at 350xg at 4°C, the medium discarded, and the cells resuspended in 1ml of annexin buffer. Five µl of annexin V FITC conjugate was added to the cell suspension and incubated at room temperature for 10 minutes, before addition of PI to a final concentration of 1.5µg/ml and vortexing. After 1 minute incubation at room temperature, the cells were placed on ice and the apoptotic status of the cells determined on the FACscan, using the Cell Quest software.

2.5.7.3 Caspase 3/7 activity

Caspase activity assay was performed using the Caspase-Glo 3/7 assay system (Promega), a luminescent assay which measures caspase 3 and 7 activities, as described previously (Howells *et al.*, 2007). Caspase 3 and 7 are members of the cysteine aspartic acid-specific protease family and play a key effector role in apoptosis (Nicholson and Thornberry, 1997).

Cells were seeded at $1x10^4$ cells per well on a white 96-well plate (ViewPlate, Perkin-Elmer) and left to adhere overnight. Medium was removed and replaced with 50µl of

fresh medium containing appropriate concentrations of treatment agents and incubated for designated times.

All reagents were equilibrated at room temperature prior to use. Caspase 3/7 buffer was added to Caspase 3/7 substrate and mixed by inverting until dissolved. Fifty µl of this was added to each well and the plate sealed. Plates were agitated for 30 seconds on a plate mixer and incubated in the dark at room temperature for 1 hour, prior to reading luminescence on a Fluostar Optima (BMG Labtech, Offenberg, Germany). Luminescence was proportional to caspase activity and expressed as fold change from DMSO controls. All values were normalised to a blank control (DMSO treated medium and Caspase3/7 reagent).

2.6 MICROARRAY ANALYSIS OF CHANGES IN GENE EXPRESSION

2.6.1 Preparation of cells and RNA extraction

Nine medium flasks of AsPC-1 cells were grown from 3 separate batches of cells to a final confluence of no more than 60%. Cells were then routinely passaged. Cells ($5x10^6$) were counted and seeded into nine medium flasks with 10ml of RPMI medium + 10% FCS. These were incubated overnight and left to adhere. Cells were then treated with 5μM of GSI-I in 10mls of medium for 12 and 24 hours, or as a DMSO control. Treatments were performed in triplicate, giving nine flasks.

2.6.1.1 Preparation of RNA

The following steps were performed under strict RNase-free conditions.
The nine flasks were then routinely passaged and $5x10^6$ cells from each flask reserved in 15ml RNase-free centrifuge tubes. The cells were then pelleted for 10 minutes at 12,000 rpm and the medium aspirated, leaving the cell pellet for RNA isolation.

RNA was isolated using the Qiagen RNeasy kit and the kit protocol followed (a brief summary is given below). All stages are performed at room temperature.

The cell pellets were loosened and 600μl of Buffer RLT containing 6μl of β-mercaptoethanol added and vortexed. Cells were homogenised by passing 10x through a 23G needle fitted to an RNase-free syringe. 600μl of 70% ethanol (diluted in RNase-free dH_2O) was added and mixed by pipetting.

A 600µl aliquot of the cell solution was transferred to an RNeasy spin column contained in a 2ml collection tube and centrifuged for 30 seconds at 12,000 rpm. The flow-through was discarded. The process was repeated for the remaining 600µl of cell solution in the same spin column. Buffer RW1 (700µl) was added to the spin column, centrifuged for 30 seconds at 12,000 rpm, and the flow-through discarded. Buffer RPE (500µl, previously diluted 1 in 5 with 100% ethanol) was added to the spin column, centrifuged for 30 seconds at 12,000 rpm, and the flow-through discarded. This was repeated with another 500µl of Buffer RPE. The spin column was placed over a fresh 2ml collection tube and centrifuged for 1 minute at 12,000 rpm to eliminate residual buffer.

The spin column was transferred to a fresh 2ml collection tube and the RNA eluted from the column by centrifugation (1 minute at 12,000 rpm) using two aliquots of 40µl RNase-free dH_2O. RNA purification was determined (see 2.9.3) and the RNA stored at -70°C until microarray analysis.

2.6.1.2 Determination of RNA purification

The concentration of RNA can be determined by measuring the absorbance at 260 nm (A_{260}) in a spectrophotometer. An absorbance of 1 unit at 260 nm corresponds to 40µg of RNA per ml. The ratio of the readings at 260 nm and 280 nm (A_{260}/A_{280}) provides an estimate of the purity of RNA with respect to contaminants that absorb in the UV, such as protein. Pure RNA has an A_{260}/A_{280} ratio of 1.9-2.1.

Ten µl of RNA eluant was added to 90µl RNase-free dH_2O, in a curvette, and the absorbance at 260 nm and 280 nm measured in a spectrophotometer (zeroed using RNase-free dH_2O).

2.6.2 RNA target preparation for microarray analysis

RNA target preparation was performed using GeneChip® Eurkaryotic Poly-A RNA Control Kit, GeneChip® Expression 3'-Amplification Reagents One-Cycle cDNA Synthesis Kit, GeneChip® Expression 3'-Amplification Reagents for IVT (*In Vitro* Transcription) Labelling, GeneChip® 3'-Amplification Reagents Hybridization Control Kit, GeneChip® Hybridization, Wash and Stain Kit(Affymetrix) following the manufacturer's instructions. These are briefly detailed below. At each step all reagents were mixed by flicking the tube, followed by brief centrifugation to collect liquid in the bottom of the tube unless stated otherwise.

2.6.2.1 First strand cDNA synthesis

Five µg of RNA sample was mixed with 2µl of T7-Oligo(dT) Primer, 2µl of diluted poly-A RNA controls, made up to 12µl with RNase-free dH_2O to create the primer mix. *In vitro* synthesised polyadenylated (poly-A) transcripts of *B.subtilis* genes not present in eukaryotic samples (*lys*, *phe*, *thr*, and *dap*) were spiked into the RNA samples to provide exogenous controls. These were diluted in poly-A control dilution buffer in serial dilutions to give a 1:10,000 final dilution, 2µl of which was added to the mix. This was incubated for 10 minutes at 70°C, and then cooled for 2 minutes at 4°C.

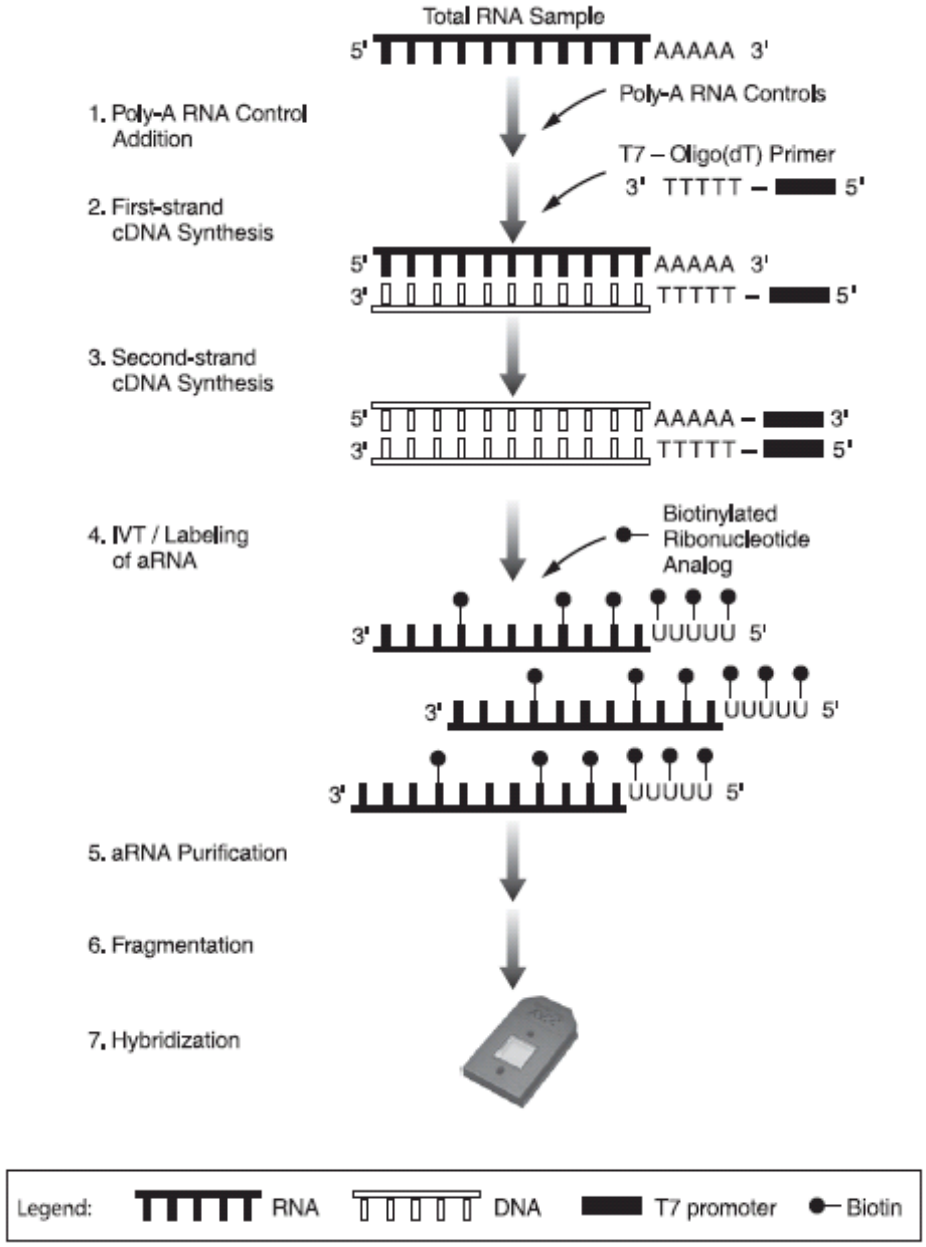

Figure 2.2 – Schematic diagram of microarray analysis
Adapted from manufacturer's handbook

The first-strand mix (4µl 1st strand reaction mix, 2µl 0.1M DTT, 1µl 10mM dNTP) was added to the primer mix and incubated at 42°C for 2 minutes. One µl Superscript II was added and incubated for 1 hours at 42°C, before cooling for 2 minutes at 4°C.

2.6.2.2 Second strand cDNA synthesis

The second-strand mix (91µl RNase-free dH_20, 30µl 5x2nd strand mix, 3µl 10mM dNTP, 1µl *E.coli* DNA ligase, 4µl *E.coli* DNA polymerase I, 1µl RNase H) was added to the first-strand mix and incubated for 2 hours at 16°C. Two µl T4 DNA polymerase was then added and incubated for 5 minutes at 16°C, before adding 10µl 0.5M EDTA.

2.6.2.3 cDNA clean-up

cDNA binding buffer (600µl) was added to the double-stranded cDNA mix and vortexed. Then 400µl was added to a cDNA clean-up spin column in a collection tube, centrifuged for 1 minute at 12,000 rpm, and flow-through discarded. This was repeated in the same column for the remaining mix. cDNA wash buffer (750µl) was added to the column over a fresh collection tube, centrifuged for 1 minute, and flow-through discarded. The columns were dried by centrifugation for 5 minutes at maximum speed with the cap open. Columns were then placed over fresh collection tubes and 14µl of cDNA elution buffer added to the spin column membrane. This was incubated for 1 minute at room temperature, before centrifugation for 1 minute at maximum speed.

2.6.2.4 Synthesis of biotin-labelled cRNA

The eluted cDNA was added to an RNase-free microfuge tube and the following added: 4µl 10x IVT labelling buffer, 12µl IVT labelling NTP mix, 4µl IVT labelling enzyme mix, RNase-free dH_2O to a total volume of 40µl. This was incubated for 16 hours at 37°C.

2.6.2.5 Clean-up and quantification of biotin-labelled cRNA

Sixty µl RNase-free dH2O was added with vortexing for 3 seconds, followed by 350µl IVT cRNA binding buffer, and further 3 seconds vortexing. Ethanol (250µl) was added and mixed by pipetting. The sample (700µl) was then applied to a cRNA clean-up spin column in a collection tube, centrifuged for 15 seconds at 12,000 rpm, and collection tube and flow-through discarded. IVT cRNA wash buffer (500µl) was added to the spin column, centrifuged over a new collection tube for 15 seconds at 12,000 rpm, and flow-through discarded. Then 500µl 80% ethanol (in RNase-free dH_2O) was added to the column, centrifuged and flow-through discarded. The spin column was then dried by centrifugation for 5 minutes at maximum speed with the cap open. The cRNA was then eluted using 11µl of RNase-free dH_2O applied to the column membrane and centrifuged for 1 minute at maximum speed. This was repeated with 10µl of RNase-free dH_2O.

cRNA was then quantified using an Agilent 2100 Bioanalyzer (Agilent Technologies, West Lothian, U.K.) and RNA Nano LabChip (Agilent Technologies) and the adjusted cRNA yield calculated to reflect carryover of unlabelled total RNA.

$$\textbf{Adjusted cRNA yield} = \mathbf{RNA_m - (RNA_i)(y)}$$

RNA_m = amount of cRNA (µg)

RNA_i = starting amount of total RNA (µg)

Y = fraction of cDNA reaction used in IVT

2.6.2.6 Fragmentation of cRNA

Twenty µg of cRNA (adjusted yield) was added to 8µl of 5x fragmentation buffer and RNAase-free dH_2O to a total volume of 40µl, incubated at 94°C for 35 minutes, then placed on ice. This fragmented full-length cRNA to 35-200 base fragments by metal-induced hydrolysis prior to hybridisation. The cRNA was then analysed on the Bioanalyzer to quantitate and ensure sufficient fragmentation.

2.6.3 Hybridisation

MES stock buffer (12x) and 2x Hybridisation buffer were made fresh (see 2.2).

A hybridisation cocktail was made of 15µg of fragmented cRNA, 5µl 3nM Control Oligonucleotide B2, 15µl 20x Eukaryotic Hybridisation controls, 3µl 10mg/ml Herring sperm DNA, 3µl 50mg/ml BSA, 150µl 2x Hybridisation buffer, 30µl DMSO, RNase-free dH_2O to a final volume of 300µl. This was heated for 5 minutes at 99°C. The Eukaryotic Hybridisation controls were heated for 5 minutes at 65°C to resuspend the cRNA prior to aliquotting.

The GeneChip® Human Genome U133 Plus 2.0 arrays were allowed to equilibrate to room temperature, then filled with 200µl 1x Hybridisation buffer and incubated in the hybridisation oven (640, Affymetrix) at 45°C for 10 minutes with rotation.

Hybidisation cocktail was heated at 45°C for 5 minutes, and then centrifuged for 5 minutes at maximum speed to remove insoluble material. The hybridisation buffer was removed from the array cartridges, and then they were filled with 200µl of hybridisation cocktail, avoiding insoluble material. The arrays were then placed in the hybridisation oven at 45°C for 16 hours and 60 rpm rotation.

2.6.4 Washing and staining

Wash buffers A and B, and 2x Stain buffer were made up fresh (see 2.2). Fifty mg goat IgG stock was resuspended in 5ml 150mM NaCl. SAPE stain solution was made up fresh and kept on ice in black eppendorps (see 2.2). For each array 1200µl was made up and split into two 600µl aliquots. The antibody solution mix was made up fresh (600µl per array) in eppendorps (see 2.2).

After hybridisation, the hybridisation cocktail was removed and replaced with 200µl of wash buffer A and the arrays were placed in the fluidics station. Washing and staining of the arrays was performed using the Affymetrix fluidics station 200, operated using the Microarray suite. The fluidics station was primed prior to use and wash buffers A and B placed in buffer reservoir A and B respectively. The automatic wash and staining sequence is given below:

- Wash 1 – 10 cycles of 2 mixes per cycle with wash buffer A at 25°C
- Wash 2 – 4 cycles of 15 mixes per cycle with wash buffer B at 50°C
- Stain – 10 minutes in SAPE solution at 25°C
- Post-stain wash – 10 cycles of 4 mixes per cycle with wash buffer A at 25°C
- 2nd Stain – 10 minutes in antibody solution at 25°C
- 3rd Stain – 10 minutes in SAPE solution at 25°C
- Final wash – 15 cycles of 4 mixes per cycle with wash buffer A at 30°C

The array cartridges were then ejected from the fluidics station and any bubbles removed by filling with additional wash buffer A.

2.6.5 Scanning arrays

The probe arrays were scanned using the Affymetrix GeneChip® Scanner 3000 (Affymetrix), controlled using the Microarray Suite.

2.6.6 Data analysis

Microarray data were analysed using the GeneSifter™ software (Geospitza Inc, Seattle, USA) and Microsoft Excel. The relative expression level of each gene was determined by comparing the signal intensity of each gene in the array after correction for background and normalisation. The expression profiles were then compared between treatment groups using the Student *t* test for unpaired data (controlling the false discovery rate using the Benjamini-Hochberg multiple comparisons procedure; Benjamini and Hochberg, 1995). Adjusted P values <0.05 were considered significant.

2.7 METHODS – MASS SPECTROMETRY

2.7.1 Solid phase extraction

Oasis® HLB columns (Waters, 30mg, 1cc) were mounted on a vacuum manifold, which was maintained at a pressure of approximately 20kPa. Each sample was mixed with an equal volume of 4% phosphoric acid, and left on ice for 1 hour. Columns were primed with 1ml of HPLC methanol, and washed with 1ml of HPLC water, before applying the samples. After washing the columns with HPLC water (1ml), samples were eluted using 1ml of 40% acetonitrile in 0.1% trifluoroacetic acid (TFA). Elutions were reduced in a centrifugal evaporator for 40 minutes, and then freeze-dried. Samples were stored at -80°C, and reconstituted in 100µl ammonium bicarbonate ph 7.4 prior to analysis.

2.7.2 Size-exclusion filtration

Microcon® filters (10,000 Da molecular weight cut off) were twice washed with 500µl HPLC water (14000g at 4°C) for 20 minutes. Samples were then passed through the prepared filter devices for 45 minutes. Samples were then refrigerated at -20°C until required for immunoprecipitation.

2.7.3 Sample preparation for Mass Spectrometry

Prior to analysis samples were acidified with an equal volume of 0.1% TFA and then mixed 1:1 with matrix (α-cyano-4-hydroxy-cinnamic acid dissolved in acetonitrile/methanol (50:50, v/v, 2mg/ml).

2.7.4 Mass Spectrometry

Analysis was conducted using a Q-Tof Ultima Global instrument (Waters, Manchester, UK) in positive ionisation mode. Each well on the MALDI target plate (12 x 1wells, Waters, Manchester, UK) was spotted with 1µl of sample, then air dried. Each spot received 100 laser ablations. Analysis of the sample produced a graph of intensity against mass/charge ratio (detection range 800-3000 m/z). For method validation, 2 spots were analysed for each sample, and for the main study, 4 spots were analysed. Mass Lynx software (Version 4.1, Waters, Manchester, UK) was used to process the data.

2.8 STATISTICAL ANALYSIS

All statistical analyses were performed using Statistical Package for the Social Sciences 18.0® (SPSS, Chicago, Illinois, USA). In order to look for associations between different proteins, the percentages of tumour stained were compared using Spearman's correlation coefficient. Results from this test produced a correlation coefficient, indicating the strength of the association and a P value indicating significance. Chi-squared and Fisher's exact tests were used to analyse categorical data. The Mann-Whitney U test was used to compare continuous variables between independent groups, with the Wilcoxon test used to compare continuous variables between related groups. Where greater than two independent groups were compared, these were first analysed using the Kruskal-Wallis test, followed by the Mann-Whitney test to determine where significant difference occurred. Univariate prognostic significance of variables was determined by means of univariate Cox regression analysis, Kaplan-Meier analysis and application of the log-rank test. Multivariable analysis was performed using all variables with $P<0.10$ on univariate analysis, through their entry into a Cox proportional hazards regression analysis using a stepwise backward procedure. Statistical significance for all tests was defined as $P<0.05$. All statistical techniques employed in the study were approved by Dr John Bankart (Department of Health Sciences, University of Leicester) and have been employed previously by CDM for similar analyses in peer-review publications (Mann *et al.*, 2007, 2007a, 2009; Doucas *et al*., 2008; Neal *et al.*, 2011).

CHAPTER 3

NOTCH EXPRESSION IN PANCREATIC ADENOCARCINOMA *IN VIVO*

3.1 INTRODUCTION

Pancreatic ductal adenocarcinoma is associated with a poor prognosis, due to its late presentation, and aggressive invasive and metastatic potential. The ability to determine the prognosis and recurrence risk for individual patients with pancreatic carcinoma would help guide surgical and chemotherapeutic treatment according to individual risk. To this end, several markers have previously been investigated in this disease. Various possible prognostic markers of survival have been identified, including socio-economic status (Lim *et al*, 2003; Cress *et al*, 2006), operative factors (Benassai *et al*, 2000; Wagner *et al*, 2004; Sohn *et al*, 2000), and tumour characteristics, including tumour size, perineural invasion, microvascular invasion, local lymph node metastases, resection margin status, and tumour differentiation (Sohn *et al*, 2000; Neoptolemos *et al*, 2001; Wagner *et al*, 2004; Kuhlmann *et al*, 2004; Garcea *et al*, 2007). Serum tumour markers, in particular CA 19.9, have also been evaluated and found to be predictive of prognosis (Ferrone *et al*, 2006). Recently attention has turned towards the prognostic value of serum markers of inflammation, the basis of which being that it is not only the intrinsic properties of the tumour cells that determine tumour progression, but also that of the host inflammatory response (Coussens and Werb, 2002). Pre-operative serum C-reactive protein (Jamieson *et al*, 2005) and neutrophil-lymphocyte ratio (NLR) (Bhatti *et al*, 2010; Garcea *et al*, 2010) have both been found to independently predict prognosis following resection of pancreatic adenocarcinoma.

Molecular biomarkers are attractive diagnostic and prognostic indicators. In addition biomarkers that display prognostic significance offer the potential as novel therapeutic targets. Multiple molecular markers have been found to be associated with prognosis in pancreatic adenocarcinoma, including tumour suppressor genes, apoptotic proteins, growth

factors and receptors, matrix metalloproteinases and angiogenic proteins and receptors (reviewed in Garcea *et al*, 2005 and Ansari *et al*, 2011). Molecular biomarkers may be derived from resected tissue specimens or biopsies, potentially allowing prognostication or predicting response to treatment. In addition the presence of these markers in surrogate tissues such as serum, faeces or bile, may allow monitoring of disease progression or response to chemotherapy, as well as aiding earlier initial diagnosis or even providing a screening tool.

Whilst it has been previously demonstrated that the Notch pathway is up-regulated in pancreatic carcinoma (Miyamoto *et al*, 2003; Buchler *et al*, 2005; Doucas *et al*, 2008), no data exist examining the role of Notch in the progression of the disease or relation to tumour phenotype. The experiments in this chapter will, for the first time, examine the expression of Notch pathway constituents in pancreatic adenocarcinoma, with particular reference to disease progression. In addition the relationships between individual Notch proteins will be assessed. Notch expression will be also be correlated with clinicopathological characteristics and prognosis, associations that have yet to be examined in pancreatic adenocarcinoma.

3.2 PATIENT DEMOGRAPHICS

Local ethical committee approval (REC 7176) was obtained to use both archival tissue and freshly collected specimens from patients with pancreatic adenocarcinoma undergoing surgery or biopsy. These patients were identified from the University Hospitals of Leicester MDT database. Written consent was obtained for the study. Data were obtained from patient case notes, pathology and radiology computer systems. Survival status was determined by analysing hospital records and General Practitioner records. Demographic, operative and histology data were collected, in addition to performing immunohistochemistry on tissue specimens.

Patients with resectable pancreatic head tumours underwent a pancreaticoduodenectomy (either standard or pylorus-preserving) with an isolated Roux-en-Y pancreaticojejunostomy. Those with pancreatic tail tumours underwent distal pancreatectomy. Patients with positive intra-operative pancreatic resection margins proceeded to a total pancreatectomy. Where curative resection was not deemed feasible, patients underwent a combined hepaticojejunostomy-en-Y and gastrojejunostomy for palliation (Biliary bypass).

3.2.1 Resected group

Forty-two patients who underwent potentially curative resection of pancreatic adenocarcinoma between October 2000 and May 2007 were included in this study. Patients with ampullary tumours and distal cholangiocarcinomas were excluded. Pancreatic adenocarcinoma tissue was available from all patients. In addition, background uninvolved pancreatic tissue was available in 35 patients, and involved local lymph nodes in 16 patients.

Clinicopathological data for these patients are displayed in Table 3.1. Twenty-four (57.1%) were male and 18 (42.9%) were female, with a median age of 64 years (range 30-80 years) at the time of surgery. Thirty-six patients (85.7%) underwent pancreaticoduodenectomy for tumour of the pancreatic head, 4 patients (9.5%) underwent distal pancreatectomy for tumours of the pancreatic tail, and 2 patients (4.8%) underwent total pancreatectomy for positive intra-operative resection margins on frozen section. Twelve patients (28.6%) underwent pre-operative stenting via ERCP.

Histopathological characteristics

The median tumour size on histology was 29mm (range 10-50mm). Four tumours (9.5%) were well differentiated, 19 (45.2%) moderately differentiated, and 18 (42.9%) were poorly differentiated. A median of 9.5 lymph nodes (range 1-32) were recovered in the resected specimen, with 20 patients (47.6%) having clear lymph nodes and 22 patients (52.4%) lymph node metastases. Of those with positive lymph nodes, a median of 2 nodes contained metastatic tumour (range 1-8), yielding a median of 33.3% (range 10-100%). Microvascular invasion was identified in 33.3% of tumours (n=14) and perineural infiltration in 66.7% (n=28). A R_0 resection (negative resection margin) was achieved in 64.3% of patients.

3.2.2 Unresectable group

Fifty patients in whom tumour tissue samples were collected for unresectable pancreatic adenocarcinoma between January 2003 and January 2007 were included in this study. Twenty-one (42%) were male and 29 (58%) were female, with a median age of 68.4 years (range 43.9-80.9 years). Twenty-six were unresectable based upon locally advanced disease or vascular involvement therefore tissue was from the pancreatic primary, and 24 had

metastatic disease. Of these, 14 had tissue from liver metastases, 8 peritoneal disease and 2 distant involved lymph nodes.

3.2.3 Long-term survival

Patient survival was updated as of 1st January 2011. In patients undergoing potentially curative resection, median follow-up was 30.6 months (mean 40.1 months, range 1-122 months) with no patient lost to follow-up. As of January 2011, seven patients (16.7%) were alive, four of whom were disease-free. Two patients died of unrelated illnesses. A total of 36 patients (88%) had developed recurrent disease at follow-up. The overall median survival was 30.5 months (95% confidence interval (CI) 29.5-31.5 months), giving 1-year, 3-year and 5-year overall survival rates of 87.5%, 32.5% and 21.3% respectively (Figure 3.1). The disease-free median survival was 25.0 months (95% CI 17.7-32.3 months), giving 1-, 3-, and 5-year disease-free survival rates of 64.1%, 25.6% and 16.6% respectively. Median survival following detection of recurrent disease was 5.2 months (range 0.3-36.0 months).

In patients with unresectable tumours and who therefore received palliative treatment, with or without palliative chemotherapy, median follow-up was 5.9 months (mean 6.9 months, range 1.0-18.2 months). As of January 2011, all patients had died. The overall median survival was 5.9 months (95% CI 3.4-8.4 months) giving 6- and 12-month survival rates of 48.9% and 17.0% ($p<0.0001$ vs. resectable overall survival (log rank test), Figure 3.1).

Table 3.1 – Clinicopathological data of patients undergoing potentially curative resection for pancreatic adenocarcinoma (n=42)

	Number	%	Median	Range
Gender				
Male	24	57.1	-	-
Female	18	42.9	-	-
Age (years)	-	-	64	30-80
Serology at presentation				
CA 19-9 (U/ml)	-	-	320	3-10,000
Alkaline Phosphatase (IU/L)	-	-	258	39-6881
Alanine transaminase (IU/L)	-	-	91	18-474
Bilirubin (µmol/L)	-	-	146	5-410
WCC ($x10^9$/L)	-	-	7.5	3.8-20.6
Lymphocytes ($x10^9$/L)	-	-	1.5	0.7-3.0
Neutrophils ($x10^9$/L)	-	-	5.0	2.0-16.2
NLR	-	-	3.7	1.1-11.9
Albumin (g/L)	-	-	36	29-47
Creatinine (µmol/L)	-	-	72	49-139
Operative intervention				
Pancreaticoduodenectomy	36	85.7	-	-
Distal pancreatectomy	4	9.5	-	-
Total pancreatectomy	2	4.8	-	-
Tumour characteristics				
Tumour diameter (mm)	-	-	29	10-50
Differentiations				
Well	4	9.5	-	-
Moderate	19	45.2	-	-
Poor	18	42.9	-	-
No data	1	2.4		
Nodal status				
Positive	22	52.4	-	-
Negative	20	47.6	-	-
Microvessel invasion				
Yes	14	33.3	-	-
No	25	59.5	-	-
No data	3	7.1		
Perineural infiltration				
Yes	28	66.7	-	-
No	12	28.6	-	-
No data	2	4.8		
Resection margin				
Positive	15	35.7	-	-
Negative	27	64.3	-	-

WCC, White cell count; NLR, Neutrophil/lymphocyte ratio.

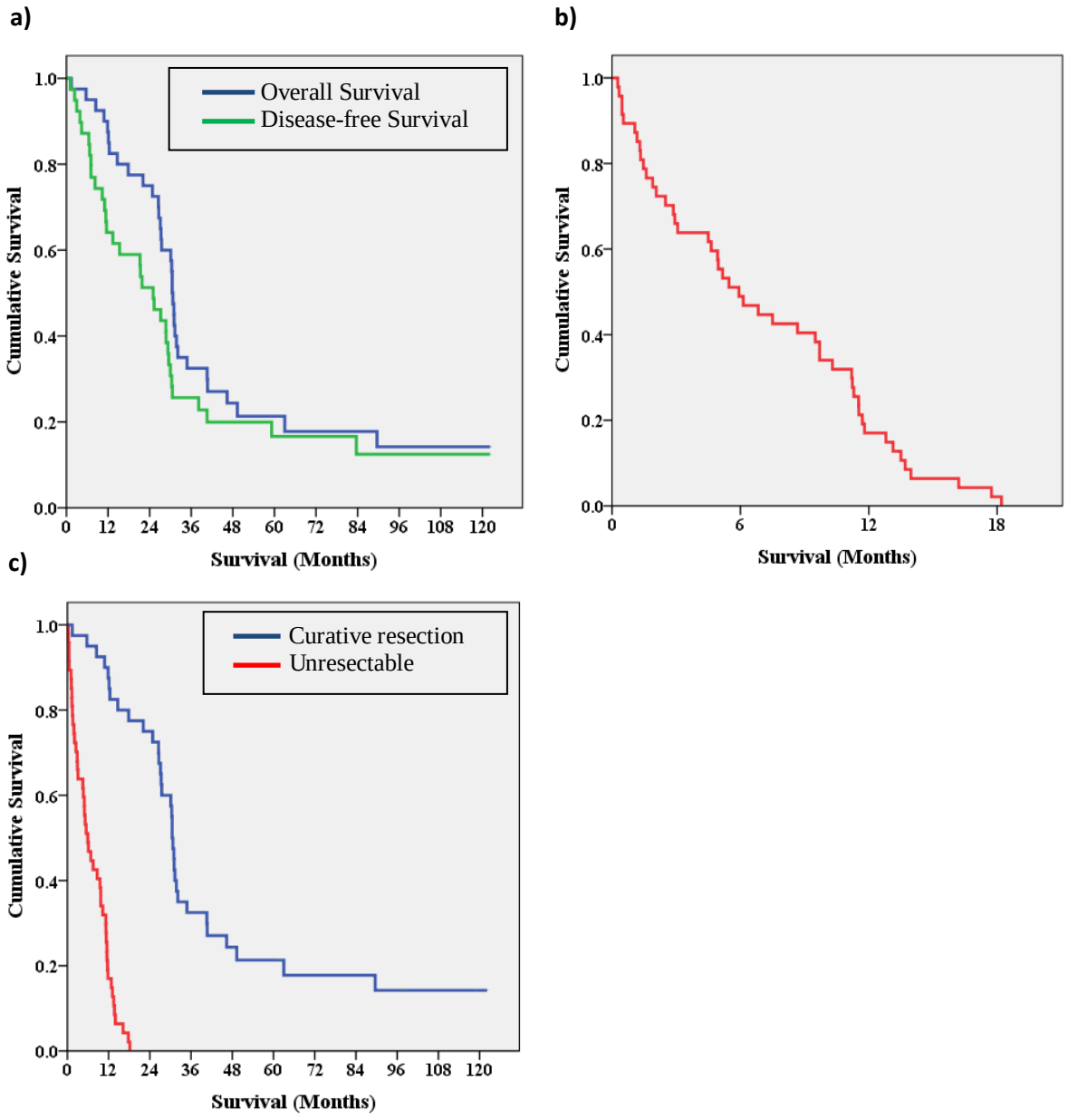

Figure 3.1 – Survival in patients with pancreatic adenocarcinoma
Kaplan Meier curves for a) Overall and disease-free survival in patients undergoing potentially curative resection for pancreatic adenocarcinoma; b) Overall survival for patients undergoing bypass surgery for unresectable pancreatic adenocarcinoma; c) Comparing overall survival for patients undergoing potentially curative resection and unresectable patients ($p<0.001$, log rank test).

3.2.4 Risk factor analysis for factors associated with survival

Univariate and multivariate long-term survival analyses (for overall and disease-free survival) were performed in the absence of biomarker information to provide baseline prognostic information for the study population. Results of univariate analysis for associations with survival in patients undergoing potentially curative resection are shown in Table 3.2. Results of multivariate analyses (including results for all variables entered into the last round of regression analysis) are shown in Table 3.3.

Lymph node involvement, positive resection margins, CA19.9 ≥320 U/ml, and perineural invasion were entered into the regression model for both overall and disease-free survival, with microvascular invasion also entered for overall survival. Lymph node involvement ($p=0.006$) and positive resection margins ($p=0.020$) were found to be independently associated with poor overall survival in patients undergoing resection with curative intent. CA19.9 ($p=0.005$) and perineural invasion ($p=0.016$) were found to be independently associated with reduced disease-free survival. Kaplan-Meier survival curves demonstrating these associations are shown in Figure 3.2. There was no difference in either overall ($p=0.618$) or disease-free survival ($p=0.954$) when patients with head of pancreas adenocarcinomas were compared to those with body/tail tumours, therefore the entire group was used for further survival analysis.

Table 3.2 – Univariate Cox regression survival analyses for all patients undergoing potentially-curative resection for pancreatic adenocarcinoma (n=42).

	Overall Survival		Disease-free Survival	
	Hazard Ratio (95% CI)	**P**	**Hazard Ratio (95% CI)**	**P**
Gender: male/female	0.702 (0.351-1.404)	0.317	0.913 (0.457-1.825)	0.797
Age: ≥64/<64 years	0.899 (0.447-1.809)	0.766	0.972 (0.489-1.933)	0.936
CA19.9 ≥320/<320 (U/ml)	2.828 (1.288-6.212)	**0.010**	2.743 (1.239-6.069)	**0.013**
Alk Phos ≥258/<258 (IU/L)	0.939 (0.457-1.930)	0.864	1.082 (0.529-2.215)	0.829
ALT ≥91/<91 (IU/L)	2.017 (0.442-4.136)	0.155	1.665 (0.812-3.413)	0.164
Bilirubin ≥146/<146 (μmol/L)	1.134 (0.559-2.299)	0.728	1.279 (0.626-2.614)	0.499
WCC: ≥7.5/<7.5 ($x10^9$/L)	0.641 (0.315-1.305)	0.220	0.801 (0.394-1.628)	0.540
Lymphocytes: ≥1.5/<1.5 ($x10^9$/L)	1.040 (0.511-2.114)	0.914	0.998 (0.489-2.039)	0.997
Neutrophils: ≥5.0/<5.0 ($x10^9$/L)	0.657 (0.321-1.342)	0.249	0.780 (0.383-1.588)	0.494
NLR: ≥5/<5	0.862 (0.405-1.836)	0.701	0.744 (0.349-1.590)	0.446
Albumin: ≥36/<36 (g/L)	1.015 (0.494-2.089)	0.967	0.841 (0.411-1.722)	0.637
Creatinine: ≥72/<72 (μmol/L)	0.732 (0.360-1.489)	0.390	0.764 (0.376-1.554)	0.458
Tumour diameter: ≥29/<29 (mm)	0.839 (0.407-1.729)	0.634	0.845 (0.412-1.730)	0.644
Tumour differentiation: poor vs. well/moderate	1.286 (0.616-2.687)	0.503	0.985 (0.477-2.033)	0.967
Nodal status: +/-	3.441 (1.535-7.578)	**0.003**	3.438 (1.566-7.548)	**0.002**
Microvessel invasion: +/-	1.716 (0.921-3.584)	0.100	1.822 (0.874-3.799)	0.109
Perineural invasion: +/-	1.723 (0.890-3.758)	0.098	2.208 (1.001-4.872)	**0.050**
Resection margin: positive/negative	1.536 (1.075-2.193)	**0.018**	1.431 (0.881-2.160)	0.081

WCC, White cell count; ALT, alanine transaminase; NLR, neutrophil/lymphocyte ratio; CI, confidence interval

Table 3.3 – Multivariate Cox regression survival analyses following potentially-curative resection for pancreatic adenocarcinoma (n=42)

	Overall Survival		Disease-free Survival	
	Hazard Ratio (95% CI)	**P**	**Hazard Ratio (95% CI)**	**P**
Nodal status: +/-	3.005 (1.133-7.976)	**0.027**	1.696 (0.599-4.803)	0.320
Resection margin: positive/negative	1.645 (1.104-2.457)	**0.015**		
CA19.9 ≥320/<320 U/ml			3.313 (1.440-7.619)	**0.005**
Perineural invasion: +/-	1.540 (0.586-4.049)	0.381	2.965 (1.224-7.185)	**0.016**

CI, confidence interval

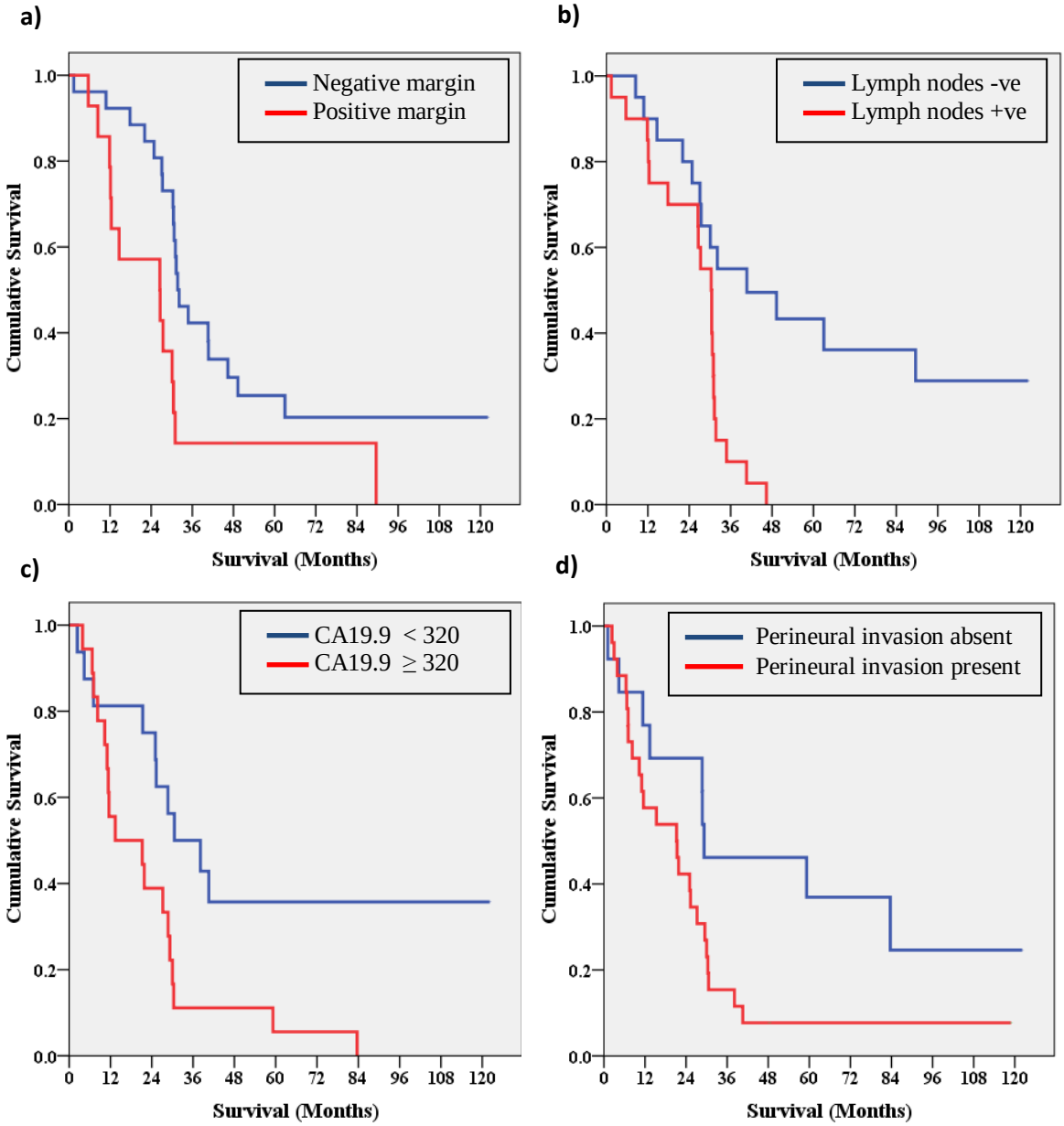

Figure 3.2 – Clinicopathological risk factors of adverse outcome
Kaplan-Meier survival curves for conventional clinicopathological prognostic factors independently associated with overall (a, b) and disease-free (c, d) survival in patients undergoing resection of pancreatic adenocarcinoma with curative intent (n=42): a) Resection margin involvement (p=0.015, log-rank test), b) Lymph node involvement (p=0.002, log-rank test), c) Serum CA19.9 level (p= 0.010, log-rank test), d) Perineural invasion (p=0.045, log-rank test).

3.3 RESULTS

3.3.1 Notch expression

3.3.1.1 Notch-1

Some degree of cytoplasmic Notch-1 staining was identified in the cancer cells of all resected pancreatic cancer specimens (Figure 3.3; Table 3.4). A median of 75% of ductal carcinoma cells scored stained positive for cytoplasmic Notch-1, ranging from 15% to 100%. Cytoplasmic Notch-1 expression was up-regulated in tumour tissue compared to background normal pancreatic tissue in 28 of the 35 patients (80.0%) for whom tissue was available, with a median of 27.5% of normal ductal cells displaying cytoplasmic expression ($p<0.001$ compared to tumour tissue). Nuclear Notch-1 staining, suggesting pathway activation, was not identified in any ductal cells in normal pancreatic tissue, however was identified in cancer cells of 11 patients with resected pancreatic adenocarcinoma (26.2%, $p<0.001$ compared to background pancreas).

Cytoplasmic Notch-1 expression was significantly positively correlated with cytoplasmic HES-1 expression in ductal adenocarcinoma cells ($p=0.020$, Table 3.5). Similarly, nuclear Notch-1 expression and nuclear HES-1 expression were significantly associated ($p=0.013$). Nuclear Notch-1 expression was significantly inversely associated with cytoplasmic Notch-4 expression ($p=0.006$), and cytoplasmic Notch-1 expression was significantly inversely associated with nuclear Notch-4 expression ($p=0.039$). Neither nuclear Notch-1 expression nor cytoplasmic Notch-1 expression were found to be associated with any of the clinicopathological factors investigated, nor to differ with tumour location (Table 3.6).

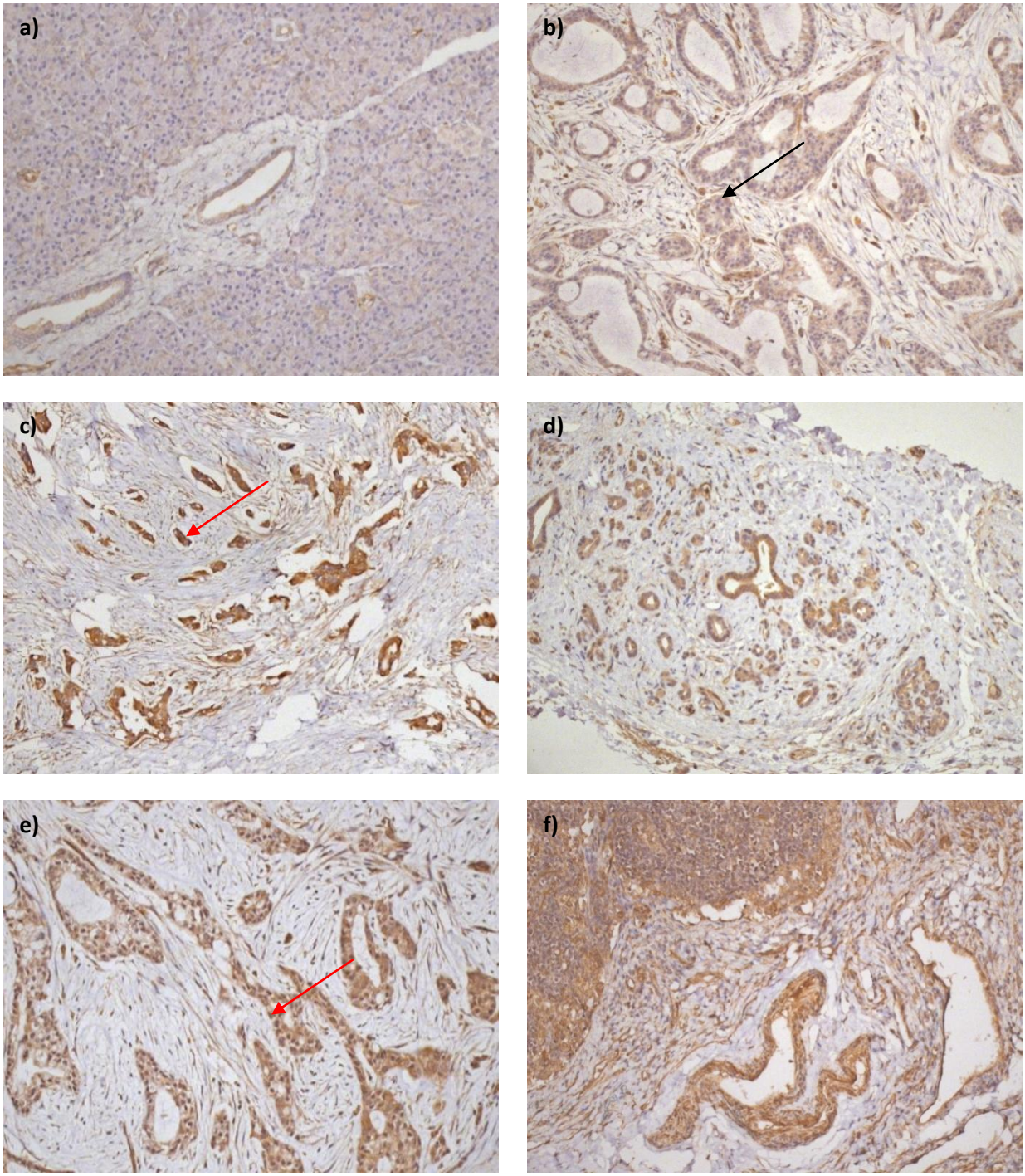

Figure 3.3 – Immunohistochemical expression of Notch-1 in normal pancreas and pancreatic adenocarcinoma
a) Notch-1 expression was detected in the cytoplasm of normal pancreatic ductal epithelium, however no nuclear staining was present; b) resected pancreatic adenocarcinoma specimen demonstrating cytoplasmic staining but negative nuclear staining for Notch-1 (black arrow); c-e) unresectable pancreatic adenocarcinoma displaying strong cytoplasmic Notch-1 staining and positive nuclear staining (red arrows); f) strong cytoplasmic staining and nuclear staining seen in distant lymph node metastases.
(Original magnification, all 20x)

Table 3.4 – Expression of the Notch pathway constituents in normal pancreas, early and advanced pancreatic adenocarcinoma.

		Background pancreas (n=35)	Resectable disease		Advanced disease		
			Pancreatic tissue (n=42)	Local lymph nodes (n=16)	Overall (n=50)	Locally advanced (n=26)	Metastatic (n=24)
Notch-1	Nuclear n(%)	0 (0.0%)	11 (26.2%)*	6 (37.5%)*	35 (70%)*†	16 (61.5%)*†	19 (79.2%)*†
	Cytoplasmic %(range)	27.5% (0-50)	75% (15-100%)*	50% (25-95%)*	30% (5-95%)*†	35% (15-90%)*†	45% (5-65%)*†
Notch-3	Nuclear n(%)	0 (0.0%)	20 (47.6%)*	10 (62.5%)*	45 (90%)*†	23 (88.5%)*†	22 (91.7%)*†
	Cytoplasmic %(range)	30% (0-85)	45% (5-85%)*	45% (30-90%)*	45% (15-90%)*	40% (15-85%)*	65% (20-90%)*δ
Notch-4	Nuclear n(%)	0 (0.0%)	8 (19%)*	3 (18.8%)*	34 (68%)*†	18 (69.2%)*†	16 (66.7%)*†
	Cytoplasmic %(range)	20% (0-50%)	70% (20-95%)*	45% (20-90%)*	40% (5-85%)*†	45% (5-80%)*†	45% (15-85%)*†
HES-1	Nuclear n(%)	8 (22.9%)	33 (78.6%)*	12 (75%)*	50 (100%)*†	26 (100%)*†	24 (100%)*†
	Cytoplasmic %(range)	45% (5-85%)	50% (20-95%)	45% (5-95%)	40% (15-95%)†	42.5% (15-90%)	40% (15-95%)
HEY-1	Nuclear n(%)	0 (0%)	11 (26.2%)*	7 (50%)*	38 (76%)*†	18 (69.2%)*†	20 (83.3%)*†
	Cytoplasmic %(range)	25% (0-45%)	65% (35-100%)*	70% (45-100%)*	70% (50-100%)*	75% (55-100)*	70% (50-100%)*

* $p<0.05$ compared to background pancreas; †$p<0.05$ compared to resectable pancreatic carcinoma tissue; δ$p<0.05$ compared to locally advanced disease

Table 3.5 – Correlations between Notch protein expression in resected pancreatic adenocarcinoma specimens (n = 42).

		Notch-1 nucl	**Notch-1** cyto	**Notch-3** nucl	**Notch-3** cyto	**Notch-4** nucl	**Notch-4** cyto	**HES-1** nucl	**HES-1** cyto	**HEY-1** nucl	**HEY-1** cyto
Notch-1 nucl	Coeff.	1.000	.024	.280	-.129	.179	-.411**	.339*	-.169	.023	.159
	Sig.		.880	.069	.410	.250	**.006**	**.013**	.292	.885	.308
Notch-1 cyto	Coeff.	.024	1.000	.174	.121	-.316*	-.236	-.183	.362*	-.086	.086
	Sig.	.880		.263	.440	**.039**	.128	.247	**.020**	.584	.583
Notch-3 nucl	Coeff.	.380	.174	1.000	.047	.168	.393**	-.023	.164	.493**	.135
	Sig.	.069	.263		.765	.283	**.009**	.884	.306	**.001**	.388
Notch-3 cyto	Coeff.	-.129	.121	.047	1.000	-.003	.157	.290	.269	-.103	.555**
	Sig.	.410	.440	.765		.984	.315	.062	.089	.511	**.000**
Notch-4 nucl	Coeff.	.179	-.316*	3168	-.003	1.000	.049	.157	-.209	.179	-.074
	Sig.	.250	**.039**	.283	.984		.757	.320	.189	.250	.636
Notch-4 cyto	Coeff.	-.411**	-.236	.393**	.157	.049	1.000	.157	-.161	.006	.156
	Sig.	**.006**	.128	**.009**	.315	.757		.320	.315	.967	.319
HES-1 nucl	Coeff.	.339*	-.183	.023	.290	.157	-.201	1.000	.094	-.014	.090
	Sig.	**.013**	.247	.884	.062	.320	.203		.561	.932	.570
HES-1 cyto	Coeff.	-.169	.362*	.164	.269	-.209	-.161	.094	1.000	-.087	.183
	Sig.	.292	**.020**	.306	.089	.189	.315	.561		.590	.252
HEY-1 nucl	Coeff.	.023	-.086	.493**	-.103	.179	.006	-.014	-.087	1.000	-.062
	Sig.	.885	.584	**.001**	.511	.250	.967	.932	.590		.691
HEY-1 cyto	Coeff.	.159	.086	.135	.555**	-.074	.156	.090	.183	-.062	1.000
	Sig.	.308	.583	.388	**.000**	.636	.319	.570	.252	.691	

Nucl, nuclear; cyto, cytoplasmic; coeff, Spearman's rank correlation coefficient; *, correlation is significant at the 0.05 level (2-tailed); **, correlation is significant at the 0.01 level (2-tailed). Significant p-values are in bold.

Table 3.6 – Associations of nuclear and cytoplasmic Notch-1 expression with clinicopathological variables

Factor	Category	Nuclear Notch-1 expression			Cytoplasmic Notch-1 expression	
		Present	Absent	P*	Median (range)	P**
Gender	Male	5	19	0.287	62.5% (30-100%)	0.805
	Female	6	12		77.5% (15-95%)	
Age	≥64 years	5	11	0.407	67.5% (15-100%)	0.242
	<64 years	6	20		75% (25-98%)	
CA19.9	≥320 (U/ml)	7	12	0.251	65% (15-100%)	0.860
	<320 (U/ml)	4	15		75% (25-95%)	
Alk Phos	≥258 (IU/L)	7	14	0.305	75% (15-90%)	0.745
	<258 (IU/L)	4	15		65% (25-100%)	
ALT	≥91 (IU/L)	7	13	0.240	75% (15-90%)	0.598
	<91 (IU/L)	4	16		57.5% (25-100%)	
Bilirubin	≥146 (µmol/L)	5	15	0.500	75% (15-90%)	0.871
	<146 (µmol/L)	6	14		60% (25-100%)	
WCC	≥7.5 ($x10^9$/L)	6	14	0.500	67.5% (16-98%)	0.735
	<7.5 ($x10^9$/L)	5	15		75% (24-91%)	
Lymphocytes	≥1.5 ($x10^9$/L)	6	14	0.500	60% (15-100%)	0.776
	<1.5 ($x10^9$/L)	5	15		75% (35-90%)	
Neutrophils	≥5.0 ($x10^9$/L)	6	14	0.578	65% (15-100%)	0.957
	<5.0 ($x10^9$/L)	5	15		75% (25-90%)	
NLR	≥5.0	2	10	0.275	57.5% (35-90%)	0.152
	<5.0	9	19		75% (25-100%)	
Albumin	≥36 (g/L)	5	18	0.276	65% (25-100%)	0.722
	<36 (g/L)	6	11		75% (15-95%)	
Creatinine	≥72 (µmol/L)	6	14	0.500	62.5% (15-100%)	0.561
	<72 (µmol/L)	5	15		75% (25-90%)	
Tumour diameter	≥29mm	5	14	0.643	75% (25-90%)	0.793
	<29mm	5	14		70% (15-100%)	
Tumour differentiation	Poor	5	13	0.623	70% (25-90%)	0.663
	Well/Mod	6	16		75% (15-100%)	
Nodal status	Positive	6	16	0.574	65% (15-100%)	0.930
	Negative	5	14		72.5% (25-100%)	
Microvessel invasion	Present	2	12	0.177	77.5% (25-95%)	0.710
	Absent	9	18		70% (15-100%)	
Perineural invasion	Present	5	23	0.088	57.5% (15-95%)	0.103
	Absent	6	8		77.5% (40-100%)	
Resection margin	Positive	6	9	0.261	75% (15-100%)	0.906
	Negative	5	22		70 (35-95%)	

*, Chi squared or Fisher's exact test as appropriate; **, Mann-Whitney U test
Alk Phos, alkaline phosphatase; ALT, alanine transaminase; NLR, neutrophil/lymphocyte ratio

3.3.1.2 Notch-3

Similar to cytoplasmic Notch-1 staining, cytoplasmic Notch-3 staining was identified in cancer cells of all resected pancreatic adenocarcinoma specimens (Figure 3.4, Table 3.4). A median of 45% of ductal carcinoma cells stained positive for cytoplasmic Notch-3, ranging from 5% to 85%. Cytoplasmic Notch-3 expression was up-regulated in tumour tissue compared to background pancreatic tissue in 21 of 35 patients (60.0%), with a median of 30% of normal ductal cells displaying cytoplasmic expression ($p<0.001$ compared to tumour tissue). Nuclear Notch-3 staining was negative in normal pancreatic ductal cells, however was positive in cancer cells of 20 patients with resected pancreatic adenocarcinoma (47.6%, $p<0.001$ compared to background pancreas).

Nuclear Notch-3 expression was highly significantly associated with nuclear HEY-1 expression in resected pancreatic adenocarcinoma specimens ($p=0.001$; Table 3.5). Similarly, cytoplasmic Notch-3 was significantly correlated with cytoplasmic HEY-1 expression ($p<0.001$). In addition, nuclear Notch-3 expression was positively associated with cytoplasmic Notch-4 expression ($p=0.009$). Cytoplasmic Notch-3 expression was not associated with any of the clinicopathological factors investigated. Nuclear Notch-3 expression was associated with the presence of lymph node metastases in resected adenocarcinoma specimens and demonstrated a trend towards association with elevated CA19.9 level ($p=0.054$; Table 3.7). Neither nuclear nor cytoplasmic Notch-3 expression differed between patients with head of pancreas compared to body/tail tumours.

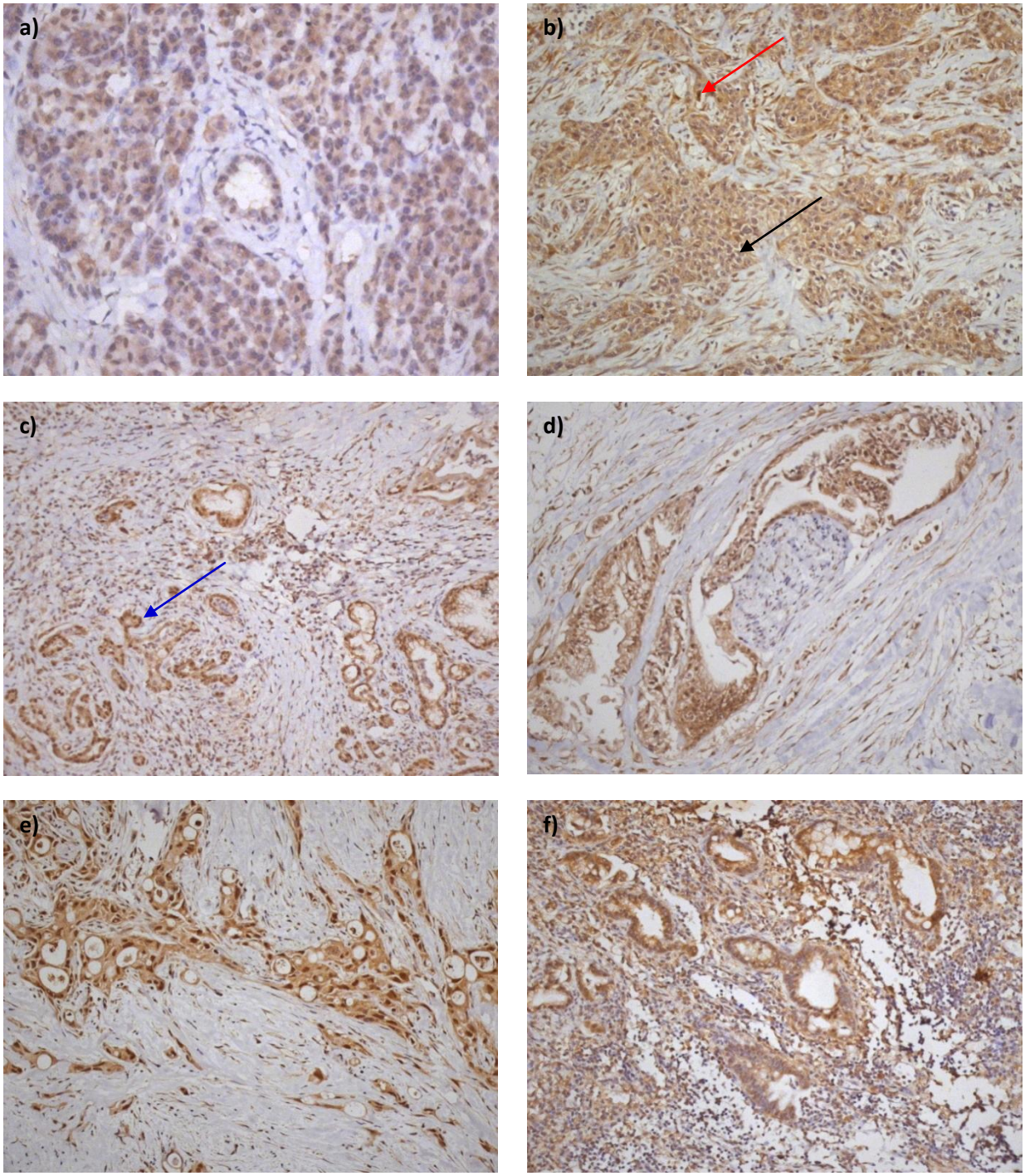

Figure 3.4 – Immunohistochemical expression of Notch-3 in normal pancreas and pancreatic adenocarcinoma
a) Notch-3 was detected in the cytoplasm of normal pancreatic ductal epithelial cells, however no nuclear staining was present; b) resected pancreatic carcinoma specimen demonstrating strong cytoplasmic Notch-3 staining and nuclei with positive (red arrow) and negative (black arrow) Notch-3 staining; c) resected pancreatic carcinoma demonstrating largely nuclear staining (blue arrow); d) nuclear staining in an area of perineural invasion; e) strong cytoplasmic and nuclear staining in an unresectable specimen; f) Notch-3 staining in a metastatic deposit in a local lymph node
(Original magnification, all 20x, except a) 40x)

Table 3.7 – Associations of nuclear and cytoplasmic Notch-3 expression with clinicopathological variables

Factor	Category	Nuclear Notch-3 expression			Cytoplasmic Notch-3 expression	
		Present	Absent	P*	Median (range)	P**
Gender	Male	13	11	0.378	60% (5-85%)	0.105
	Female	8	10		45% (20-85%)	
Age	≥64 years	5	11	0.055	60% (25-85%)	0.130
	<64 years	16	10		42.5% (5-85%)	
CA19.9	≥320 (U/ml)	14	7	0.054	45% (20-85%)	0.670
	<320 (U/ml)	6	11		45% (5-85%)	
Alk Phos	≥258 (IU/L)	9	13	0.264	45% (5-80%)	0.807
	<258 (IU/L)	11	9		45% (10-85%)	
ALT	≥91 (IU/L)	11	8	0.172	47.5% (20-85%)	0.441
	<91 (IU/L)	9	12		45% (5-85%)	
Bilirubin	≥146 (µmol/L)	10	11	0.376	47.5% (20-85%)	0.223
	<146 (µmol/L)	12	9		45% (5-85%)	
WCC	≥7.5 ($x10^9$/L)	10	11	1.000	47.5% (15-75%)	0.871
	<7.5 ($x10^9$/L)	10	11		45% (5-85%)	
Lymphocytes	≥1.5 ($x10^9$/L)	12	9	0.376	45% (10-85%)	0.588
	<1.5 ($x10^9$/L)	9	12		50% (5-85%)	
Neutrophils	≥5.0 ($x10^9$/L)	10	12	0.500	47.5% (15-75%)	0.267
	<5.0 ($x10^9$/L)	11	9		40% (5-85%)	
NLR	≥5.0	4	9	0.150	45% (5-70%)	0.965
	<5.0	17	12		45% (15-85%)	
Albumin	≥36 (g/L)	11	13	0.500	47.5% (5-85%)	0.712
	<36 (g/L)	9	9		45% (20-75%)	
Creatinine	≥72 (µmol/L)	10	11	0.624	50% (15-85%)	0.379
	<72 (µmol/L)	11	10		45% (5-85%)	
Tumour diameter	≥29mm	8	11	0.191	45% (5-85%)	0.672
	<29mm	12	9		45% (20-85%)	
Tumour differentiation	Poor	9	9	0.624	45% (5-85%)	0.295
	Well/Mod	12	11		55% (10-85%)	
Nodal status	Positive	15	7	**0.015**	45% (20-85%)	0.597
	Negative	6	13		45% (5-85%)	
Microvessel invasion	Present	7	7	0.585	40% (20-80%)	0.650
	Absent	14	13		45% (5-85%)	
Perineural invasion	Present	15	13	0.372	55% (20-85%)	0.112
	Absent	6	8		40% (5-85%)	
Resection margin	Positive	8	7	0.582	45% (20-85%)	0.318
	Negative	13	14		45% (5-75%)	

*, Chi squared or Fisher's exact test as appropriate; **, Mann-Whitney U test
Alk Phos, alkaline phosphatase; ALT, alanine transaminase; NLR, neutrophil/lymphocyte ratio

3.3.1.3 Notch-4

Cytoplasmic Notch-4 expression was detected in cancer cells of all resected pancreatic adenocarcinoma specimens with a median of 70% of ductal carcinoma cells demonstrating cytoplasmic staining (range 20% to 95%) (Table 3.4, Figure 3.5). Cytoplasmic Notch-4 staining was up-regulated in the tumour tissue in 33 of 35 patients compared to background pancreas ductal cells (94.3%), with a median of 20% of normal ductal cells displaying cytoplasmic staining ($p<0.001$ compared to tumour tissue). Nuclear Notch-4 staining was negative in background normal ductal cells, however was positive in the cancer cells of 8 patients with resected pancreatic adenocarcinoma (19.0%, $p=0.009$ compared to background pancreas).

Significant inverse associations were noted between nuclear Notch-4 expression and cytoplasmic Notch-1 expression ($p=0.039$), as well as cytoplasmic Notch-4 expression and nuclear Notch-1 expression ($p=0.006$; Table 3.5). Cytoplasmic Notch-4 expression was also associated with nuclear Notch-3 staining ($p=0.009$). Neither cytoplasmic or nuclear staining of Notch-4 were associated with any clinicopathological variable investigated, although there were trends towards increased cytoplasmic Notch-4 expression being associated with well/moderate tumour differentiation and negative lymph node status ($p=0.086$ and 0.050 respectively, Table 3.8). Neither nuclear nor cytoplasmic Notch-4 expression differed between patients with head of pancreas compared to body/tail tumours.

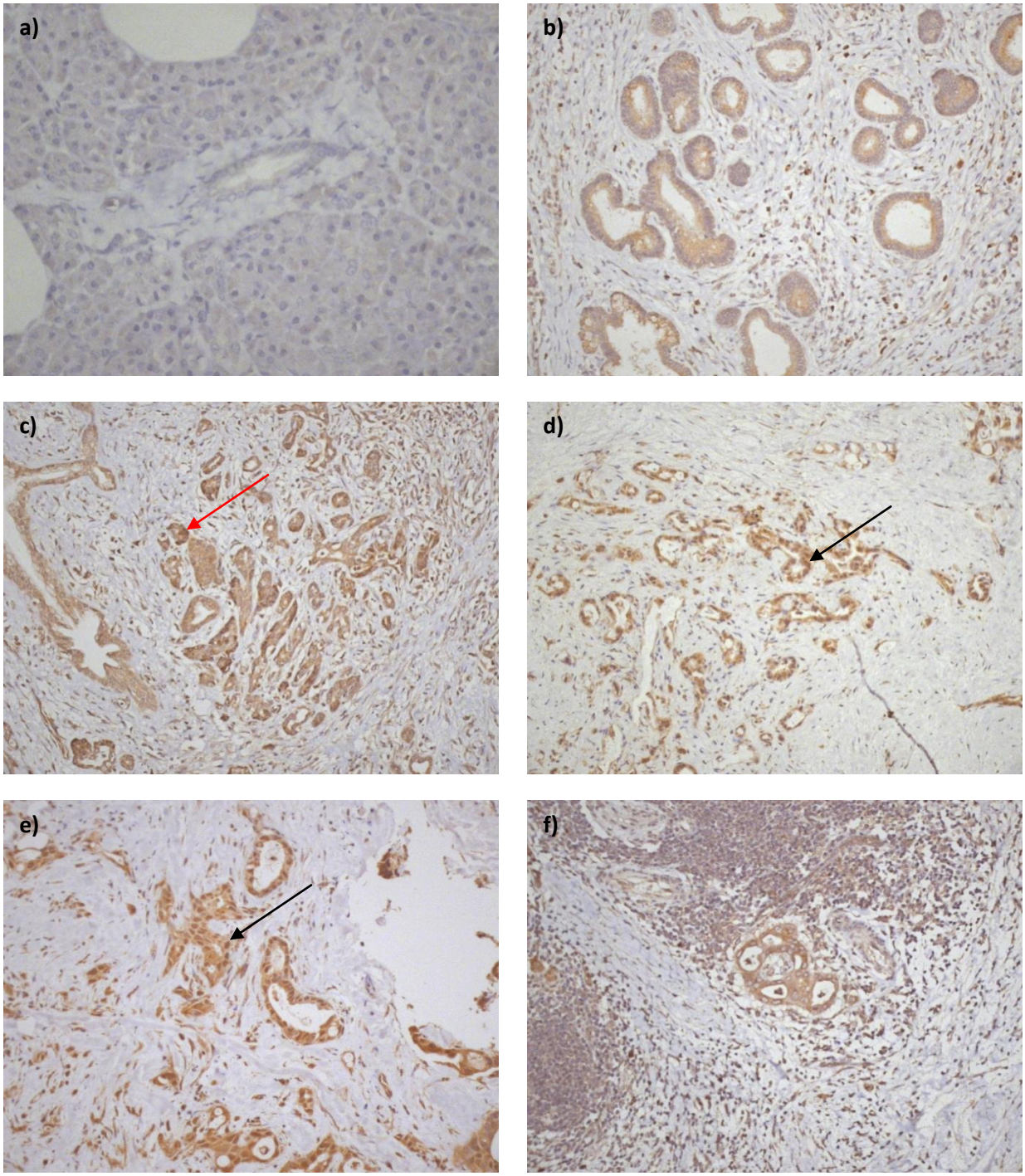

Figure 3.5 – Immunohistochemical expression of Notch-4 in normal pancreas and pancreatic adenocarcinoma
a) Cytoplasmic Notch-4 expression was weak in normal ductal epithelial cells; b) resectable pancreatic adenocarcinoma demonstrating cytoplasmic, but not nuclear expression of Notch-4; c) resected pancreatic adenocarcinoma demonstrating nuclear Notch-4 staining (red arrow); d,e) unresectable pancreatic adenocarcinoma specimens demonstrating a high percentage of nuclear Notch-4 staining (black arrows); f) metastatic deposit in a local lymph node demonstrating cytoplasmic, but not nuclear Notch-4 staining.
(Original magnification, all 20x, except a) 40x)

Table 3.8 – Associations of nuclear and cytoplasmic Notch-4 expression with clinicopathological variables

Factor	Category	Nuclear Notch-4 expression			Cytoplasmic Notch-4 expression	
		Present	Absent	P*	Median (range)	P**
Gender	Male	3	21	0.197	55% (20-95%)	0.270
	Female	5	13		70% (20-95%)	
Age	≥64 years	2	14	0.336	70% (20-95%)	0.721
	<64 years	6	20		54% (20-95%)	
CA19.9	≥320 (U/ml)	5	16	0.478	50% (20-90%)	0.317
	<320 (U/ml)	3	14		70% (20-95%)	
Alk Phos	≥258 (IU/L)	4	18	0.441	70% (20-95%)	0.455
	<258 (IU/L)	4	15		65% (20-95%)	
ALT	≥91 (IU/L)	6	15	0.204	55% (20-90%)	0.569
	<91 (IU/L)	2	18		70% (25-95%)	
Bilirubin	≥146 (µmol/L)	4	16	0.500	70% (25-95%)	0.167
	<146 (µmol/L)	4	17		55% (20-95%)	
WCC	≥7.5 ($x10^9$/L)	4	17	0.500	70% (20-95%)	0.807
	<7.5 ($x10^9$/L)	4	16		65% (20-95%)	
Lymphocytes	≥1.5 ($x10^9$/L)	5	16	0.500	70% (20-95%)	0.665
	<1.5 ($x10^9$/L)	3	17		67.5% (25-95%)	
Neutrophils	≥5.0 ($x10^9$/L)	3	19	0.164	70% (20-95%)	0.674
	<5.0 ($x10^9$/L)	5	14		65% (20-95%)	
NLR	≥5.0	1	12	0.081	70% (25-95%)	0.859
	<5.0	7	21		65% (20-95%)	
Albumin	≥36 (g/L)	5	19	0.649	70% (20-95%)	0.222
	<36 (g/L)	3	14		65% (20-85%)	
Creatinine	≥72 (µmol/L)	4	17	0.500	72.5% (20-95%)	0.473
	<72 (µmol/L)	4	16		50% (20-95%)	
Tumour diameter	≥29mm	3	16	0.346	65% (20-95%)	0.661
	<29mm	5	14		50% (35-95%)	
Tumour differentiation	Poor	4	14	0.383	45% (20-95%)	0.086
	Well/Mod	4	19		75% (25-95%)	
Nodal status	Positive	5	16	0.406	45% (20-95%)	0.050
	Negative	3	17		75% (20-95%)	
Microvessel invasion	Present	3	11	0.565	67.5% (20-95%)	0.890
	Absent	5	22		65% (20-95%)	
Perineural invasion	Present	4	23	0.240	70% (20-95%)	0.584
	Absent	4	10		55% (20-95%)	
Resection margin	Positive	3	11	0.605	65% (25-95%)	0.969
	Negative	5	22		70% (20-95%)	

*, Chi squared or Fisher's exact test as appropriate; **, Mann-Whitney U test
Alk Phos, alkaline phosphatase; ALT, alanine transaminase; NLR, neutrophil/lymphocyte ratio

3.3.1.4 HES-1

Cytoplasmic HES-1 staining was detected to some degree in cancer cells of all resected adenocarcinoma specimens with a median of 50% of ductal carcinoma cells demonstrating cytoplasmic staining (range 20% to 95%; Table 3.4). Cytoplasmic HES-1 staining was up-regulated in the tumour cells compared to background ductal cells in only 8 of 35 patients (22.9%), with a median of 45% staining in the cytoplasm of normal ductal cells ($p=0.530$ compared to tumour tissue). Nuclear HES-1 staining was identified in the background normal ductal cells of 8 patients (22.9%), but was positive in the cancer cells of 33 patients with resected pancreatic adenocarcinoma (78.6%, $p<0.001$ compared to background pancreas).

Nuclear HES-1 expression was significantly associated with nuclear Notch-1 expression ($p=0.013$) and cytoplasmic HES-1 expression was significantly correlated with cytoplasmic Notch-1 expression ($p=0.020$; Table 3.5)). Neither cytoplasmic nor nuclear staining of HES-1 were associated with any clinicopathological variable investigated, although there was a trend towards nuclear expression being associated with perineural invasion ($p=0.073$, Table 3.9). Neither nuclear nor cytoplasmic HES-1 expression differed between patients with head of pancreas compared to body/tail tumours.

3.3.1.5 HEY-1

Cytoplasmic HEY-1 staining was detected in cancer cells of all resected adenocarcinoma specimens with a median of 65% of ductal carcinoma cells demonstrating cytoplasmic staining (range 35% to 100%; Table 3.4). Cytoplasmic HEY-1 staining was up-regulated in

the tumour cells compared to background ductal cells in 33 of 35 patients (94.2%), with a median of 25% in the cytoplasm of normal ductal cells ($p<0.001$ compared to tumour tissue). Nuclear HEY-1 staining was negative in background normal ductal cells, but was positive in the cancer cells of 11 patient with resected adenocarcinoma specimens (26.2%, $p=0.001$ compared to background pancreas).

There were significant associations between nuclear expression of HEY-1 and Notch-3 ($p=0.001$) and cytoplasmic expression of HEY-1 and Notch-3 ($p<0.001$; Table 3.5). Positive nuclear HEY-1 staining in ductal adenocarcinoma cells was strongly associated with the presence of local lymph node metastases and microvessel invasion (both $p=0.003$), as well as perineural invasion ($p=0.048$) and younger patient age ($p=0.022$). Of note, on examination of HEY-1 immunohistochemistry, nuclear expression was frequently positive in areas of perineural invasion. Cytoplasmic HEY-1 was not associated with any clinicopathological variables. Neither nuclear nor cytoplasmic HEY-1 expression differed between patients with head of pancreas compared to body/tail tumours.

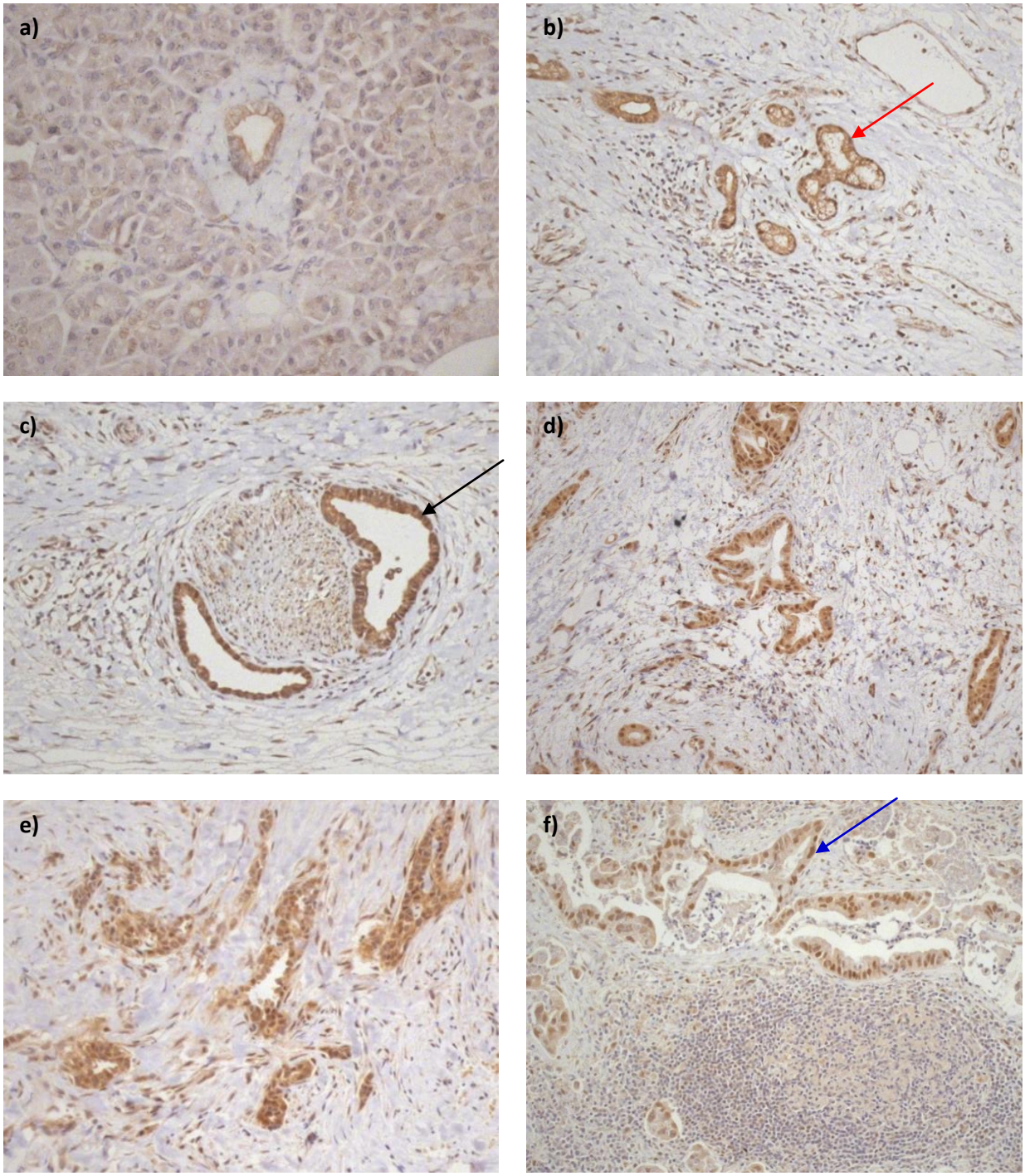

Figure 3.6 – Immunohistochemical expression of HES-1 in normal pancreas and pancreatic adenocarcinoma
a) Normal pancreatic ductal epithelium demonstrating cytoplasmic HES-1 staining, but not nuclear HES-1 expression; b) Resected pancreatic adenocarcinoma demonstrating cytoplasmic and nuclear HES-1 staining (red arrow); c) Area of perineural invasion in a resected pancreatic adenocarcinoma demonstrating nuclear expression (black arrow); d,e) unresectable pancreatic adenocarcinoma demonstrating cytoplasmic and nuclear HES-1 expression; f) distant lymph node metastases demonstrating weak cytoplasmic staining and positive nuclear HES-1 expression (blue arrow).
(Original magnification, all 20x, except a) 40x)

Table 3.9 – Associations of nuclear and cytoplasmic HES-1 expression with clinicopathological variables

Factor	Category	Nuclear HES-1 expression		P	Cytoplasmic HES-1 expression	
		Present	Absent		Median (range)	P
Gender	Male	20	4	0.216	45% (20-90%)	0.083
	Female	13	5		50% (25-95%)	
Age	≥64 years	14	3	0.314	40% (20-80%)	0.742
	<64 years	19	6		50% (25-95%)	
CA19.9	≥320 (U/ml)	15	6	0.222	45% (25-90%)	0.502
	<320 (U/ml)	14	2		55% (20-95%)	
Alk Phos	≥258 (IU/L)	17	5	0.442	45% (20-80%)	0.207
	<258 (IU/L)	16	3		50% (25-95%)	
ALT	≥91 (IU/L)	18	3	0.317	45% (20-90%)	0.608
	<91 (IU/L)	15	5		48% (25-95%)	
Bilirubin	≥146 (µmol/L)	17	4	0.622	45% (25-90%)	0.618
	<146 (µmol/L)	16	4		50% (20-95%)	
WCC	≥7.5 ($x10^9$/L)	16	4	0.622	50% (25-95%)	0.538
	<7.5 ($x10^9$/L)	17	4		45% (20-90%)	
Lymphocytes	≥1.5 ($x10^9$/L)	14	6	0.101	45% (20-95%)	0.305
	<1.5 ($x10^9$/L)	19	2		50% (30-90%)	
Neutrophils	≥5.0 ($x10^9$/L)	18	4	0.558	50% (25-95%)	0.930
	<5.0 ($x10^9$/L)	15	4		50% (20-90%)	
NLR	≥5.0	12	1	0.209	45% (35-70%)	0.975
	<5.0	21	7		45% (20-95%)	
Albumin	≥36 (g/L)	17	6	0.217	45% (20-95%)	0.735
	<36 (g/L)	16	2		50% (25-90%)	
Creatinine	≥72 (µmol/L)	17	4	0.622	45% (20-95%)	0.747
	<72 (µmol/L)	16	4		45% (28-90%)	
Tumour diameter	≥29mm	18	2	0.303	50% (20-85%)	0.691
	<29mm	15	4		45% (25-95%)	
Tumour differentiation	Poor	15	3	0.508	45% (20-90%)	0.917
	Well/Mod	18	5		50% (25-95%)	
Nodal status	Positive	18	3	0.319	45% (25-95%)	0.744
	Negative	15	5		50% (20-85%)	
Microvessel invasion	Present	12	2	0.479	50% (20-95%)	0.600
	Absent	21	6		45% (25-90%)	
Perineural invasion	Present	24	3	0.073	48% (24-95%)	0.283
	Absent	9	5		45% (20-70%)	
Resection margin	Positive	12	3	0.885	50% (25-90%)	0.623
	Negative	21	5		45% (20-95%)	

*, Chi squared or Fisher's exact test as appropriate; **, Mann-Whitney U test
Alk Phos, alkaline phosphatase; ALT, alanine transaminase; NLR, neutrophil/lymphocyte ratio

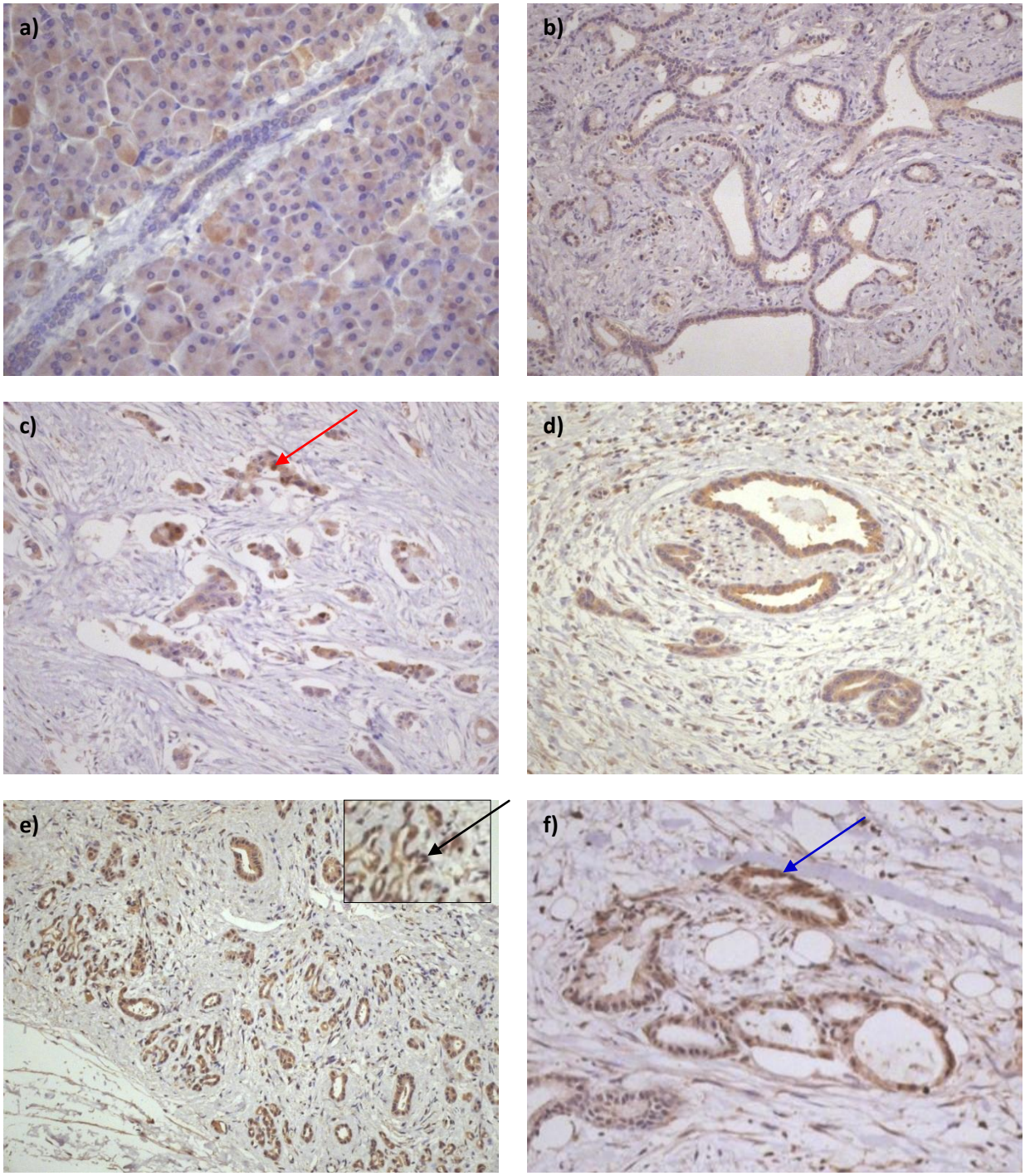

Figure 3.7 – Immunohistochemical expression of HEY-1 in normal pancreas and pancreatic adenocarcinoma
a) Longitudinal view of a normal pancreatic duct; b) resected pancreatic adenocarcinoma demonstrating weak cytoplasmic but no nuclear staining; c) resected adenocarcinoma specimen demonstrating nuclear expression (red arrow); d) area of perineural invasion in a resected tumour demonstrating cytoplasmic staining; e) unresectable tumour demonstrating cytoplasmic and positive nuclear expression of HEY-1 (see magnified insert, black arrow); f) peritoneal metastasis demonstrating cytoplasmic and nuclear staining (blue arrow) (Original magnification, all 20x, except a) 40x)

Table 3.10 – Associations of nuclear and cytoplasmic HEY-1 expression with clinicopathological variables

Factor	Category	Nuclear HEY-1 expression		P	Cytoplasmic HEY-1 expression	
		Present	Absent		Median (range)	P
Gender	Male	5	19	0.287	65% (40-90%)	0.254
	Female	6	12		60% (35-100%)	
Age	≥64 years	1	15	**0.022**	65% (35-100%)	0.492
	<64 years	10	16		65% (55-95%)	
CA19.9	≥320 (U/ml)	6	15	0.510	60% (35-90%)	0.154
	<320 (U/ml)	4	13		65% (40-100%)	
Alk Phos	≥258 (IU/L)	4	17	0.183	65% (40-90%	0.989
	<258 (IU/L)	7	12		60% (35-100%)	
ALT	≥91 (IU/L)	6	14	0.500	65% (35-95%)	0.465
	<91 (IU/L)	5	15		65% (40-100%)	
Bilirubin	≥146 (µmo/L)	4	16	0.240	65% (45-100%)	0.343
	<146 (µmol/L)	7	13		55% (35-75%)	
WCC	≥7.5 ($x10^9$/L)	6	14	0.500	65% (35-100%)	0.892
	<7.5 ($x10^9$/L)	5	15		60% (35-90%)	
Lymphocytes	≥1.5 ($x10^9$/L)	8	12	0.078	55% (35-75%)	0.490
	<1.5 ($x10^9$/L)	3	17		65% (40-100%)	
Neutrophils	≥5.0 ($x10^9$/L)	5	16	0.422	65% (45-100%)	0.597
	<5.0 ($x10^9$/L)	6	13		55% (35-95%)	
NLR	≥5.0	2	10	0.275	65% (50-100%)	0.658
	<5.0	9	19		40% (35-75%)	
Albumin	≥36 (g/L)	6	17	0.546	65% (50-100%)	0.055
	<36 (g/L)	5	12		55% (35-85%)	
Creatinine	≥72 (µmol/L)	5	15	0.500	65% (40-100%)	0.285
	<72 (µmol/L)	6	14		55% (35-85%)	
Tumour diameter	≥29mm	4	16	0.238	65% (35-95%)	0.827
	<29mm	7	13		65% (40-100%)	
Tumour differentiation	Poor	4	14	0.503	60% (35-85%)	0.157
	Well/Mod	6	16		65% (45-100%)	
Nodal status	Positive	10	12	**0.003**	55% (35-90%)	0.614
	Negative	1	18		55% (40-100%)	
Microvessel invasion	Present	8	6	**0.003**	50% (35-90%)	0.109
	Absent	3	22		65% (40-100%)	
Perineural invasion	Present	10	18	**0.048**	65% (35-100%)	0.749
	Absent	1	11		55% (40-80%)	
Resection margin	Positive	4	11	0.837	65% (40-100%)	0.875
	Negative	7	20		50% (35-90%)	

*, Chi squared or Fisher's exact test as appropriate; **, Mann-Whitney U test
Alk Phos, alkaline phosphatase; ALT, alanine transaminase; NLR, neutrophil/lymphocyte ratio

3.3.2 Notch expression in local lymph node metastases

Of those patients with positive local lymph node metastases following resection of pancreatic adenocarcinoma, there was no difference in nuclear expression of Notch-1 (37.5% vs.26.2%, p=0.369), Notch-3 (62.5% vs. 47.6%, p=0.179), Notch-4 (18.8% vs. 19.0%, p=0.624) or HES-1 (75.0% vs. 78.6%, p=0.303) in metastatic adenocarcinoma cells compared to those in the pancreatic primary (Table 3.4). In addition, there was no difference in cytoplasmic expression of Notch-1 (p=0.679), Notch-3 (p=0.211), Notch-4 (p=0.637), HES-1 (p=0.530) or HEY-1 (p=0.126) between the two groups. Only nuclear HEY-1 showed a trend towards significant difference between the two groups, with positive nuclear expression higher in local lymph metastases than the pancreatic primary (50.0% vs. 26.2%, p=0.074).

3.3.3 Notch expression in advanced pancreatic adenocarcinoma

When all patients with advanced pancreatic adenocarcinoma (either locally advanced or metastatic) were analysed, positive nuclear expression of Notch-1 (70.0% vs. 26.2%, p<0.001), Notch-3 (90.0% vs. 47.6%, p<0.001), Notch-4 (68.0% vs. 19.0%, p<0.001), HES-1 (100% vs. 78.6%, p=0.001) and HEY-1 (76.0% vs. 26.2%, p<0.001) were found to be significantly increased compared to the expression in patients with resected tumours (Table 3.4). Cytoplasmic staining of Notch-1 (median 30% vs. 75%, p<0.001), Notch-4 (median 40% vs. 70%, p=0.001) and HES-1 (median 40% vs. 50%, p=0.023) were significantly reduced in advanced pancreatic cancer cells compared to those from resected tumours. There was no change in cytoplasmic staining of Notch-3 (p=0.953) or HEY-1 (p=0.945) between the two groups.

When the patients with metastatic disease were compared to those with locally advanced disease, there was no difference in nuclear expression of any of the biomarkers, or cytoplasmic expression of Notch-1, -4, HES-1 or HEY-1. Only cytoplasmic expression of Notch-3 significantly differed between the groups, being higher in those patients with distant metastases compared to locally advanced disease (median staining 65% vs. 40%, p=0.018).

3.3.4 Survival analyses

3.3.4.1 Univariate analyses

Survival analyses were performed to associate the expression of individual biomarkers with overall and disease-free survival following resection with curative intent of pancreatic adenocarcinoma (Table 3.11). Kaplan-Meier curves displaying survival according to expression of individual biomarkers are shown in Figures 3.8-3.12.

Expression of nuclear Notch-1 was associated with a significantly shorter overall survival. For patients undergoing potentially curative resection, the 5-year survival for patients with nuclear Notch-1 expression was 18.2% (median 14.7 months, 95% CI 1.4-30.3 months) and 22.1% without nuclear expression (median 31.3 months, 95% CI 30.0-32.6 months, p=0.044 log-rank; Figure 3.8). Nuclear Notch-1 expression was associated with a reduced disease-free survival, with 5-year disease-free survival of 18.2% in patients with nuclear expression (median 11.6 months, 95% CI 4.8-18.4 months) and 20.4% in patients without nuclear expression (median 28.7 months, 95% CI 23.2-34.2 months), although this failed to reach statistical significance (p=0.184 log-rank). Up-regulated expression of cytoplasmic Notch-1

Table 3.11 – Univariate Cox regression survival analyses for Notch pathway biomarkers for all patients undergoing potentially-curative resection for pancreatic adenocarcinoma (n=42).

	Overall Survival		Disease-free Survival	
	Hazard Ratio (95% CI)	**P**	**Hazard Ratio (95% CI)**	**P**
Notch-1 nuclear expression: +/-	2.128 (1.003-4.525)	**0.049**	1.658 (0.781-3.521)	0.188
Notch-1 cytoplasmic expression: ≥50%/<50% staining	0.626 (0.311-1.261)	0.190	0.700 (0.349-1.407)	0.317
Notch-3 nuclear expression: +/-	2.541 (1.213-5.324)	**0.013**	2.380 (1.166-4.858)	**0.017**
Notch-3 cytoplasmic expression: ≥50%/<50% staining	1.516 (0.760-3.023)	0.238	1.768 (0.868-3.600)	0.116
Notch-4 nuclear expression: +/-	1.155 (0.445-2.998)	0.768	0.898 (0.345-2.340)	0.826
Notch-4 cytoplasmic expression: ≥50%/<50% staining	0.550 (0.274-1.103)	0.092	0.596 (0.298-1.190)	0.142
HES-1 nuclear expression: +/-	1.252 (0.514-3.053)	0.621	1.444 (0.553-3.769)	0.453
HES- cytoplasmic expression: ≥50%/<50% staining	0.689 (0.317-1.498)	0.347	0.595 (0.273-1.296)	0.191
HEY-1 nuclear expression: +/-	2.998 (1.326-6.778)	**0.008**	3.498 (1.583-7.690)	**0.002**
HEY-1 cytoplasmic expression: ≥50%/<50% staining	0.803 (0.307-2.100)	0.654	0.676 (0.260-1.763)	0.424

CI, confidence interval

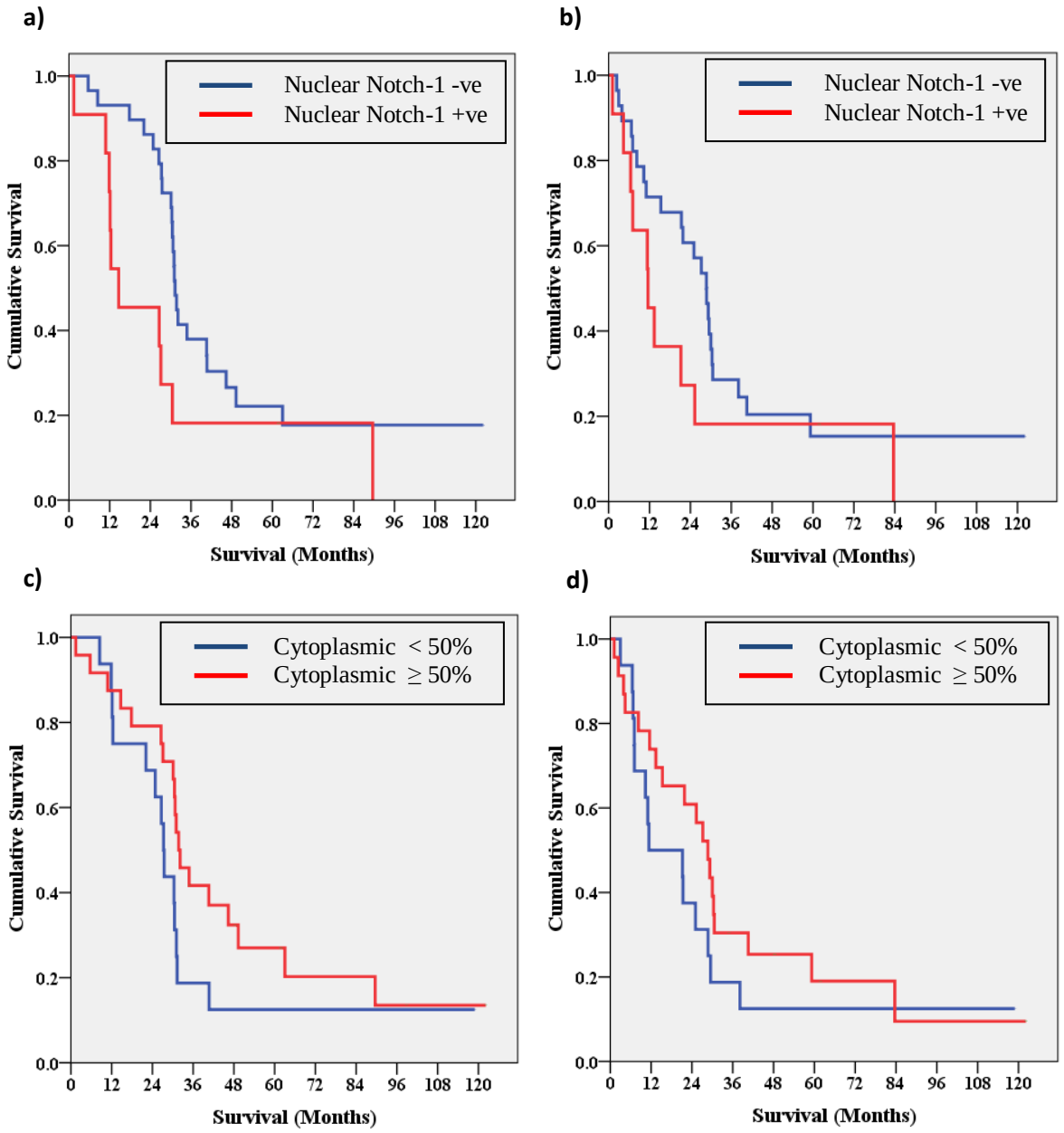

Figure 3.8 – Impact of Notch-1 expression on survival
Kaplan-Meier survival curves demonstrating the impact of nuclear Notch-1 expression on a) overall and b) disease-free survival (p=0.044 and 0.184 log-rank respectively); and the impact of Notch-1 cytoplasmic expression on c) overall and d) disease-free survival (p=0.186 and 0.315 log-rank respectively).

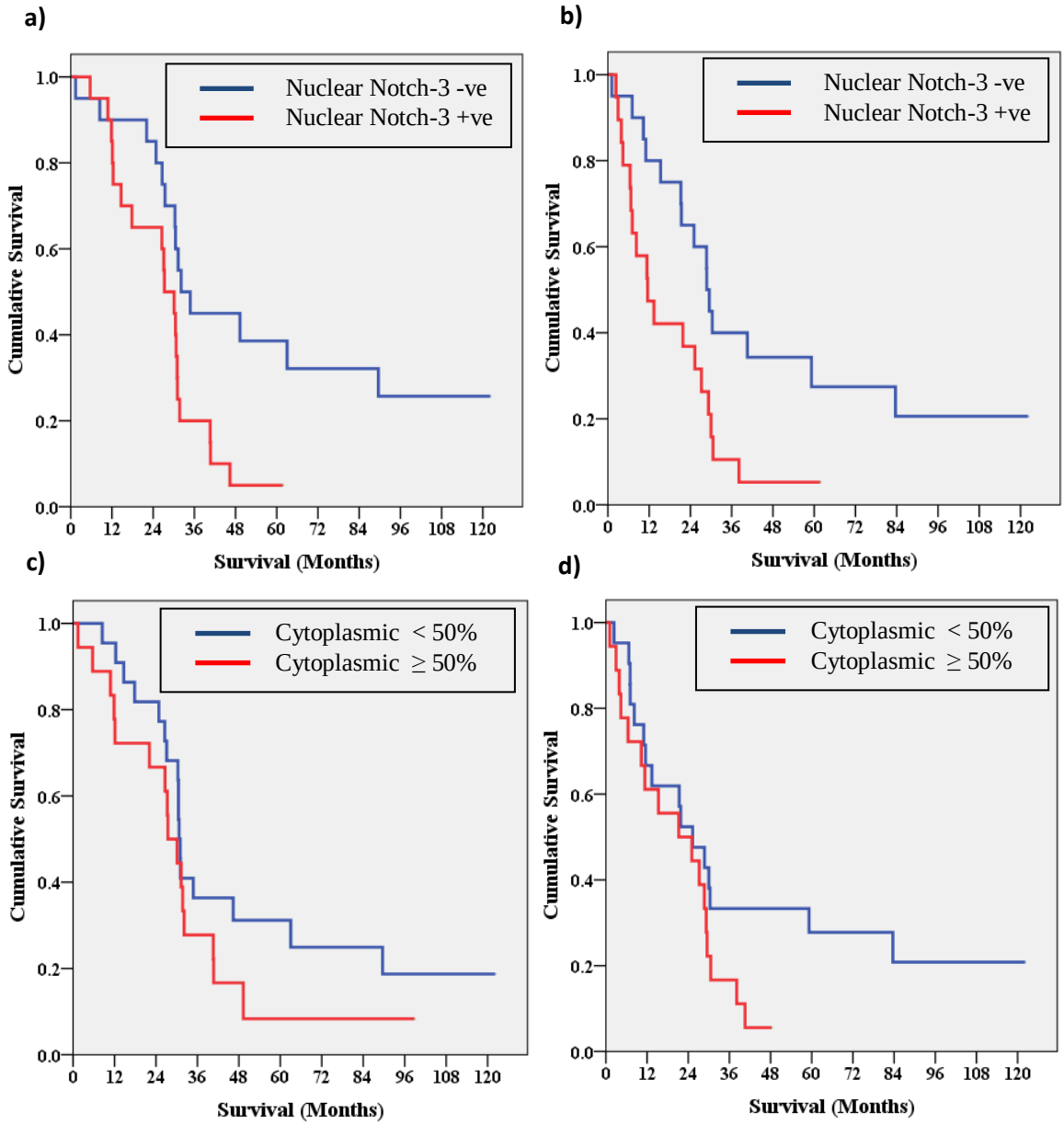

Figure 3.9 – Impact of Notch-3 expression on survival
Kaplan-Meier survival curves demonstrating the impact of nuclear Notch-3 expression on a) overall and b) disease-free survival (p=0.011 and 0.014 log-rank respectively); and the impact of Notch-3 cytoplasmic expression on c) overall and d) disease-free survival (p=0.234 and 0.112 log-rank respectively).

(≥50% cells staining) was not associated with either overall (median 31.7 months, 95% CI 26.8-36.7 months vs. 27.3 months, 95% CI 25.7-28.9 months, p=0.186 log-rank) or disease-free survival (median 28.7 months, 95% CI 22.5-34.9 months vs. 11.4 months, 95% CI 1.2-31.4 months, p=0.315 log-rank).

Nuclear Notch-3 expression was associated with significantly shorter overall and disease-free survival following resection. The 5-year overall survival for patients with nuclear Notch-3 expression was 5.0% (median 27.3 months, 95% CI 20.7-33.9 months) and 38.6% for patients without nuclear expression (median 32.1 months, 95% CI 24.5-39.8 months, p=0.011 log-rank; Figure 3.9). The 5-year disease-free survival following resection for patients with nuclear Notch-3 expression was 5.3% (median 11.7 months, 95% CI 4.3-18.9 months) compared to 27.4% in patients without nuclear expression (median 28.7 months, 95% CI 27.0-30.5 months, p=0.014 log-rank). Up-regulated expression of cytoplasmic Notch-3 (≥50% cells staining) was not associated with either overall (median 27.5 months, 95% CI 21.6-33.3 months vs. 30.7 months, 95% CI 30.1-31.3 months, p=0.234 log-rank) or disease-free

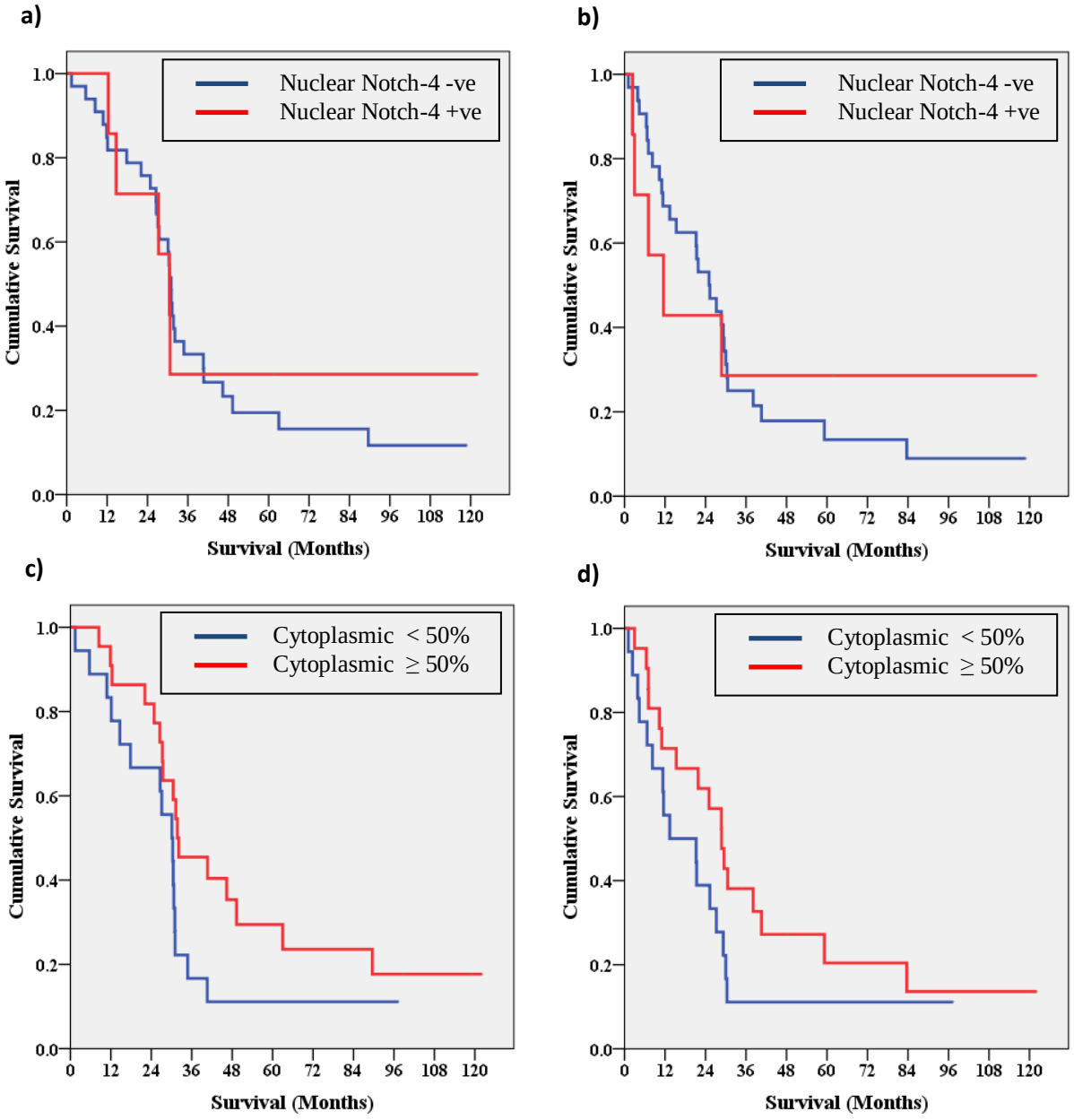

Figure 3.10 – Impact of Notch-4 expression on survival
Kaplan-Meier survival curves demonstrating the impact of nuclear Notch-4 expression on a) overall and b) disease-free survival (p=0.767 and 0.826 log-rank respectively); and the impact of Notch-4 cytoplasmic expression on c) overall and d) disease-free survival (p=0.087 and 0.234 log-rank respectively).

survival (median 21.2 months, 95% CI 4.1-41.4 months vs. 25.3 months, 95% CI 14.3-36.3 months, p=0.112 log-rank).

Nuclear expression of Notch-4 had no impact on overall or disease-free survival. The median overall survival for patients expressing nuclear Notch-4 was 30.5 months (95% CI 22.3-38.7 months) compared to 31.0 months (95% CI 29.6-32.4 months) in patients with negative expression (p=0.767 log-rank; Figure 3.10). The median disease-free survival of patients expressing nuclear Notch-4 was 11.6 months (95% CI 1.1-23.0 months) compared to 25.0 months (95% CI 16.9-33.1 months) in patients with negative expression (p=0.826 log-rank). Up-regulated expression of cytoplasmic Notch-4 (≥50% cells staining) was associated with a trend towards improved overall survival with 5-year survival rates of 29.5% compared to 11.1% (median 31.7 months, 95% CI 20.3-43.1 months vs. 30.1 months, 95% CI 23.3-36.9 months, p=0.087 log-rank).not associated with either overall (median 27.5 months, 95% CI 21.6-33.3 months vs. 30.7 months, 95% CI 30.1-31.3 months, p=0.234 log-rank). An association with improved disease-free survival was also seen, although this did not reach statistical significance (median 28.7 months, 95% CI 22.1-35.4 months vs. 13.4 months, 95% CI 0.0-33.5 months, p=0.138 log-rank).

Expression of nuclear HES-1 had no association with overall or disease-free survival. The median overall survival for patients expressing nuclear HES-1 was 30.4 months (95% CI 26.2-34.6 months) compared to 46.4 months (95% CI 14.8-77.9 months) in those with negative expression (p=0.620 log-rank). The median disease-free survival of patients expressing nuclear HES-1 was 21.8 months (95% CI 16.2-27.4 months) compared to 30.0 months (95% CI 1.4-74.0 months) in those with negative expression (p=0.450 log-rank).

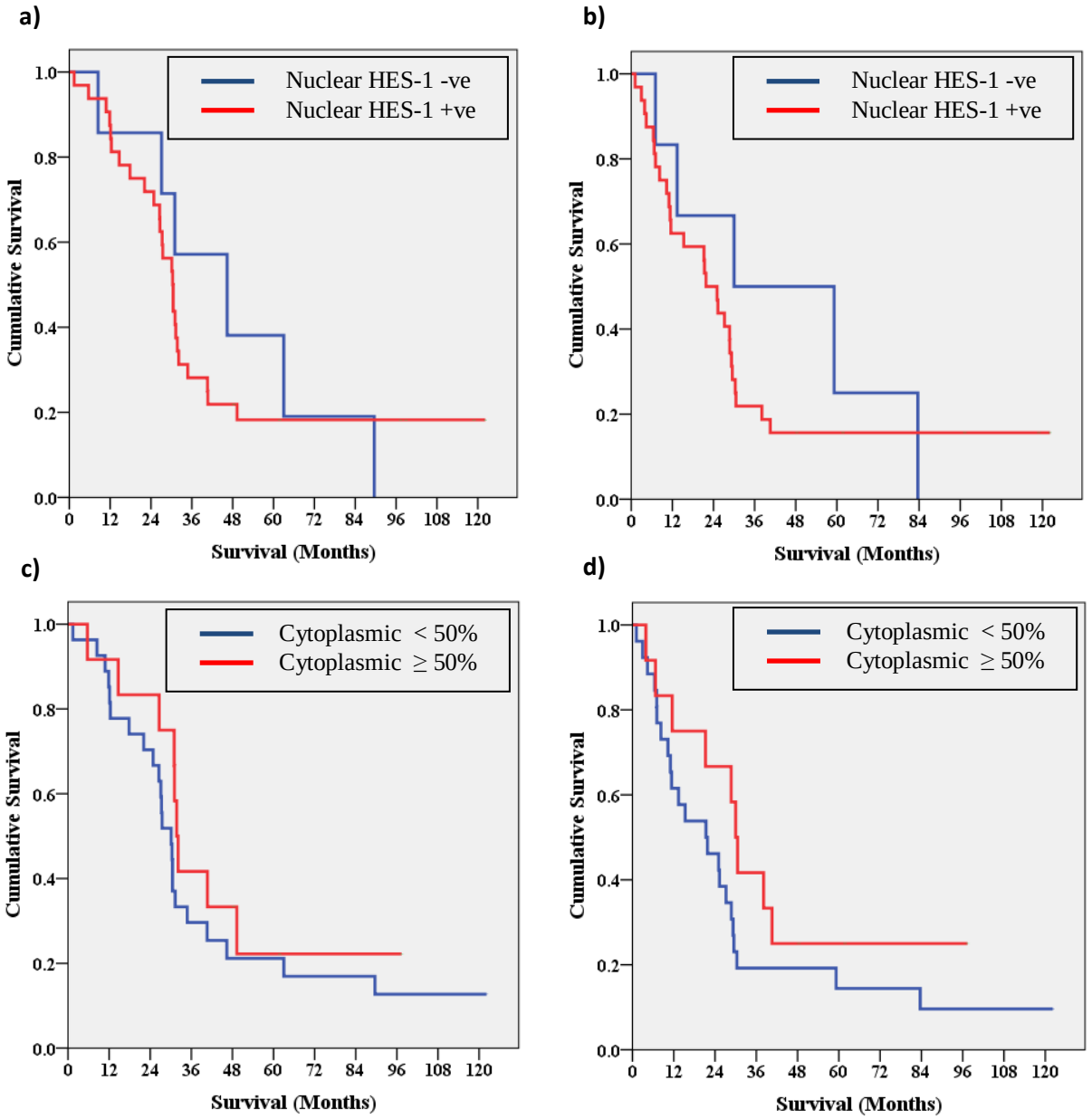

Figure 3.11 – Impact of HES-1 expression on survival
Kaplan-Meier survival curves demonstrating the impact of nuclear HES-1 expression on a) overall and b) disease-free survival (p=0.620 and 0.450 log-rank respectively); and the impact of HES-1 cytoplasmic expression on c) overall and d) disease-free survival (p=0.343 and 0.187 log-rank respectively).

Similarly, up-regulated expression of cytoplasmic HES-1 (≥50% cells staining) was not associated with either overall (median 31.7 months, 95% CI 29.9-33.5 months vs. 30.1 months, 95% CI 24.9-35.3 months, p=0.343 log-rank) or disease-free survival (median 30.0 months, 95% CI 26.8-33.2 months vs. 21.4 months, 95% CI 6.8-36.9 months, p=0.187 log-rank).

Nuclear HEY-1 expression was associated with shorter overall and disease-free survival following resection, both at a highly significant level. The 5-year overall survival for patients with nuclear HES-1 expression was 0.0% (median 26.5 months, 95% CI 11.9-41.2 months) and 28.4% for patients without nuclear expression (median 31.3 months, 95% CI 25.5-37.1 months, p=0.006 log-rank; Figure 3.12). The 5-year disease-free survival following resection for patient with nuclear HEY-1 expression was 0.0% (median 7.1 months, 95% CI 6.4-7.7 months) compared to 22.3% in patients without nuclear expression (median 28.7 months, 95% CI 25.1-32.4 months, p=0.001 log-rank). Up-regulated expression of cytoplasmic HEY-1 (≥50% cells staining) was not associated with either overall (median 30.5 months, 95% CI 26.9-34.1 months vs. 37.1 months, 95% CI 30.6-32.8 months, p=0.653 log-rank) or disease-free survival (median 31.4 months, 95% CI 7.9-34.8 months vs. 29.5 months, 95% CI 27.4-31.6 months, p=0.421 log-rank).

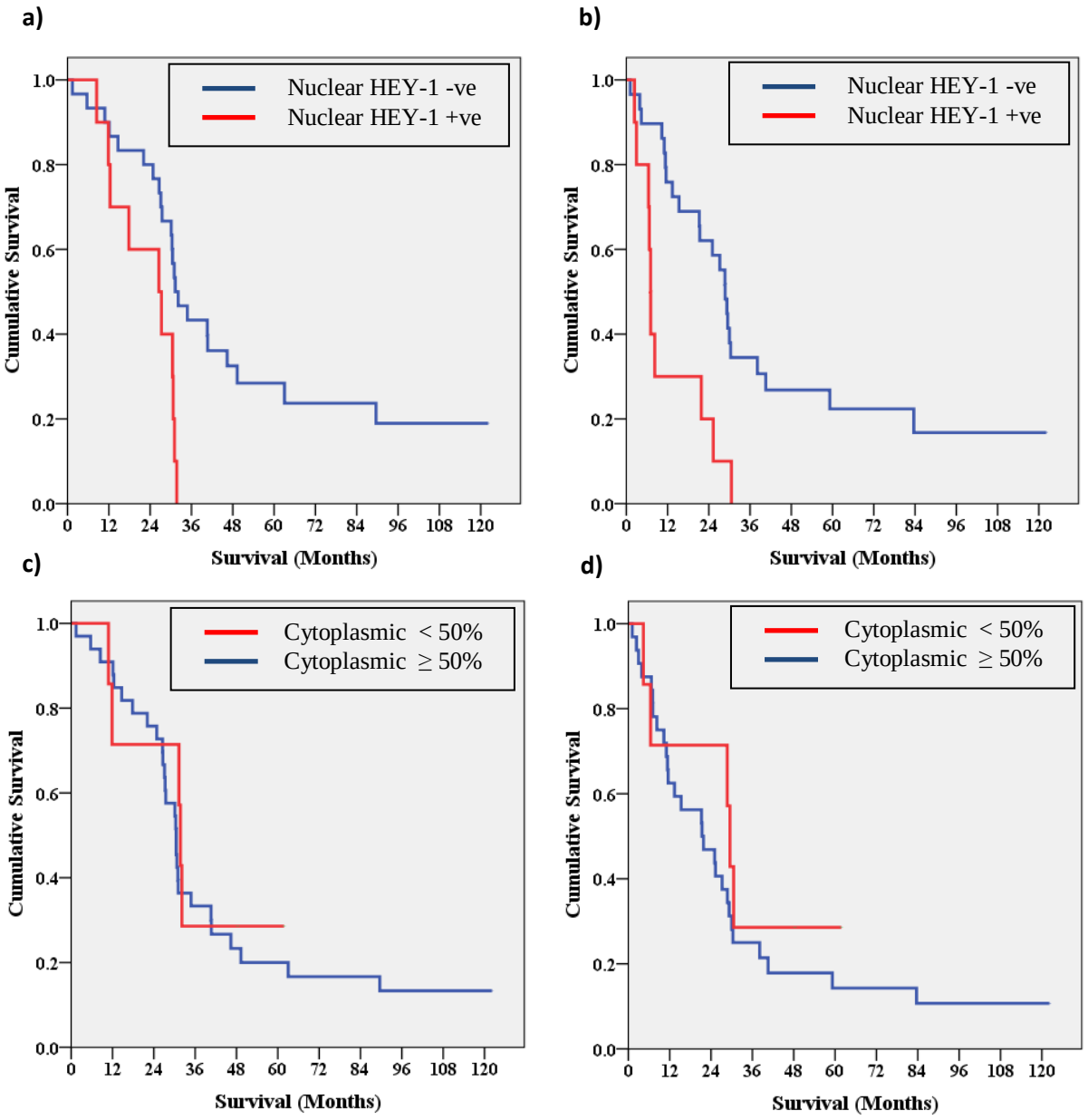

Figure 3.12 – Impact of HEY-1 expression on survival
Kaplan-Meier survival curves demonstrating the impact of nuclear HEY-1 expression on a) overall and b) disease-free survival (p=0.006 and 0.001 log-rank respectively); and the impact of HEY-1 cytoplasmic expression on c) overall and d) disease-free survival (p=0.653 and 0.421 log-rank respectively).

3.3.4.2 Multivariate analyses

Variables with $p<0.100$ on univariate analysis were incorporated in multivariate analyses that also included all clinicopathological variables with $p<0.100$ on univariate analysis (Table 3.2). Results from the final round of multivariate regression analysis for overall and disease-free survival are shown in Table 3.12.

In addition to CA19.9 level and resection margin status, nuclear HEY-1 expression also maintained independent prognostic significance on multivariate analysis (Table 3.12a). Nuclear HEY-1 expression was independently associated with shortened overall survival ($p=0.003$) and shortened disease-free survival ($p=0.010$). Nuclear Notch-3 expression also demonstrated non-significant trends towards shortened overall and disease-free survival ($p=0.120$ and $p=0.096$ respectively, removed at final round of regression analysis). Cytoplasmic Notch-4 expression did not maintain significance on multivariate survival analysis. When only patients who underwent a R_0 resection (i.e. potentially curative resection) were considered, CA19.9, lymph node status, nuclear Notch-3 and nuclear HEY-1 expression all had $p<0.100$ on univariate analysis when examining overall survival. For disease-free survival, CA19.9, lymph node status, perineural infiltration, nuclear Notch-3 expression, cytoplasmic Notch-3 expression and nuclear HEY-1 expression all had $p<0.100$ on univariate analysis. These variables were incorporated into a multivariate model (Table 3.12b). Nuclear HEY-1 expression was maintained as an independent prognostic factor for both overall ($p=0.003$) and disease-free survival ($p=0.010$), along with serum CA19.9 level (overall survival $p=0.031$; disease-free survival $p=0.004$). The same variables maintained significance when only patients with head of pancreas adenocarcinomas were analysed.

Table 3.12 – Multivariate Cox regression survival analyses, including Notch biomarkers, following potentially-curative resection for a) all patients with pancreatic adenocarcinoma (n=42); b) those patients undergoing a R_0 resection (n=27)

a)

	Overall Survival		Disease-free Survival	
	Hazard Ratio (95% CI)	**P**	**Hazard Ratio (95% CI)**	**P**
Resection margin: positive/negative	2.967 (1.172-7.512)	**0.022**		
CA19.9 ≥320/<320 (U/ml)			3.767 (1.631-8.702)	**0.002**
Perineural invasion: +/-			2.341 (0.899-6.093)	0.081
Notch-3 nuclear expression: +/-	3.466 (1.455-8.254)	0.120	2.446 (0.854-7.009)	0.096
Notch-4cytoplasmic expression: ≥50%/<50%	0.496 (0.217-1.134)	0.096		
HEY-1 nuclear expression: +/-	4.305 (1.661-11.158)	**0.003**	3.359 (1.339-8.427)	**0.010**

b)

	Overall Survival		Disease-free Survival	
	Hazard Ratio (95% CI)	**P**	**Hazard Ratio (95% CI)**	**P**
CA19.9 ≥320/<320 (U/ml)	2.922 (1.106-7.722)	**0.031**	5.323 (1.699-16.677)	**0.004**
Notch-3 nuclear expression: +/-	2.340 (0.861-6.359)	0.096	2.380 (0.816-6.942)	0.112
HEY-1 nuclear expression: +/-	4.139 (1.220-14.041)	**0.023**	5.545 (1.693-18.157)	**0.005**

CI, confidence interval

Interestingly, if nuclear HEY-1 was excluded from the multivariate analysis, nuclear Notch-3 staining became independently predictive of outcome for both overall and disease-free survival for all patients (p=0.007 and 0.048) and those undergoing R_0 resections (disease-free survival only; p=0.030). This provides evidence that it is the Notch-3 pathway, acting via HEY-1, that is associated with poor prognosis.

3.3.5 Combining biomarkers

Combinations of biomarkers may enable generation of more accurate prognostic information. Nuclear HEY-1 expression and serum CA19.9 level were chosen due to their independent prognostic power on multivariate analysis for all patients (disease-free survival) and those having undergone a R_0 resection. Patients were scored for the presence of serum CA19.9 level ≥320 and positive nuclear HEY-1 expression, with a minimum score of 0 and a maximum of 2. When all resected patients were analysed, this score was significantly associated with both overall and disease-free survival. Five year overall survival was 43.8% for patients with a score of 0, 10.0% with a score of 1, and 0.0% with a score of 2 (median 49.3 months, 95% CI 21.3-77.3 months; 30.1 months, 95% CI 25.1-35.1 months; and 26.5 months, 95% CI 7.9-45.2 months respectively, p=0.001 log-rank; Figure 3.13). Five year disease-free survival was 38.1% for patients with a score of 0, 5.3% with a score of 1, and 0.0% with a score of 2 (median 38.1 months, 95% CI 24.2-52.0 months; 21.2 months, 95% CI 1.7-40.8 months; and 7.1 months, 95% CI 6.2-8.0 months respectively, p<0.001 log-rank). When only patients who had undergone a R_0 resection were investigated, this score remained significantly associated with both overall and disease-free survival. Five year overall survival was 46.7% for patients with a score of 0, 15.4% with a score of 1, and 0.0% with a score of 2 (median 49.3 months, 95% CI 46.2-53.1 months; 31.7 months, 95% CI 30.5-33.0

months; and 27.3 months, 95% CI 12.2-42.5 months respectively, p=0.007). Five year disease-free survival for this group of patients was 36.0% for patients with as score of 1, 8.3% with a score of 1, and 0.0% with as score of 2 (median 38.1 months, 95% CI 12.4-63.8 months; 27.2 months, 95% CI 1.2-53.2 months; and 8.3 months, 95% CI 0.0-16.7 months respectively, p=0.041 log-rank).

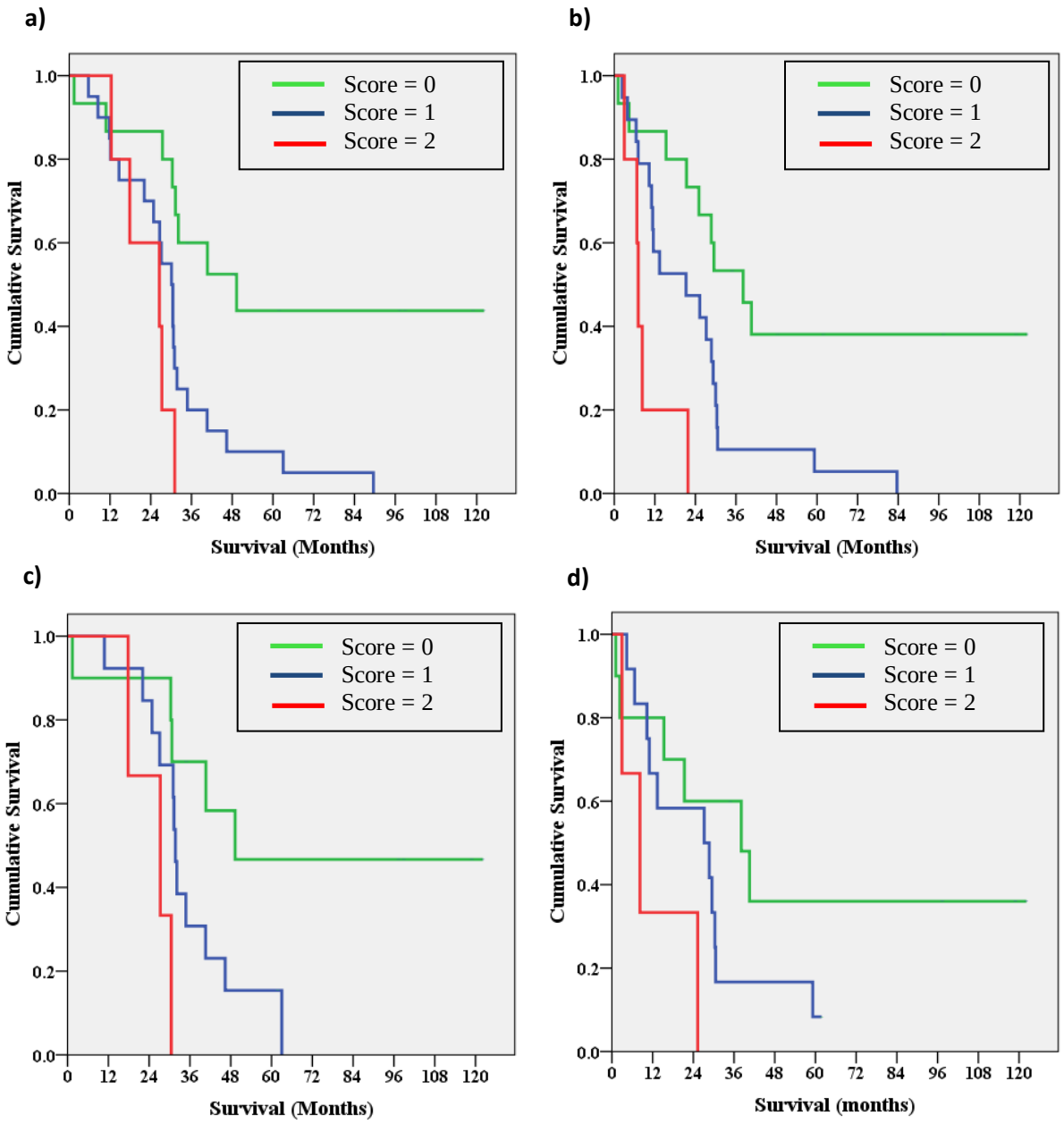

Figure 3.13 – Impact of combining biomarkers on survival
Kaplan-Meier survival curves demonstrating the impact of a score based upon CA 19.9 level and nuclear HEY-1 expression on a) overall and b) disease-free survival for all patients (p=0.001 and <0.001 log-rank respectively); and on c) overall and d) disease-free survival for patients undergoing a R_0 resection (p=0.007 and 0.041 log-rank respectively).

3.4 DISCUSSION

This chapter reports a large immunohistochemical assessment of the Notch pathway in pancreatic ductal adenocarcinoma. It is the first study to examine the alterations in Notch expression throughout disease progression from early, through advanced local disease to metastatic disease. This is also the first time that the expression patterns of individual Notch pathway constituents have been correlated with each other in pancreatic carcinoma. Finally, this is the first study to correlate the expression of Notch pathway constituents with clinicopathological factors and ultimately examine their use as predictors of survival.

Miyamoto *et al* (2003) used microarray analysis to demonstrate significant up-regulation of Notch-2, Notch-3, Notch-4, delta-1 and jagged-1 in resected pancreatic adenocarcinoma specimens compared to normal pancreas. This was associated with the up-regulation of several Notch target genes, including HES-1, HES-4, HEY-1 and HEY-L, suggesting that the up-regulation of the Notch pathway was functional. These findings were validated using RT-PCR. They further performed immunohistochemistry for Notch-1, Notch-2, Notch-3, Notch-4 and HES-1 on a panel of 34 resected adenocarcinoma specimens and normal pancreas. They found little expression of the four receptors in normal ductal epithelial cells; however they found moderate-high expression of the receptors in adenocarcinoma specimens, associated with a 7-fold increase in cells expressing HES-1 in adenocarcinoma specimens compared to normal ductal epithelium. The results of this study also found cytoplasmic Notch-1, Notch-3 and Notch-4 to be up-regulated in pancreatic carcinoma compared to normal ductal epithelium. However an up-regulation of nuclear localisation of the Notch receptors in resected pancreatic adenocarcinoma specimens, as well of nuclear expression of the target genes, HES-1 and HEY-1, was observed. Target gene activation and nuclear

localisation provide firm evidence that the Notch-1, Notch-3 and Notch-4 pathways are up-regulated in pancreatic carcinoma. In addition, nuclear expression of all proteins was up-regulated in advanced compared to resectable disease. This suggests that the Notch pathway may be important in disease progression and metastasis. These findings are in line with Buchler *et al* (2004) who demonstrated strong immunostaining of the Notch receptors and their ligands in areas of neurovascular invasion in pancreatic adenocarcinoma. In addition, Notch-1 inhibition has been shown to reduce pancreatic cancer cell invasion *in vitro*, with associated reductions in MMP-9, VEGF, and NF-κB DNA-binding activity (Wang *et al*, 2006 and 2006b), all known to play important roles in tumour cell invasion and metastasis (Nagakawa *et al*, 2002; Xiong *et al*, 2004).

This is the first study to correlate individual Notch proteins and downstream targets with each other. Nuclear expression of Notch-1 and HES-1 were found to be positively correlated. Nuclear localisation of Notch-1 is strongly suggestive of pathway activation and the association with HES-1 is unsurprising, and in line with existing data that suggest that HES-1 is a major effector of Notch-1. Similarly, nuclear Notch-3 expression is positively correlated with nuclear HEY-1 expression, but not HES-1, which supports previous data that HES-1 is under Notch-1 regulation, whilst Notch-3 is thought to act through HEY-1 (Haruki *et al*, 2005; Konishi *et al*, 2007; Lin *et al*, 2010). Intracellular Notch-3 has previously been shown to be a poor activator of HES-1 and HES-5, and in fact to act as a repressor by blocking Notch-1-mediated activation of HES-1 and HES-5 promotors *in vitro* (Beatus *et al*, 1999). Competition for access to RBK-Jκ/CSL, or for a common co-activator, may explain these findings. Notch-3 and Notch-4 are known to be structurally divergent from Notch-1 and Notch-2, lacking the transactivation domain in the cytoplasmic portion of the receptor (Radtke *et al*, 2004), and unlike Notch-1, Notch-3 contains 34 instead of 36 EGF-like repeats

(Bellavia *et al*, 2008). Despite these data, no negative correlation between Notch-3 and HES-1 was found in this study. Nuclear Notch-1 was found to be negatively correlated with cytoplasmic Notch-4 in this study, as were nuclear Notch-4 and cytoplasmic Notch-1. No data exist in the literature examining this relationship, however this may suggest a negative feedback relationship or antagonism between the two receptor pathways – these data need validating with *in vitro* experiments. Similarly, nuclear Notch-3 and cytoplasmic Notch-4 were found to be positively correlated. This may be a coincidental finding or suggest a relationship between the two pathways. Again this would need further investigation with *in vitro* experimentation.

Although the correlation of Notch expression with tumour characteristics has been recently investigated in several malignancies (Chang *et al*, 2010; Jung *et al*, 2010; Donnem *et al*, 2010; Wang *et al*, 2009a and 2010b), this is the first study to examine these relationships in pancreatic adenocarcinoma. Although neither Notch-1 nor Notch-4 provided any significant associations, nuclear Notch-3 expression was associated with the presence of local lymph node metastases in resected pancreatic adenocarcinoma specimens. Similarly, nuclear HEY-1 expression was associated with the presence of nodal metastases, and perineural and microvascular invasion. Nuclear HES-1 was associated with a trend towards being associated with perineural invasion. These data would suggest that Notch activation, particularly through HEY-1 is associated with a more aggressive tumour phenotype. HEY-1 is the main target of Notch-3, which itself has been found to be associated with lymph node metastases in patients with ovarian carcinoma (Jung *et al*, 2010). Buchler *et al* (2005) demonstrated increased expression of the Notch pathway ligand, Jagged 1, particularly in areas of perineural invasion and invasion into surrounding tissues. In combination with serial increase in nuclear Notch receptor and target protein expression seen in advanced pancreatic

adenocarcinoma compared to early disease, this suggests that the Notch pathway is involved in tumour invasion and metastasis.

This study demonstrates nuclear HEY-1 to be predictive of overall and disease-free survival, independent of other known prognostic indicators. In other words, nuclear HEY-1 expression may serve as a potential biomarker for prognosis prediction. Identifying biomarkers of prognosis may help guide use of adjuvant therapies following surgery and may uncover novel therapeutic targets. Notch pathway activation in tumour cells has been associated with clinical outcome in other solid tumours (Table 3.13), including transitional cell carcinoma of the bladder (Shi *et al*, 2008), breast (Jubb *et al*, 2010), lung (Donnem *et al*, 2010), ovarian (Jung *et al*, 2010), prostatic (Santagata *et al*, 2004), and renal cell carcinoma (Wu *et al*, 2011). In addition to nuclear HEY-1 expression, nuclear Notch-3 expression was also included in the multivariate survival analysis, but did not quite reach significance. Notch-3 is known to act through HEY-1 (Haruki *et al*, 2005; Konishi *et al*, 2007), and this suggests that the Notch-3 pathway is important in the progression of pancreatic adenocarcinoma. A pilot study in which the author was involved found nuclear Notch-3 expression to be associated with unresectability – 0 of 10 patients with nuclear Notch-3 expression were resectable, compared to 6 of 13 without nuclear Notch-3 staining (Doucas *et al*, 2008. This however, was a much smaller series of patients (23 vs. 92 patients). Notch-3 has been shown to be important in several solid tumours (Pierfelice *et al*, 2011; Haruki *et al*, 2005), and Notch-3 gene amplifications (19p13.12) have been detected in breast (Yamaguchi *et al*, 2008) and ovarian carcinoma (Park *et al*, 2006), although this has yet to be detected in pancreatic adenocarcinoma. It has also been associated with a poor prognosis in ovarian carcinoma (Jung *et al*, 2010), and resistance to carboplatin chemotherapy (Park *et al*, 2010). The mechanisms by which the Notch-3 pathway contribute to tumour progression have yet to be

determined, however it has been reported to prevent apoptosis by cross-talking with the MAPK pathway and regulating Bim (Konishi *et al*, 2010), and also by acting through the proto-oncogene, Pbx1 (Park *et al*, 2008)

The predictive power of isolated molecular biomarkers is very limited. Combining groups of molecular biomarkers, along with the more traditional clinical and pathophysiological data is likely to be superior and might lead to a robust and accurate assessment of cancer prediction and prognosis. This study demonstrated that nuclear HEY-1 expression combined with CA 19.9 levels can be used to create a score which allows stratification of prognosis following resection of pancreatic adenocarcinoma. Other molecular prognostic markers in pancreatic carcinoma (reviewed in Garcea *et al*, 2005) need to be investigated in this, and larger, cohorts of patients in order to develop an optimal panel of biomarkers for prognostication.

This study has several potential limitations. Firstly it involved retrospective collection of data and this has meant that the clinicopathological data set was partially incomplete. Due to the nature of the disease, the number of patients with resectable pancreatic carcinoma used in the study was small, however the series is comparable or greater in number than the majority of studies of pancreatic adenocarcinoma in the literature. It is likely that expanding the patient numbers may provide further associations, however this would necessitate multicentre cooperation. There has been some concern with regards to antigen degradation in formalin-fixed, paraffin-embedded tissue (Vis *et al*, 2000; Xie *et al*, 2011). Attempts were made to limit this by only using specimens collected since 2000; however this will always remain a limitation of this type of research.

In summary, these data demonstrate that the Notch pathway is up-regulated in pancreatic carcinoma, and that a progressive up-regulation is seen with advanced disease. They also demonstrate that in particular activation of Notch-3 through its target gene, HEY-1, is associated with an aggressive tumour phenotype and an adverse prognosis. This suggests that these markers may have a future role as prognostic biomarkers.

Table 3.13 – Studies examining the relationship of the Notch pathway as prognostic biomarkers in solid malignancies

Tumour	Study	N	Specimen	Method	Marker	Univariate	Multivariate*
Bladder	Shi *et al*, 2008	70	Tissue	IHC	Notch-1	Increased DFS	N.S
					Notch-2	N.S	-
					Notch-3	N.S	-
					Jagged-1	Increased DFS	HR 3.09
					DLL-1	N.S	-
Breast	Jubb *et al*, 2010	156	Tissue	IHC	DLL-4	Reduced OS	HR 1.55
	Reedijk *et al*, 2008a	887	Tissue	RT-PCR	Jagged-1	Reduced DFS	-
	Dickson *et al*, 2007	127	Tissue	IHC	Jagged-1	Reduced OS	-
			Tissue	RT-PCR	Jagged-1	Reduced OS	-
	Reedijk *et al*, 2005	50	Tissue	mRNA ISH	Notch-1	Reduced OS and DFS	-
					Notch-3	Reduced OS	-
					Jagged-1	Reduced OS	-
					Notch-2	N.S	-
					Notch-4	N.S	-
					Jagged-2	N.S	-
					DLL-1	N.S	-
					DLL-3	N.S	-
					DLL-4	N.S	-
	Parr *et al*, 2004	97	Tissue	IHC/RT-PCR	Notch-1	Reduced OS	-
					Notch-2	Increased OS	-
Cervical	Yeasmin *et al*, 2010	70	Tissue	IHC	Notch-3 (nuclear)	Reduced OS	N.S
Colon	Reedijk *et al*, 2008	130	Tissue	IHC	HES-1	N.S	-
Gastric	Yeh *et al*, 2009	96	Tissue	IHC	Notch-1	N.S	-
					Jagged-1	Reduced OS	-
Head and Neck	Lin *et al*, 2010a	59	Tissue	IHC	Notch-1	Reduced OS	-
					Jagged-1	Reduced OS	-
NB	Chang *et al*, 2010	85	Tissue	IHC	Notch-1	Reduced OS	HR 2.69

Table 3.13 cont.

NSCLC	Donnem *et al*, 2010	335	Tissue	IHC	Notch-1 (tumour)	Reduced DSS	N.S
					Notch-4 (tumour)	Reduced DSS	HR 1.55
					Notch-4 (stromal)	Increased DSS	N.S
					Jagged-1 (stromal)	Increased DSS	N.S
					DLL-4	Increased DSS	HR 1.89
	Haruki *et al*, 2005	207	Tissue	IHC	Notch-3	N.S	
Ovarian	Park *et al*, 2010	78	Effusion	RT-PCR	Notch-3	Reduced OS and PFS†	Not done
	Jung *et al*, 2010	75	Tissue	IHC	Notch-3	Reduced OS	HR 9.36
					Jagged-1		N.S
					Jagged-2		N.S
	Wang *et al*, 2010c	61	Tissue	IHC	HES-1	Reduced OS and DFS	N.S
					HES-5	N.S	N.S
Prostate	Santagata *et al*, 2004	95	Tissue	IHC	Jagged-1	Reduced DFS	HR 3.51
RCC	Wu *et al*, 2011	129	Tissue	IHC	Jagged-1	Reduced OS and DFS	OS HR 2.56
							DFS HR 2.4

NB, Neuroblastoma, NSCLC, non-small cell lung cancer; RCC, renal cell carcinoma; IHC, immunohistochemistry; RT-PCR, reverse transcriptase, polymer chain reaction; ISH, *in-situ* hybridisation; DLL, delta-like; DFS, disease-free survival; OS, overall survival; DSS, disease-specific survival; PFS, progression free survival; N.S, not significant; -, not performed; HR, hazards ratio; *hazards ratio only given if found to be independently prognostic on multivariate analysis; † in patients with recurrent disease on carboplatin chemotherapy

CHAPTER 4

POTENTIAL THERAPEUTIC MODULATION

OF THE NOTCH PATHWAY

4.1 INTRODUCTION

As data suggesting Notch plays an important role in the carcinogenesis of several malignancies emerge, attention has focused towards potential therapeutic modulation of this pathway. Inhibition of the gamma secretase enzyme responsible for liberating the active intracellular fragment (ICN) of the Notch receptor is an attractive proposition. Gamma secretase inhibitors (GSIs) were initially developed for Alzheimer's disease to reduce β-amyloid accumulation and have proved safe and generally well tolerated in clinical trials (Siemers *et al*, 2006 and 2007; Fleisher *et al*, 2008).

Much interest has focused on the therapeutic potential of this class of agents in haematological malignancies, with *in vitro* data suggesting benefit in T-cell acute lymphoblastic leukaemia (T-ALL) (Lewis *et al*, 2007; De Keersmaecker *et al*, 2008; O'Neil *et al*, 2006; Kindler *et al*, 2008), β-cell chronic lymphocytic leukaemia (Rosati *et al*, 2009), β-lymphoma (Lan *et al*, 2006), and myeloma (Nefedova *et al*, 2008). In further *in vitro* studies, gamma secretase inhibition has also been shown beneficial in a range of solid malignancies, including ovarian carcinoma (Park *et al*, 2006), breast carcinoma (Zang *et al*, 2007; Farnie *et al*, 2007; Nam *et al*, 2008; Osipio *et al*, 2008) both oestrogen-receptor positive (Rizzo *et al*, 2008) and negative (Lee *et al*, 2008), cholangiocarcinoma (Ishimura *et al*, 2005), hepatoma (Suwanjunee *et al*, 2008), lung carcinoma (Konishi *et al*, 2007), colon carcinoma (Zhang H *et al*, 2008), osteosarcoma (Zhang *et al*, 2008a), and Kaposi's sarcoma (Curry *et al*, 2005 and 2007). GSIs are currently commencing clinical trials in patients with T-cell acute lymphoblastic leukaemia (Deangelo *et al*, 2006) and breast carcinoma (Merck)

Few data exist regarding the effect of treatment with gamma secretase inhibitors in pancreatic adenocarcinoma cell lines. The experiments described in this chapter examined the effects of GSI treatment on Notch expression and on cell proliferation, viability, cell cycle and apoptosis, in addition to treatment in combination with other anti-cancer agents. They also investigate the effect of individual Notch receptor knockdown on the cell lines.

4.2 RESULTS

4.2.1 Basal Notch protein expression in human pancreatic carcinoma cell lines

It was initially important to determine the basal levels of Notch protein expression in the four pancreatic carcinoma cell lines when grown under normal conditions, in order to see whether levels were easily and reproducibly detectable, and significantly different between cell lines.

Figure 4.1 depicts basal level of Notch-1, -3, and -4 under normal growth conditions in the ASPC-1, BxPC-3, MIAPaCa-2, and PANC-1 cell lines. All four cell lines expressed the active intracellular Notch-1 (ICN-1; ~110kDa) to some degree, with ASPC-1, BxPC-3 and MIAPaCa-2 cells showing relatively greater expression than PANC-1 cells. In addition, a second band was observed below the 110kDa band in all cell lines, particularly in the PANC-1 cell line. This band has previously been identified in other cell lines in the literature (Callahan *et al*, 2000), and may represent either an isoform of the intracellular active portion of the Notch-1 receptor, or an intermediate degradation product. A band representing the full length Notch-1 receptor is shown at greater than 200kDa (exact weight 272.5kDa) in all four cell lines.

Active Notch-3 (ICN-3) is represented by a band at ~120kDa. Active Notch-3 was expressed very strongly by ASPC-1, however expression was only very weak in the other three cell lines examined. Similar to the Notch-1 electrophoresis, two additional bands were seen at a very similar molecular weight. These have not been previously

reported, however again are likely to represent isoforms of the active Notch-3. A band representing the full length Notch-3 protein was detected after running the bands further down the gel, at >200kDa (exact weight 244kDa; Figure 4.1b).

The active intracellular portion of Notch-4 (ICN-4) is represented by a band at ~60kDa. Active Notch-4 was expressed by both MIAPaCa-2 and PANC-1 cell lines. When the film was hyper-exposed, a small amount of active Notch-4 was expressed by ASPC-1 cells. BxPC-3 cells did not express Notch-4 protein.

Attempts were made to assess the Notch-2 status of these four cell lines. Despite numerous attempts to optimise antibodies against Notch-2 from several manufacturers no clear bands were identified in any cell lines, therefore it was decided to continue investigation into Notch-1, -3, and -4. Three of these cell lines were taken forward for further experiments based on their combination of Notch protein expression and suitability for the assays to be used.

a)

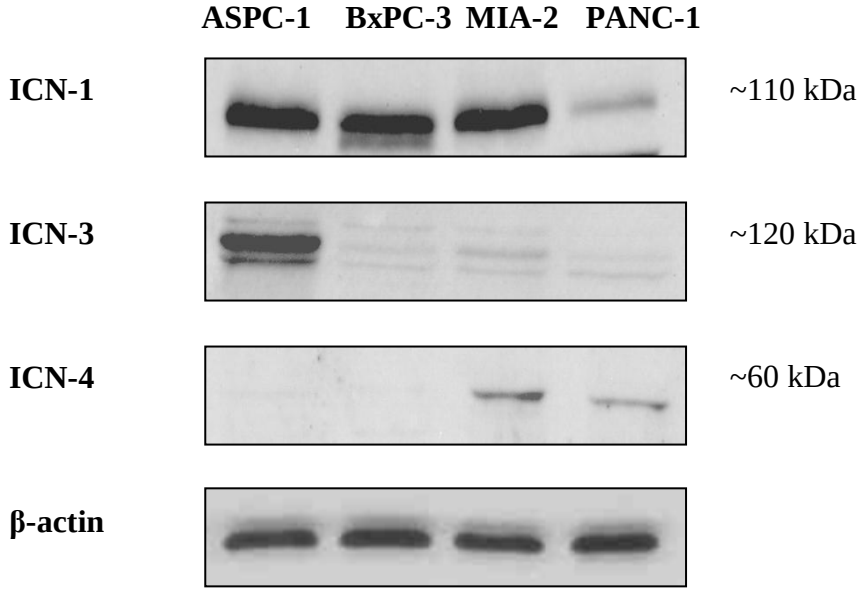

b)

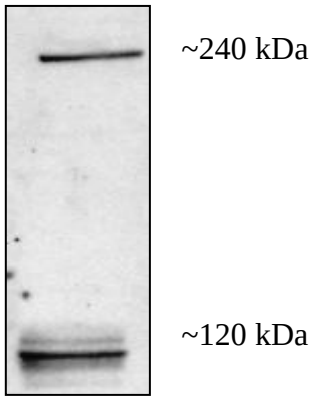

Figure 4.1 – Basal Notch protein expression
a) Western blots demonstrating basal expression of the active intracellular portions (ICN) of Notch-1, -3 and -4 in four pancreatic carcinoma cell lines grown to 70% confluence, b) western blot demonstrating full length Notch-3 in ASPC-1 cells

4.2.2 The effect of gamma secretase inhibition in pancreatic carcinoma cells – treatment with L-685,458 (GSI-X)

L-685,458 (GSI-X; {1S-benzyl-4R-[1-(1S-carbamoyl-2-phenethylcarbamoyl)-1S-3-methylbutylcarbamoyl]-2R-hydroxy-5-phenylpentyl}carbamic acid *tert*-butyl ester; Figure 4.2) has previously been reported to be a potent non-competitive inhibitor of gamma secretase activation by binding to presenilin and functioning as a transition state analog mimic at the catalytic site of an aspartyl protease (Doerfler *et al*, 2001; Li *et al*, 2000; Shearman *et al*, 2000; Tian *et al*, 2002; Weidemann *et al*, 2002). It has been shown to have 50-100 fold greater selectivity for gamma secretase than other aspartyl proteases (Shearman *et al*, 2000). L-685,458 has been shown inhibit release of active intracellular Notch-1 (Figueroa *et al*, 2002; Ikeuchi T *et al*, 2002; Martys-Zage *et al*, 2000) and the Notch target genes HES-1 and HEY-1 (Dahlqvist *et al*, 2003; Kang *et al*, 2005; Zayzafoon *et al*, 2004). L-685,458 also dose-dependently inhibited the growth of human tongue carcinoma Tca8113 cells by inducing G_0-G_1 cell cycle arrest and apoptosis (Yao *et al*, 2007).

Treatment with L-685,458 resulted in a small down-regulation of active intracellular Notch-3 (ICN-3) expression in ASPC-1 cells, but did not affect expression of ICN-1 or ICN-4 in any cell line (Figure 4.2). No significant effect was seen on cell growth or cell viability following treatment with L-685,458 (Figure 4.3). Apoptosis was not detected to a significant level in any of the pancreatic carcinoma cell lines. This was the case for concentrations up to 20μM and treatment times up to 72 hours (Figure 4.3).

a)

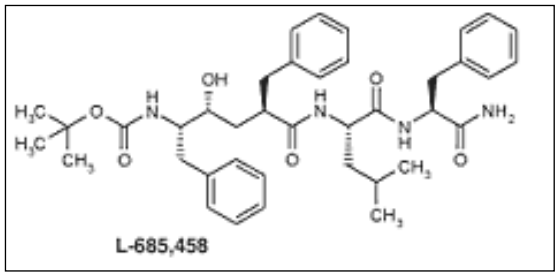

Molecular formula	Molecular weight
$C_{39}H_{52}N_4O_6$	672.85

b)

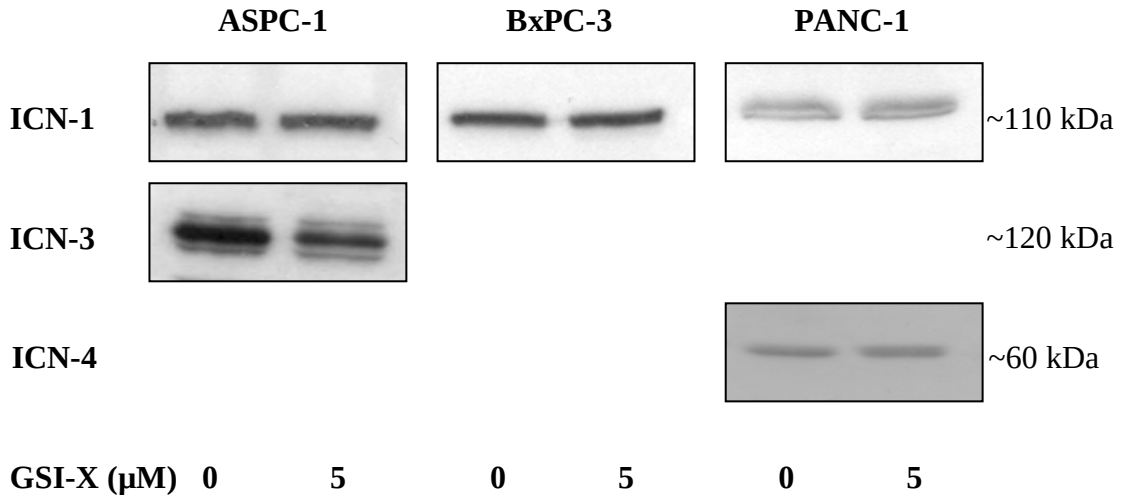

Figure 4.2 – Effect of the gamma secretase inhibitor L-685,458 (GSI-X) on Notch expression in pancreatic adenocarcinoma cell lines
a) Chemical structure of L-685,458 (GSI-X); b) Effect of 48 hours treatment with 5µM L-685,458 (GSI-X) or DMSO control on expression of active intracellular Notch-1, -3 and -4 in pancreatic adenocarcinoma cell lines *in vitro.*

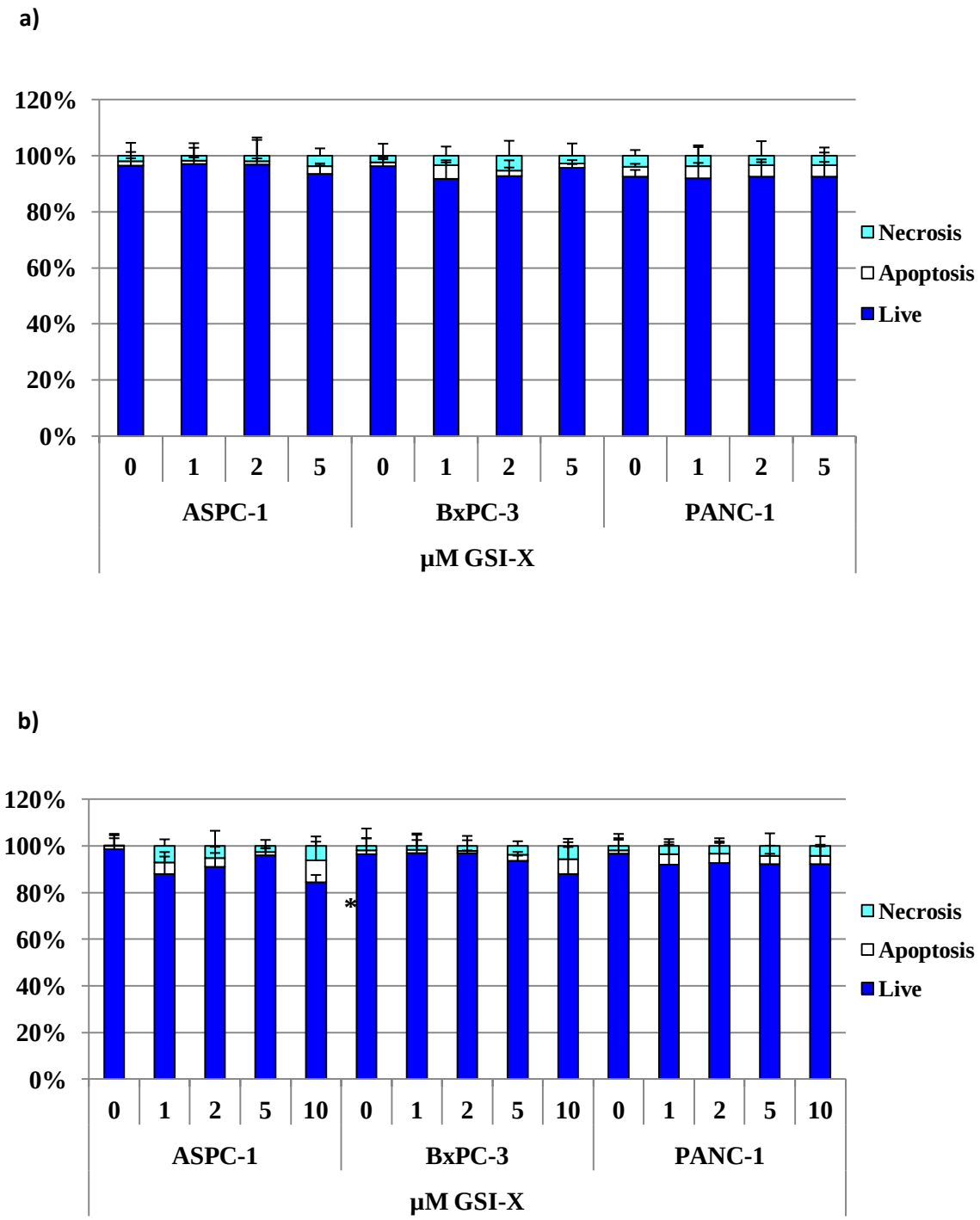

Figure 4.3 – Effect of GSI-X on pancreatic adenocarcinoma cell lines *in vitro*
Annexin V/PI staining of three pancreatic adenocarcinoma cell lines following treatment with increasing doses of GSI-X (µM) or DMSO control for a) 24 hours or b) 48 hours. Bars represent proportion of cells that are live (blue), apoptotic (white), and necrotic (cyan). Charts show mean and standard deviation. *$p<0.05$ compared to DMSO control.

4.2.3 The effect of gamma secretase inhibition in pancreatic carcinoma cells – treatment with Z-Leu-Leu-Nle-CHO (GSI-I)

A structurally distinct gamma secretase inhibitor was used to determine whether inhibition of Notch-1 and Notch-4 activation could be achieved. GSI-I (Z-Leu-Leu-Nle-CHO), is a tripeptide aldehyde inhibitor previously shown to be a potent inhibitor of Notch pathway activation. It has been shown to block Notch-1, Notch-2 and Notch-4 activation in Kaposi's sarcoma cells (Curry *et al*, 2005). This was associated with induction of G_2-M cell cycle arrest followed by apoptosis, an effect which was abrogated by enforced expression of ICN-1, ICN-2 or ICN-4 by retroviral vector transduction (Curry *et al*, 2005; 2007). GSI-I treatment also resulted in growth inhibition or tumour regression, associated with apoptosis, in a murine xenograft model of Kaposi's sarcoma (Curry *et al*, 2005), and reduced cell proliferation and induced apoptosis in ovarian carcinoma cell lines over-expressing Notch-3 (Park *et al*, 2006)

Treatment with GSI-I resulted in a dose-dependent reduction in expression of ICN-1 in all cell lines following 48 hours of treatment (figure 4.4). ICN-3 expression was reduced in ASPC-1 following 48 hours of treatment. ICN-4 expression was reduced in PANC-1 cell line following 48 hours of treatment. Treatment with GSI-I also inhibited expression of the target protein HES-1 in a dose-dependent manner in all cell lines. Treatment with GSI-I resulted in a significant reduction in proportion of live cells and induction of apoptosis compared to DMSO control or treatment with GSI-X in all three cell lines. All further experiments were therefore carried out with GSI-I.

a)

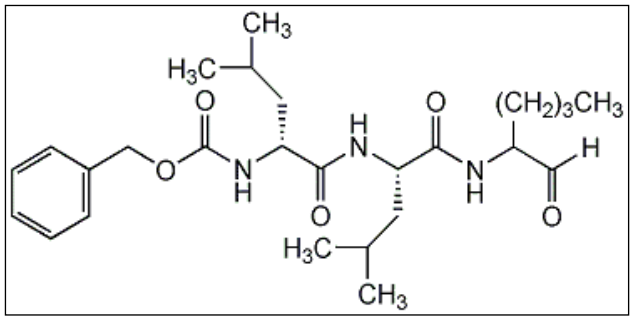

Molecular formula	Molecular weight
$C_{26}H_{41}N_3O_5$	475.6

b)

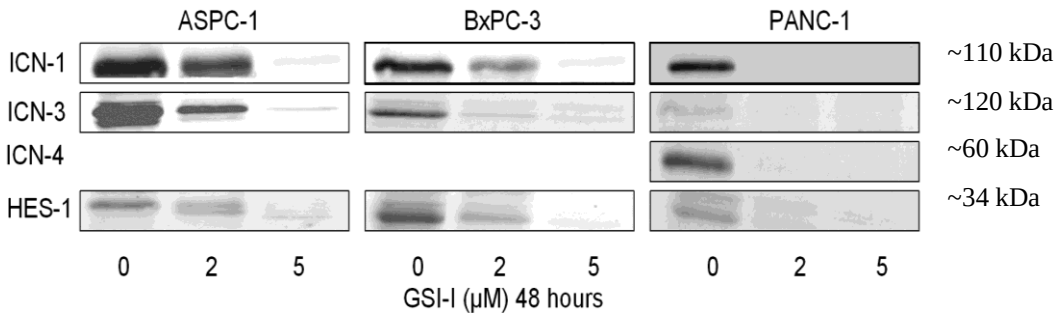

c)

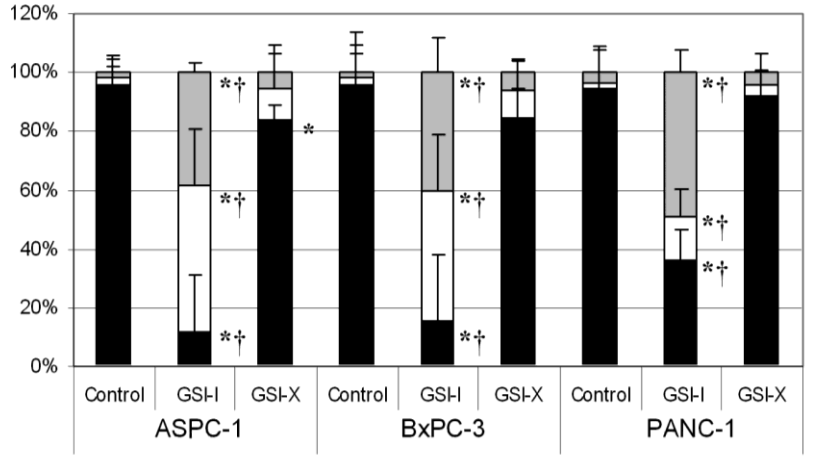

Figure 4.4 – Effect of GSI-I on pancreatic adenocarcinoma cell lines *in vitro*

a) Chemical structure of Z-Leu-Leu-Nle-CHO (GSI-I);
b) Western blots showing effect on active intracellular Notch (ICN)-1, -3, -4 and HES-1 following treatment with GSI-I for 48 hours in ASPC-1, BxPC-3, and PANC-1 pancreatic adenocarcinoma cell lines;
c) Annexin V/PI staining to assess apoptosis and necrosis in cells treated with either 10μM GSI-I or 10μM GSI-X for 48 hours. Bars represent proportion of cells that are live (black), apoptotic (white), and necrotic (grey). Charts show mean and standard deviation. *p<0.05 compared to DMSO; †p<0.05 compared to GSI-X.

4.2.3.1 Cell viability

The effect of GSI-I on cell viability was next determined, using ATP levels as an endpoint as described in 2.5.7.1. Figure 4.5 illustrates the reduction in cellular ATP levels following treatment of the pancreatic carcinoma cell lines ASPC-1, BxPC-3, and PANC-1 with GSI-I, and shows a clear difference in sensitivity among the cell lines.

ASPC-1 was the most sensitive line, followed by BxPC-3, with PANC-1 the most resistant. Following 72 hours of treatment with 10μM, ATP levels were <1% of DMSO control in ASPC-1 cells, compared to 2% in BxPC-3 and 15% in PANC-1 cells. Treatment resulted in a dose- and time-dependent reduction in cell viability in all cell lines. Approximate IC_{50} values were calculated for all 3 cell lines by plotting the luminescence as a percent of the DMSO control against increasing GSI-I concentrations (Table 4.1).

Table 4.1 – IC_{50} values for a panel of pancreatic carcinoma cell lines following treatment with GSI-I.

	24 hours	**48 hours**	**72 hours**
ASPC-1	2.78μM	0.89μM	0.68μM
BxPC-3	4.40μM	2.85μM	1.59μM
PANC-1	9.55μM	6.92μM	3.65μM

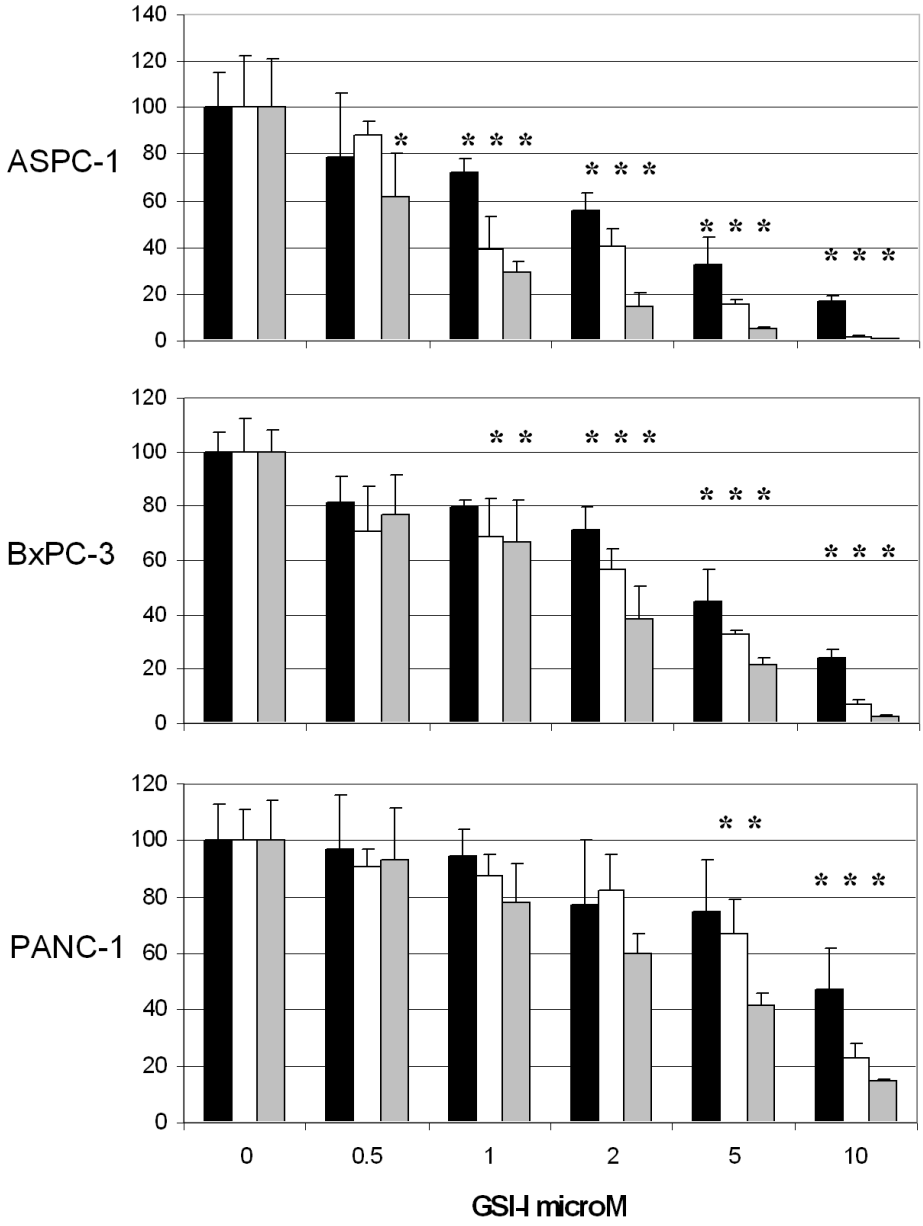

Figure 4.5 – Effect of GSI-I on cell viability in pancreatic adenocarcinoma cells
ATP levels following treatment for 24 (black bars), 48 (white bars) and 72 hours (grey bars) of treatment with GSI-I. Charts show mean and standard deviation. *p<0.05 compared to DMSO control.

4.2.3.2 Cell proliferation

Cell growth and proliferation assays were performed over a period of 72 hours to determine if GSI-I possessed cytostatic activity. Treatment resulted in reduced cellular proliferation as measured by cell count. Sensitivity was in the order ASPC-1>BxPC-3>PANC-1 (205-fold, 66-fold and 51-fold respectively, following treatment with 5μM (Figure 4.6).

4.2.3.3 Cell cycle analysis

To further investigate the decrease in proliferation, flow cytometric analysis was used to determine the DNA content following treatment with GSI-I. This analysis indicates whether the inhibition of proliferation induced by GSI-I was due to alterations in cell cycle distribution and at which point in the cell cycle this occurred. Only adherent live cells were analysed, excluding late apoptotic and necrotic floating cells, which would accumulate in the sub-G_1 area.

Cell cycle arrest is characterised by an accumulation of cells within specific areas of the cell cycle, which can be demonstrated by alterations in the peaks obtained after analysis of DNA of treated cells compared to controls. Following 8 and 12 hours of treatment with GSI-I, no significant alteration in cell cycle distribution was apparent in any cell line (data not shown). Following 24 hours of treatment, ASPC-1 demonstrated

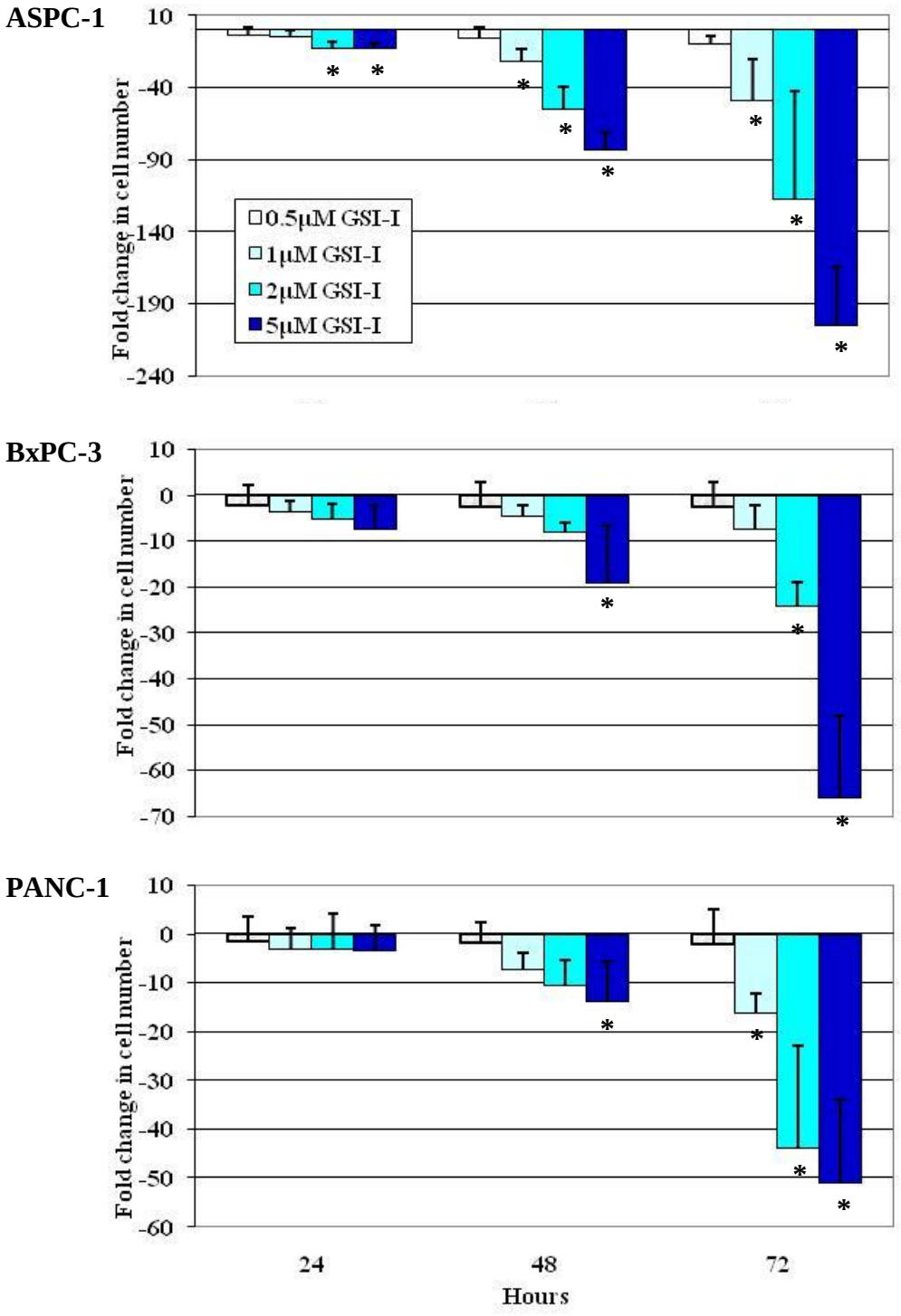

Figure 4.6 – Effect of GSI-I on proliferation in pancreatic adenocarcinoma cells
Cell proliferation measured by cell count following treatment with GSI-I. Data are expressed as change compared to DMSO control. Charts show mean and standard deviation. *$p<0.05$ compared to DMSO control.

significant accumulation in G_2/M at doses of 1μM and greater (42% at 5μM; Figure 4.7). Interestingly at 1μM, a significant increase of cells in G_1 was also seen (19% increase), suggesting combined G_1 and G_2M arrest at this dose. BxPC-3 and PANC-1 both demonstrated significant increases in G_2M population at doses of 1μM and above, with both lines having >70% of cells in G_2M after treatment with 5μM. In all cell lines, arrest was maintained at 72 hours following treatment (data not shown). Bar charts demonstrating the percentage of cells in each phase of the cell cycle following 24 hours of treatment with increasing concentrations of GSI-I are shown in Figure 4.7.

4.2.3.4 Assessment of apoptosis in response to GSI-I

To determine the extent of apoptosis occurring in response to treatment with GSI-I, the ASPC-1, BxPC-3 and PANC-1 cells were stained with FITC-conjugated annexin V and PI (described in 2.5.7.2). Figure 4.4c shows the comparative effects upon apoptosis of treating the three cell lines with GSI-I or L-685,458. Treatment with 10μM GSI-I resulted in a significant reduction in the live cell population compared to treatment with L-685,458 of DMSO control, associated with significant induction of apoptosis and increase in necrotic cells in all three cell lines.

The induction of apoptosis following treatment with GSI-I was confirmed via a time course of treatment up to 24 hours with 5μM (Figure 4.8). ASPC-1 and BxPC-3 demonstrated a time-dependent increase in apoptosis, with apoptosis first occurring

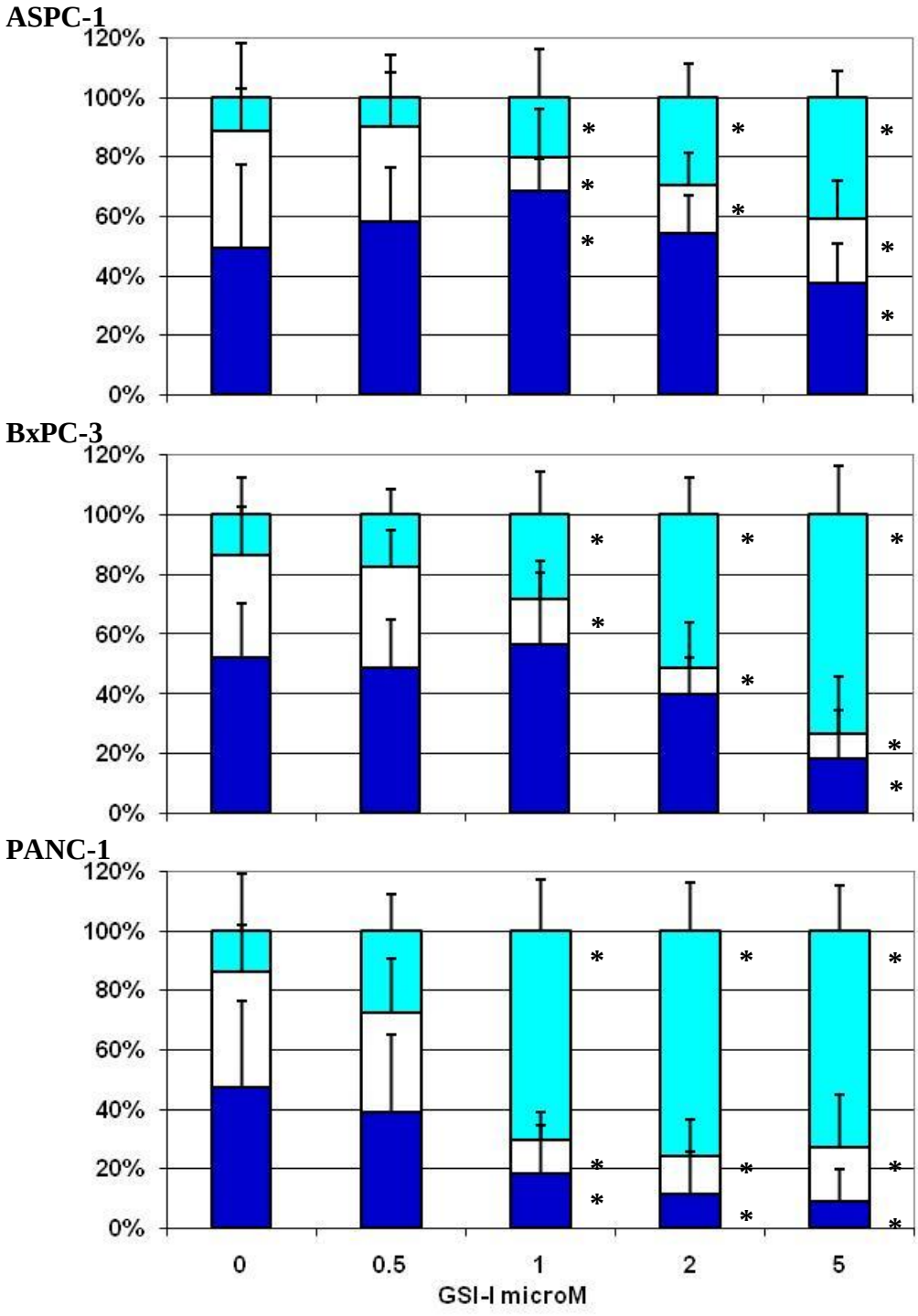

Figure 4.7 – Effect of GSI-I on cell cycle in pancreatic adenocarcinoma cells.
FACS cell cycle analysis of PI stained cells following treatment for 24 hours. (blue bars=G_1; white bars=S; cyan bars=G_2/M). *$p<0.05$ compared to DMSO control.

after 4 hours of treatment in ASPC-1 cells, reaching significant levels in both cell lines after 8 hours of treatment. PANC-1 demonstrated a significant increase in necrosis by 20 hours without significant induction of apoptosis.

Figure 4.9 demonstrates annexin V/PI results following treatment with increasing doses of GSI-I. Following 24 hours of treatment, PANC-1 cells exhibited the least sensitivity to GSI-I, undergoing a significant 18% increase in necrosis after treatment with 5μM and 45% with 10μM, with only a 9% increase in apoptosis occurring upon treatment with 10μM. In contrast, BxPC-3 underwent a significant 21% increase in apoptosis and 10% increase in necrosis after treatment with 1μM. ASPC-1 was the most sensitive line, with a significant 16% increase in apoptosis and 12% increase in necrosis after treatment with 0.5μM.

Effector Caspase 3/7 activity is another measure of apoptosis which can be used to corroborate data from annexin V/PI binding. Significant induction of caspase 3/7 activity was seen following 24 hours treatment with 0.5μM GSI-I in ASPC-1 cells and 1μM in BxPC-3 cells (Figure 4.11). Significant induction of caspase 3/7 activity only occurred following treatment with 5μM GSI-I for 24 hours in PANC-1 cells.

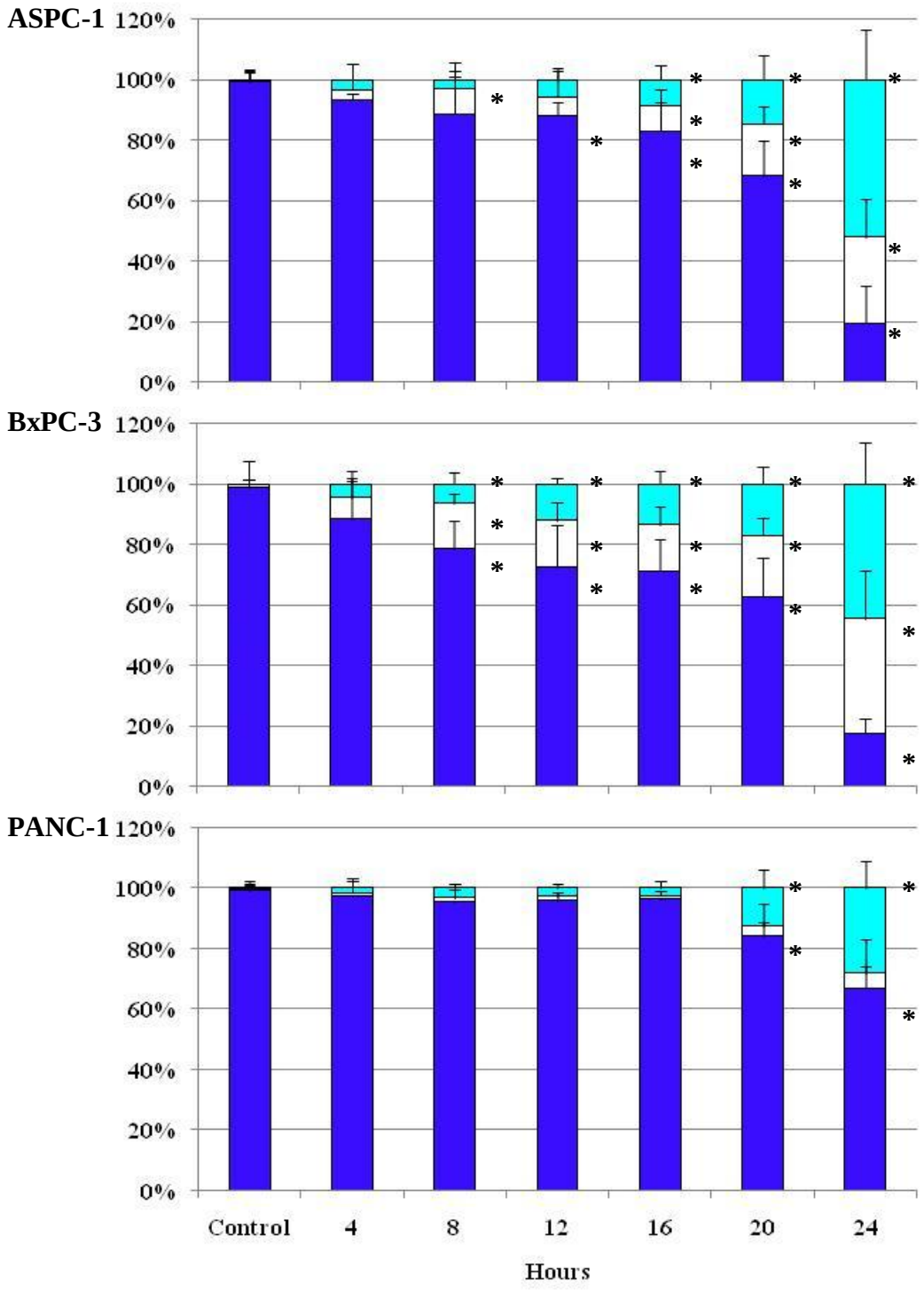

Figure 4.8 – Effect of GSI-I on apoptosis in pancreatic adenocarcinoma cells at early time points.
Annexin V/PI staining for apoptosis in cell lines treated for up to 24 hours with 5µM GSI-I. Blue bars represent live, white bars apoptotic, and cyan bars necrotic populations. *$p<0.05$ compared to DMSO control.

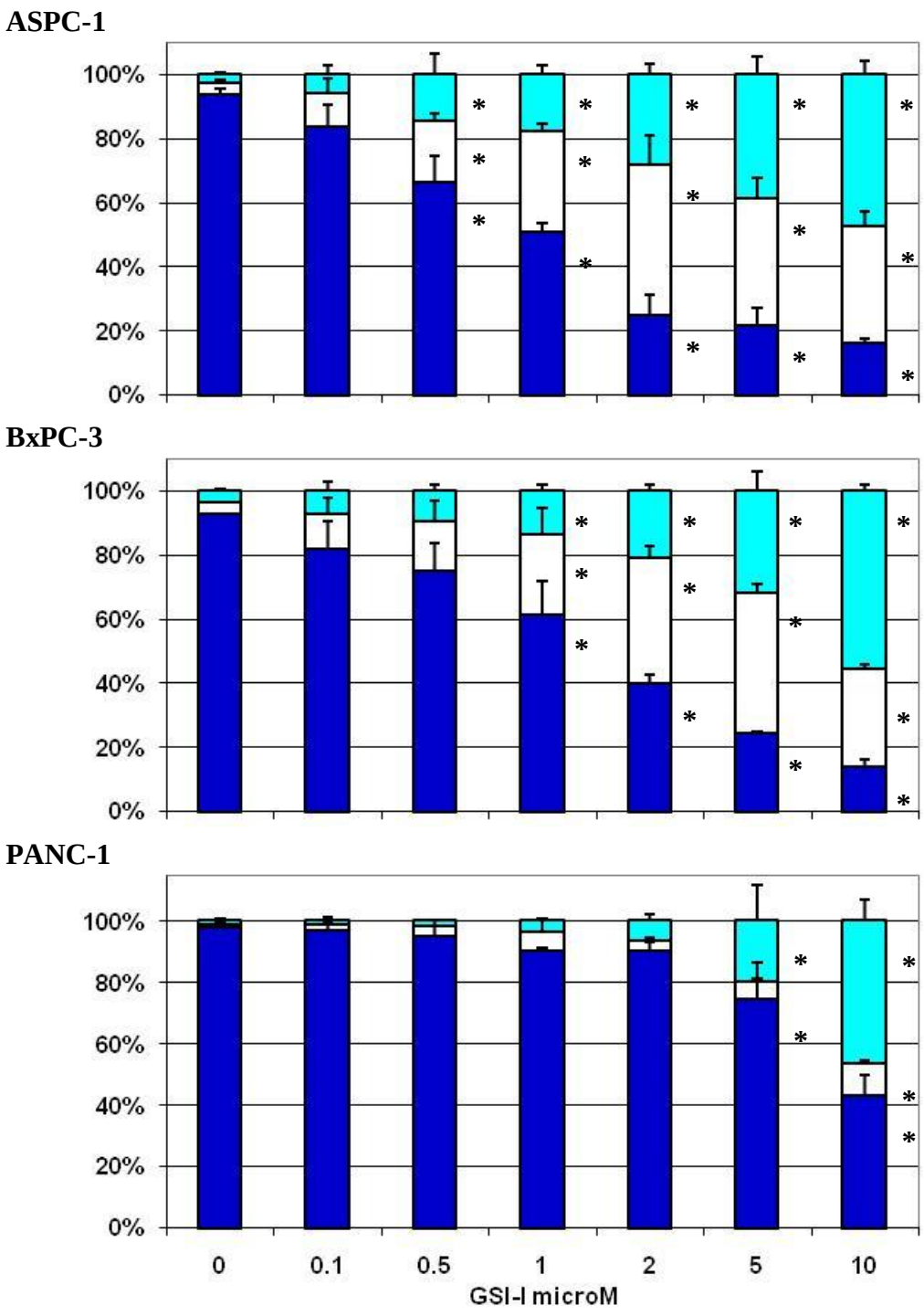

Figure 4.9 – Effect of GSI-I on apoptosis in pancreatic adenocarcinoma cells. Annexin V/PI staining for apoptosis in cell lines treated for 24 hours with GSI-I. Blue bars represent live, white bars apoptotic, and cyan bars necrotic populations. *$p<0.05$ compared to DMSO control.

The cell lines were exposed to GSI-I for longer periods of time to determine the effect of prolonged treatment on apoptosis and necrosis. Figure 4.10 demonstrates treatment of ASPC-1, BxPC-3 and PANC-1 cell lines with GSI-I for 48 and 72 hours. By 72 hours, very few live ASPC-1 (2%) or BxPC-3 (5%) cells remained following treatment with 5μM and with only 18% in the PANC-1 line.

4.2.4 The effect of curcumin on pancreatic carcinoma cell lines

Curcumin is a promising dietary agent with chemopreventive and chemotherapeutic potential. It has been shown to induce apoptosis in a variety of cancer cell lines (Howells *et al*, 2007). It has previously been shown to augment the cytotoxic effects of gemcitabine in pancreatic adenocarcinoma cell lines (Kunnumakkara *et al*, 2007; Li *et al*, 2005). This polyphenol has also been shown to inhibit Notch-1 activity in BxPC-3 and PANC-1 cell lines (Wang *et al*, 2006c), however the effect on other Notch protein expression has not been investigated. Treatment with curcumin resulted in a small reduction in ICN-1 expression in the three lines (Figure 4.12a – displays western blot for ASPC-1 cells). It also resulted in decreased ICN-3 in ASPC-1 and ICN-4 in PANC-1 cells, inhibiting Notch-3 with greater potency than 1 or 4. A small reduction in HES-1 expression was seen in all cell lines following treatment with 5μM for 48 hours (Figure 4.12a – displays western blot for ASPC-1 cells).

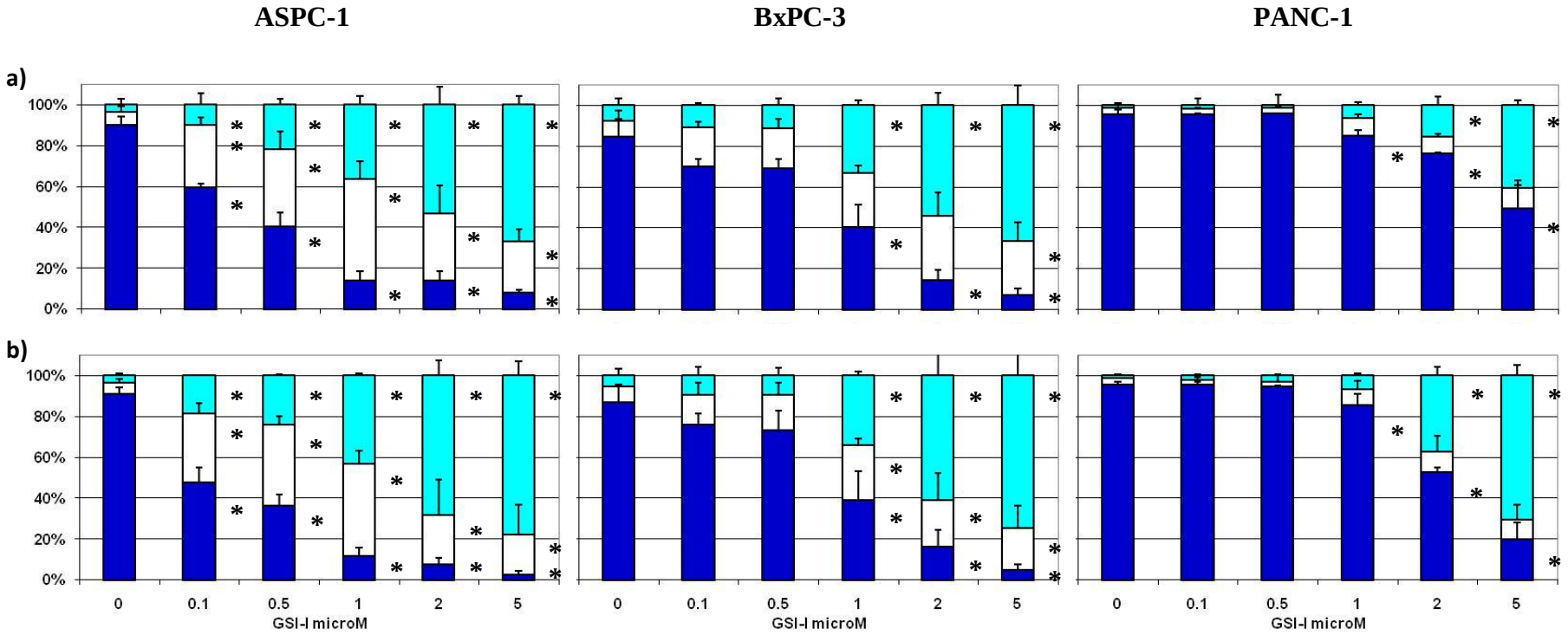

Figure 4.10 – Effect of prolonged treatment with GSI-I on apoptosis in pancreatic adenocarcinoma cells.
Annexin V/PI staining for apoptosis in cell lines treated for a) 48 and b) 72 hours with GSI-I. Blue bars represent live, white bars apoptotic, and cyan bars necrotic populations. *$p<0.05$ compared to DMSO control.

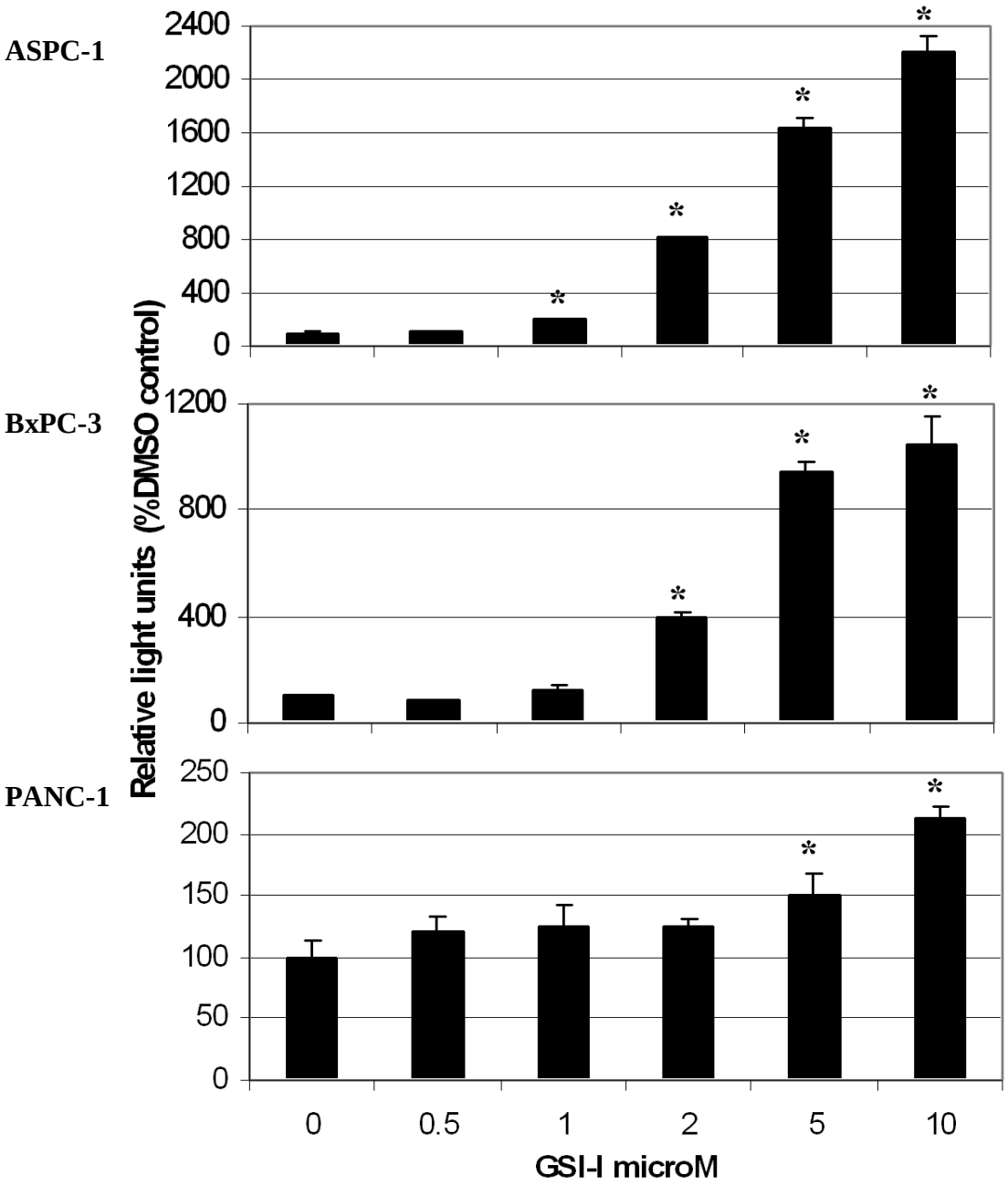

Figure 4.11 – Caspase 3/7 activation following treatment with GSI-I.
ASPC-1, BxPC-3, and PANC-1 pancreatic adenocarcinoma cell lines were treated for 24 hours. *$p<0.05$ compared to DMSO control.

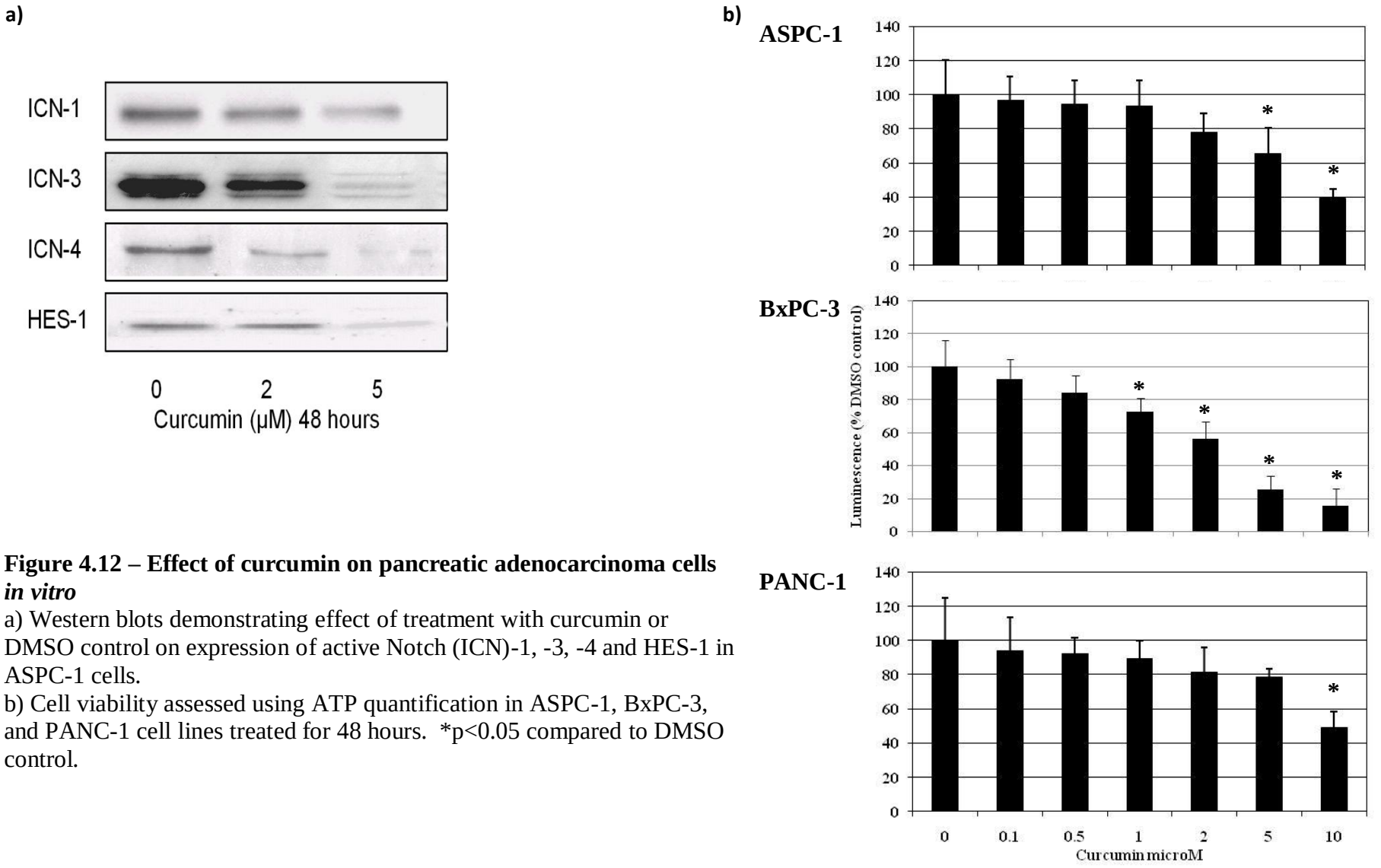

Figure 4.12 – Effect of curcumin on pancreatic adenocarcinoma cells *in vitro*

a) Western blots demonstrating effect of treatment with curcumin or DMSO control on expression of active Notch (ICN)-1, -3, -4 and HES-1 in ASPC-1 cells.

b) Cell viability assessed using ATP quantification in ASPC-1, BxPC-3, and PANC-1 cell lines treated for 48 hours. *$p<0.05$ compared to DMSO control.

Treatment with curcumin for 48 hours resulted in a reduction in cell viability in all three cell lines investigated (Figure 4.12b). BxPC-3 was the most sensitive cell line, with a significant reduction following treatment with 1µM and an IC_{50} of 2.60µM. ASPC-1 was the next most sensitive cell line, with a significant reduction in viability following treatment with 5µM and an IC_{50} of 7.99µM. PANC-1 was the least sensitive line, with a significant reduction in viability seen following treatment with 10µM of curcumin and an IC_{50} of 9.85µM.

Curcumin was shown to induce apoptosis in both ASPC-1 and BxPC-3 cell lines following treatment for 48 hours (Figure 4.13). BxPC-3 was the most sensitive cell line, with a significant reduction in live cell population associated with induction of apoptosis following treatment with 2.5µM for 48 hours. A significant induction of apoptosis was seen in ASPC-1 cells following treatment with 5µM for 48 hours. No significant reduction in live cell population or induction of apoptosis was seen in PANC-1 cells treated for 48 hour with 10µM (Figure 4.16). When treated with higher doses of curcumin for 72 hours, a larger proportion of ASPC-1 and BxPC-3 cells became necrotic (Figure 4.13).

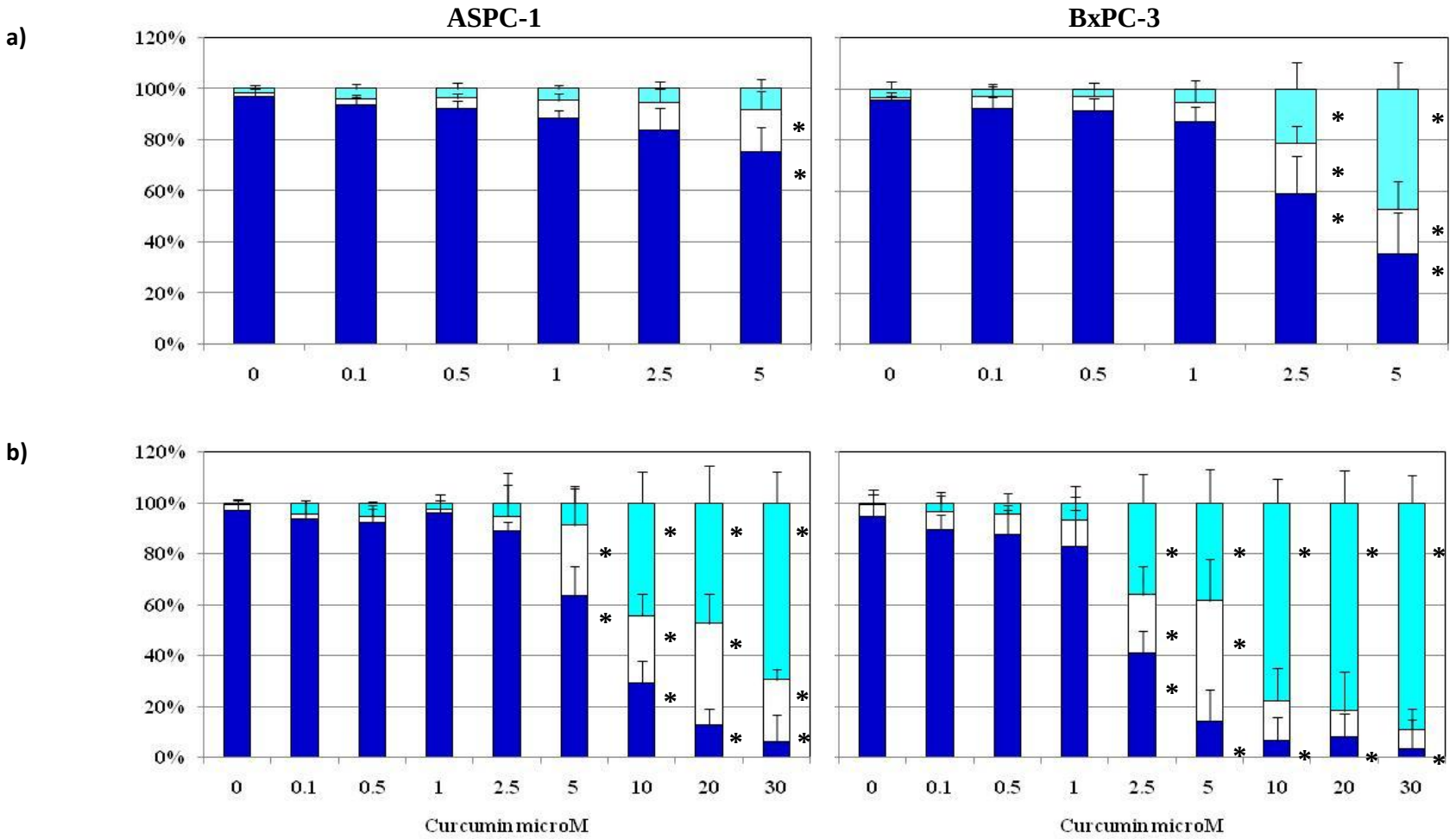

Figure 4.13 – Effect of curcumin on apoptosis in pancreatic adenocarcinoma cells
Annexin V/PI staining for apoptosis in ASPC-1 and BxPC-3 pancreatic cancer cell lines treated for a) 48 and b) 72 hours with curcumin. Blue bars represent live, white bars apoptotic, and cyan bars necrotic populations. *$p<0.05$ compared to DMSO control.

4.2.5 Combination treatment with GSI-I and gemcitabine

Gemcitabine is currently the first line of chemotherapy for patients with advanced pancreatic adenocarcinoma. The effect of gemcitabine on Notch protein expression was assessed. Treatment with gemcitabine for 48 hours had no effect on ICN-1, -3, -4 or HES-1 expression, suggesting, as expected, that its effects are independent of the Notch pathway (data not shown). The effectiveness of GSI-I in combination with gemcitabine *in vitro* was next determined. ASPC-1 and BxPC-3 cells responded to treatment with 100nM of gemcitabine for 48 hours, with 51% and 31% reduction in ATP levels respectively (Figures 4.14; 4.15). PANC-1 was relatively more resistant to gemcitabine with a 17% reduction (Figure 4.16). Combined treatment with GSI-I and gemcitabine resulted in significantly greater reduction in ATP levels compared to treatment with either agent alone in all three cell lines (Figures 4.14-4.16).

The contribution of apoptosis to these findings was next investigated using annexin V staining, which demonstrated significant reduction in live cells in ASPC-1 and BxPC-3 cell lines treated with the combination compared to either agent alone (Figures 4.14; 4.15). This was associated with an increase in apoptotic and necrotic cells. PANC-1 cells demonstrated a reduction in live cells, associated with an increase in necrotic cells on treatment with both GSI-I and gemcitabine compared to treatment with gemcitabine alone (Figure 4.16). Combined treatment resulted in an additional 11% reduction in live cells compared to GSI-I alone, however this failed to reach significance ($p=0.24$). Annexin V assay data were corroborated by measurement of effector caspase (3/7) activity, demonstrating greater activity in ASPC-1 and BxPC-3 following treatment with both agents compared to either alone (Figure 4.17). No

induction of caspase activity was seen in PANC-1 following treatment with gemcitabine. Induction of caspase activity was seen following treatment with both gemcitabine and GSI-I, however this was similar to that following GSI-I alone.

4.2.6 Combination treatment with GSI-I and curcumin

Combination treatments may act in additive or synergistic fashion, lowering the doses required for pharmacological activity, with the potential to minimise toxicity. The combination of curcumin and GSI-I was therefore assessed in the three pancreatic carcinoma cell lines, ASPC-1, BxPC-3, and PANC-1. Treatment with curcumin resulted in a significant reduction in viability in all three cell lines (sensitivity BxPC-3>ASPC-1>PANC-1; Figures 4.14-4.16). Combination treatment with GSI-I and curcumin resulted in significant reduction in viability compared to treatment with either agent alone in all cell lines, and this combination was more effective than GSI-I with gemcitabine.

Annexin V staining was used to assess the contribution of apoptosis to these findings. Combined treatment in ASPC-1 cells resulted in a significant reduction in live cells, associated with an increase in apoptotic and necrotic cells compared to treatment with either agent alone (Figure 4.14). Combined treatment in BxPC-3 resulted in a significant reduction in live cells, associated with an increase in necrotic cells compared to treatment with either agent alone. However no change in the apoptotic population was seen (Figure 4.15). Despite the significant reduction in ATP levels seen upon treatment of PANC-1 cells with 10μM curcumin, no significant change in

the percentage of live, apoptotic or necrotic cells was seen, suggesting a cytostatic rather than cytocidal effect (Figure 4.16). Combination treatment resulted in a significant reduction in live cells compared to curcumin alone, and an additional 18% reduction in live cells compared to GSI-I alone, although this failed to reach statistical significance ($p=0.08$). Caspase 3/7 activity was significantly increased in ASPC-1 cells following treatment with curcumin and GSI-I compared to either agent alone (Figure 4.17). In BxPC-3 cells, although there was induction of caspase 3/7 activity following treatment with both agents, this was similar to either agent alone. PANC-1 demonstrated no additional induction of caspase 3/7 activity with both agents over GSI-I alone.

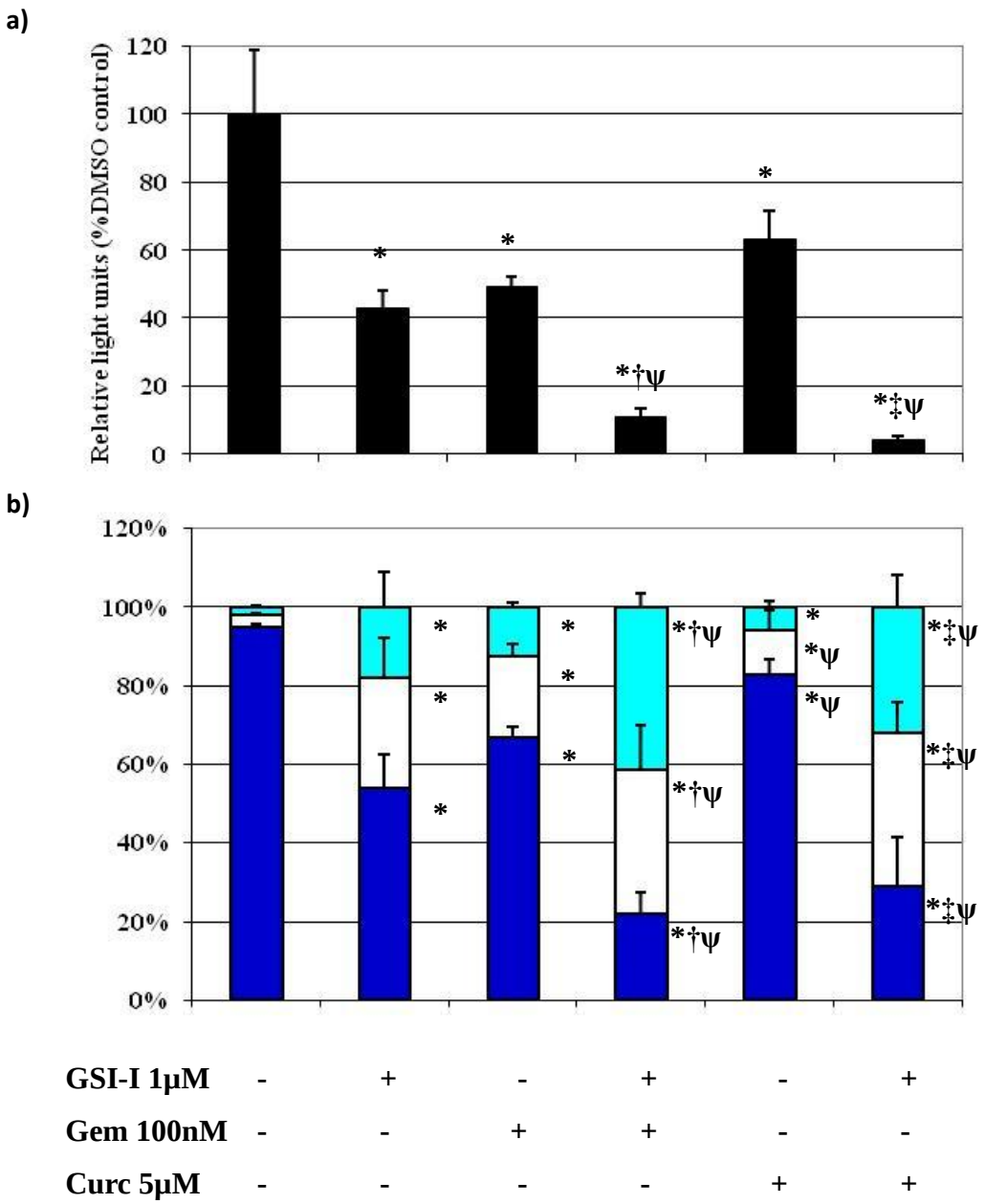

Figure 4.14 – Effect of combining GSI-I with gemcitabine or curcumin in ASPC-1 cells.

a) ATP levels following treatment with GSI-I +/- gemcitabine or curcumin for 48 hours. b) Apoptosis as assessed by AnnexinV/PI staining following treatment for 48 hours (Blue bars represent live, white bars apoptotic, and cyan bars necrotic populations). *p<0.05 compared to DMSO control; †p<0.05 compared to treatment with gemcitabine alone; ‡p<0.05 compared to treatment with curcumin alone; ψp<0.05 compared to GSI-I alone.

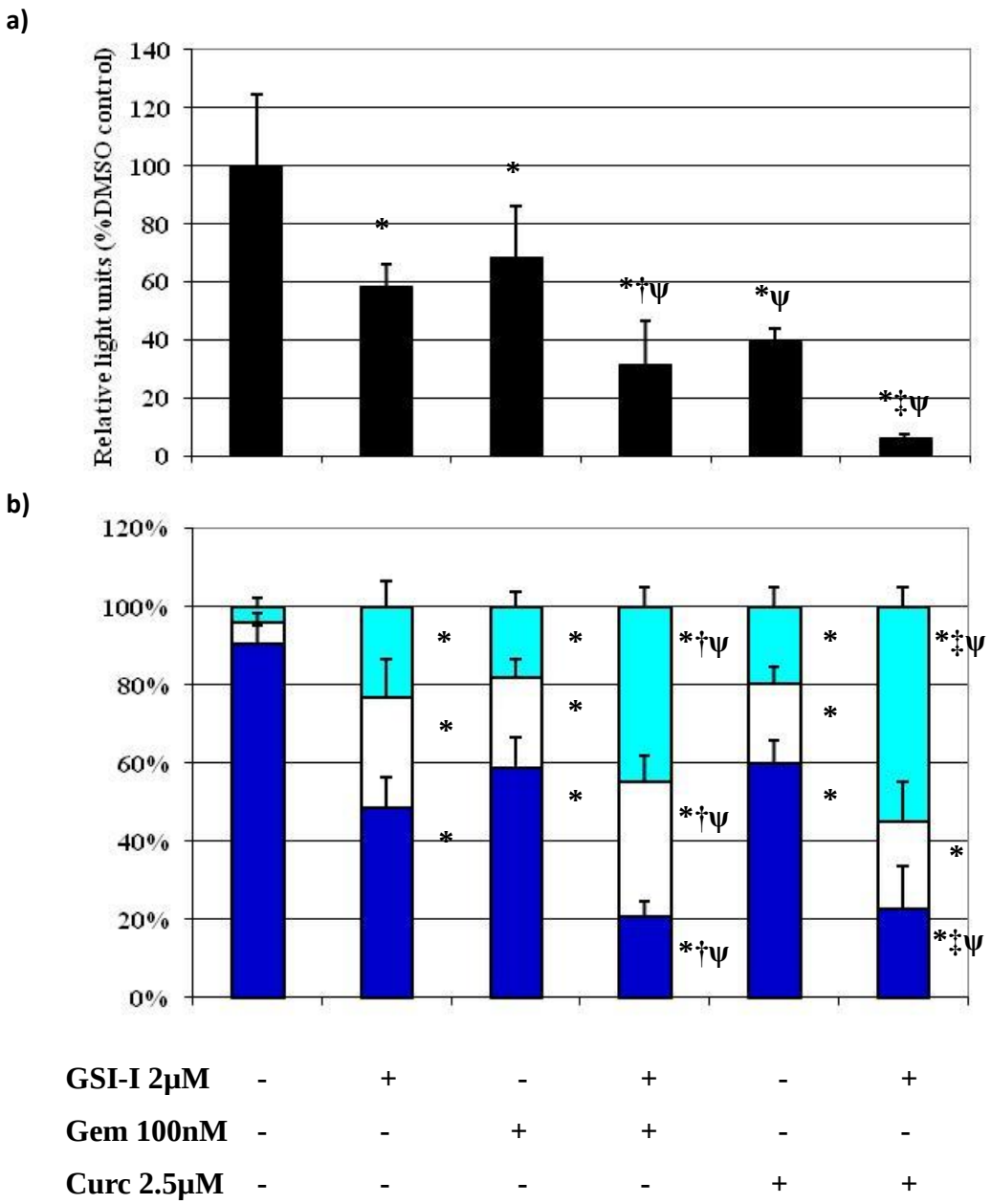

Figure 4.15 – Effect of combining GSI-I with gemcitabine or curcumin in BxPC-3 cells.

a) ATP levels following treatment with GSI-I +/- gemcitabine or curcumin for 48 hours. b) Apoptosis as assessed by AnnexinV/PI staining following treatment for 48 hours (Blue bars represent live, white bars apoptotic, and cyan bars necrotic populations). *p<0.05 compared to DMSO control; †p<0.05 compared to treatment with gemcitabine alone; ‡p<0.05 compared to treatment with curcumin alone; ψp<0.05 compared to GSI-I alone.

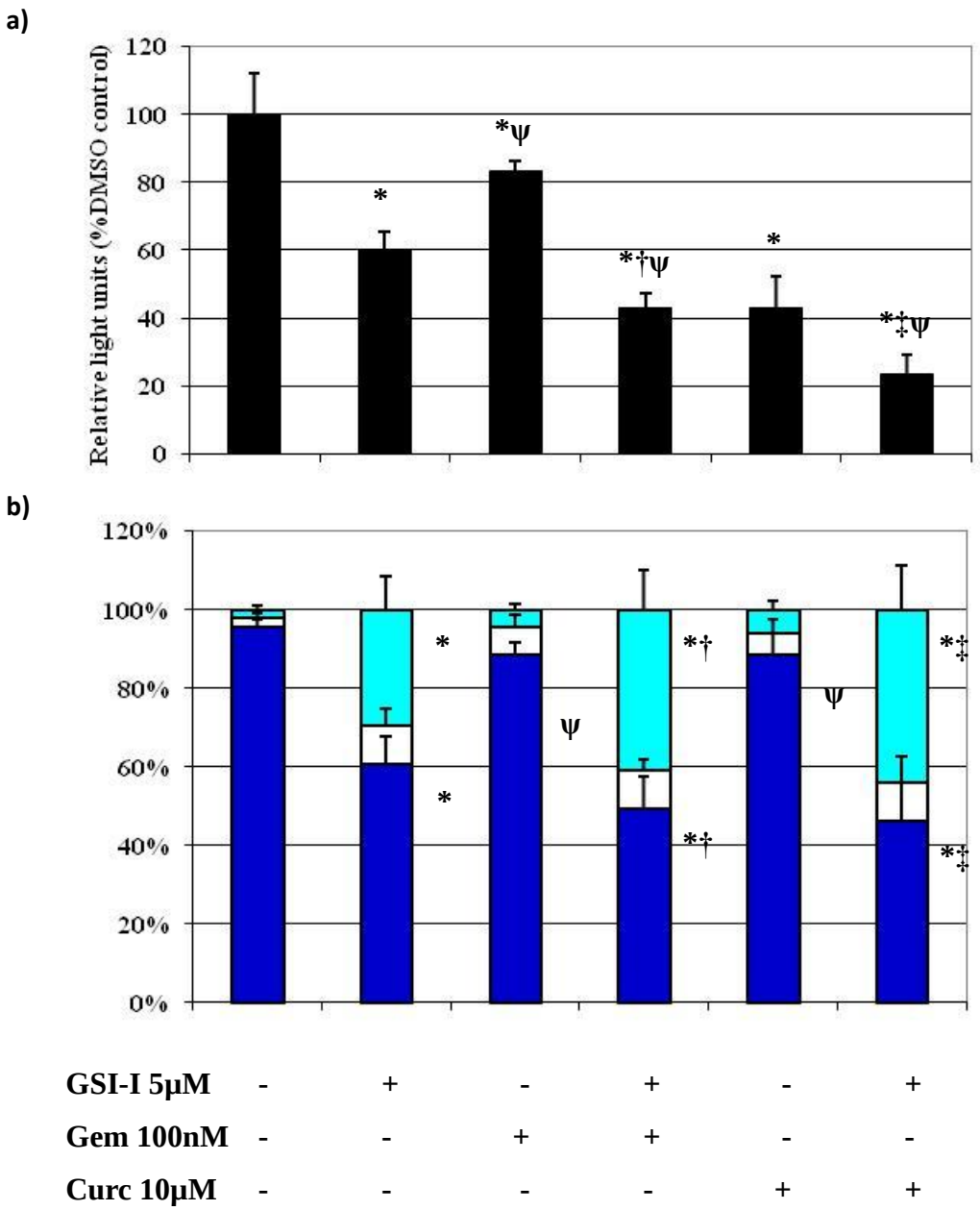

Figure 4.16 – Effect of combining GSI-I with gemcitabine or curcumin in PANC-1 cells.

a) ATP levels following treatment with GSI-I +/- gemcitabine or curcumin for 48 hours. b) Apoptosis as assessed by AnnexinV/PI staining following treatment for 48 hours (Blue bars represent live, white bars apoptotic, and cyan bars necrotic populations). *$p<0.05$ compared to DMSO control; †$p<0.05$ compared to treatment with gemcitabine alone; ‡$p<0.05$ compared to treatment with curcumin alone; ψ$p<0.05$ compared to GSI-I alone.

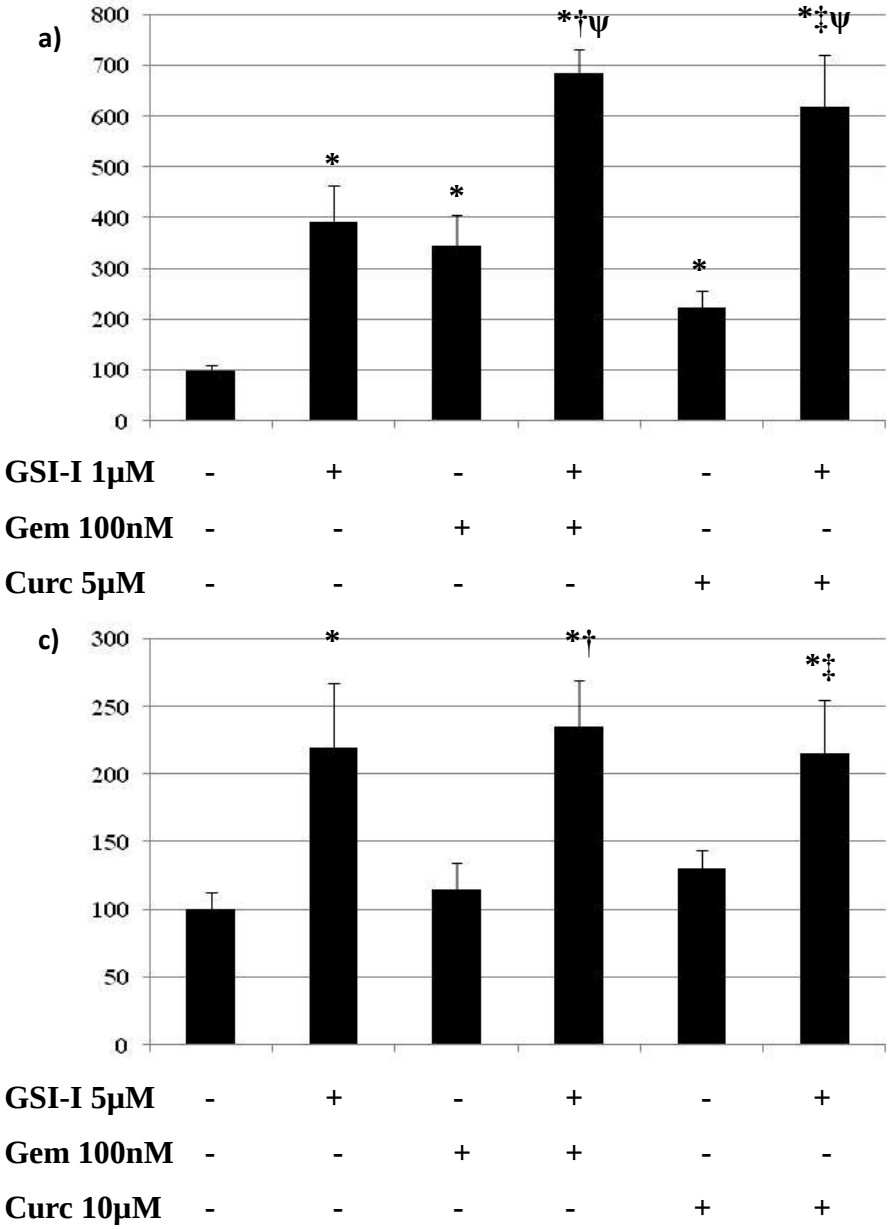

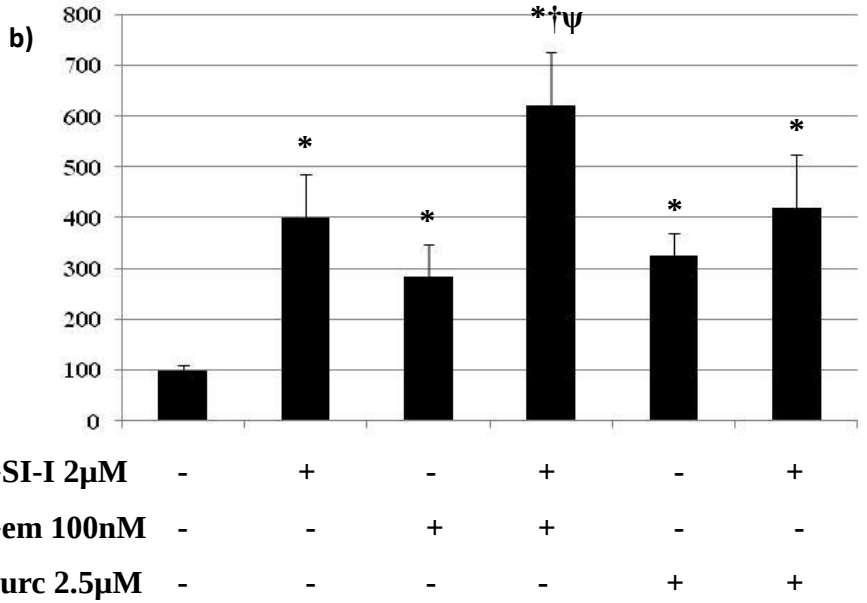

Figure 4.17– Caspase 3/7 activation following combination treatment of pancreatic adenocarcinoma cell lines.
Caspase 3/7 activation following 24 hours of treatment with combinations of GSI-I, curcumin and gemcitabine in a) ASPC-1; b) BxPC-3; and c) PANC-1 pancreatic cancer cell lines. *$p<0.05$ compared to DMSO control; †$p<0.05$ compared to treatment with gemcitabine alone; ‡$p<0.05$ compared to treatment with curcumin alone; ψ$p<0.05$ compared to GSI-I alone.

4.2.7 Microarray analysis following GSI-I treatment

To assess the effect of GSI-I on a larger array of genes, microarray analysis was performed on ASPC-1 cells following treatment with 5μM GSI-I for 12 and 24 hours in triplicate using GeneChip® Human Genome U133 Plus 2.0 arrays which allows the analysis of over 40,000 gene transcripts. Genes with ≥1.5 fold change and adjusted $p<0.05$ on Benjamini and Hochberg post-hoc analysis were considered. Alterations in 1068 and 713 genes were seen 12 and 24 hours of treatment respectively.

4.2.7.1 Effect of GSI-I on Notch-related genes

The effect of GSI-I on all genes classified by gene ontology as being involved in the Notch pathway was analysed (Table 4.2; Figure 4.18). Consistent with previous data in this chapter, GSI-I resulted in down-regulation of the target gene HES-1, as well as HEY-1, both ICN-CSL dependent targets. Similarly, PBX1 and NRARP have both previously been shown to be target genes of Notch, and both were found to be down-regulated. PBX1 has been shown to be essential for proliferation in ovarian carcinoma (Park *et al*, 2008) and to maintain myeloid progenitor cells in an undifferentiated state (Sykes *et al*, 2004). It has been found to be a target gene of Notch-3 in ovarian (Park *et al*, 2008), cervical (Yeasmin *et al*, 2010), and breast carcinoma (Xiao *et al*, 2011). The NRARP gene is also activated by Notch signalling, and acts as a negative feedback regulator, with its protein forming an inhibitory complex with ICN-CSL, blocking downstream gene transcription (Lamar *et al*, 2001; Krebs *et al*, 2001; Yun and Bevan, 2003; Pirot *et al*, 2004).

The Deltex genes allow Notch to act via a CSL-independent pathway and their transcription is regulated by Notch (Matsuno *et al*, 1995 and 1998). Consistent with this, Deltex-1 and -4 were both down-regulated following GSI-I treatment. Deltex-3 however was up-regulated. Little is known about the differing functions between the Deltex isoforms, with the majority of data in the literature pertaining to Deltex-1. Deltex-1 is known to be a Notch-1 target gene. However it also has Notch-independent mechanisms of expression (Matsuno *et al*, 1998). Deltex-1 acts in a negative feedback manner, targeting ICN-1 for ubiquitinisation and proteosome-mediated degradation (Zhang *et al*, 2010). HES-1 mediates this by direct transcriptional repression of the Deltex-1 promoter.

Alterations in the expression of a number of Notch inhibitors were also seen. NUMB and NUMBL were both up-regulated following gamma secretase inhibition. NUMB and NUMBL are known to be inhibitors of Notch (Frise *et al*, 1996). Chapman *et al* (2006) have previously demonstrated that not only do these two proteins inhibit Notch, but that also high levels of Notch inhibit NUMB and NUMBL through an ICN, but not HEY-1 or HES-1, -dependent mechanism. It would therefore make sense that a down-regulation of ICN following gamma secretase inhibition would result in the observed up-regulation of NUMB and NUMBL. Up-regulation was seen in a number of other inhibitors of the Notch pathway, including SEL1L, which is thought to be involved in targeting ICN-1 for ubiquitinisation (Li et al, 2010; Biunno *et al*, 2006), and the CSL co-repressors, CTBP1, HDAC2, and NCOR2. Differential expression was seen in CSL co-activators, with MAML3 and PCAF-1 up-regulated, and MAML2 and SNW1 down-regulated. It is not clear why these changes have

occurred. It may be that they are the result of 'extra-Notch' effects of gamma secretase inhibition, however further experimentation is needed.

Mind bomb and Fringe are both groups of genes that are important for interaction between the Notch receptors and their ligands. Mind bomb proteins are essential for Notch activation by Delta and Jagged ligands through promoting internalisation and endocytosis of the ligand in the signalling cell (Itoh *et al*, 2003; Koo *et al*, 2005). They were down-regulated following gamma secretase inhibition. Fringe (lunatic fringe, LFNG; manic fringe, MFNG; radical fringe, RFNG) are known to encode proteins with furose-specific β-1.3 N-acetylglucosaminyltransferase activity, which fucosylate the EGF-like repeats of the extracellular portion of Notch receptors, again necessary for Notch-ligand interaction. Both lunatic and manic fringe were down-regulated following GSI-I, however radical fringe was up-regulated. The explanations for these changes are not apparent; it may be that Mind bomb and lunatic and manic fringe are involved in a positive feedback loop following Notch activation, however no supporting data are present in the literature. Clearly if these targets are validated , this is an area for further research.

Table 4.2 – Microarray analysis of the effect of GSI-I on Notch-related gene expression in ASPC-1 pancreatic adenocarcinoma cells.

Gene symbol	Gene name	Change at 12 hours		Change at 24 hours	
		Fold change	Direction	Fold change	Direction
ADAM10	ADAM metalloprotease domain 10	1.55	Down	-	-
ADAM17	ADAM metalloprotease domain 17	1.57	Up	3.99	Up
CTBP1	C-terminal binding protein 1	1.52	Down	2.24	Up
DLL3	Delta-like-3	6.37	Down	2.99	Down
DTX1	Deltex homolog 1	3.89	Down	-	-
DTX3	Deltex 3 homolog	3.06	Up	2.89	Up
DTX4	Deltex 4 homolog	2.67	Down	1.67	Down
DVL2	Dishevelled homolog-2	-	-	1.52	Down
DVL3	Dishevelled homolog-3	-	-	1.5	Up
HDAC2	Histone deacetylase-2	-	-	2.56	Up
HES1	Hairy and enhancer of split-1	1.78	Down	2.32	Down
HEY1	Hairy/enhancer of split with YRPW motif-1	1.85	Down	1.99	Down
JAG1	Jagged-1	-	-	2.22	Up
JAG2	Jagged-2	2.55	Down	3.91	Down
LFNG	LFNG O-fucosylpeptide 3-beta-N-acetylglucosaminyltransferase	-	-	2.63	Down
MAML2	Mastermind-like 2	2.78	Down	-	-
MAML3	Mastermind-like 3	-	-	6.49	Up
MFNG	MFNG O-fucosylpeptide 3-beta-N-acetylglucosaminyltransferase	-	-	3.67	Down
MIB1	Mindbomb homolog 1	1.61	Down		
MIB2	Mindbomb homolog 2	7.44	Down	2.09	Down
NCOR2	Nuclear receptor co-repressor 2	1.95	Up	2.1	Up
NOTCH2	Notch homolog-2	1.98	Down	-	-
NOTCH3	Notch homolog-3	2.05	Down	-	-
NRARP	Notch-regulated ankyrin repeat protein	1.62	Down	2.07	Down
NUMB	Numb homolog	-	-	7.12	Up
NUMBL	Numb homolog-like	-	-	1.57	Up
PCAF	P300/CBP-associated factor	-	-	2.82	Up

Table 4.2 cont.

PSEN1	Presenilin-1	9.17	Down	3.03	Down
PSEN2	Presenilin-2	2.44	Down	2.08	Down
PBX1	PBX1 (Hypothetical LOC100131938)	4.3	Down	2.02	Down
RBPJ	Recombination signal binding protein for immunoglobulin kappa J region	-	-	2.45	Up
RBPJL	Recombination signal binding protein for immunoglobulin kappa J region-like	-	-	1.62	Up
RFNG	RFNG O-fucosylpeptide 3-beta-N-acetylglucosaminyltransferase	-	-	1.91	Up
SEL1L	Sel-1 suppressor of lin-12-like	1.84	Up	1.55	Up
SNW1	SNW domain containing 1	1.59	Down	-	-
TP63	Tumor protein p63	1.82	Down	4.8	Down

Up-regulated genes in red; down-regulated genes in green. - = no change. Genes with ≥1.5 fold change and adjusted $p<0.05$ on Benjamini and Hochberg post-hoc analysis were considered

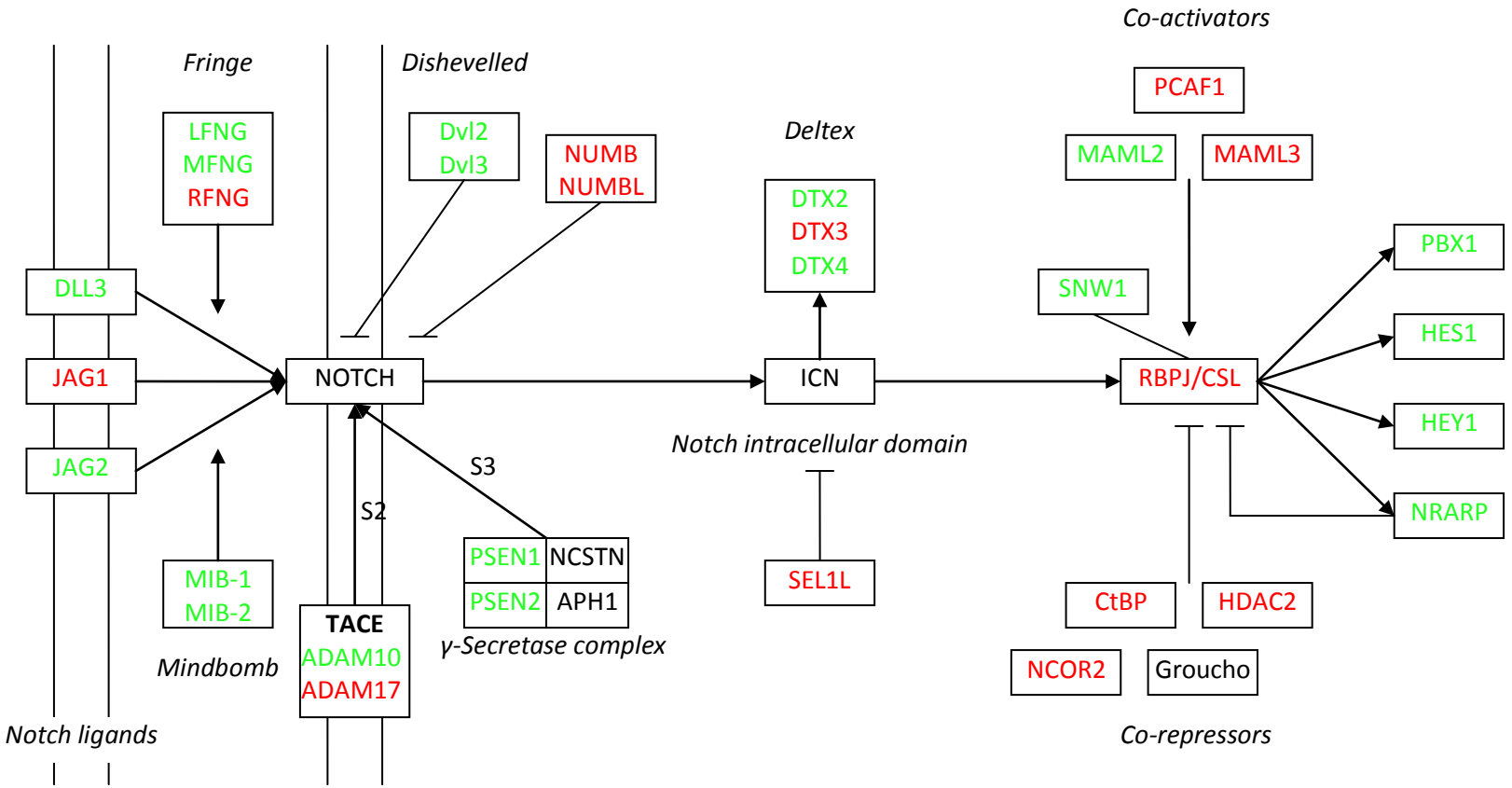

Figure 4.18 – Microarray analysis of the effect of gamma secretase inhibition using GSI-I on the Notch pathway in ASPC-1 cells. Up-regulated genes in red, down-regulated genes in green.

4.2.7.2 Effect of GSI-I on genes involved in cell cycle and apoptosis

To explain the effects of GSI-I reported in this chapter the data, the impact on genes involved in cell cycle and apoptosis was assessed using the microarray data. Following treatment with GSI-I, significant changes were found in 107 genes associated with cell cycle progression and 69 genes known to be involved in apoptosis.

Apoptosis was first seen in ASPC-1 cells after 8 hours following treatment with 5µM GSI-I. Up-regulation of multiple pro-apoptotic genes was seen on microarray after 12 hours of treatment, including AIFM2, ANXA1, BCL2L13, BTG1, CARD10, Clusterin, DAP3, DEDD2, FAF1, HIPK2, HSP1, PP1R15A, SH3KBP1, and Sequestrosome 1. Associated down-regulation was seen in a number of anti-apoptotic proteins, including BAG1, FAIM, NUAK2, Phosducin-like 3, SGPP1, SOCS2, and TNFAIP8.

In this study, GSI-I treatment resulted in G_2M cell cycle arrest in ASPC-1 cells, with an additional G_1 arrest at lower doses. Significant changes were found in genes that regulate the G_1/S and G_2/M transitions and thus may help to explain the findings seen. Cyclin D_1, cyclin D_2, CDK2, CDK4, and CDK6 were all down-regulated following treatment, the majority at 12 hours. These are all known to be important in G_1S progression (Ho *et al*, 2002). CDKN1A (p21) was up-regulated at 24 hours, and is known to inhibit cyclin-CDK2 and –CDK4 complexes. In addition, up-regulation of BCCIP was seen, over-expression of which is known to result in G_1 arrest by

enhancing the inhibitory activity of p21 towards CDK2 (Meng *et al*, 2004). Changes in several other G_1/S regulators were also seen. Accumulation of C11orf82 (Noxin) is also known to result in G_1 arrest, and this was up up-regulated following 12 hours of treatment (Nakaya *et al*, 2007). Accumulation of both HBP1 (Yee *et al*, 2004) and PML (Le *et al*, 1998) has previously been shown to inhibit exit from G_1; both were significantly up-regulated following GSI-I treatment. Similarly, RB1CC1 is known to block progression into S-phase via inducing Rb1 expression (Chano *et al*, 2002); this was again up-regulated following GSI-I treatment.

Alterations in the expression of several genes important in G_2/M were seen and may explain the arrest in this phase following treatment with GSI-I. Cyclin F (Bai *et al*, 1994) and CDCA3 (Ayad *et al*, 2003) are both required for progress in S-phase; both are down-regulated following GSI-I treatment. Cyclin B_1 and CDC2 are both required for entry into mitosis and are down-regulated after 24 hours treatment. CDKN1A (p21), which inhibits CDC2, is up-regulated. GADD45A which is known to result in G_2/M arrest by inhibiting CDC2 kinase activity, is also up-regulated (Jin *et al*, 2002). In addition, multiple genes which are known to be important for progress through mitosis are down-regulated following GSI-I treatment, including AURKA, AURKB, ANAPCM, BUB1B, BUB3, BORA (C13orf34), CDC20, FAM33A, FBXO5, KIF23, NEK2, and NSL1. Together these findings may explain the G_2M arrest seen in previous experiments.

Table 4.3 – Microarray analysis of the effect of GSI-I on cell-cycle gene expression in ASPC-1 pancreatic adenocarcinoma cells.

Gene symbol	Gene name	Change at 12 hours		Change at 24 hours	
		Fold change	Direction	Fold change	Direction
ANAPC13	Anaphase promoting complex subunit 13	2.00	Down	-	-
ANLN	Anillin, actin binding protein	1.73	Down	2.20	Down
APPL1	Adaptor protein, phosphotyrosine interaction, PH domain and leucine zipper containing 1	1.84	Down	-	-
ASNS	Asparagine synthetase	2.82	Up	-	-
AURKA	Aurora kinase A	-	-	1.91	Down
AURKB	Aurora kinase B	1.99	Down	-	-
BCCIP	BRCA2 and CDKN1A interacting protein	1.89	Up	-	-
BLM	Bloom syndrome	-	-	1.57	Down
BRCA2	Breast cancer 2, early onset	2.63	Down		
BUB1B	BUB1 budding uninhibited by benzimidazoles 1 homolog beta	-	-	2.03	Down
BUB3	BUB3 budding uninhibited by benzimidazoles 3 homolog	-	-	1.69	Down
C11orf82	Chromosome 11 open reading frame 82	1.85	Up	-	-
C13orf34	Chromosome 13 open reading frame 34	-	-	1.89	Down
CASP8AP2	CASP8 associated protein 2	1.61	Down	-	-
CCNB1	Cyclin B1	-	-	1.74	Down
CCNB2	Cyclin B2	-	-	2.37	Down
CCND1	Cyclin D1	2.53	Down	-	-
CCND2	Cyclin D2	3.41	Down	-	-
CCNF	Cyclin F	1.85	Down	-	-
CCNG1	Cyclin G1	1.59	Down	-	-
CDC2	Cell division cycle 2, G1 to S and G2 to M	-	-	2.43	Down
CDC20	Cell division cycle 20 homolog	-	-	2.10	Down
CDCA3	Cell division cycle associated 3	-	-	2.26	Down
CDCA5	Cell division cycle associated 5	-	-	2.19	Down
CDK2	Cyclin-dependent kinase 2	1.83	Down	-	-
CDK4	Cyclin-dependent kinase 4	-	-	2.68	Down
CDK6	Cyclin-dependent kinase 6	1.60	Down	-	-
CDKN1A	Cyclin-dependent kinase inhibitor 1A	-	-	3.85	Up
CDKN2	Cyclin-dependent kinase inhibitor 2A	1.56	Down	-	-

Table 4.3 cont.

CDKN3	Cyclin-dependent kinase inhibitor 3 (CDK2-associated dual specificity phosphatase)	-	-	1.82	Down
CIT	Citron (rho-interacting, serine/threonine kinase 21)	-	-	2.05	Down
CKS2	CDC28 protein kinase regulatory subunit 2	-	-	1.80	Down
DUSP1	Dual specificity phosphatase 1	5.18	Up	4.15	Up
EID1	EP300 interacting inhibitor of differentiation 1	2.44	Down	-	-
ERCC6L	Excision repair cross-complementing rodent repair deficiency, complementation group 6-like	-	-	2.55	Down
EXO1	Exonuclease 1	2.81	Down	2.78	Down
FAM33A	Family with sequence similarity 33, member A	1.88	Down	-	-
FBXO5	F-box protein 5	-	-	3.81	Down
GADD45A	Growth arrest and DNA-damage-inducible, alpha	2.31	Up	-	-
GAS7	Growth arrest-specific 7	5.67	Up	-	-
HBP1	HMG-box transcription factor 1	2.55	Up	2.66	Up
HELLS	Helicase, lymphoid-specific	-	-	2.18	Down
HEXIM1	Hexamethylene bis-acetamide inducible 1	-	-	1.59	Up
HMGA2	High mobility group AT-hook 2	3.51	Down	2.27	Up
HTATIP2	HIV-1 Tat interactive protein 2	-	-	2.28	Up
JUB	Jub, ajuba homolog	3.26	Down	1.70	Down
KIF23	Kinesin family member 23	-	-	3.13	Down
KLK10	Kallikrein-related peptidase 10	2.37	Down	2.22	Down
MAEA	Macrophage erythroblast attacher	-	-	1.75	Down
MAPK6	Mitogen-activated protein kinase 6	1.87	Up	-	-
MCM3	Minichromosome maintenance complex component 3	2.39	Down	-	-
MCM7	Minichromosome maintenance complex component 7	-	-	1.95	Down
MDC1	Mediator of DNA damage checkpoint 1	1.98	Down	-	-
MKI67	Antigen identified by monoclonal antibody Ki-67	1.75	Down	2.25	Down
NCAPD2	Non-SMC condensin I complex, subunit D2	-	-	1.70	Down
NDE1	NudE nuclear distribution gene E homolog 1	1.55	Down	-	-
NEK2	NIMA (never in mitosis gene a)-related kinase 2	-	-	2.20	Down
NF2	Neurofibromin 2 (merlin)	1.71	Down	-	-
NPM1	Nucleophosmin (nucleolar phosphoprotein B23, numatrin)	-	-	1.66	Down
NSL1	NSL1, MIND kinetochore complex component, homolog	1.79	Down	-	-
NUSAP1	Nucleolar and spindle associated protein 1	-	-	2.00	Down

Table 4.3 cont.

PBXO5	F-box protein 5	3.34	Down	-	-
PLK2	Polo-like kinase 2	2.14	Down	-	-
PML	Promyelocytic leukemia	-	-	5.94	Up
PMS1	PMS1 postmeiotic segregation increased 1	2.88	Down	-	-
PPP1CC	Protein phosphatase 1, catalytic subunit, gamma isoform	-	-	1.59	Down
PPP1R15A	Protein phosphatase 1, regulatory (inhibitor) subunit 15A	4.69	Up	-	-
PRC1	Protein regulator of cytokinesis 1	-	-	1.83	Down
PSMA1	Proteasome (prosome, macropain) subunit, alpha type, 1	1.59	Up	1.63	Up
PSMA2	Proteasome (prosome, macropain) subunit, alpha type, 2	-	-	1.84	Up
PSMA4	Proteasome (prosome, macropain) subunit, alpha type, 4	-	-	1.76	Up
PSMA5	Proteasome (prosome, macropain) subunit, alpha type, 5	1.73	Up	2.12	Up
PSMA6	Proteasome (prosome, macropain) subunit, alpha type, 6	-	-	1.58	Up
PSMB2	Proteasome (prosome, macropain) subunit, beta type, 2	-	-	1.58	Up
PSMB7	Proteasome (prosome, macropain) subunit, beta type, 7	6.51	Up	1.74	Up
PSMB9	Proteasome (prosome, macropain) subunit, beta type, 9	2.64	Down	-	-
PSMC1	Proteasome (prosome, macropain) 26S subunit, ATPase, 1	-	-	1.88	Up
PSMC2	Proteasome (prosome, macropain) 26S subunit, ATPase, 2	-	-	1.99	Up
PSMD1	Proteasome (prosome, macropain) 26S subunit, non-ATPase, 1	3.23	Up	-	-
PSMD2	Proteasome (prosome, macropain) 26S subunit, non-ATPase, 2	2.49	Up	1.91	Up
PSMD6	Proteasome (prosome, macropain) 26S subunit, non-ATPase, 6	2.8	Up	2.60	Up
PSMD12	Proteasome (prosome, macropain) 26S subunit, non-ATPase, 12	2.65	Up	1.86	Up
PSMD13	Proteasome (prosome, macropain) 26S subunit, non-ATPase, 13	2.08	Up	-	-
PSMD14	Proteasome (prosome, macropain) 26S subunit, non-ATPase, 14	2.29	Up	2.36	Up
RACGAP1	Rac GTPase activating protein 1	-	-	1.89	Down
RAD1	RAD1 homolog	-	-	1.75	Down
RAD51L1	RAD51-like 1	2.05	Down	-	-
RAN	RAN, member RAS oncogene family	-	-	1.99	Down
RASSF4	Ras association (RalGDS/AF-6) domain family member 4	-	-	2.92	Down
RB1CC1	RB1-inducible coiled-coil 1	2.21	Up	2.06	Up
RBBP4	Retinoblastoma binding protein 4	1.74	Down	-	-
RINT1	RAD50 interactor 1	1.78	Up	-	-
SKP1	S-phase kinase-associated protein 1	-	-	1.84	Up
SKP2	S-phase kinase-associated protein 2 (p45)	3.03	Down	2.20	Down

Table 4.3 cont.

SMC1A	Structural maintenance of chromosomes 1A	-	-	2.00	Down
SMC4	Structural maintenance of chromosomes 4	-	-	2.28	Down
SPAG5	Sperm associated antigen 5	-	-	1.88	Down
SPC24	SPC24, NDC80 kinetochore complex component, homolog	1.85	Down	-	-
SPC25	SPC25, NDC80 kinetochore complex component, homolog	-	-	2.63	Down
TIMELESS	Timeless homolog	-	-	2.00	Down
TP53	Tumor protein p53	-	-	2.15	Down
TPD52L1	Tumor protein D52-like 1	1.90	Down	-	-
TUBB	Tubulin, beta	2.56	Down	2.26	Down
UBB	Ubiquitin B	2.49	Up	-	-
ZRF1	Zuotin related factor 1	2.02	Up	-	-
ZWILCH	Zwilch, kinetochore associated, homolog	-	-	2.00	Down
ZZEF1	Zinc finger, ZZ-type with EF-hand domain 1	2.03	Up	2.10	Up

Up-regulated genes in red; down-regulated genes in green. - = no change. Genes with ≥1.5 fold change and adjusted $p<0.05$ on Benjamini and Hochberg post-hoc analysis were considered

Table 4.4 – Microarray analysis of the effect of GSI-I on apoptosis gene expression in ASPC-1 pancreatic adenocarcinoma cells.

Gene symbol	Gene name	Effect	Change at 12 hours		Change at 24 hours	
			Fold change	Direction	Fold change	Direction
AIFM2	Apoptosis-inducing factor, mitochondrion-associated, 2	Pro	2.08	Up	1.7	Up
ASNS	Asparagine synthetase	Anti	2.82	Up	-	-
ANXA1	Annexin A1	Pro	1.55	Up	1.99	Up
BAG1	BCL2-associated athanogene 1	Anti	3.09	Down	1.56	Down
BAG3	BCL2-associated athanogene 3	Anti	2.9	Up	-	-
BCL2L13	BCL2-like 13	Pro	1.72	Up	1.67	Up
BNIP3	BCL2/adenovirus E1B 19kDa interacting protein 3	Pro	-	-	2.35	Up
BNIP3L	BCL2/adenovirus E1B 19kDa interacting protein 3-like	Pro	-	-	2.95	Up
BTG1	B-cell translocation gene 1, anti-proliferative	Pro	1.95	Up	-	-
BUB1B	BUB1 budding uninhibited by benzimidazoles 1 homolog beta	Pro	-	-	2.03	Down
C11orf82	Chromosome 11 open reading frame 82	Anti	1.85	Up	-	-
CAPN10	Calpain 10	Pro	-	-	6.65	Up
CARD10	Caspase recruitment domain family, member 10	Pro	1.9	Up	-	-
CASP1	Caspase 1	Pro	2.57	Down	-	-
CASP8AP2	CASP8 associated protein 2	Pro	1.61	Down	-	-
CDC2	Cell division cycle 2	Anti	-	-	2.43	Down
CDKN1A	Cyclin-dependent kinase inhibitor 1A	Anti	-	-	3.85	Up
CDKN2A	Cyclin-dependent kinase inhibitor 2A	Pro	1.56	Down	-	-
CEBPG	CCAAT/enhancer binding protein (C/EBP), gamma	Pro	2.2	Up	-	-
CFLAR	CASP8 and FADD-like apoptosis regulator	Anti	-	-	2.24	Up
CLU	Clusterin	Pro	2.4	Up	3.65	Up
CYCS	Cytochrome C	Pro	5.84	Down	1.94	Down
DAP3	Death associated protein 3	Pro	2.07	Up	-	-
DEDD2	Death effector domain containing 2	Pro	2.35	Up	-	-
FAF1	Fas (TNFRSF6) associated factor 1	Pro	1.71	Up	-	-
FAIM	Fas apoptotic inhibitory molecule	Anti	1.75	Down	-	-
FIS1	Fission 1 (mitochondrial outer membrane) homolog	Pro	1.53	Down	1.58	Down
GADD45A	Growth arrest and DNA-damage-inducible, alpha	Pro	2.31	Up	-	-
GCLC	Glutamate-cysteine ligase, catalytic subunit	Anti	2.22	Up	-	-
GCLM	Glutamate-cysteine ligase	Anti	3.27	Up	-	-

Table 4.4 cont.

HIPK2	Homeodomain interacting protein kinase 2	Pro	1.8	Up	1.97	Up
HMOX1	Hemeoxygenase-1	Anti	3.89	Up	-	-
HSP1	Heat shock protein 1	Pro	1.79	Up	1.54	Down
HSPA1B	Heat shock protein 1B	Anti	17.17	Up	-	-
HSPA5	Heat shock protein 5	Anti	2.21	Up	-	-
HTATIP2	HIV-1 Tat interactive protein 2	Anti	-	-	2.28	Up
IFIH1	Interferon induced with helicase C domain 1	Pro	1.93	Up	-	-
IGF1R	Insulin-like growth factor 1 receptor	Anti	1.57	Down	-	-
IGFBP3	Insulin-like growth factor binding protein 3	Pro	3.11	Down	-	-
IL6	Interleukin 6	Anti	-	-	2.01	Up
KIAA1967		Pro	13.49	Down	-	-
MAL	Mal, T-cell differentiation protein	Pro	2.58	Down	-	-
MBD4	Methyl-CpG binding domain protein 4	Pro	1.67	Up	-	-
NPM1	Nucleophosmin (nucleolar phosphoprotein B23, numatrin)	Anti	-	-	1.66	Down
NUAK2	NUAK family, SNF1-like kinase, 2	Anti	2.26	Down	-	-
PDCL3	Phosducin-like 3	Anti	1.55	Down	-	-
PEA15	Phosphoprotein enriched in astrocytes 15	Anti	2.06	Up	-	-
PML	Promyelocytic leukemia	Pro	-	-	5.94	Up
PPP1R15A	Protein phosphatase 1, regulatory (inhibitor) subunit 15A	Pro	4.69	Up	-	-
PSEN1	Presenilin 1	Anti	1.79	Up	-	-
RB1CC1	RB1-inducible coiled-coil 1	Anti	2.21	Up	2.06	Up
RTN3	Reticulon 3	Pro	-	-	1.58	Up
SELS	Selenoprotein S	Anti	1.92	Up	-	-
SERINC3	Serine incorporator 3	Pro	-	-	1.96	Up
SERPINB2	Serpin peptidase inhibitor, clade B (ovalbumin), member 2	Anti	2.47	Up	-	-
SH3KBP1	SH3-domain kinase binding protein 1	Pro	1.86	Up	-	-
SGPP1	Sphingosine-1-phosphate phosphatase 1	Anti	3.03	Down	-	-
SOCS2	Suppressor of cytokine signaling 2	Anti	1.64	Down	-	-
SOD1	Superoxide dismutase 1	Pro	-	-	2.2	Up
SQSTM1	Sequestrosome 1	Pro	13.01	Up	16.99	Up
TM2D1	TM2 domain containing 1	Pro	1.59	Up	-	-
TAX1BP1	Tax1 (human T-cell leukemia virus type I) binding protein 1	Anti	2.45	Up	-	-
TIAL1	TIA1 cytotoxic granule-associated RNA binding protein-like 1	Pro	1.75	Up	-	-

Table 4.4 cont.

TNFAIP8	Tumor necrosis factor, alpha-induced protein 8	Anti	1.67	Down	-	-
TOP2A	Topoisomerase (DNA) II alpha	Pro	-	-	2.21	Down
TP53	Tumor protein p53	Pro	-	-	2.15	Down
TPD52L1	Tumor protein D52-like 1	Pro	1.9	Down	-	-
TUBB	Tubulin, beta	Pro	2.56	Down	2.26	Down
VCP	Valosin-containing protein	Anti	2.21	Up	1.63	Up

Up-regulated genes in red; down-regulated genes in green. - = no change. Genes with ≥1.5 fold change and adjusted $p<0.05$ on Benjamini and Hochberg post-hoc analysis were considered

4.2.8 Effect of individual Notch receptor knockdown

Gamma secretase inhibitors may therefore be promising therapeutic agents in pancreatic carcinoma. Whilst they clearly result in Notch inactivation, the extent to which the effects seen are related to Notch has not been determined, and the changes seen may be due to Notch-independent 'off-target' effects. To determine the effects of the individual Notch receptors, siRNA transfection was utilised to knockdown each Notch receptor individually. Transfection was optimised in all cell lines prior to examining end points (see Materials and Methods).

4.2.8.1 Notch-1 knockdown in pancreatic adenocarcinoma cell lines

To assess the role of Notch-1, the effect of Notch-1 knockdown using siRNA was assessed in ASPC-1, BxPC-3 and PANC-1 cell lines. Significant knockdown of intracellular Notch-1 was achieved in all three cell lines (Figure 4.19) with a >70% knockdown in ASPC-1 cell line, 55% in BxPC-3 cells and >90% in PANC-1 cells. Notch-1 knockdown resulted in a significant reduction in ATP levels at 48 hours compared to control siRNA transfection in ASPC-1 and BxPC-3 cell lines indicating loss of cellular viability (Figure 4.20). ATP levels were reduced in ASPC-1 cells by 38% and BxPC-3 by 55%. No effect on ATP levels was seen following Notch-1 knockdown in PANC-1 cells.

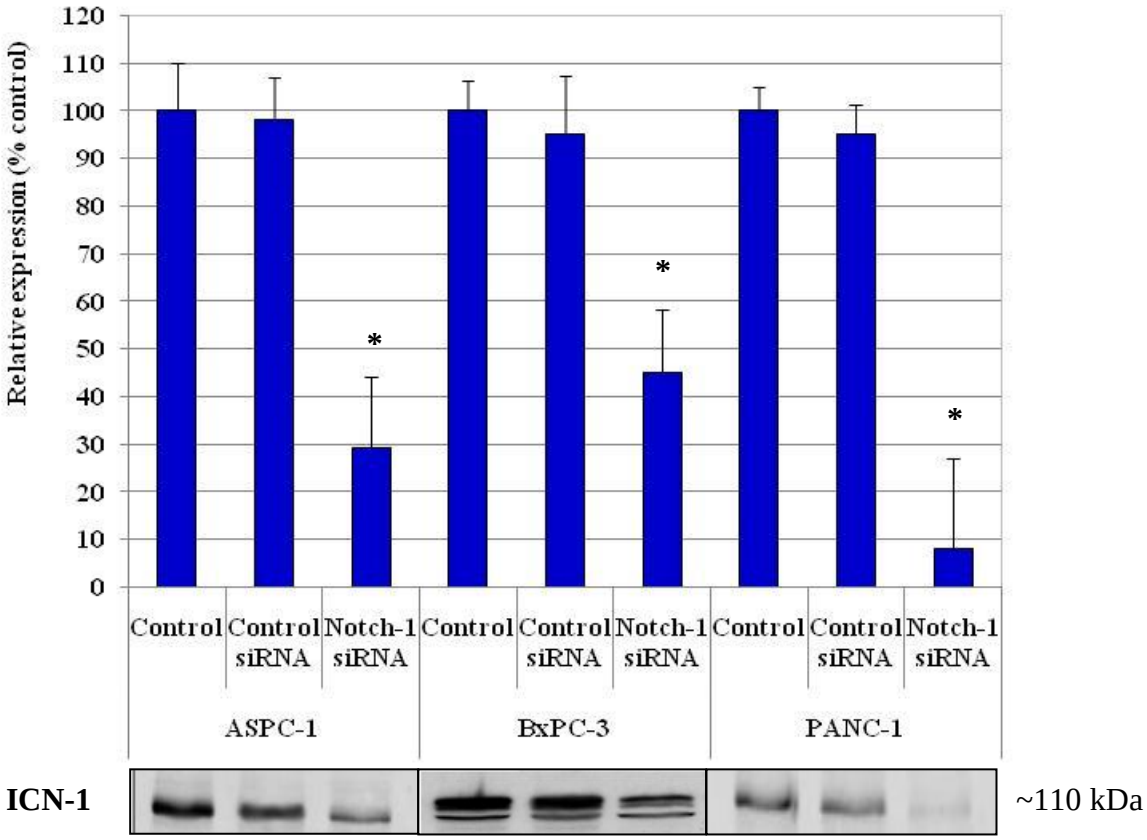

Figure 4.19 – Notch-1 knockdown
Knockdown of intracellular Notch-1 at 48 hours following transfection with Notch-1 siRNA in ASPC-1, BxPC-3 and PANC-1 cells. Bar chart demonstrates average expression from 3 experiments, relative to control, with error bars displaying standard deviation. Representative western blots are shown. *$p<0.05$ compared to control siRNA.

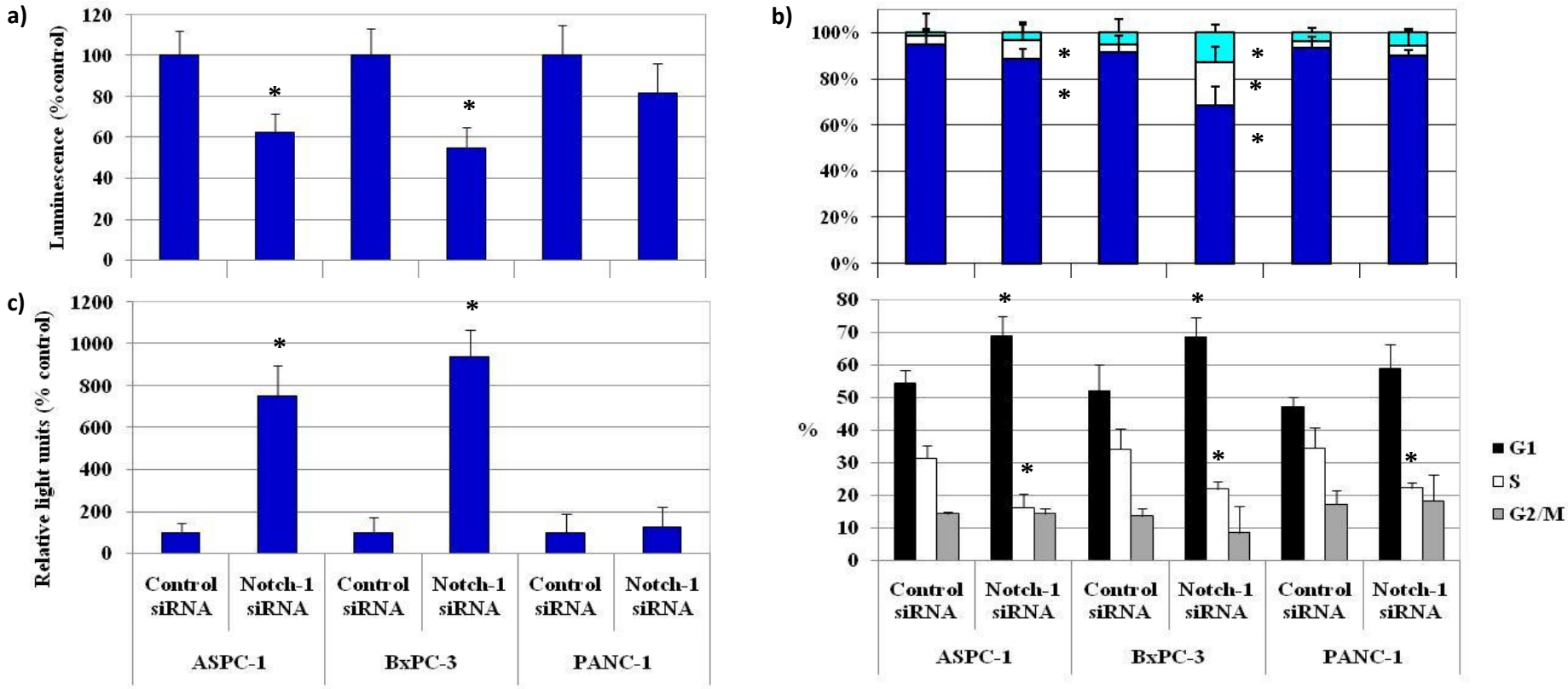

Figure 4.20 – Effect of Notch-1 knockdown on pancreatic adenocarcinoma cell lines.
Effect of Notch-1 siRNA knockdown on a) ATP levels at 48 hours; b) Annexin V/PI staining at 48 hours (blue bars represent live cells, white bars apoptotic, and cyan bars necrotic cell populations); c) Caspase 3/7 activity at 24 hours; d) cell cycle distribution at 48 hours following transfection in ASPC-1, BxPC-3, and PANC-1 pancreatic adenocarcinoma cell lines. Charts shown mean and standard deviation. *$p<0.05$ compared to transfection with control siRNA.

Notch-1 knockdown by siRNA transfection resulted in a reduction in live cells and induction of apoptosis, as assessed by the Annexin V/PI assay in ASPC-1 and BxPC-3 cell lines (Figure 4.20). Again no effect was seen in PANC-1 cells. These results were confirmed using the Caspase 3/7 assay, which showed a 7-fold increase in caspase activity in ASPC-1 cells and a 9-fold increase in BxPC-3 cells following Notch-1 knockdown compared to control siRNA transfection (Figure 4.20). No increase in caspase 3/7 activity was seen in PANC-1 cells.

Notch-1 knockdown resulted in an increase in cells in G_1 48 hours following transfection, associated with a reduction in the S-phase population in all three cell lines, indicating G_1 cell cycle arrest (Figure 4.20).

4.2.8.2 Notch-3 knockdown in pancreatic adenocarcinoma cell lines

The effect of intracellular Notch-3 knockdown was investigated in ASPC-1, BxPC-3 and PANC-1 cell lines using Notch-3 siRNA. It should be noted that BxPC-3 and PANC-1 express minimal levels of Notch-3 compared to ASPC-1. Greater than 70% knockdown of Notch-3 siRNA was achievable in ASPC-1 cells, however only 43% knock-down was achievable in BxPC-3 and 30% in PANC-1 (Figure 4.21). Notch-3 knockdown resulted in a significant reduction in ATP levels at 48 hours in ASPC-1 cells by 30% (Figure 4.22). No significant change in ATP levels was seen in either of the other two cell lines.

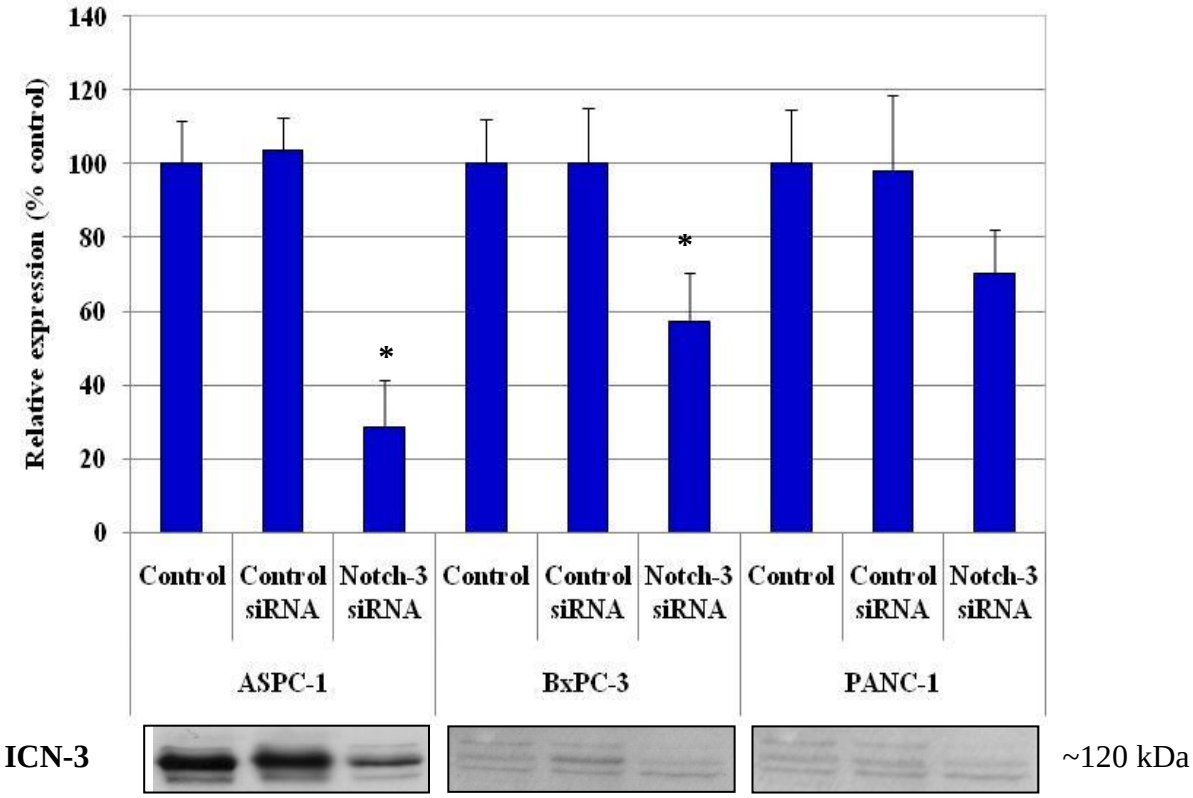

Figure 4.21 – Notch-3 knockdown
Knockdown of intracellular Notch-3 at 48 hours following transfection with Notch-3 siRNA in ASPC-1, BxPC-3 and PANC-1 cells. Bar chart demonstrates average expression from 3 experiments, relative to actin control, with error bars displaying standard deviation. Representative western blots are shown. *$p<0.05$ compared to control siRNA.

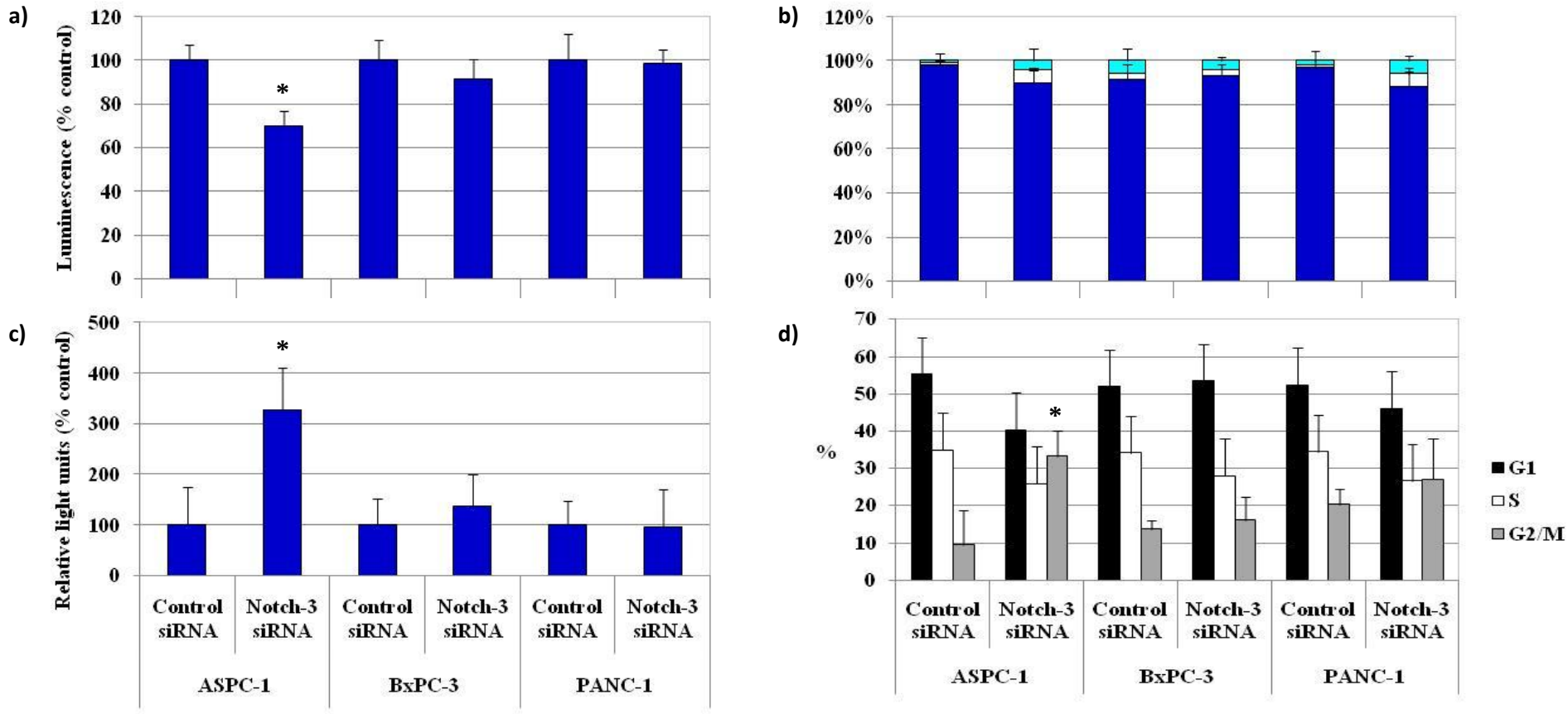

Figure 4.22 – Effect of Notch-3 knockdown on pancreatic adenocarcinoma cell lines.
Effect of Notch-3 siRNA knockdown on a) ATP levels at 48 hours; b) Annexin V/PI staining at 48 hours (blue bars represent live cells, white bars apoptotic, and cyan bars necrotic cell populations); c) Caspase 3/7 activity at 24 hours; d) cell cycle distribution at 48 hours following transfection in ASPC-1, BxPC-3, and PANC-1 pancreatic adenocarcinoma cell lines. Charts shown mean and standard deviation. *$p<0.05$ compared to transfection with control siRNA.

Notch-3 knockdown did not result in an alteration of the viable cell population as determined by annexin/PI staining at 48 hours post transfection in any of the three cell lines (Figure 4.22). However caspase 3/7 activity was increased over 3-fold 24 hours following Notch-3 siRNA transfection in ASPC-1 cells, indicating induction of apoptosis (Figure 4.22). No such increase in activity was seen in BxPC-3 or PANC-1 cells. Similarly, no alteration in cell cycle distribution was seen following Notch-3 knockdown in BxPC-3 or PANC-1 cells. However in ASPC-1 cells, an increase in G_2M cells was accompanied by a reduction in G_1 and S-phase cells, indicating G_2M cell cycle arrest (Figure 4.22).

4.2.8.3 Notch-4 knockdown in the PANC-1 pancreatic adenocarcinoma cell line

The effect of Notch-4 knockdown was investigated only in PANC-1 cells as ASPC-1 and BxPC-3 cell lines have been shown not to express intracellular Notch-4 (see Chapter 4). Knockdown of intracellular Notch-4 >70% was achievable by siRNA transfection in this cell line at 48 hours post transfection (Figure 4.23). Notch-4 knockdown did not translate into any significant change in ATP levels, Annexin V/PI staining (Figure 5.14), Caspase 3/7 activity or cell cycle distribution (Figure 4.23), indicating no effect on cell viability, proliferation or induction of apoptosis.

4.2.8.4 Combined Notch knockdown in ASPC-1 cells

The effect of combined Notch knockdown was investigated in ASPC-1 cells. Notch-1 knockdown did not alter expression of active Notch-3 or result in active Notch-4 expression (Figure 4.24). Similarly, Notch-3 knockdown did not alter intracellular

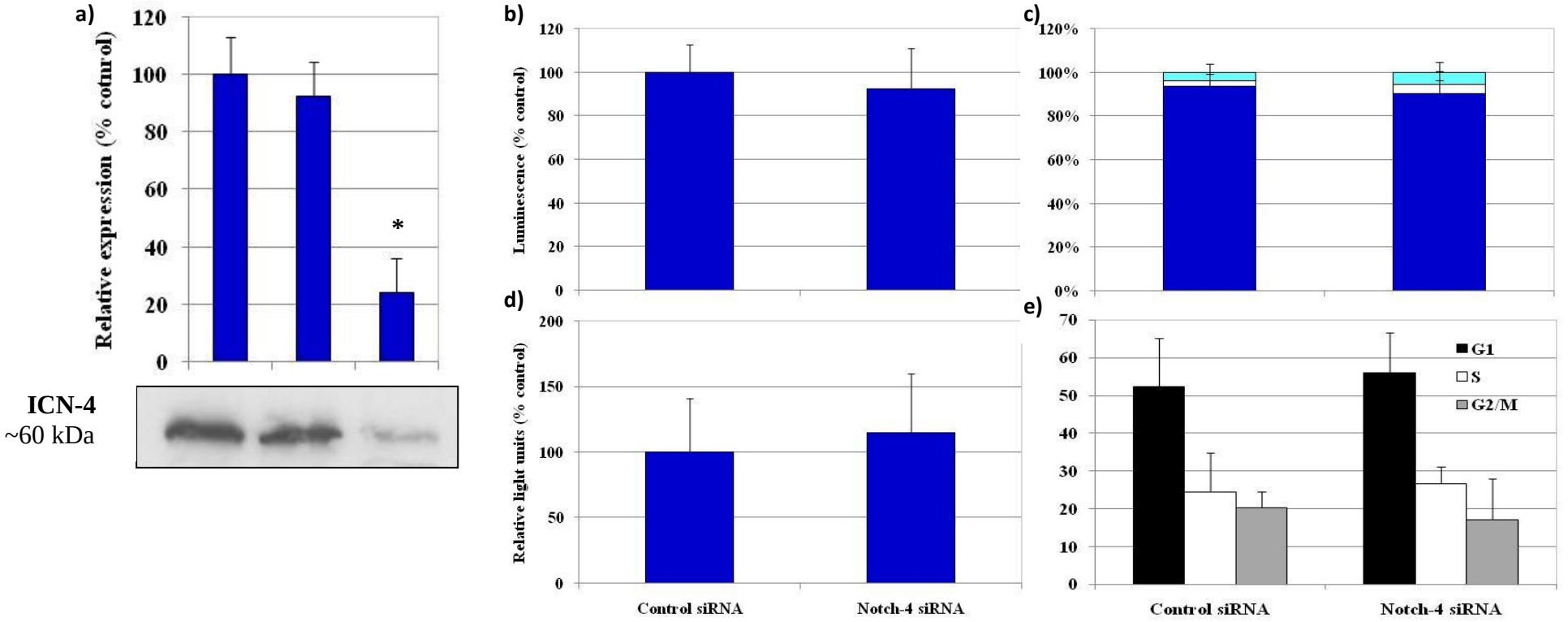

Figure 4.23 – Effect of Notch-4 knockdown on PANC-1 pancreatic adenocarcinoma cell line.
Effect of Notch-4 knockdown on a) expression of intracellular Notch-4 (ICN-4) at 48 hours following transfection relative to actin expression; b) ATP levels at 48 hours; c) Annexin V/PI staining at 48 hours (blue bars represent live cells, white bars apoptotic, and cyan bars necrotic cell populations); d) Caspase 3/7 activity at 24 hours; e) cell cycle distribution at 48 hours following transfection in ASPC-1, BxPC-3, and PANC-1 pancreatic adenocarcinoma cell lines. Charts shown mean of 3 experiments and standard deviation. Representative western blots are shown. *$p<0.05$ compared to transfection with control siRNA

Notch-1 expression or induce Notch-4 expression. These findings suggest that these signalling pathways act independently in this cell line. Notch-1 knockdown resulted in down regulation of HES-1, and a small reduction in HEY-1 expression, both target proteins of the Notch pathway. Notch-3 knockdown resulted in a reduction in HEY-1 expression, however no change in HES-1 expression was seen.

Combined knockdown of intracellular Notch-1 and Notch-3 was possible in the ASPC-1 cell line. Transfection of both Notch-1 and Notch-3 siRNA resulted in a 55% and 52% knockdown in Notch-1 and -3 respectively (Figure 4.24). A reduction in HES-1 and HEY-1 target proteins was seen in these cells. No induction of Notch-4 expression was seen. Attempts were made to investigate the effect of combined Notch-1 and -4 knockdown in PANC-1 cells, however combination knockdown was not achieved in this cell line using chemical transfection.

Combined Notch-1 and -3 resulted in a significantly greater reduction in ATP levels compared to knockdown of either alone (Figure 4.25). No alteration in Annexin V/PI staining was seen compared to Notch-1 knockdown alone, suggesting no additional induction of apoptosis (Figure 4.25). Notch-1 knockdown was again found to result in an increased proportion of cells in the G_1-phase at the expense of S-phase (Figure 4.25). Notch-3 knockdown again resulted in an increased in the G_2M population at the expense of G_1. Combined knockdown of the two proteins resulted in a significant increase in the G_1 population compared to control siRNA and Notch-3 knockdown – this was similar to Notch-1 knockdown alone. In addition, a significant increase in G_2M population was seen compared to control or Notch-1 knockdown – this was

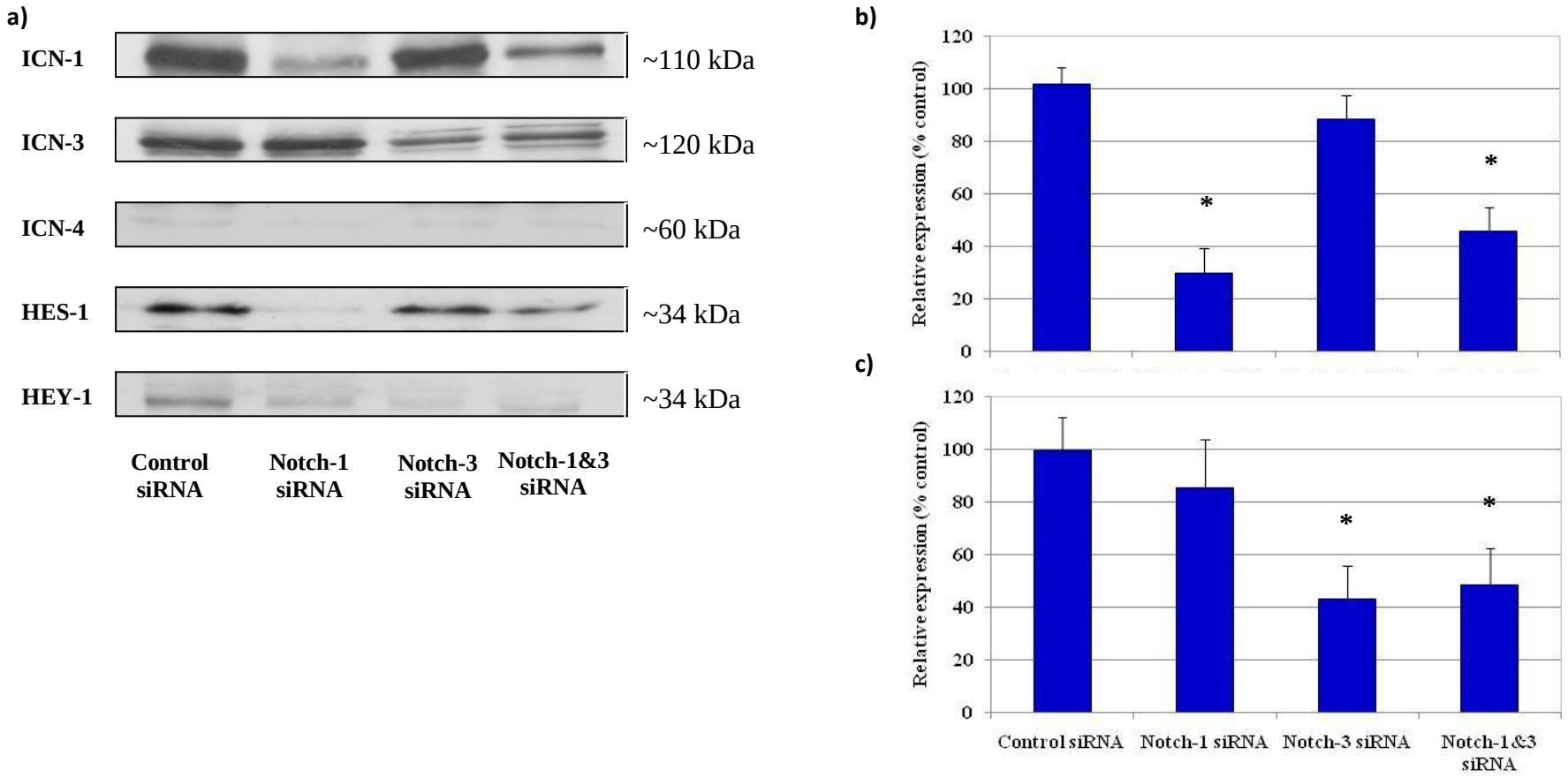

Figure 4.24 – Effect of Notch-1 and Notch-3 knockdown, alone and in combination, on Notch expression in ASPC-1 cells.
Effect of Notch-1 and Notch-3 knockdown, alone and in combination, on expression of intracellular Notch-1, -3, -4, HES-1 and HEY-1 in ASPC-1 pancreatic adenocarcinoma cells; a) representative western blots; knockdown of b) intracellular Notch-1 and c) Notch-3 at 48 hours following transfection. Data are expressed relative to actin levels. Charts shown mean of 3 experiments, with error bars displaying standard deviation. *$p<0.05$ compared to transfection with control siRNA.

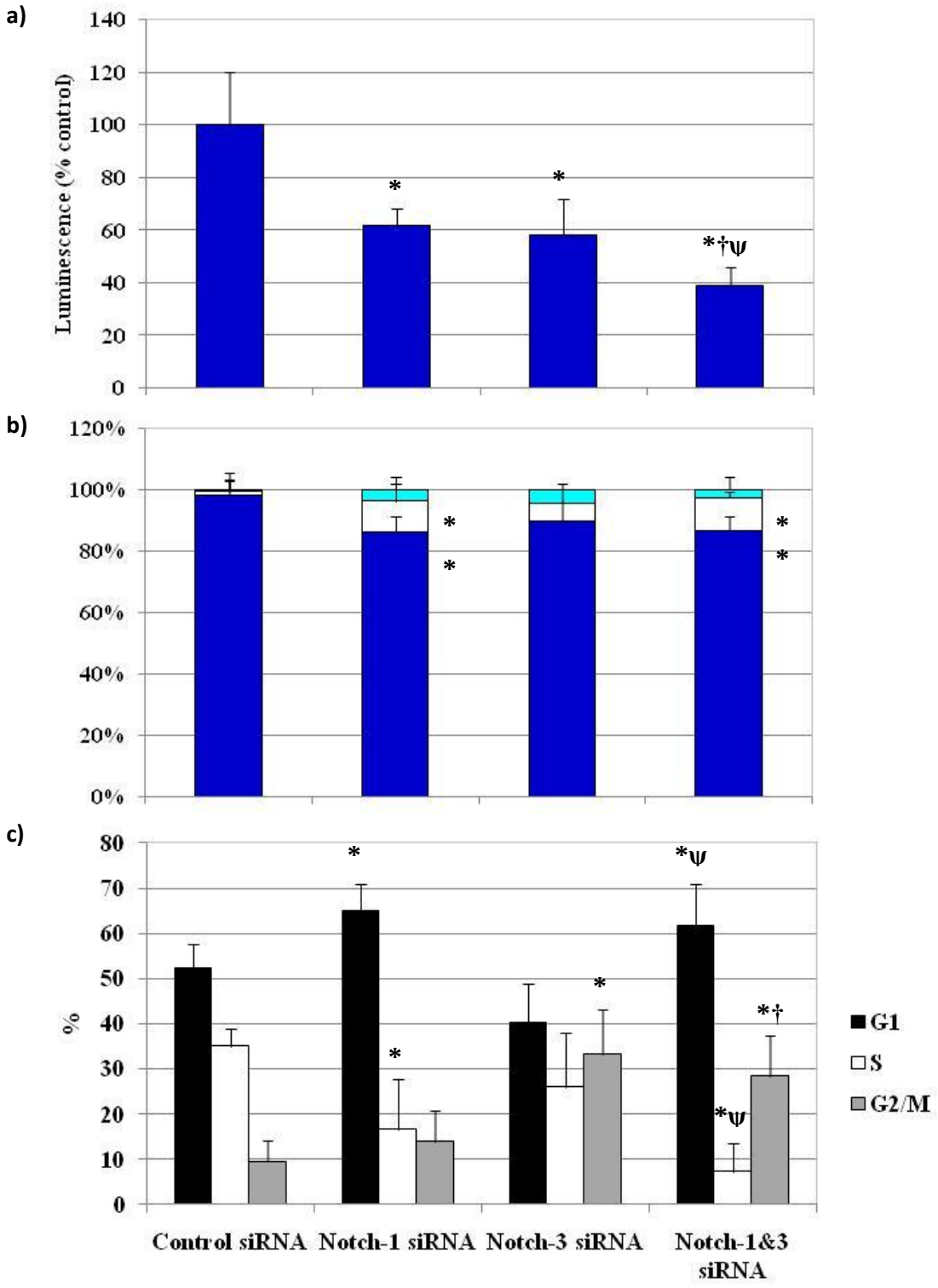

Figure 4.25 – Effect of combined Notch-1 and Notch-3 knockdown in ASPC-1
Effect of combined Notch-1 and Notch-3 siRNA knockdown on a) ATP levels at 48 hours; b) Annexin V/PI staining at 48 hours (blue bars represent live cells, white bars apoptotic, and cyan bars necrotic cell populations); c) cell cycle distribution at 48 hours following transfection. Charts show mean and standard deviation. *$p<0.05$ compared to control siRNA; †$p<0.05$ compared to Notch-1 siRNA; ψ$p<0.05$ compared to Notch-3 siRNA.

similar to Notch-3 knockdown alone. These changes were at the expense of a reduction in S-phase cells. These findings may suggest a combined G_1 and G_2M cell cycle arrest following Notch-1 and Notch-3 knockdown. The addition of Notch-4 siRNA to Notch-1 and -3 siRNAs did not alter these results.

4.2.9 Effect of gamma secretase inhibition on other signalling pathways

The phenotypic changes in ASPC-1 seen with combined Notch-1, -3, and -4 knockdown suggest that the effects of gamma secretase inhibition are mediated, at least in part, through inhibition of the Notch pathway, but do not prove that all the anti-tumour effects are Notch-dependent. Gamma-secretase is known to regulate proteolysis of several other transmembrane proteins, including Erb4, APP, and E-cadherin (Ni *et al*, 2001; Dalrymple *et al*, 2005; Dovey *et al*, 2001). The microarray data generated following treatment of ASPC-1 with GSI-I were reanalysed to determine the impact upon other pathways known to be important in pancreatic carcinoma, namely the JAK-STAT, Hedgehog, MAP kinase, NF-κB and Wnt pathways. Again a cut off of ≥1.5-fold change and $p<0.05$ were used. The results are given in Table 4.5. No Hedgehog pathway constituents were affected.

Table 4.5 – Microarray analysis of the effect of GSI-I on other signalling pathways important in pancreatic carcinogenesis in ASPC-1 pancreatic adenocarcinoma cells.

Gene symbol	Gene name	Fold change	Direction
JAK-STAT pathway			
IFNAR2	Interferon (alpha, beta and omega) receptor 2	1.95	Down
LEPR	Leptin receptor	1.86	Up
STAM	Signal transducing adaptor molecule	1.82	Up
MAP Kinase pathway			
RASGRP4	RAS guanyl releasing protein 4	9.73	Up
DUSP1	Dual specificity phosphatase 1	4.15	Up
MAP3K6	Mitogen-activated protein kinase kinase kinase 6	3.13	Down
DUSP6	Dual specificity phosphatase 6	1.96	Down
MAPK9	Mitogen-activated protein kinase 9	1.58	Up
NF-κB pathway			
IKKG	Inhibitor of kappa light polypeptide gene enhancer, kinase gamma	1.58	Down
Wnt pathway			
FZD2	Frizzled homolog 2	1.94	Down
FZD10	Frizzled homolog 10	1.91	Down
SKP1	S-phase kinase-associated protein 1	1.84	Up
DVL2	Dishevelled-2	1.52	Down
DVL3	Dishevelled-3	1.5	Up

Up-regulated genes in red; down-regulated genes in green. Genes with ≥1.5 fold change and adjusted $p<0.05$ on Benjamini and Hochberg post-hoc analysis were considered

Data in the literature demonstrate that increased NF-κB activity can promote growth, inhibit apoptosis, promote angiogenesis, invasion and metastasis, and chemoresistance in pancreatic cancer (Holcomb *et al*, 2008). The gamma secretase inhibitor down-regulated IKKγ, which phosphorylates IKKβ targeting it for degradation, resulting in NF-κB activation. This change is more likely to be Notch-dependent. There is known to be extensive cross-talk between the two pathways, and Wang *et al* (2006 and 2006b) have shown Notch-1 knockdown to reduce NF-κB activity.

GSI-I treatment resulted in down-regulation of Frizzled 2 and 10, as well as dishevelled-2. Dishevelled-3 however was up-regulated. Frizzled are transmembrane receptors, which when activated, activate dishevelled which inhibits the Axin/GSK-3β/APC complex, increasing β-catenin levels and translocation to the nucleus, where it associates with T cell factor-4 causing transcriptional activation of target genes. Cyclin D_1, a target of the Wnt-pathway, is also reduced by GSI treatment (Table 4.3). A γ-secretase cleavage is known to cleave E-cadherin, resulting in disassociation of E-cadherin, β-catenin and α-catenin from the cytoskeleton, thus increasing β-catenin activity (Marambaud *et al*, 2002). Thus a gamma secretase inhibitor may reduce cyclin D_1 expression. Equally however the changes may be explained by cross-talk between the Notch and Wnt signalling pathways. Several previous studies have linked Notch and Wnt in both agonist and antagonist relationships (Axelrod *et al*, 1996; Fre *et al*, 2009). Clearly these changes need validation and further investigation.

4.3 DISCUSSION

These data confirm previous reports that Notch activation occurs in pancreatic carcinoma cells *in vitro*, and provide evidence that modulation of this pathway using gamma secretase inhibition is a promising therapeutic avenue. It is the first study to use microarray analysis in order to elucidate the mechanisms behind the GSI-I effects seen. The only previous study to investigate a role for GSIs in pancreatic cancer used the MTT assay to demonstrate a reduction in growth of BxPC-3 cells following treatment with DAPT (Kimura *et al*, 2007). To date, no published study has investigated gamma secretase inhibitors, alone or in combination in more than one pancreatic carcinoma cell line, for effects on cell proliferation, viability, apoptosis, and cell-cycle distribution.

Treatment with GSI-I, the more effective of two inhibitors investigated, resulted in inactivation of the Notch pathway in three treated lines, as evidenced by down-regulated ICN-1, -3, -4 and HES-1 (as well as HEY-1 on microarray analysis). GSI-I has been previously shown to block Notch-1, -2 and -4 activation in Kaposi Sarcoma cells (Curry *et al*, 2005) and Notch-3 activation in ovarian carcinoma cells (Park *et al*, 2006). Although GSI-X was previously reported as a specific and potent inhibitor of the Notch pathway (Martys-Zage *et al*, 2000; Sun *et al*, 2005), in these experiments it was only found to affect Notch-3 activation, with no effect on Notch-1, -4 or HES-1, suggesting differential selectivity in these cell lines. Even then, it had only a comparatively small effect on intracellular Notch-3 compared to GSI-I. Rooman *et al* (2006) found GSI-X had no effect on HES-1 mRNA, but reduced Hey-1 and Hey-2 mRNA in metaplastic pancreatic exocrine cells. This supports previous data that

HES-1 is under Notch-1 regulation, while Notch-3 is thought to act through Hey-1 (Haruki *et al*, 2005; Konishi *et al*, 2007). Indeed, Notch-3 has been shown to inhibit Notch-1-mediated activation of HES-1 and –5 promotors (Beatus *et al*, 1999).

Treatment with GSI-I resulted in reduction in cell viability to some degree in all cell lines investigated. This was associated with induction of apoptosis in ASPC-1 and BxPC-3 cell lines. In the PANC-1 line the majority of affected cells appeared to progress straight to necrosis. As no defect in apoptosis in PANC-1 cells is reported, this is likely to be a treatment-related finding. Treatment with GSI-I resulted in reduced cell proliferation in all lines along with an increased proportion of cells in G_2/M, with an additional increase in the G_1 population only in ASPC-1 cells at lower doses. Wang *et al* (2006a) found specific Notch-1 inhibition using siRNA to induce G_0/G_1 arrest in BxPC-3 and PANC-1 cells. The discrepancy may be related to the specific blockade of Notch-1 using siRNA, whereas GSI-I prevents activation of all Notch receptors. GSI-I treatment increased the percentage of Kaposi's sarcoma cells in G_2/M phase (Curry *et al*, 2005, 2007). However, these authors found that siRNA inhibition of Notch-1 also resulted in a significant increase in cells in G_2/M. Other studies have found treatment with other GSIs and specific Notch-1 inhibition to result in G_0/G_1 arrest, although these studies have all been in cells derived from haematological malignancies (Chan *et al*, 2007; Lewis *et al*, 2007; Sharma *et al*, 2006; Lan *et al*, 2006)

Curcumin is a promising anticancer dietary agent, derived from turmeric, with published evidence indicating its potential in pancreatic carcinoma, both alone and in

combination with gemcitabine (Li *et al*, 2005; Kunnumakkara *et al*, 2007). It has been shown to inhibit active Notch-1 expression in Raji cells (Chen *et al*, 2007) and to decrease Notch-1 mRNA and protein levels in BxPC-3 and PANC-1 cells, with some inhibition of HES-1 expression (Wang *et al* 2006c). In these experiments it was found that curcumin down-regulated ICN-1 and HES-1 protein expression, using a more physiologically achievable dose and treatment for a shorter period (48 hours). Curcumin also decreased levels of ICN-3 and ICN-4, which may suggest that it possesses GSI activity. Indeed, Narlawar *et al* (2007) synthesised curcumin-derived oxazoles and pyrazoles, which were potent inhibitors of gamma-secretase.

The Notch receptors are known to have context and cancer-specific effects on carcinogenesis, for example Notch-1 is oncogenic in T-cell leukaemia and breast cancer (Stylianou *et al*, 2006; Weng *et al*, 2004), whilst loss of Notch-1 has these effects in medulloblastoma, skin cancer and HCC (Qi *et al*, 2003; Fan *et al*, 2004; Nicolas *et al*, 2003). Notch-1 was found to be up-regulated in pancreatic carcinoma compared to normal pancreas, with progressive up-regulation with advanced disease (Chapter 3). The experiments in this chapter demonstrate pro-tumorigenic effects of Notch-1 in pancreatic adenocarcinoma. Knockdown of Notch-1 resulted in a reduction in ATP levels and an induction of apoptosis in ASPC-1 and BxPC-3 cells, but not in PANC-1 cells. Wang *et al* (2006a) demonstrated that Notch-1 knockdown resulted in inhibited cell growth and induction of apoptosis in BxPC-3, HPAC and PANC-1 cells. In addition cells transfected with constitutively active Notch-1 resulted in increased tumour cell growth. It is not clear why that study found Notch-1 knockdown to result in PANC-1 cell line apoptosis, where as the current study did not. The siRNAs used were from the same company (Santa Cruz Biotechnology) and

the same transfection reagent was used (Lipofectamine 2000, Invitrogen). Also they did not report percentage of protein level knockdown, however on examining representative western blots, the knockdown achieved in the current study was at least comparable. The main difference is the assays used to detect apoptosis and this may account for the difference – this current study used Annexin V/PI staining and Caspase 3/7 activation, whilst Wang *et al* used Histone/DNA fragment ELISA. In addition it must be remembered that although immortalised cell lines descend from the same parental cell, the multiple passages may result in alterations of genotype. No other data relating to this are available in the literature. Further studies by the same group (Wang *et al*, 2006a and 2006c) found that Notch-1 knockdown using siRNA promoted cancer cell growth inhibition and apoptosis induced by the dietary chemopreventive agents genistein and curcumin, where as transfection with constitutively active Notch-1 reduced the effectiveness of both agents. Several mechanisms have been suggested for the anti-apoptotic function of Notch-1, including alterations in the NF-κβ pathway, PI3K-Akt pathway, and the JNK pathway. Wang *et al* (2006, 2006a and 2006b found that Notch-1 knockdown using siRNA in BxPC-3 cells resulted in a decrease NF-κβ DNA binding activity, where as transfection with Notch-1 cDNA resulted in an increase in NF-κβ binding activity. NF-κβ is known to play an important role in pancreatic carcinoma, mediating survival signals that inhibit apoptosis and promote cancer cell growth, and is constitutively active in 70% of human pancreatic adenocarcinoma (Liptay *et al*, 2003; Sclabas *et al*, 2005). Other studies have found Notch-1 to cross-talk with the NF- κβ pathway. Kamstrup *et al* (2010) found Notch-1 knockdown in cutaneous T cell lymphoma cells to result in inhibition of NF-κβ. Notch-1 has been found to strongly induce NF- κβ promoter activity and the expression of several NF- κβ subunits and NF- κβ binding activity

(Jang *et al*, 2004). It also interacts with the p50 subunit to retain the active NF- κβ in the nucleus leading to sustained activation (Shin *et al*, 2006; Wang et al, 2001). Similarly, Song *et al* (2008) found that inhibition of Notch-1 using siRNA in cervical cancer cells resulted in a reduction in NF-κβ activity, whereas constitutively active Notch-1 increased NF-κβ activity. TNFα-stimulated IKK activity was shown to be Notch-1 dependent, and Notch-1 was found in association with IKKα at IKKα-stimulated promoters and was required for IKKα to associate with these promoters. In a study using cervical cancer cells, Nair *et al* (2003) suggested that the anti-apoptotic effects on Notch-1 may be mediated in part through the PI3K-PKB/Akt pathway. Sade *et al* (2004) found that enforced expression of active Notch-1 in T-cells significantly increased the expression of the anti-apoptotic proteins Bcl-XL, IAP-2, and FLIP (FLICE-like inhibitor protein). The anti-apoptotic effects of active Notch-1 in abrogating TRAIL-induced apoptosis were found to be dependent upon PI3K activation of Akt-PKB as assessed by pAkt-Thr^{308} expression, with the effects being abolished by the PI3K inhibitors LY294002 and Wortmannin. Similarly, the effects were blocked by the Notch inhibitor, Numb. Other studies have provided additional evidence of the link between Notch-1 and the PI3K-Akt-mTOR pathway, demonstrating Notch-1 knockdown to result in down-regulation of pAkt and mTOR in colorectal cancer cells (Koduru *et al*, 2010), glioma cells (Zhao *et al*, 2010) and T-ALL cells (Guo *et al*, 2010). In addition, Wang *et al* (2010) found Notch-1 knockdown in prostate cancer cells to result in down-regulation of pAkt and FoxM1 (Forkhead Box M1 transcription factor), which is known to be up-regulated in pancreatic carcinoma (Wang *et al*, 2007a) and can be controlled by Akt expression (Major *et al*, 2004; Wang *et al*, 2010a). Jang *et al* (2004) found that Notch-1 knockdown sensitised murine erythroleukemia cells to apoptosis triggered by anti-

cancer agents (hydroxyurea, nocodazole, cisplatin), and that this was associated with phosphorylation of c-Jun N-terminal kinase (JNK) -1 and -2, whilst constitutive activation of Notch-1 abolished these effects. In addition, in the same cells expression of constitutively active Notch-1 resulted in Bcl-XL up-regulation, and Notch-1 knockdown resulted in lower levels of Bcl-XL expression.

The current study found Notch-1 knockdown to result in G_1 arrest in ASPC-1 and BxPC-3 cell lines. Notch-1 knockdown in pancreatic carcinoma cells has been associated with a reduction in cyclin A1, cyclin D1 and CDK-2, which are known to regulate the G_1-S cell cycle transition, and an increase in p21 and p27 (Wang *et al*, 2006c), members of the KIP/CIP family which interact with the cyclinA-Cdk2, cyclinE-Cdk2 and cyclinD-cdk4 complexes and inhibit their activities (Aprelikova *et al*, 1995; Bartek *et al*, 1997). Guo *et al* (2009) found similar changes in T-ALL cells with Notch-1 knockdown. Sarmento *et al* (2005) provided further detail of the mechanisms behind these changes, finding that ligand dependent and independent activation of Notch-1 induced transcription of the S phase kinase-associated protein 2 (SKP2) that targets proteins for degradation. This resulted in proteasome-mediated degradation of p27Kip1 and p21(waf1/cip1), causing premature entry into S phase. Silencing of SKP2 using siRNA abolished the effect of Notch on G_1-S progression and p27 and p21 levels. Curry *et al* (2007) found Notch-1 silencing using siRNA to result in G_2M cell cycle arrest in Kaposi sarcoma cells, associated with increased NF-κβ activity and cyclin B1 levels.

This is the first study to investigate the effects of Notch-3 knockdown on proliferation, cell cycle and apoptosis in pancreatic carcinoma cell lines. Notch-3 was found to be up-regulated in pancreatic adenocarcinoma compared to normal pancreas (Chapter 3). In addition, increased levels of nuclear expression were associated with advanced disease, suggesting Notch-3 to be important in the progression of the disease. The data presented demonstrated that ASPC-3 was the only cell line to express active Notch-3 to any extent. Knockdown using siRNA resulted in a reduction in ATP levels in ASPC-1 cells, as well as G_2M cell cycle arrest. An increase in caspase 3/7 activity was seen indicating induction of apoptosis, although no changes were seen on Annexin V/PI analysis. No changes were seen in BxPC-3 or PANC-1 cells. Taken together, these data confirm Notch-3 to be important in pancreatic carcinoma and a potential therapeutic target. A recent study by Yao *et al* (2010) published after the experiments in this chapter were performed, using BxPC-3 and PANC-1 cells, found that Notch-3 knockdown using transfection of a vector-based siRNA, enhanced gemcitabine-induced cytotoxicity associated with induction of apoptosis. They also found that Notch-3 knockdown resulted in suppression of Akt activity, confirming a previously reported correlation identified by immunohistochemistry (Doucas *et al*, 2008). The results from chapter 3 suggest Notch-3 and its target protein HEY-1 are associated with poor long-term survival following resection for pancreatic adenocarcinoma. Few data in the literature examines the role of Notch-3 in malignancy and the mechanisms via which it mediates its effects remain largely unexplored. Notch-3 is likely to play a role in ovarian (Jung *et al*, 2010), cervical (Yeasmin *et al*, 2010), lung (Konishi *et al*, 2010) and HCC (Gramantieri *et al*, 2007). Over-expression has been associated with

aggressive disease, poorer prognosis, and chemo-resistance in cervical and serous ovarian carcinomas (Yeasmin *et al*, 2010; Jung *et al*, 2010).

The effect of Notch-4 knockdown in pancreatic carcinoma has not previously been reported. Notch-4 was found to be over-expressed in pancreatic carcinoma compared to normal pancreas (Chapter 3). Whilst no data exists pertaining to pancreatic carcinoma, Notch-4 is known to play an important role in other solid malignancies, including breast (Soriano *et al*, 2000; Raafat *et al*, 2009; Gallahan and Callahan, 1997; Harrison *et al*, 2010). In this study, Notch-4 knockdown was only investigated in PANC-1 cells as it did not appear to be present in ASPC-1 or BxPC-3 cells. Knockdown of Notch-4 did not result in any change in cell viability, apoptosis or cell cycle distribution. Despite satisfactory knockdown being achieved in this study (>70% knockdown), these finding may mean that the remaining low levels of Notch-4 are sufficient for PANC-1 cell survival and proliferation. The only way to resolve this would be to achieve 100% knockdown, which despite optimisation, was not possible in these experiments.

Combined knockdown of Notch-1 and Notch-3 has not previously been reported in the literature, and was achievable in ASPC-1 cells, although at some expense to the overall level of knockdown achieved. Interestingly, although combined knockdown produced no increase in apoptosis over Notch-1 knockdown alone, knockdown of both proteins resulted in combined G_1 and G_2/M cell cycle arrest, accounting for the additional reduction in ATP-levels over knockdown of each protein individually. This confirms the previous findings that Notch-1 knockdown results in G_1-arrest in

this cell line and Notch-3 knockdown results in G_2M arrest, and that they act through different mechanisms. Although attempts were made to synchronise cells in $G_{0/1}$ prior to treatment using serum starvation, in order to confirm these results it would be necessary to repeat the experiments using a chemical block such as Nocodazole to synchronise all cells.

Knockdown of Notch-1 did not affect Notch-3 expression and vice versa. Expression of Notch-4 was not enforced by knockdown of either protein. These results suggest that in ASPC-1 cells these receptors act via different pathways and are not interlinked in feedback loops. HES-1 is known to be a target protein of Notch-1, and these findings confirm that this is the case in pancreatic adenocarcinoma cells. These data suggest that HEY-1 is a target of Notch-1, confirming previous data in breast cancer cells (Stylianou *et al*, 2006). The siRNA data also suggest that Notch-3 acts through HEY-1 rather than HES-1. This may be a cell-specific finding; Notch-3 has been shown to act through both HEY-1 and HES-1 in HepG2 HCC cells and HeLa cervical cancer cells (Giovannini *et al*, 2009). However in lung cancer cells, HES-1 has been shown to act independently of Notch-3 activation (Lin *et al*, 2010; Konishi *et al*, 2007; Haruki *et al*, 2005). These findings are in agreement with data from Chapter 3 which showed significant immunohistochemical associations between expression of nuclear Notch-1 and nuclear HES-1, and nuclear Notch-3 and nuclear HEY-1.

Whilst the phenotypic changes in ASPC-1 seen with combined Notch-1, -3, and -4 knockdown are similar to those seen following treatment with GSI-I, they are clearly not of the same magnitude. There may be several reasons for this. Notch-2 was not

investigated in this study due to problems obtaining a suitable antibody. A recent study suggested Notch-2 to be important in the progression of PanIN lesions (Mazur *et al*, 2010). Although adequate levels of Notch knockdown were achieved, this was not complete and indeed seemed to less than that achievable with GSI-I treatment. It may be that only small levels of protein are sufficient for biological function and therefore the siRNA knockdown was insufficient. Transfection of siRNAs is useful for investigating the immediate effects of inhibiting specific genes, however gene silencing is transient and is therefore unsuitable when prolonged inhibition of gene expression is necessary as it would require multiple or continuous administration of the siRNA. Similarly it is not useful for analysis of loss-of-function phenotypes over long periods of time. Several studies have demonstrated that siRNA degradation peaks 36-48 hours after introduction. This may partially enable the discrepancy in results, however experiments performed during optimisation demonstrated knockdown to be maintained from 12 to 48 hours post-transfection, although efficiency was reduced by 72 hours. Transfection of cells treated with GSI-I with vectors expressing constitutively active Notch may allow the contribution of each Notch to the effects seen to be determined.

This is the first study to use microarray to assess the changes in gene expression following treatment of pancreatic cancer cells with a gamma secretase inhibitor. It demonstrates effects on a number of downstream targets and regulators of the Notch pathway, as well as potential mechanisms for the induction of apoptosis and cell cycle arrest seen. These findings would need to be validated using RT-PCR analysis. Microarray is a useful tool to screen large numbers of genes following treatment. There are however a number of limitations. Firstly it is expensive, which limited

further experiments in the current study. Secondly it reports change in a huge number of genes and produces a quantity of data which can be unmanageable. Thirdly, the final product of gene expression is protein where as microarray looks at RNA levels. In this study a cut off of 1.5-fold change was used, which is standard in the literature. It is possible however, that a smaller fold change in RNA level could produce a biologically relevant change.

These results suggests that the effects of gamma secretase inhibition are mediated, at least in part, through inhibition of the Notch pathway, but do not prove that all the antitumour effects are Notch-dependent. Gamma-secretase is known to regulate proteolysis of several other transmembrane proteins, including Erb4, APP, and E-cadherin (Ni *et al*, 2001; Dalrymple *et al*, 2005; Dovey *et al*, 2001). The microarray data in this study suggest the NF-κB and Wnt pathways may be involved, however validation and further clarification is needed. Studies in other cancers, however, suggest that the majority of GSI-related antitumour effects are through inhibition of Notch. Zhang *et al* (2008a) showed that GSI-reduced invasion of osteosarcoma cells was reversed following transfection of active Notch-1. Lewis *et al* (2007) showed reversal of GSI-mediated G_0/G_1 cell cycle arrest and apoptosis following transfection with active Notch-1, and Sharma *et al* (2006) demonstrated that transfection of intracellular Notch-1 rescued GSI-induced growth arrest and apoptosis in T-cell leukaemia cells. In Kaposi's sarcoma cells, transfection with retroviral vectors expressing active Notch-1, -2 or –4 resulted in reduced GSI-mediated inhibition of cell proliferation (Curry *et al*, 2005). Chan *et al* (2007) demonstrated that Notch-1 retroviral transduction rescued GSI-induced hypophosphorylation of signalling proteins in the mTOR pathway.

Results from these experiments demonstrate for the first time that pharmacological inhibition of the Notch pathway with GSIs may enhance the effect of gemcitabine. In addition, the combination of GSI-I and curcumin is shown to be effective. They also demonstrate that Notch-1 and Notch-3, but not Notch-4 are important in pancreatic carcinoma cell proliferation and survival, and that they act independently of each other. These data support the hypothesis that inhibition of Notch activation using GSI is a promising therapeutic approach in pancreatic carcinoma, but that some effects may be via Notch-independent pathways.

CHAPTER 5

EFFECT OF GAMMA SECRETASE INHIBITION IN A XENOGRAFT MODEL OF PANCREATIC ADENOCARCINOMA

5.1 INTRODUCTION

Given the promising therapeutic potential of gamma secretase inhibition (Chapter 4), and to enable translation to the clinic, an alternative gamma secretase inhibitor, a preclinical tool compound (MRK003) of one already trialled in humans (MK0752) was chosen for further investigation.

MK-0752 is an orally-active gamma secretase inhibitor manufactured by Merck Pharmaceuticals Inc. The chemical name is cis-4-[(4-chlorophenyl) sulfonyl]-4-(2,5-difluorophenyl) cyclohexanepropanoic acid and its empirical formula is $C_{21}H_{20}ClF_2O_4SNa$, with a molecular weight of 464.89. MK-0752 was initially developed for the treatment of Alzheimer's disease, with the aim to inhibit gamma-secretase mediated cleavage of the amyloid precursor protein and prevent formation of Aβ peptides (Siemers *et al*, 2006 and 2007). Although promising reductions in Aβ production were produced in animal models and humans, development for this indication was discontinued due to a narrow therapeutic index. Subsequently, MK-0752 has been developed for the treatment of solid tumours.

MK-0752 is known to have unfavourable pharmacokinetic characteristics in mice and therefore MRK-003 has been used for preclinical studies and was supplied by the company. MRK-003 performs similarly to MK-0752 in *in vitro* assessments. MRK-003 has been shown to be a potent inhibitor of gamma-secretase with a subnanomolar *in vitro* potency for the inhibition of Aβ secretion and Notch receptor cleavage in SH-SY5Y SPA4CT and HEK293 cells (Sparey *et al,* 2005; Lewis *et al,* 2007). *In vitro* studies show that it can induce G_1 cell cycle arrest, decrease cell viability, and cause apoptosis in T-ALL cell lines carrying Notch activating mutations (Lewis *et al,* 2007).

In vivo studies show suppression of formation of spontaneous mammary tumours in *neu*T transgenic mouse tumour model. MRK-003 has also been shown to inhibit Notch-3 activation, inhibit growth and induce apoptosis in lung cancer cell lines *in vitro*, and inhibit tumour growth *in vivo* in a mouse xenograft model (Konishi *et al*, 2007). Clinical studies evaluating MK-0752 in T-ALL (De Angelo *et al*, 2006; NCT00100152) have been performed, and further studies investigating its use in breast carcinoma (Krop *et al*, 2006; NCT00106145; NCT00645333; NCT00756717) and paediatric central nervous system malignancies (NCT 00572182) are currently underway.

The experiments described in this chapter examined the effects of MRK-003 on pancreatic adenocarcinoma cells *in vitro* and *in vivo*, alone and in combination with other anti-cancer agents.

5.2 RESULTS

5.2.1 *In vitro* studies

5.2.1.1 Effect on Notch protein expression

Treatment with MRK-003 resulted in a small reduction in ICN-1 expression in all three cell lines following 48 hours of treatment (Figure 5.1). ICN-3 expression was reduced in ASPC-1 following 48 hours of treatment. No effect was seen on ICN-4 expression. Treatment with MRK-003 resulted in a small reduction in expression of the Notch target protein HES-1 in ASPC-1 cells. No reduction was seen in BxPC-3 or PANC-1 cells.

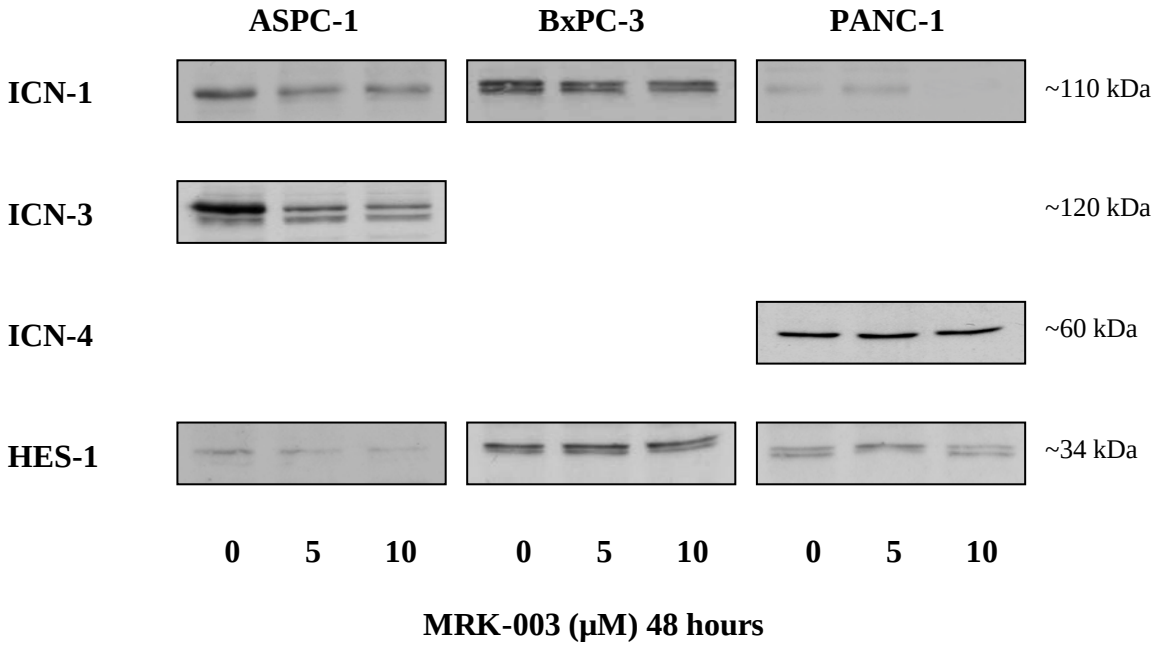

Figure 5.1 – Effect of MRK-003 on Notch protein expression in pancreatic adenocarcinoma cell lines.
Representative western blots showing effect on active intracellular Notch (ICN)-1, -3, -4 and HES-1 following treatment with MRK-003 for 48 hours compared to DMSO control (n=3 all experiments).

5.2.1.2 Effect on cell line proliferation

Treatment with MRK-003 caused a reduction in proliferation in all three pancreatic adenocarcinoma cell lines (Figure 5.2). ASPC-1 was the most sensitive cell line, followed by BxPC-3, then PANC-1. After treatment with 5μM for 72 hours, ASPC-1 showed a significant reduction in proliferation to 57.7% compared to DMSO control ($p=0.002$, Mann-Whitney (MW) test). Proliferation in BxPC-3 was 73.5% compared to DMSO control ($p=0.004$, MW-test). Proliferation in PANC-1 cells was 80.7% of DMSO controls following treatment with 10μM MRK-003 ($p=0.029$, MW-test). No significant reduction in proliferation was seen following treatment with 5μM in this cell line. Reduced proliferation was associated with G_1 cell cycle arrest in all cell lines.

5.2.1.3 Effect on cell viability

The effect of MRK-003 on cell viability was next determined, using ATP levels as an endpoint. Figure 5.3 illustrates the dose- and time-dependent reduction in cellular ATP levels following treatment of ASPC-1, BxPC-3, and PANC-1 after 24 and 48 hours, and shows a clear difference in sensitivity among the cell lines. ASPC-1 was the most sensitive line with a significant reduction in cell viability after treatment with 2μM at 24 hours and 1μM at 48 hours. Significantly reduced viability was seen BxPC-3, with PANC-1 the most resistant.

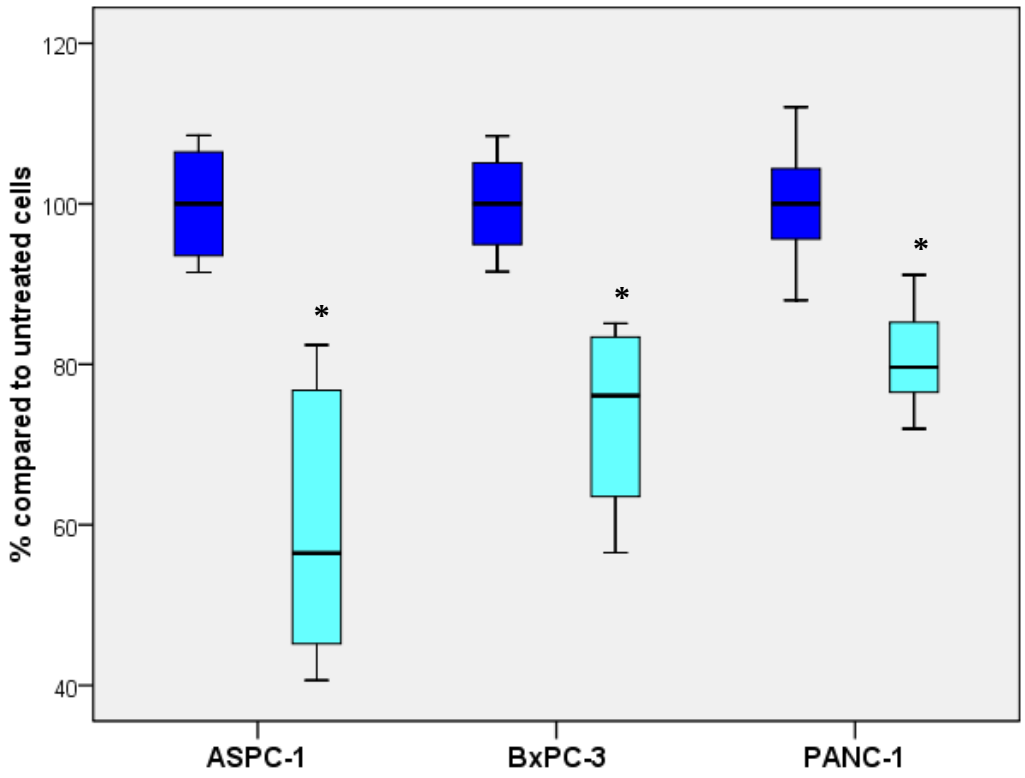

Figure 5.2 – Effect of MRK-003 on cell proliferation in pancreatic adenocarcinoma cell lines.
Box chart demonstrating reduction in cell proliferation in three pancreatic adenocarcinoma cell lines following treatment for 72 hours with 5μM (ASPC-1, BxPC-3) or 10 μM (PANC-1) of MRK-003 (pale blue). *$p<0.05$ vs. DMSO control (dark blue)

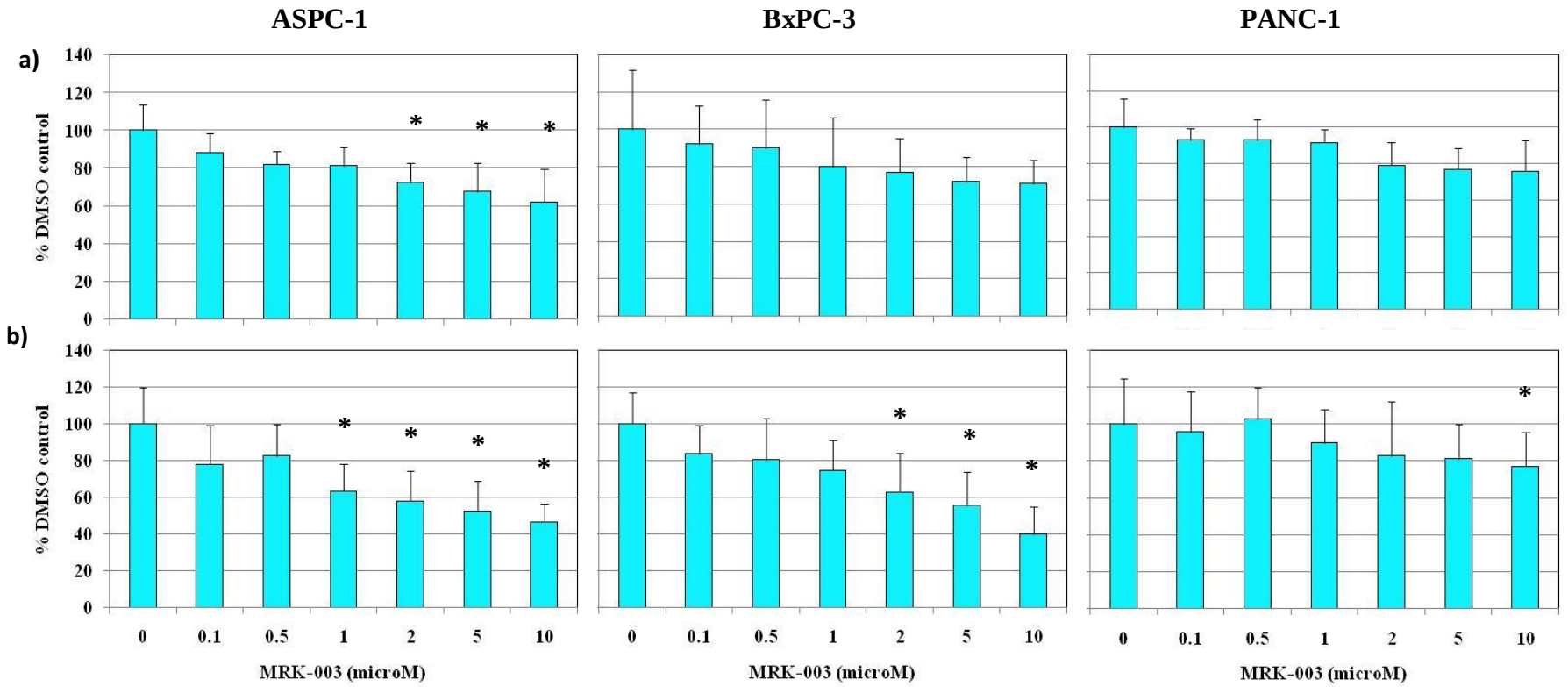

Figure 5.3 – Effect of MRK-003 on cell viability in pancreatic adenocarcinoma cells.
ATP levels following treatment for a) 24 and b) 48 hours. Charts show mean and standard deviation. *$p<0.05$ compared to DMSO control.

5.2.1.4 Effect on apoptosis

Figure 5.4 demonstrates annexin V/PI results following treatment with MRK-003 for 24 hours, with little effect seen in any cell line. ASPC-1 and BxPC-3 underwent a small but significant reduction in live cells after treatment with 10μM MRK-003. No effect was seen on PANC-1 cells. No statistically significant induction in apoptosis was seen in any of the three cell lines. Following 48 hours of treatment, a significant reduction in live cell population associated with induction of apoptosis was seen after treatment with 5μM in ASPC-1 cells and 10μM in BxPC-3 cells. Again, no effect was seen in PANC-1 cells. No significant induction in effector caspase 3/7 activity was seen following 24 hours of treatment with 5μM (ASPC-1, BxPC-3) or 10μM (PANC-1).

5.2.1.5 Combination treatment

The effectiveness of MRK-003 in combination with gemcitabine, the current first line chemotherapy agent, and curcumin, a promising dietary anti-cancer agent, was next assessed (Figures 5.5-5.7). Combined treatment with MRK-003 and gemcitabine resulted in a significantly reduced ATP level in ASPC-1 cells compared to either agent alone. This was associated with a significant reduction in live cell population on Annexin V/PI analysis, an induction of apoptosis and increase in necrotic cell population compared to either agent alone. Caspase 3/7 analysis confirmed the increased induction in apoptosis. These findings were not reciprocated in the other two cell lines. Similarly, the combination of curcumin and MRK-003 resulted in a reduction in live cells on annexin V analysis associated with an increase in necrotic cell population compared to either agent alone only in ASPC-1 cells (Figure 5.5-7).

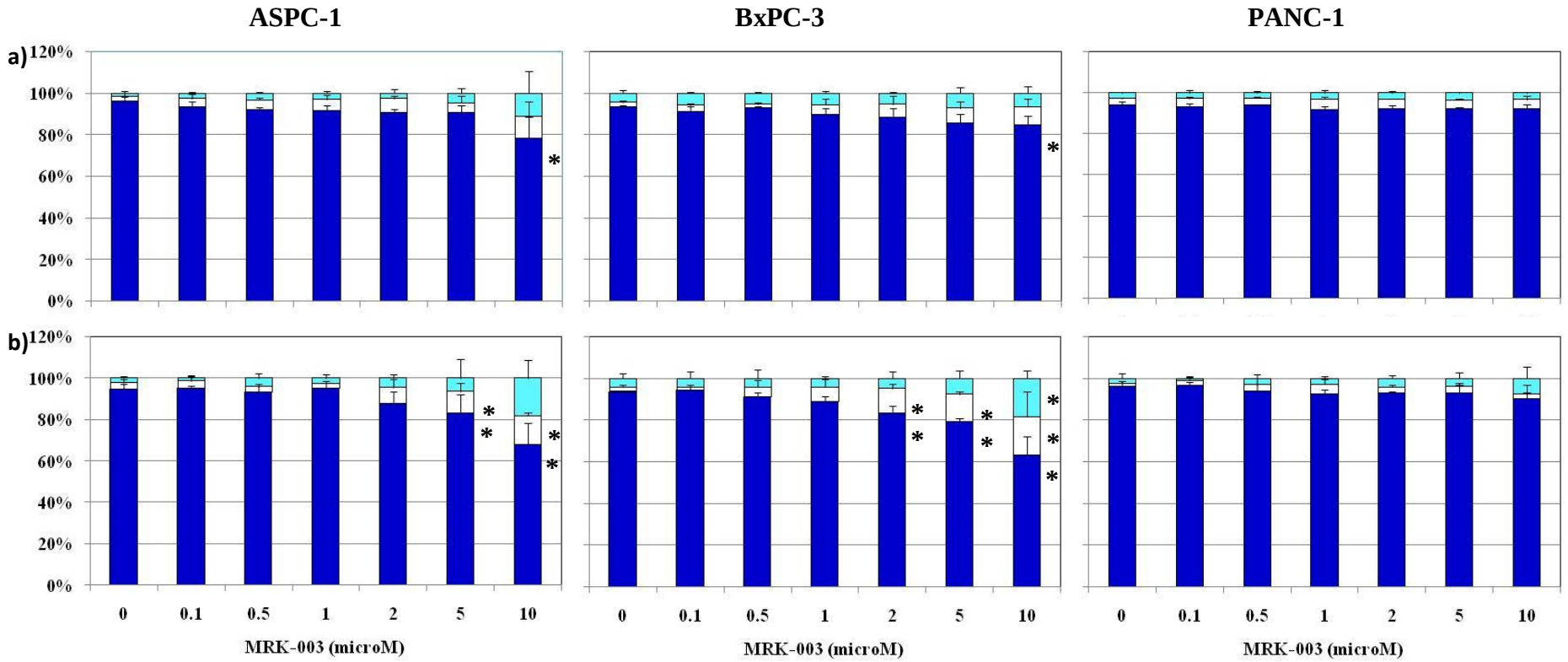

Figure 5.4 – Effect of MRK-003 on apoptosis in pancreatic adenocarcinoma cells.
Annexin V/PI staining for apoptosis in cell lines treated for a) 24 hours and b) 48 hours with MRK-003. Blue bars represent live, white bars apoptotic, and cyan bars necrotic populations. *$p<0.05$ compared to DMSO control.

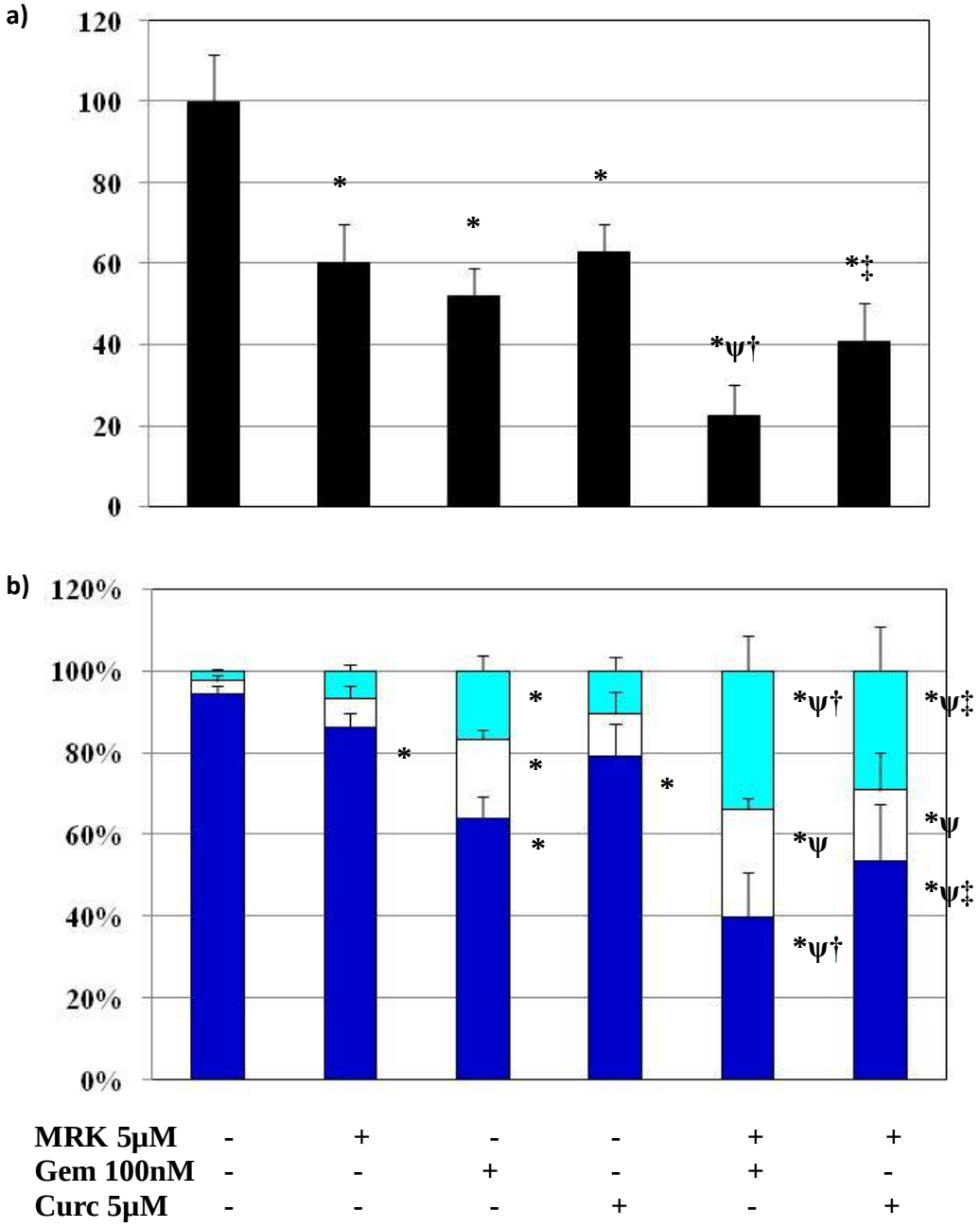

Figure 5.5 – Effect of combining MRK-003 with gemcitabine or curcumin in ASPC-1 cells.

a) Cell viability following treatment +/- gemcitabine or curcumin. b) Apoptosis as assessed by AnnexinV/PI staining (Blue, live cells; white, apoptotic cells; cyan, necrotic cells). *p<0.05 compared to DMSO control; †p<0.05 compared to treatment with gemcitabine alone; ‡p<0.05 compared to treatment with curcumin alone; ψp<0.05 compared to MRK-003 alone.

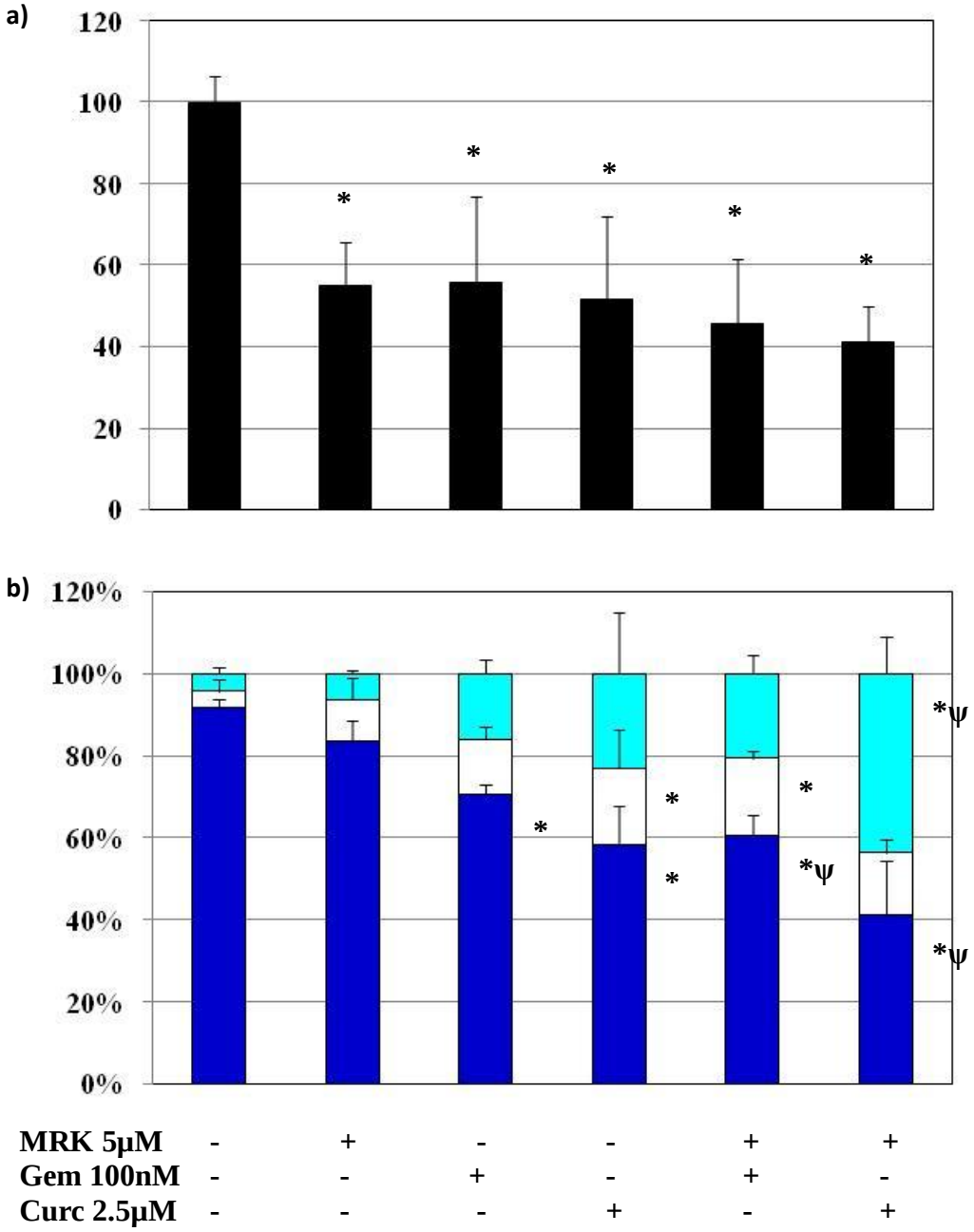

Figure 5.6 – Effect of combining MRK-003 with gemcitabine or curcumin in BxPC-3 cells.

a) Cell viability following treatment +/- gemcitabine or curcumin. b) Apoptosis as assessed by AnnexinV/PI staining (Blue, live cells; white, apoptotic cells; cyan, necrotic cells). *p<0.05 compared to DMSO control; †p<0.05 compared to treatment with gemcitabine alone; ‡p<0.05 compared to treatment with curcumin alone; ψp<0.05 compared to MRK-003 alone.

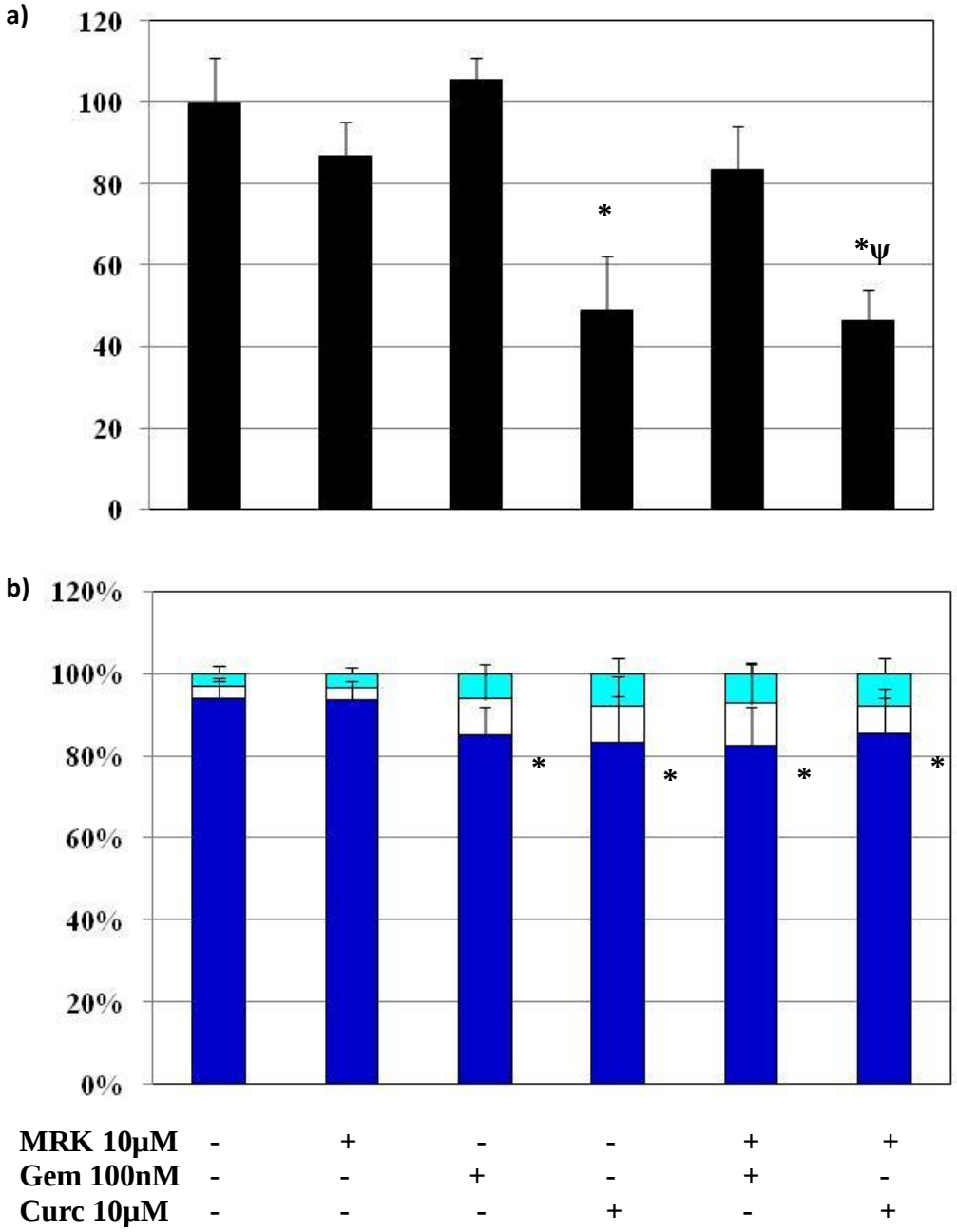

Figure 5.7 – Effect of combining MRK-003 with gemcitabine or curcumin in PANC-1 cells.

a) Cell viability following treatment +/- gemcitabine or curcumin. b) Apoptosis as assessed by AnnexinV/PI staining (Blue, live cells; white, apoptotic cells; cyan, necrotic cells). *$p<0.05$ compared to DMSO control; †$p<0.05$ compared to treatment with gemcitabine alone; ‡$p<0.05$ compared to treatment with curcumin alone; ψ$p<0.05$ compared to MRK-003 alone.

5.2.2 *In vivo* studies

Pharmacokinetic studies using MRK-003 and MK-0752 have demonstrated rapid absorption, good oral bioavailability, low clearance, and a long half life of 12 hours in plasma. Acyl glucuronidation has been identified as the major metabolic pathway, with significant enterohepatic recycling. In addition, a high level of reversible binding to plasma proteins occurs in animal models and humans.

As of July 2008 MK-0752 or placebo had been administered to 306 healthy subjects studied as part of the development into Alzheimer's disease (255 received active treatment and 51 placebo), with 192 receiving multiple dosing. In addition, 61 cancer patients have received the active treatment in studies investigating maximum-tolerated dose in T-ALL (n=8) (De Angelo *et al,* 2006) and advanced breast carcinoma (n=53) (Krop *et al,* 2006). Although generally well tolerated at low doses (<300mg daily) for two weeks, a high frequency of gastrointestinal adverse events occurred at higher doses of continuous MK-0752 (De Angelo *et al,* 2006). In patients with cancer, MK-0752 was not well tolerated when dosed continuously, particularly ≥450mg daily, with gastrointestinal toxicity and fatigue being the most prevalent dose-limiting toxicities (Krop *et al,* 2006). Daily dosing at 450mg and higher was not considered sufficiently safe or well tolerated to permit Phase II evaluation at these dose levels.

Due to the associated side-effects of continuous dosing, an intermittent dosing schedule was established using preclinical models, and confirmed to inhibit Notch

activity (Konishi *et al*, 2007). A 3-days-on/4-days-off dosing regimen resulted in decreased GI toxicity while preserving anti-tumour activity, which has subsequently been confirmed in clinical studies of patients with T-ALL and advanced breast carcinoma (total n=26, 450-600mg).

Data collected to date suggest a sufficient therapeutic window between toxicities and anti-tumour effects with an intermittent dosing schedule in humans. The aim of these experiments was to determine the effect of this dosing schedule using MRK-003 in a murine xenograft model of pancreatic adenocarcinoma.

5.2.2.1 Preparation of MRK-003 for dosing

MRK-003 was dosed as a suspension in 0.5% methylcellulose and made up fresh prior to each dosing due to a stability of 2-3 hours at room temperature. Methylcellulose (0.5%) was made up by heating 300ml of sterile dH_2O to 80°C, and then adding 5g of methylcellulose and stirring until dispersed. Cold dH_2O (700ml) was then added and stirred until fully dissolved. This was then stored at 4°C for 30mins prior to being passed through a 0.22µm filter. The solution was then stored at room temperature and opened under sterile conditions in a tissue culture hood.

An appropriate quantity of MRK-003 was weighed out and added to 0.5% methylcellulose solution to achieve the desired concentration. This was vortexed for 1 min or until the compound was no longer sticking to the bottom of the vial. This

was sonicated for 15 seconds and then placed in a sonicating water bath for 15mins at room temperature until evenly dispersed.

5.2.2.2 Xenograft model and animal husbandry

Female MF-1 nude mice (Harlan Laboratories, Oxon, U.K.) were used for the xenograft model, maintained on a normal AIN93G diet. Experiments were carried out under animal project licence 80/2167, granted to Leicester University by the United Kingdom Home Office and approved by Leicester University Local Ethics Committee for Animal Experimentation, meeting the standards required by the UKCCR for animal welfare.

Female nude mice (6-8 weeks old) were divided into 4 groups of 5 mice. ASPC-1 cells (2×10^6 cells per animal) were resuspended in 50µl ice cold serum free RPMI tissue culture medium. This was then added to 50µl of Matrigel (BD Biosciences, Oxford, UK) to give a total of 100µl which was then inoculated subcutaneously in the flank of each mouse, under light halothane anaesthesia.

Tumours were allowed to grow to 40-50mm^3 prior to commencing treatment. Once the tumours had reached the desired size, the mice were weighed, tumours callipered and the animals randomised blindly to treatment groups (Figure 5.8). All treatments were administered by gavage in an intermittent 3 day on 4 day off schedule.

- Group 1: Control group were fed normal AIN93G diet. Animals received 0.5% methyl cellulose (200µl).

- Group 2: 25mg/kg group were fed normal AIN93G diet. Animals received 25mg/kg of MK003 in 0.5% methyl cellulose (200µl).

- Group 3: 50mg/kg group were fed normal AIN93G diet. Animals received 50mg/kg of MK003 in 0.5% methyl cellulose (200µl).

- Group 4: 100mg/kg group were fed normal AIN93G diet. Animals received 100mg/kg of MK003 in 0.5% methyl cellulose (200µl).

Animals were housed by group and underwent daily general clinical observations, including diarrhoea, skin rash, skin colour and rectal prolapse. The mice were weighed once per week. Tumour volume was measured three times per week using digital callipers and was calculated using the formula = (length x width^2)/2, where length is the larger diameter of the tumour (mm). Volumes were normalised in relation to the initial (baseline) tumour size per animal in order to establish growth curves for each group (fold change). All measurements were made by the same observer. Treatment was continued for 4 weeks or until tumour burden or weight loss exceeded IACUC guidelines. At the time of sacrifice, mice were euthanised by exsanguination and the tumours excised and weighed. Tumour tissue was divided into two equal parts; one fixed in 10% buffered formalin for immunohistochemistry, the other snap frozen and stored at -80°C for future studies.

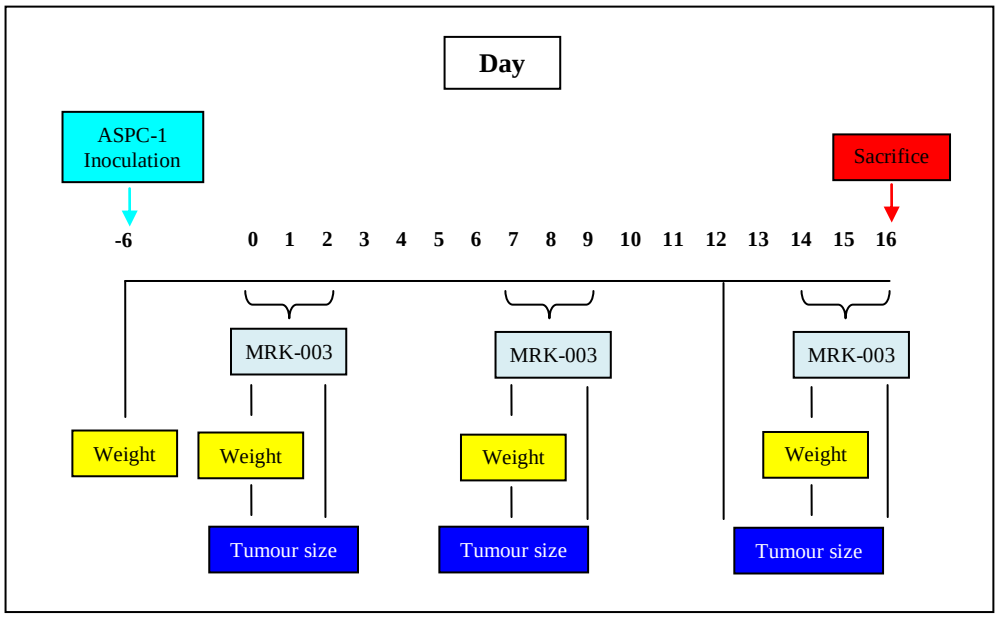

Figure 5.8 – Xenograft experiment schedule

5.2.3 *In vivo* results

5.2.3.1 MRK-003 dose-response

The treatment was administered for 16 days and the mice were sacrificed before tumour growth exceeding IACUC guidelines. Treatment with MRK-003 appeared well-tolerated with no side effects clinically apparent. Nineteen of the animals remained active and healthy throughout the study. One animal was found dead on day 12 after apparently fighting; previous to this it had appeared healthy and active. The weight of animals in all groups increased significantly throughout the study (Figure 5.9; $p<0.05$ all groups, Wilcoxon test), and there was no significant difference in animal weight between the groups at the end of treatment ($p=0.118$, KW-test).

There were no significant differences in tumour volume between the four groups at the start of treatment with MRK-003 (Figure 5.10a; p=0.536, KW-test). Growth curves displaying tumour volume and fold change in tumour volume are shown in Figure 5.11. Tumour volumes were similar at the start of the experiment, and by day 16, there was no significant difference in tumour volume between the groups. When the fold change in tumour volume from baseline was analysed, there was no significant difference between groups over these time periods.

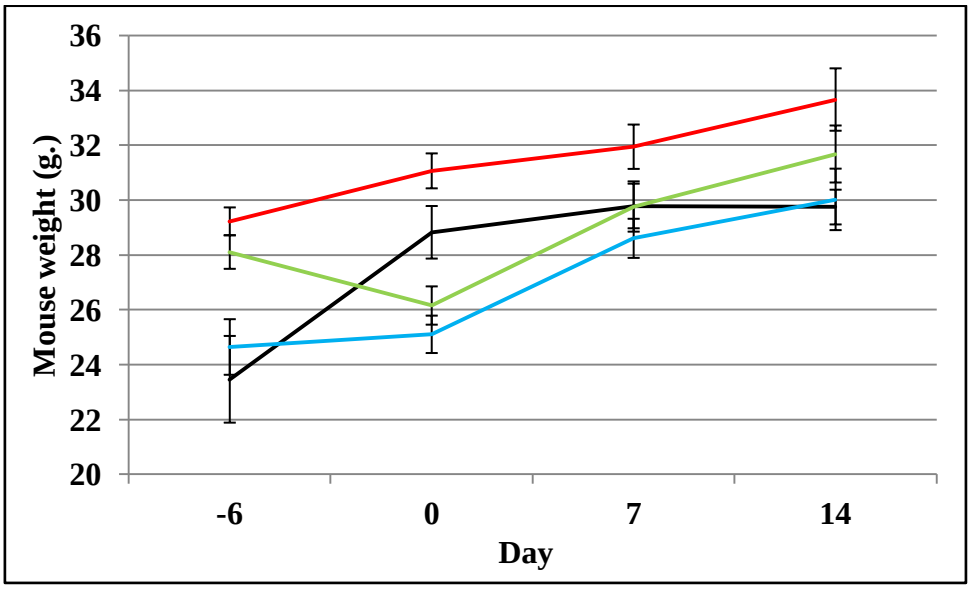

Figure 5.9 – Animal weight throughout xenograft experiment.
ASPC-1 cell inoculation occurred at day -6 and dosing with MRK-003 commenced on day 0. Groups: control (black line); 25mg/kg (blue); 50mg/kg (green); 100mg/kg (red). Values displayed are mean of 5 animals with standard error of the mean displayed as error bars.

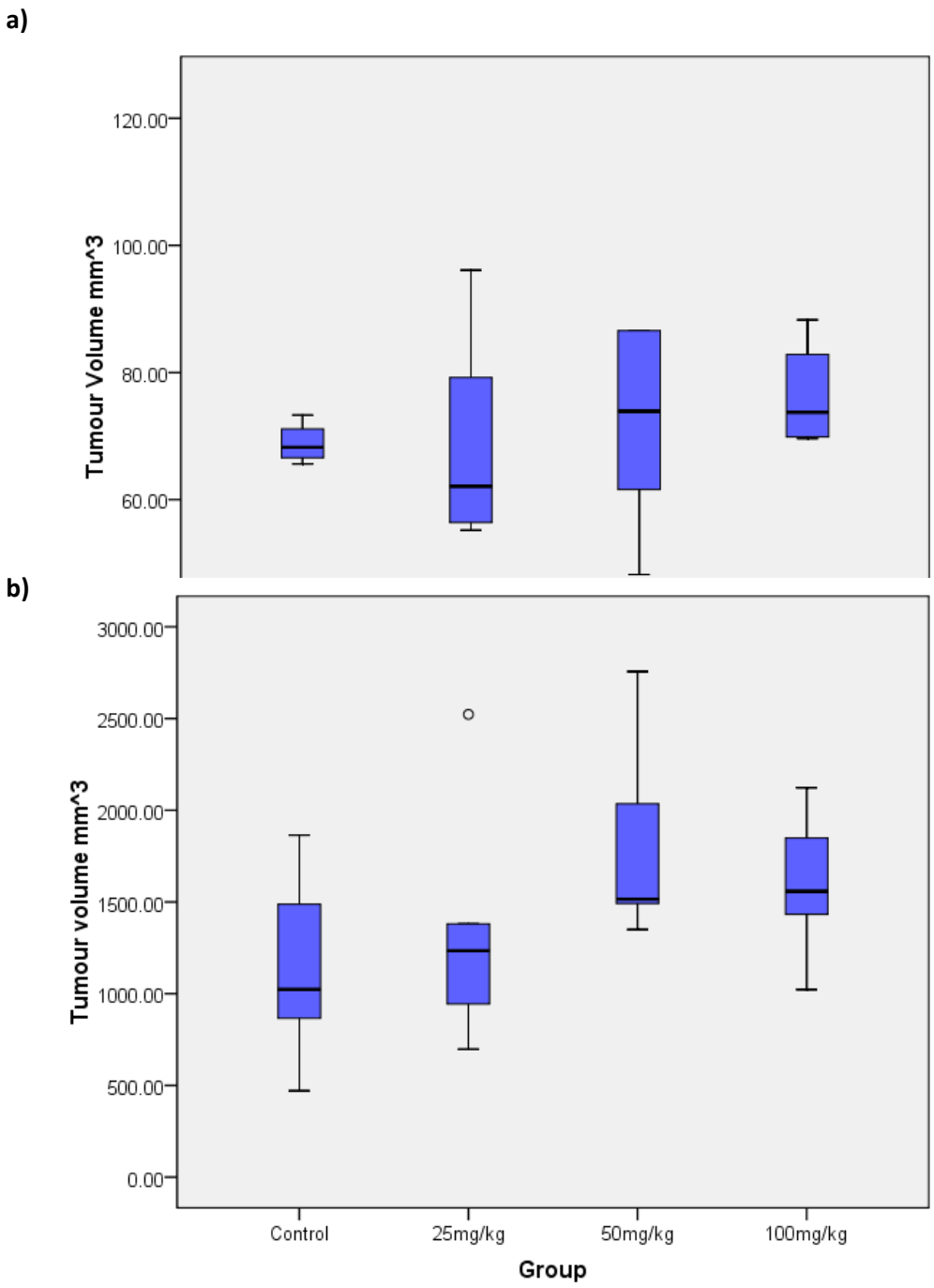

Figure 5.10– ASPC-1 xenograft tumour volume
a) At the start of treatment with MRK-003 (p=0.536; KW test), and b) at end of 16 days treatment (p=0.161).

a)

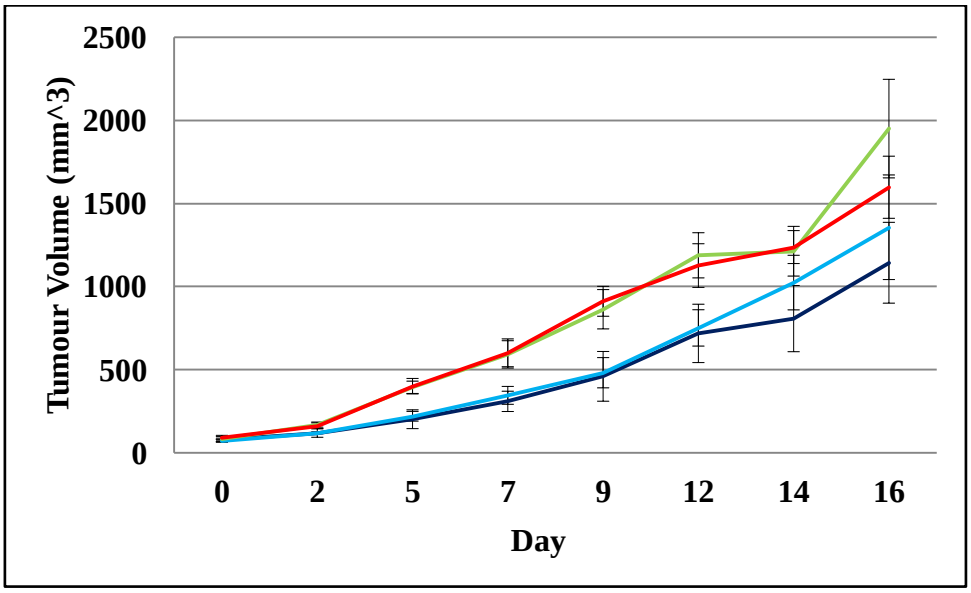

b)

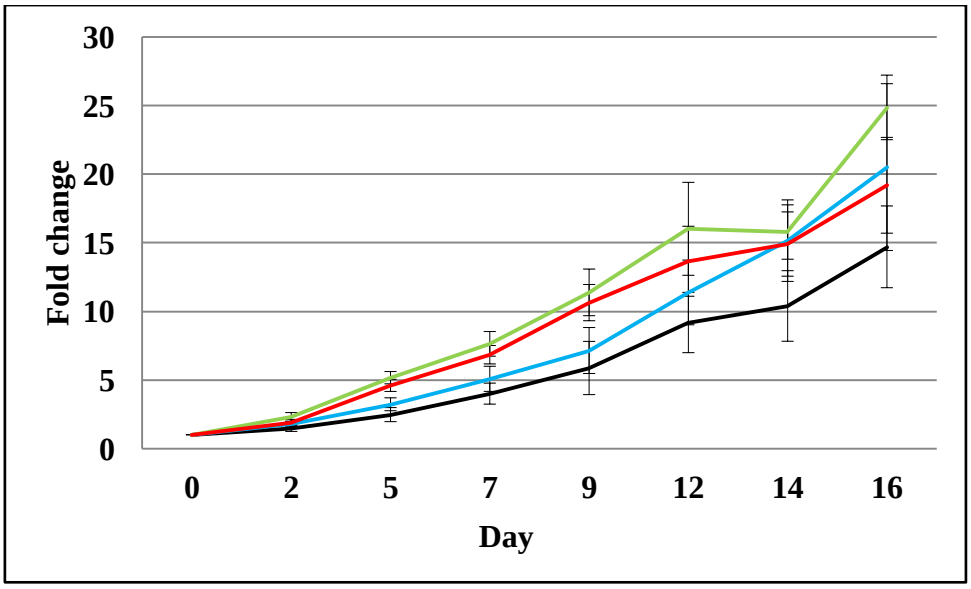

Figure 5.11 – Xenograft tumour growth following treatment with MRK-003
Growth curves displaying a) tumour volume (mm^3) and b) fold change from baseline tumour size, in a murine xenograft model of ASPC-1 pancreatic carcinoma treated with increasing doses of MRK-003. Groups: control (black line); 25mg/kg (blue); 50mg/kg (green); 100mg/kg (red). Values displayed are mean of 5 animals with standard error of the mean displayed as error bars.

5.2.3.2 Effect of MRK-003 on Ki67 staining

Tumour tissue taken at time of sacrifice and fixed in 10% buffered formalin was stained for Ki67. Ki67 antigen is the prototypic cell cycle related nuclear protein, expressed by proliferating cells in all phases of the active cell cycle (G_1, S, G_2 and M phase). It is absent in resting (G_0) cells. Ki67 antibodies are useful in establishing the cell proliferation fraction in neoplasms (immunohistochemically quantified by determining the number of Ki67 positive cells among the total number of resting cells = Ki67 index). Ki67 index was not affected by treatment with MRK-003 (Spearman's correlation coefficient 0.032, p=0.898; Figure 5.12), confirming the tumour size results.

5.2.3.3 Effect of MRK-003 on HES-1 expression

The efficacy of MRK-003 treatment on Notch pathway inactivation was examined by immunohistochemistry for HES-1 expression. The percentage of cells staining for nuclear, and therefore active, HES-1 were assessed. Treatment with MRK-003 resulted in a significant dose-dependent reduction in nuclear HES-1 expression (Spearman's correlation coefficient -0.83, p<0.001; Figure 5.13). Treatment with 100mg/kg resulted in a 36.2% reduction in nuclear HES-1 expression compared to control.

a)

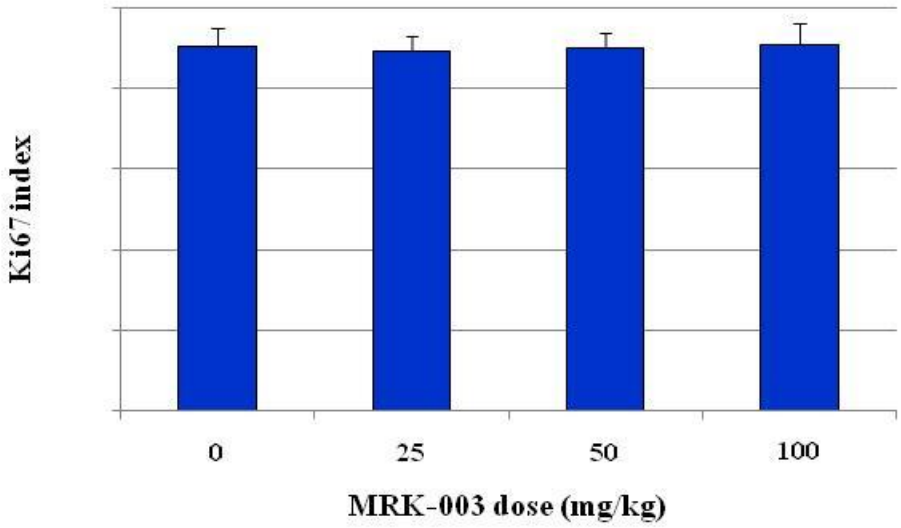

b)

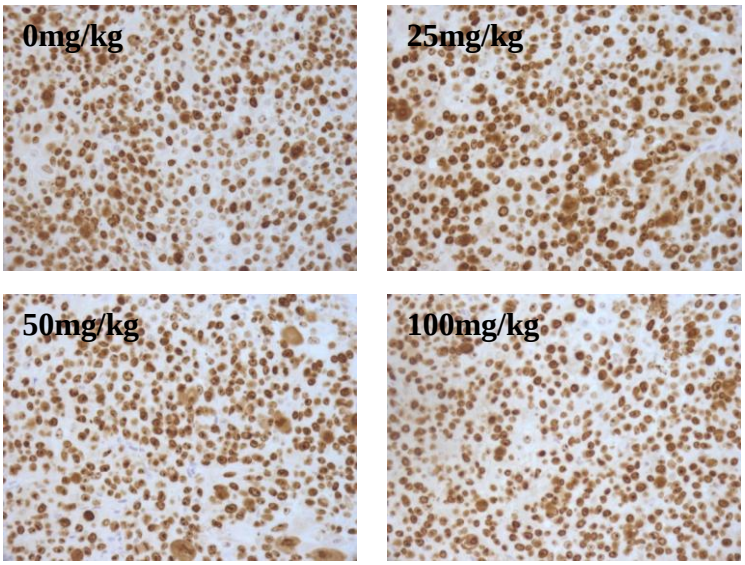

Figure 5.12– Effect of MRK-003 dosing on ASPC-1 xenograft Ki67 index.
a) Ki67 index following 16 days of treatment, p=0.898; b) Example slides

a)

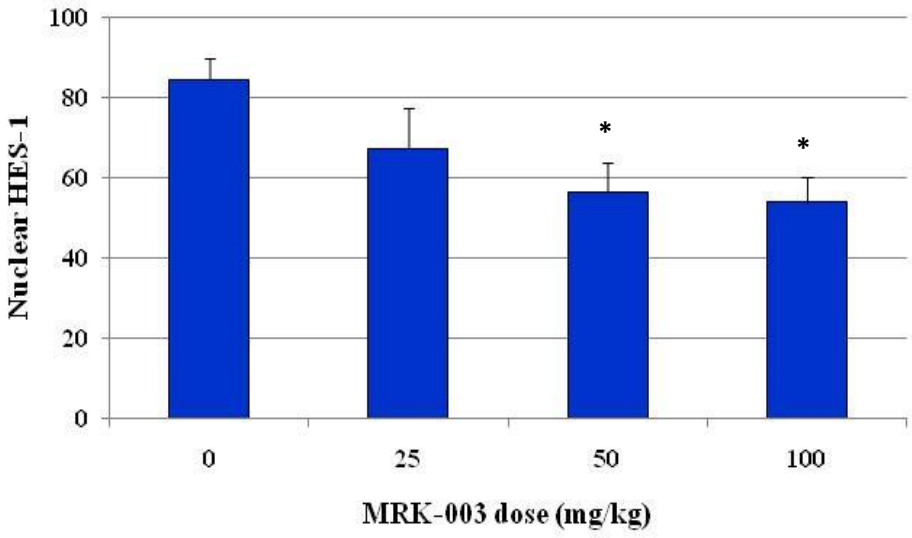

b)

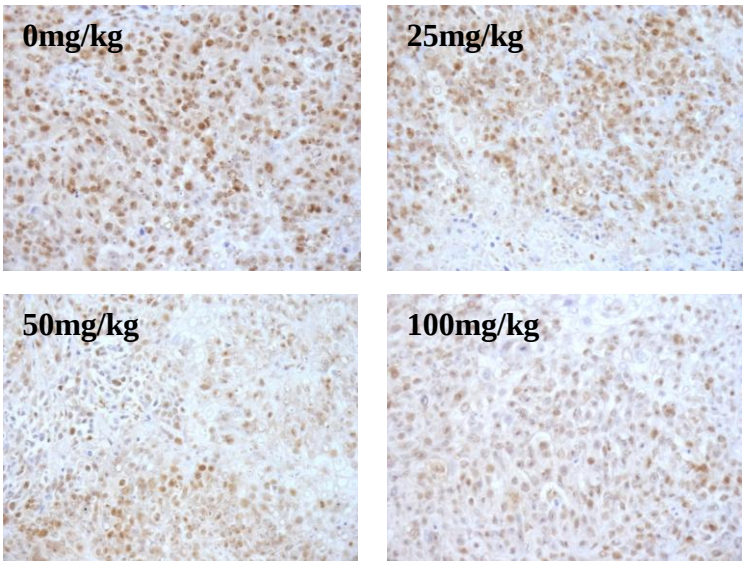

Figure 5.13 – Effect of MRK-003 dosing on ASPC-1 xenograft nuclear HES-1 expression.
a) Effect on HES-1 staining following 16 days of treatment ($p<0.001$, Spearman's; *$p<0.05$ vs. 0 mg/kg.); b) example slides.

5.3 DISCUSSION

This is the first study to investigate the effects of the gamma secretase inhibitor MRK003 on pancreatic carcinoma cell lines *in-vitro* and on tumour growth in a murine xenograft model of pancreatic carcinoma. Treatment with MRK003 resulted in a small down-regulation in active Notch-1 and Notch-3 expression *in vitro*, associated with a small reduction in HES-1 in ASPC-1 cells. No effect was seen on active Notch-4. This suggests that MRK003 is a weaker inhibitor of gamma secretase than GSI-I. Ten μM was used as this had been shown to completely knockdown intracellular Notch-1 expression in T-ALL cells (Lewis *et al*, 2007). Treatment with 1μM has been previously shown to knockdown active Notch-1 and reduce expression of HES-1 and Deltex-1 in T-ALL cells (O'Neil *et al*, 2007; Cullion *et al*, 2009). This may suggest a relative resistance to MRK003 in these pancreatic cancer cell lines.

This study found treatment with MRK003 *in vitro* to result in a reduction in cell proliferation, associated with reduced cell viability and G_1 cell cycle arrest in all three cell lines, with ASPC-1 being the most sensitive. Induction in apoptosis was seen in ASPC-1 and BxPC-3 cells after 48 hours of treatment. A study published at the time of writing demonstrated a reduction in cell proliferation in PANC-1 cells following 5 days of treatment with 5 and 10μM. They also found a small reduction in proliferation following treatment with 10μM for 72 hours, similar to this study. MRK003 has previously been found to result in G_1 arrest and induction in apoptosis in T-ALL cell lines (O'Neil *et al*, 2007; Cullion *et al*, 2009).

In this study, treatment with up to 100mg/kg of MRK003 in a three day on/four day off treatment protocol did not alter tumour growth in an ASPC-1 murine xenograft model. These results were surprising. ASPC-1 was chosen not only because it had been successfully used as a xenograft in the department previously, but also because it was the most sensitive cell line *in vitro*. MRK003 has recently been shown to have promising effects in xenograft models of lung carcinoma, breast carcinoma, and glioblastoma, as well as murine T-ALL models (Konishi *et al*, 2007; Tammam *et al*, 2009; Watters *et al*, 2009; Chen *et al*, 2010; Efferson *et al*, 2010). As previously reported in other models, this treatment schedule was well tolerated by the animals, but the lack of alteration in Ki67 staining fits with the lack of effect on tumour volume.

The question remains as to whether the absence of effect is a true result or not? Several potential explanations may exist including poor oral bioavailability and inadequate dosing. Adequate serum levels have been achieved in previous studies to knockdown HES-1, HES-5, and Deltex-1 in murine models of T-ALL and breast carcinoma (Tamman *et al*, 2009; Cullion *et al*, 2009; Watters *et al*, 2009; Efferson *et al*, 2010). The reduction of HES-1 nuclear expression seen following treatment in the current study also suggests that the agent is reaching the tumour. As only a 36% reduction in HES-1 expression was achieved in this study following treatment with 100mg/kg MRK003; it may be that higher doses should be tried in future. Although this may result in some toxicity, higher doses have previously been tolerated. Cullion *et al* (2009) treated near-end-stage disease *Tal1/Ink4/Arf*- mice with 150mg/kg MRK003 for 3 days on, 4 days off, and found that this significantly increased survival compared to placebo. Efferson *et al* (2010) found this dosing to be tolerated and to

reduce tumour growth in an ErbB2 breast cancer model. The study by Plentz *et al* (2009) used Kras p53 L/+ mice which spontaneously develop PanIN lesions, precursors of pancreatic ductal adenocarcinoma. They found that treatment with 100mg/kg in the 3 day on/4 day off intermittent dosing schedule reduced the number of PanIN lesions and development of subsequent ductal adenocarcinomas in a Notch-dependent manner. These data prove that Notch plays a role in the development of pancreatic tumours in this model but does not show that MRK003 is useful in cases of established cancer, such as those which would be targeted with chemotherapy.

Although murine models of cancer are a convenient initial method for determining the effects of a novel anti-cancer drug *in vivo*, they have several limitations which affect translational ability. Firstly, although the tumour cells are derived from human tissue, the drug is being administered within a murine environment and corresponding physiology. This is demonstrated by the utilisation of MRK003 in this chapter compared to MK-0752, which is the agent used in human trials. Secondly, by definition the mouse models must have compromised immune systems to accept the xenograft, thus altering the dynamics of the immune response on the tumour. The counter argument for this is that by the time a tumour has established and metastasised it must have escaped immuno-surveillance. The subcutaneous implantation of the xenograft will also limit comparability as the subcutaneous microenvironment may not be relevant to that of the organ site of primary or metastatic disease (Killion *et al*, 1999). One alternative to a murine xenograft model is a genetic cancer model, such as the Kras p53 L/+ mouse model which spontaneously develops precursor PanIN lesions (Plentz *et al*, 2009). These still have the limitations of murine physiology. In addition, although they can recreate one or

two of the genetic alterations characteristic of human malignancy, they cannot recreate their full complexity. Human orthotopic xenograft models may eliminate some of these limitations. In these models, tumour cells are taken from patients and injected or implanted into the equivalent organ from which the cancer originated. Although these models retain mice physiology, they have several advantages, including maintaining the complex genetic composition of human tumours and the ability to maintain site specificity. Such a model in pancreatic adenocarcinoma has been a recent development (Huynh *et al*, 2011) and may result in more meaningful outcomes from preclinical studies. However the ultimate test will always be in clinical trial.

Whilst MRK003 may prove an ineffective treatment, the *in vitro* experiments demonstrate that in ASPC-1 and BxPC-3 cells, treatment with MRK003 in combination with either gemcitabine or curcumin resulted in reduction in live cells and induction of apoptosis. These data, combined with the results from chapter 4, suggest value in combining a Notch inhibitor with gemcitabine. Although this was not investigated in this chapter due to limitations on resources, this combination has subsequently been investigated in the Kras p53 L/+ mouse model. Similarly to the results in this chapter, MRK003 produced little affect on tumour alone, however potentiated the effect of gemcitabine (*Personal Communication, Dr N. Cook, University of Cambridge*). Gamma secretase inhibition may yet be of benefit to patients with pancreatic carcinoma. A phase I/II trial investigating MK-0752 in combination with gemcitabine, in patients with metastatic pancreatic ductal adenocarcinoma has been set up in collaboration with Cambridge (Cancer Research UK). Hopefully this will provide the answer.

CHAPTER 6

NOTCH AS A PLASMA BIOMARKER

6.1 INTRODUCTION

Whilst tissue-based biomarkers are useful in providing prognostic information following biopsy or surgical resection, by their very nature they are much less useful as screening or diagnostic tools, or in monitoring response to therapy. A number of serum tumour markers have been investigated to aid diagnosis in pancreatic cancer, including CA 19.9, CEA, CAM17.1, HSP27, DU-PAN2 and MIC-1. However, either availability or relative insensitivity limits their application (Bunger *et al*, 2011). As already discussed, the Notch receptor undergoes S1, S2, and presenilin/gamma secretase-dependent S3 proteolytic cleavages, resulting in release of intracellular Notch to effect signalling. Similar to the γ and ε cleavage sites during dual-intramembrane proteolysis of the β-amyloid precursor protein (Haass and Steiner, 2002), the Notch receptor also appears to undergo an S4 cleavage near the middle of the transmembrane domain, resulting in an additional amyloid-β-like (Aβ-like) Notch fragment (Okochi *et al*, 2002, 2006; Figure 6.1). This step may be important in the degradation of the Notch transmembrane domain, and may result in secretion of a small extracellular peptide. Indeed, Okochi *et al* (2006) demonstrated that two distinct molecular species, designated Notch-1 Nβ21 and the C-terminally elongated Notch-1 Nβ25, were secreted into the extracellular fluid following transfection of HEK293 cells with Notch-1 and Jagged-1.

The aim of work presented in this chapter was firstly to determine if the degradation fragment of the Notch-1 transmembrane receptor was produced by pancreatic cancer cells *in vitro*. Secondly, it was to develop a method to detect this fragment in plasma of patients with pancreatic carcinoma, and thirdly to assess whether it could be used

as a screening/diagnostic tool. Lastly the method was extended to investigate whether similar mechanisms applied to the Notch-3 receptor.

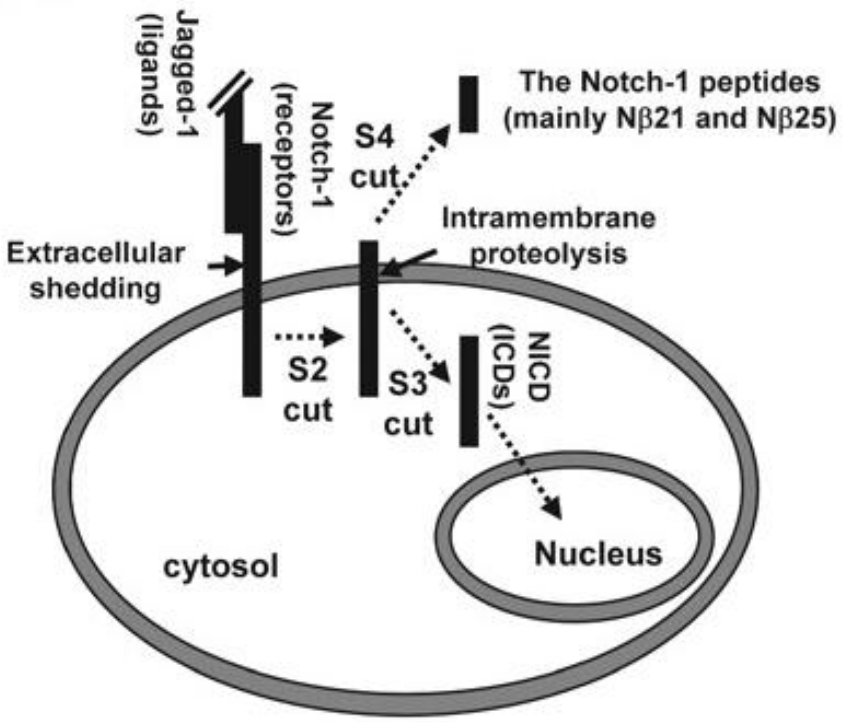

Figure 6.1 – Cleavage of Notch-1 at S4 results in extracellular secretion of the Nβ peptides. Adapted from Okochi *et al*, 2006.

6.2 METHOD DEVELOPMENT

Initial experiments focused on determining whether Notch-1 Nβ21 and Nβ25 could be detected in the media of cultured ASPC-1 pancreatic carcinoma cells, which express high levels of both Notch-1 and Notch-3. The sequences of the fragments detected by Okochi *et al* (2006) are shown below:

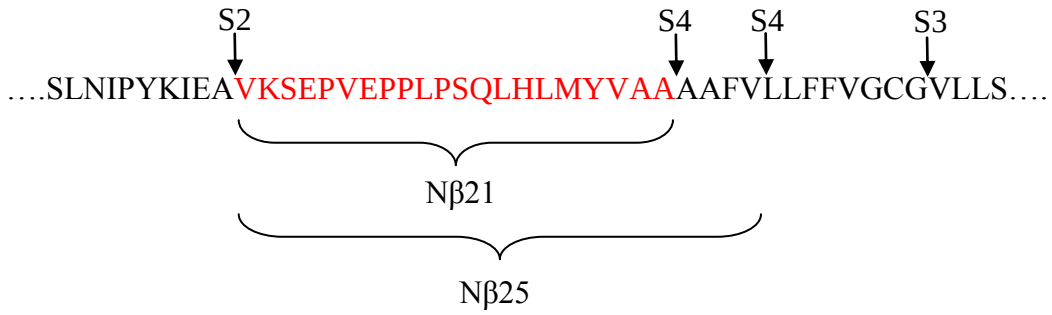

However, according to the UniProt and SwissPro databases, the above sequence was that for mouse Notch-1. The sequence for human Notch-1 is similar, but not identical (differences highlighted below in green). However, cleavage sites are conserved with the Notch-1 Nβ21 sequence between amino acids 1721-1740.

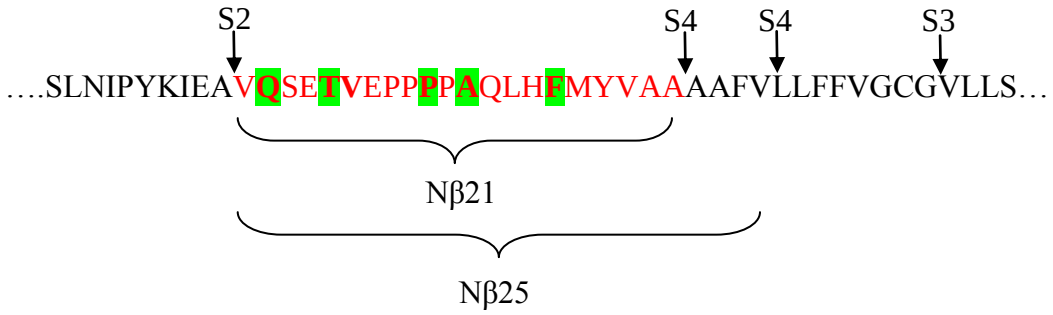

Matrix-assisted laser desorption ionisation (MALDI) mass spectrometry is based upon the bombardment of sample molecules with laser light to produce molecular ionisation. The sample is dissolved in a matrix that has a strong absorption at the laser wavelength. This mixture is applied to a target plate and, when crystallised, is subjected to laser irradiation. When the absorbed energy is transferred into excitation energy, matrix molecules locally sublimate and carry sample molecules in their plume into the gas phase, due to a proton transfer in the expanding plume. The mass to charge (m/z) ratio of each ion is then calculated by a time of flight analyser: an ion is accelerated by a determined potential between source and detector and the time that it takes to fly a fixed distance through a field-free region, known as the tube, is measured (de Hoffmann and Stoobant, 2007). The data are then processed by bioinformatic software based upon pre-existing calibration data.

ASPC-1 cells were grown to 70% confluence, following which a sample of the culture medium was removed. This underwent solid phase extraction (2.7.1) and molecular weight cut off filtration (2.7.2) prior to preparation for MALDI mass spectrometry (2.7.3 and 4). Due to the extensive number of compounds and metabolites in the culture medium, numerous peaks were seen on the mass spectrometry trace. However, there were no visible peaks at the molecular weight of interest. This was considered to be due to poor signal to noise ratio, which was likely to be replicated in human plasma.

In order to overcome this, methods to enrich the peptide were explored. The human Notch-1 Nβ21 peptide, VQSETVEPPPPAQLHFMYVAA was synthesised (Pepceuticals, Nottingham, UK), and a polyclonal rabbit antibody produced against

this (Davids Biotechnologie GmbH, Regensburg, Germany). The antibody was affinity purified by the manufacturer and was validated using ELISA, detecting the peptide at 1:300,000. The affinity of the antibody for the peptide was confirmed on dot blots prior to use.

Analysis of the peptide standard in buffer by MALDI-MS identified the most abundant isotope to have an m/z of 2312. The monoisotopic molecular weight calculated from the amino acid sequence is 2310 Da, and following positive ionisation, the [M+H]+ ion would have a mass/charge ratio of 2311 m/z. Taking into account the abundance of the carbon-13 isotope, as well as the number of carbon atoms within the peptide, the most abundant peptide isotope would be predicted to have a mass/charge ratio of 2312 m/z. The peaks seen at m/z 2334 and 2350 represent sodium and potassium adduct ions (Figures 6.2a, 6.3). The limit of detection of the pure standard was determined by analysing concentrations of 5pmol/µl down to 125fmol/µl. The lowest concentration at which a peak was observed was 250fmol/µl.

Next immunoprecipitation was investigated as an enrichment technique. Magnetic Dynabeads® (Invitrogen, UK) which have Protein G covalently bound to their surface will bind an antibody via the Fc region. Such cross-linking can be permanent to prevent co-elution. The antibody-bead complex is then incubated with the antigen of interest, which is then subsequently eluted. Protein G has been shown to strongly bind antibodies of rabbit origin, hence its use in these experiments.

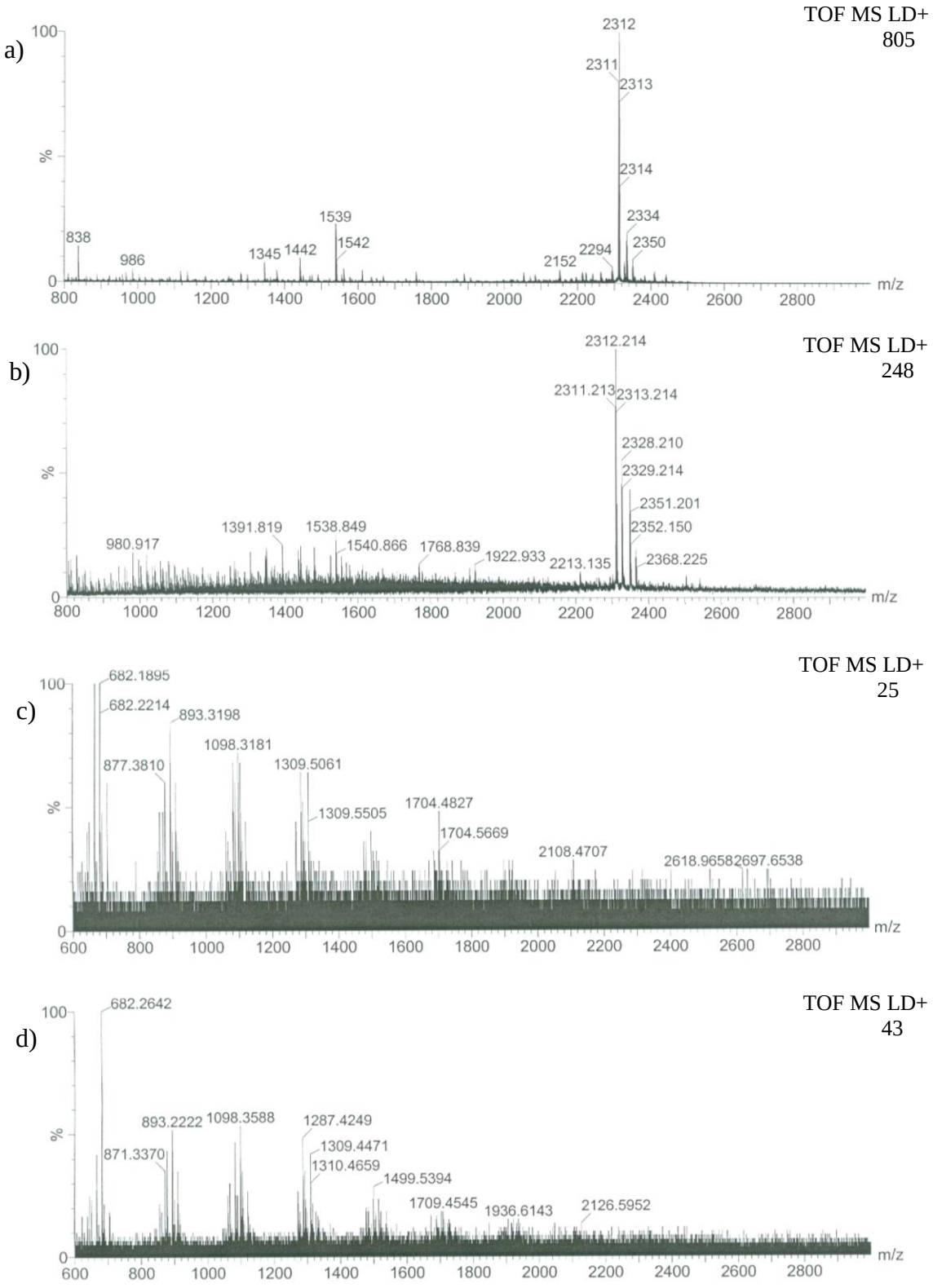

Figure 6.2 – Work-up of Notch-1 Nβ21 peptide immunoprecipitation.
Mass spectrometry traces of a) peptide standard; b) buffer spiked with peptide following immunoprecipitation and elution; c) wash following antibody-peptide binding step prior to elution; d) post-immunoprecipitation reserved buffer.

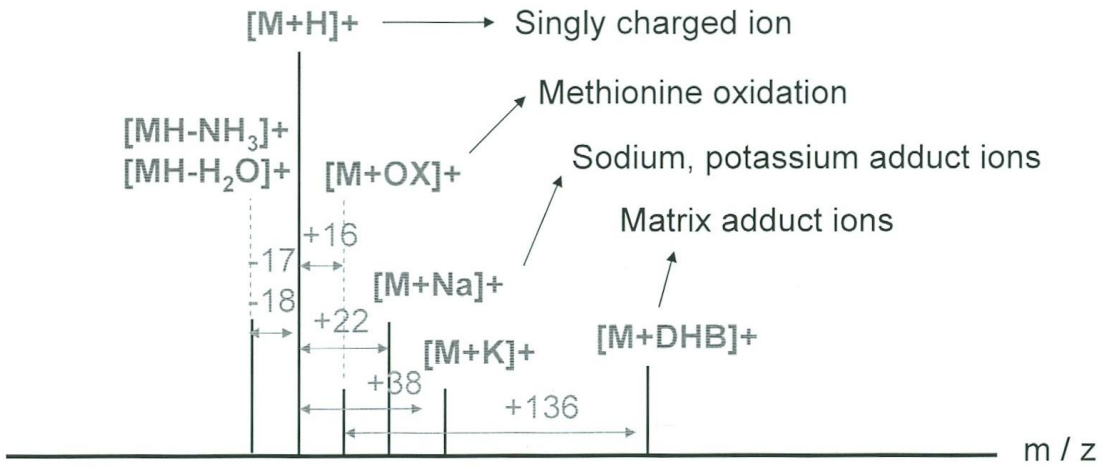

Figure 6.3 – Formation of MALDI adduct ions.
DHB, 2,5-dihydroxybenzoic acid, is a matrix used for mass spectrometry.

Briefly, the protocol for binding the antibody to the Dynabeads® was as follows. A 100µl aliquot of Dynabeads® was used for each sample. Between each step a magnetic eppendorf rack was used to isolate the beads, allowing the supernatant to be discarded. Beads were washed twice in 500µl citrate-phosphate buffer (22.4mM citric acid, 64.8mM dibasic sodium phosphate) pH 5.0 with 0.01% Tween-20, and incubated with 100µg of the anti-Notch-1 Nβ21 antibody, made up to 100µl in citrate-phosphate buffer pH 5.0. After mixing for 2 hours at room temperature to allow complexes to form, the beads were then washed three times with citrate phosphate buffer (pH 5.0) with 0.01% Tween-20, before being washed twice with 1ml triethanolamine pH 8.2. The antibody was then cross-linked to Protein G using 1ml of freshly made 20mM dimethyl pimelimidate (DMP) in 0.2M triethanolamine pH 8.2, and incubated with mixing for 30mins at room temperature. The beads were then washed once in 1ml 50mM Tris buffer pH 7.5 and three times with PBS with 0.01% Tween-20.

The efficiency of immunoprecipitation was then analysed using peptide diluted in ammonium bicarbonate pH 7.4 buffer (20pmol, 0.5pmol and 0.25 pmol). These solutions were incubated with the antibody-bound beads overnight at 4°C prior to elution, with 2x 30µl of citric acid. For all three concentrations, the appropriated m/z peak was detected. No peak was visible in the three ammonium bicarbonate washes (Figure 6.2c), demonstrating that pH elution was necessary to release the peptide from the antibody. To check elution efficiency, a further experiment with a total of 10 separate elution steps with citric acid was performed. No peak was detected in elutions 3-10, suggesting complete elution of bound peptide with the first two elutions in the investigated concentration range (Figure 6.4). In addition, no peptide was detected by mass spectrometry in the reserved buffer following immunoprecipitation (Figure 6.2d), suggesting complete uptake by the antibody-bound beads.

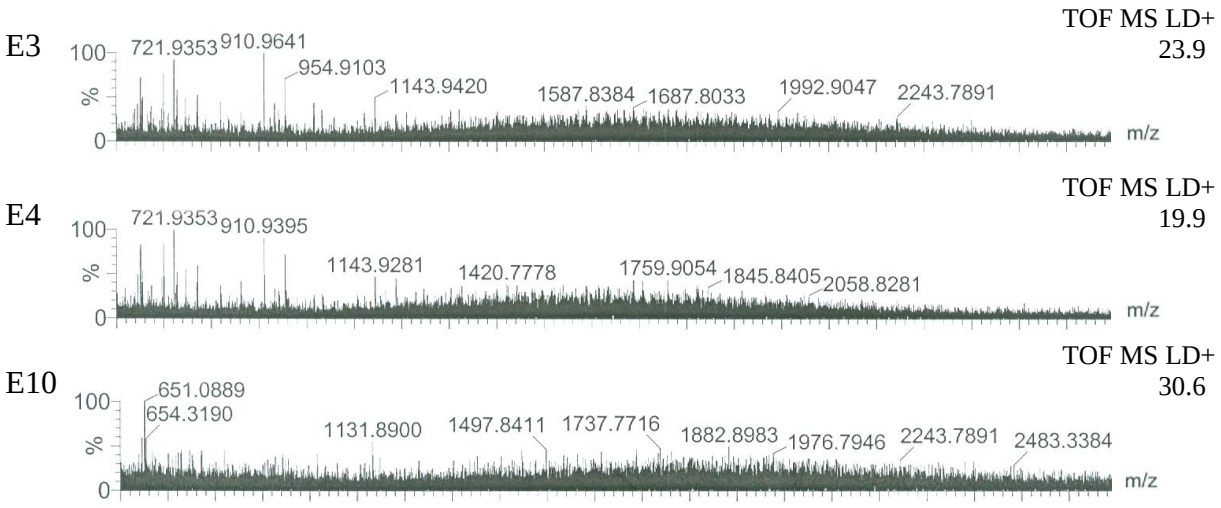

Figure 6.4 – Elution profiles following immunoprecipitation with antibody-bound Dynabeads.
Elutions (E) 3, 4, and 10 shown.

Immunoprecipitation of the peptide was then tested in spiked human plasma samples. Blood from healthy volunteers was collected in lithium-heparin coated tubes (BD Vacutainer, Becton Dickinson, Oxford, UK) and placed immediately upon ice. The samples were then centrifuged for 10mins at 2000g and 4°C to separate the plasma and the cellular fraction. The plasma was then aliquoted and stored at -80°C. Fifty µl aliquots of plasma were then spiked with 0, 25pmol or 250pmol of the Notch-1 Nβ21 peptide and subjected to solid phase extraction, centrifugal evaporation, freeze drying and size-exclusion filtration (2.7.1 and 2.7.2), before being immunoprecipitated as above. Mass spectrometry analysis demonstrated the presence of the peptide in both spiked samples, but not in the control sample. Having thus developed and validated the method, it was used to analyse patient samples.

6.3 RESULTS

6.3.1 Analysis of Notch-1 Nβ21 in human plasma samples

Plasma samples were prepared from the blood of ten patients with advanced pancreatic adenocarcinoma, collected prior to starting chemotherapy (Local Research Ethics Committee Reference 7176). Patients with advanced disease were chosen as it was hypothesised that those with greatest disease burden were more likely to have raised levels of plasma Notch-1 Nβ21. In addition, plasma samples of ten healthy controls with no past history of malignant disease were collected. All work was carried out on anonymised samples, treated identically, and all experiments performed in triplicate. Following peptide purification, four repeats for each sample were analysed using mass spectrometry.

Beads were incubated overnight with 100µl of plasma with mixing at 4°C. They were then washed three times with 50mM ammonium bicarbonate pH 7.4. The peptide was subsequently eluted using 2x 30µl washes of 0.1M citric acid pH 2.0, with supernatants combined for mass spectrometry.

The peptide was not detected in the plasma of any of the control volunteers or patients in any of the repeats (Figure 6.5b and c). In addition, no peak was seen at m/z 2700 which would represent the Notch-1 Nβ25 fragment. When the experiment was repeated, spiking one of the tumour plasma samples with 25pmol Notch-1 Nβ21, the peak was detected. This suggests that within the sensitivity of this protocol, Notch-1 Nβ21 was not present in the plasma of either the controls or cancer patients in this series.

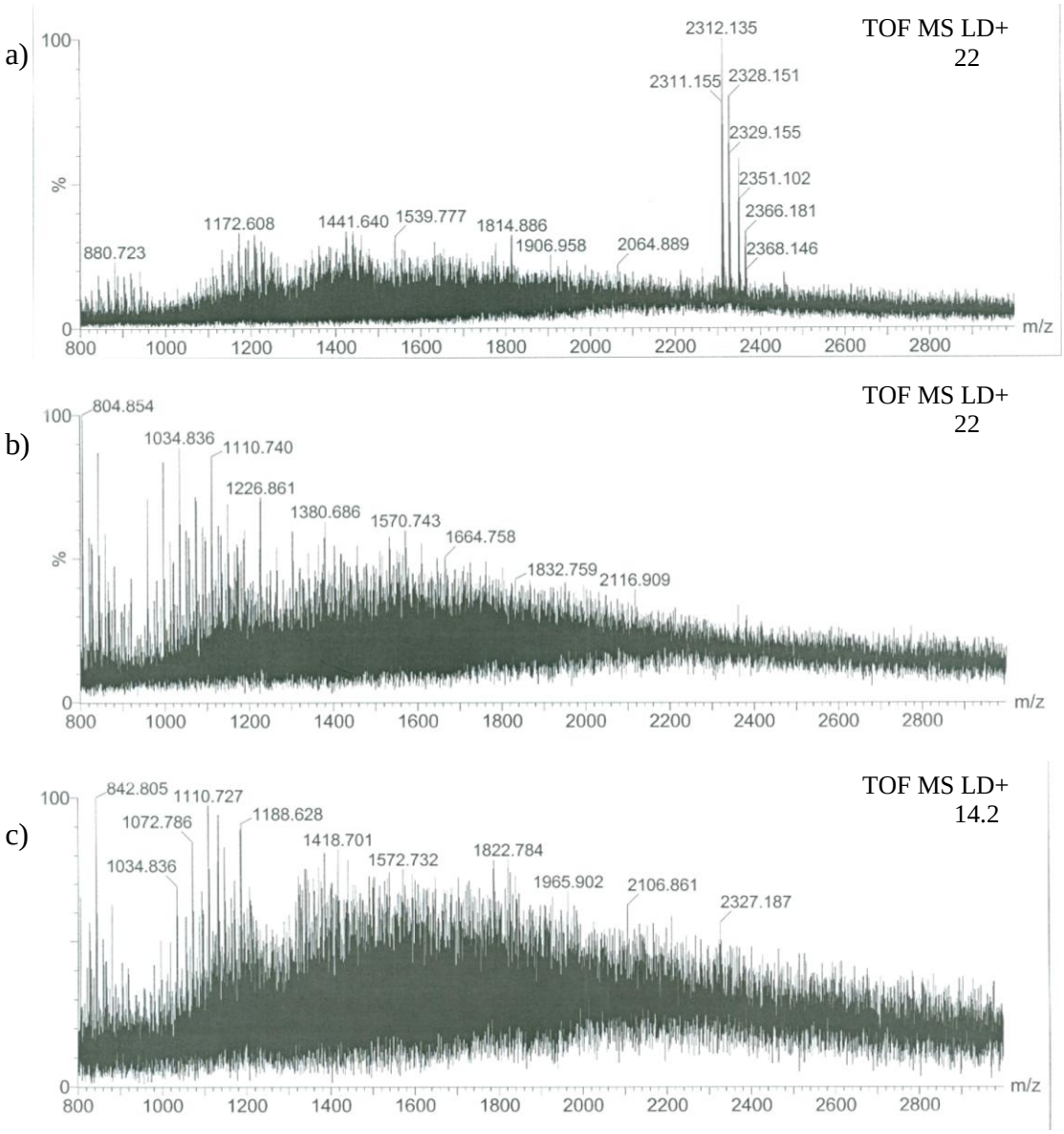

Figure 6.5 – Detection of Notch-1 Nβ21 peptide in human plasma.
Mass spectrometry analysis of a) healthy control plasma spiked with Notch-1 Nβ21; b) plasma from a healthy control participant; c) plasma from a patient with advanced pancreatic adenocarcinoma.

6.3.2 Detection of Notch-3 Nβ21 in human plasma samples

Despite the negative findings with the Notch-1 Nβ21 peptide, it was decided to perform similar investigations examining Notch-3. These experiments were performed by an intercalated *B.Sc.* student (Chris Bastianpillai), with guidance from the author. No previous work had examined potential S4 cleavage in the Notch-3 receptor. Using the UniProt database, the sequence of human Notch-3 revealed significant homology in the region of cleavage sites in human Notch-1. The published protein sequence of full length Notch-3 was aligned with that of Notch-1 in order to predict the sequence of a putative Notch-3 fragment, based on the published Notch-1 fragment.

Notch-1

Notch-3

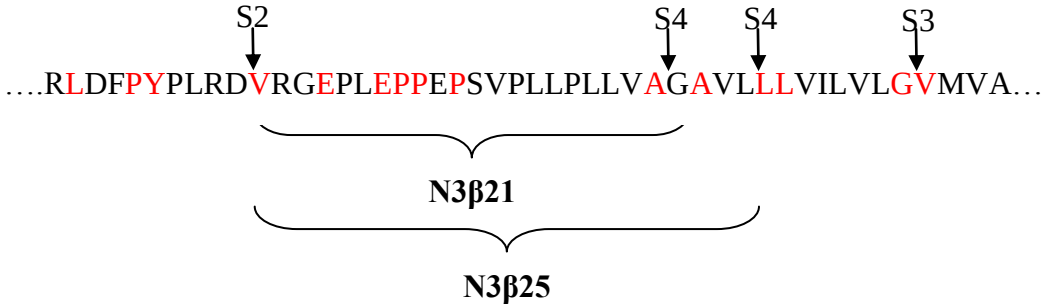

A peptide corresponding to Notch-3 Nβ21 was synthesised and the corresponding rabbit polyclonal antibody developed (Davids Biotechnologie GmbH, Regensburg, Germany). A similar work-up and validation to Notch-1 was used. The monoisotopic molecular weight calculated from the amino acid sequence is 2221Da. Following positive ionisation ([M+H]+ ion) and given the abundance of the carbon-13 isotope,

as well as the number of carbon atoms within the peptide, the most abundant peptide isotope would be predicted to have a mass/charge ratio of 2223 m/z. Analysis of the peptide standard by mass spectrometry confirmed this (Figure 6.6). The limit of detection of the pure standard was determined to be 500fmol/µl.

Immunoprecipitation was performed as for Notch-1. The *m/z* peak was detected following immunoprecipitation of peptide diluted in ammonium bicarbonate buffer to 0.25pmol. The peptide was spiked into healthy volunteer plasma (30pmol), but following immunoprecipitation and mass spectrometry, it was detected in both the control and the spiked plasma (Figure 6.6). Three further healthy volunteer unspiked samples were analysed and peaks for Notch-3 Nβ21 were observed in 2 of them, suggesting that the peptide is present in healthy volunteers in the absence of underlying malignancy.

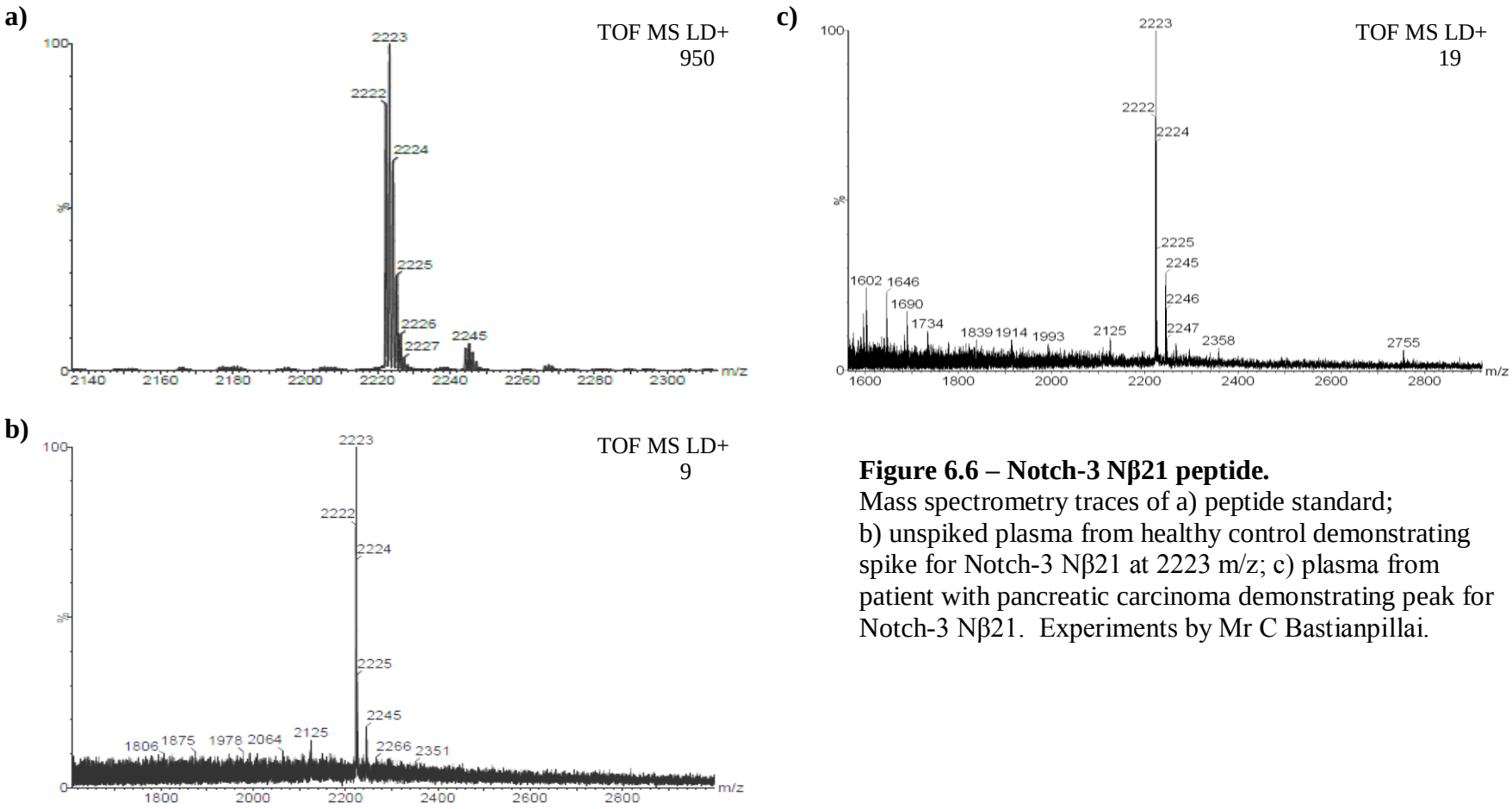

Figure 6.6 – Notch-3 Nβ21 peptide.
Mass spectrometry traces of a) peptide standard; b) unspiked plasma from healthy control demonstrating spike for Notch-3 Nβ21 at 2223 m/z; c) plasma from patient with pancreatic carcinoma demonstrating peak for Notch-3 Nβ21. Experiments by Mr C Bastianpillai.

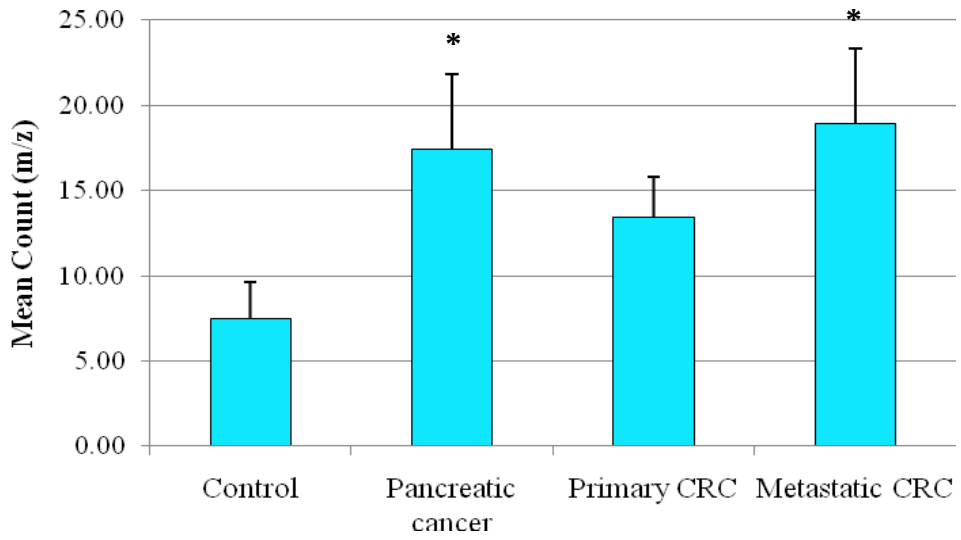

Figure 6.7 – Notch-3 Nβ21 peptide plasma expression
Mean expression of Notch-3 Nβ21 peptide in healthy age-matched controls and patients with pancreatic and colorectal malignancies. *p<0.05 *cf*. healthy controls. Error bars represent 1 SEM. Experiments by Mr C Bastianpillai.

Plasma samples from 11 patients with advanced pancreatic carcinoma were analysed as above and compared to 11 healthy age-matched controls. Following peptide purification, four repeats were analysed by mass spectrometry for each sample. The peptide was detected in 8/11 healthy controls (73%) and 10/11 (91%) patients with advanced pancreatic carcinoma (p=0.269; chi-squared). Attempts were made to quantify Notch-3 Nβ21 levels. Levels in patients with advanced pancreatic carcinoma were significantly higher than in age-matched controls (p=0.032, MW-test). To determine cancer-specificity for Notch-3 Nβ21, plasma was analysed from 14 patients with primary colorectal cancer and 15 patients with colorectal liver metastases, with Notch-3 Nβ21 identified in 86% and 93% respectively. Levels were similar to those

in patients with advanced pancreatic adenocarcinoma, demonstrating a lack of specificity for pancreatic adenocarcinoma ($p=0.951$ and 0.824 respectively, MW-test).

6.4 DISCUSSION

The identification of the novel S4 cleavage site within the transmembrane domain of the Notch-1 protein and subsequent release of the Notch-1 Aβ-like peptide fragment provided a potential target for the detection of Notch pathway activation (Okochi *et al*, 2002). This cleavage was shown to be mediated by the same presenilin-dependent γ-secretase complex responsible for the liberation of the intracellular domain which modulates target gene transcription and therefore should directly correlate with Notch activity. Subsequent work by the same group demonstrated that pathway activation by ligand binding increased production of Notch-1 Aβ-like peptide (Okochi *et al*, 2006). To date, no attempt had been made to isolate this fragment in human biological samples. In addition, S4 cleavage in the other Notch receptors had not been investigated. Based on the immunohistochemistry experiments in Chapter 3, it was hypothesised that the Notch-1 peptide fragment would be expressed at higher levels in patients with advanced pancreatic carcinoma compared to healthy controls. In addition it was hypothesised that Notch-3 would undergo a similar S4 cleavage, which would be upregulated in patients with advanced pancreatic carcinoma. The clinical aim of this work was to develop a tool that could be used, either alone or in a panel of plasma biomarkers, to assist in diagnosis and monitoring the response to therapy.

Initial method development was directed towards Notch-1. An immunoprecipitation protocol using an antibody bound to magnetic beads was developed to enrich the peptide fragment for detection using MALDI-MS. When plasma from healthy volunteers or patients with advanced pancreatic carcinoma was analysed however, no peak was detected. There may be several reasons for this. The predicted sequence of

the human peptide fragment and thus the antibody may be incorrect. The peptide fragment could be bound or 'masked' by larger proteins, such as albumin, and therefore removed during molecular weight filtration. However, when samples were spiked prior to this stage, a peak was readily detected suggesting that this is unlikely. Only 10 patients with pancreatic cancer were analysed so the negative results may be due to low sample number. However, from the immunohistochemical studies 70% of advanced tumours expressed nuclear Notch-1 suggesting at least some of the 10 samples should be positive. It would have been ideal to perform immunohistochemistry for Notch-1 and Notch-3 on biopsies of the patients used in this study. However, unfortunately insufficient tissue was available and performing extra biopsies on non-resectable tumours, with associated risks, was unethical. Lastly, it may be that the method was not sensitive enough to detect low levels of Notch-1 Nβ21. Patients with advanced pancreatic cancer were chosen for this pilot study as they have the greatest tumour burden and therefore could be expected to have the highest levels of Notch-1 Nβ21. As noted above, no data are available regarding the possible plasma levels of this peptide. With regards to other 'tumour markers', CEA and PSA concentrations are reported as ng/ml, with CEA >5ng/ml considered raised. CEA = 5ng/ml is equivalent to 25pmol/L (M_w=200kDa). The Notch-1 Nβ21 peptide was detected at an equivalent 25pmol/L when spiked into plasma. Lower concentrations were not investigated so a lower limit of sensitivity has not been defined. This would therefore need to be performed to exclude this as a reason for the negative results.

The method was used to investigate the presence of a S4 peptide fragment released upon Notch-3 activation. Notch-3 was chosen due to the high percentage (90%) of

advanced tumour demonstrating nuclear staining, and the fact that Notch-3 and its down-stream target, HEY-1, are strong indicators of poor prognosis (Chapter 3). With no published data on the existence of such a fragment, the peptide sequence was predicted from knowledge of the Notch-1 cleavage site. Method validation demonstrated detection of this peptide when spiked into control plasma. However the Notch-3 Nβ21 peptide could be detected even in unspiked samples, indicating that it is present in healthy plasma. Analysis of further plasma samples from patients with advanced pancreatic carcinoma and healthy age-matched controls revealed statistically significantly higher levels in the cancer patients ($p=0.033$). When, however, samples from patients with primary and metastatic colorectal cancer were analysed, levels were similar to that of pancreatic cancer patients. This means that, as is the case for CA19.9, the Notch-3 Nβ21 peptide on its own is not a specific biomarker for pancreatic carcinoma. These results demonstrate for the first time that a Notch-3 Aβ-like (Nβ21) peptide is released into the plasma upon S4 cleavage during Notch-3 activation, and that using this mass spectrometry method, it can be detected in plasma. The main limitation so far is the small sample size and analysis of a larger cohort is needed before drawing conclusions. Although this peptide is not specific for pancreatic carcinoma, a relative increase in plasma levels may be useful in diagnosis, and certainly warrants further investigation in combination with other biomarkers. In addition it would be interesting to correlate the change in levels before and after chemotherapy with radiological response, as a possible marker of response to treatment.

Expression of Notch-3 Nβ21 peptide appears to be significant in healthy people, a finding that may be explained by its role in propagation of vascular smooth muscle

cells, with Notch-3 upregulation having previously been linked with vascular injury (Campos *et al*, 2002). Notch-3 has been identified in patients with CADASIL syndrome (cerebral autosomal dominant arteriopathy with subcortical infarcts and leukoencephalopathy), a condition which results in recurrent strokes and vascular dementia due to vascular smooth muscle cell degeneration (Joutel *et al*, 1996). Notch-3 therefore has an important role in the homeostasis of arterial vascular smooth muscle cells in human adults, with Notch-3 acting to promote cell survival and prevent apoptosis (Kawai-Kowase and Owens, 2007; Sweeney *et al*, 2004; Wang *et al*, 2003). These findings may explain the presence of the Notch-3 Aβ-like peptide in the plasma of healthy controls.

The Notch pathway is known to be involved in colorectal carcinoma (Miyamoto and Rosenberg, 2011), with Notch-3 having been found to be significantly up-regulated in primary and metastatic colorectal cancer and to be important for tumour growth (Serafin *et al*, 2011). The elevated Notch-3 Nβ21 peptide levels in patients with colorectal cancer in this study correlate with these findings.

In summary, using this technique it has not so far been possible to detect the Notch-1 Aβ-like/Nβ21 peptide from the plasma of patients with advanced pancreatic carcinoma and further work is needed to optimise the method. Notch-3 Aβ-like/Nβ21 peptide was detected in pancreatic cancer patients, but also in healthy age-matched controls, although at lower levels. This has potential for use as part of a panel of plasma biomarkers and merits further investigation.

CHAPTER 7

GENERAL DISCUSSION

The work presented in this thesis has examined the role of the Notch pathway in pancreatic adenocarcinoma, as a prognostic indicator, disease biomarker, and therapeutic target. The studies conducted have addressed the objectives set out in section 1.4.2 and have yielded a range of novel findings regarding this family of receptors, supporting their involvement in pancreatic carcinogenesis and their potential as prognostic markers and therapeutic targets.

The Notch pathway has been implicated in the carcinogenesis of several solid and haematological malignancies, in both an oncogenic and tumour suppressive capacity. At the commencement of the current research, the role of Notch in pancreatic adenocarcinoma had only been examined in two studies assessing 26 and 46 tumours respectively (Miyamoto *et al*, 2003; Buchler *et al*, 2005). Furthermore, the biological significance of Notch upregulation, correlation between pathway constituents and association with disease progression and prognosis remained unexplored. In the present study upregulation of active Notch-1, -3, and -4, as well as targets HES-1 and HEY-1 was observed in tumours compared to normal pancreas, with sequential upregulation in advanced disease compared to early (i.e. resectable) disease. Positive correlations were documented between nuclear Notch-1 and nuclear HES-1 expression, and nuclear Notch-3 and nuclear HEY-1 expression, suggesting that these target genes are Notch receptor specific. These findings are confirmed by the knockdown experiments in chapter 4, which also suggest that there is little cross-talk between these two pathways. Notch-3 and HEY-1 were found to be strongly inversely associated with both disease-free and overall survival, with HEY-1 independently predictive of poor survival on multivariate analysis in all patients, and those undergoing a R_0 resection. This provides strong evidence for the first time that activation of the Notch-3 pathway is associated with aggressive disease and that Notch-3 has a promising role as a prognostic biomarker. In addition it suggests that this pathway in particular is important in pancreatic carcinogenesis.

Nuclear Notch-1 was found to be inversely associated with overall survival on univariate analysis, but not on multivariate analysis. Although this study is a large series relative to the literature, it would be important to confirm these results within a larger number of patients. Combining nuclear HEY-1 expression and CA19.9 level allowed the development of a scoring system that could further stratify patients undergoing resection into groups based upon prognosis. Combining these two parameters with other known molecular biomarkers of pancreatic cancer prognosis may allow development of a tool to create a molecular 'signature' to predict prognosis for individual patients and allow targeting of adjuvant treatments.

Using siRNA knockdown the current study has demonstrated that the Notch pathway is important in the growth and survival of pancreatic cancer cells and that it may be a potential therapeutic target. In addition it has helped elucidate the relative contribution of the individual Notch receptors to these findings. For the first time, Notch-1 and Notch-3 were found to be important in the maintenance of pancreatic cancer cell survival, while no effects were seen on Notch-4 knockdown. Notch-1 knockdown was found to result in a reduction in cell viability, induction of apoptosis and G_1 cell cycle arrest. These findings have been subsequently been confirmed in parallel studies by another group (Wang *et al*, 2006a-c). The data generated with regards to Notch-3 are novel and add weight to the original immunohistochemistry data that Notch-3 activation is important for disease progression. Few data exist in the literature with regards to the role of Notch-3 in carcinogenesis and the mechanisms involved, so further work is needed to expand on these findings particularly in the *in vivo* setting. This study did not examine the role of Notch-2 due to lack of a sufficiently well-validated antibody, but there are now published data to suggest it may be important in the development of pre-cancerous PanIN lesions and epithelial to mesenchymal

transition (Mazur *et al*, 2010). It is clearly important to assess the role of this Notch in pancreatic cancer and subsequent work in the author's department has been set up to address this.

The discovery of gamma secretase activation of the Notch pathway provided a promising avenue for therapeutic intervention. Given that agents which inhibited this enzyme were already being trialled in patients with Alzheimer's disease, this allowed an opportunity to rapidly translate results into the clinic for pancreatic cancer. Data generated in cell culture using GSI-I proved promising and for the first time suggested that this strategy may be of benefit to patients with pancreatic carcinoma. Treatment with GSI-I found, for the first time, reduced cell proliferation, induction of apoptosis and G_2M cell cycle arrest *in vitro*. In addition, it suggests that combination with gemcitabine or curcumin, a promising dietary anti-cancer agent, may be beneficial. The mechanisms underlying these changes were explored using microarray analysis, revealing a myriad of potential down-stream effectors of apoptotic and cell cycle alteration. In addition, changes were seen in the NF-κB, JAK-STAT and Wnt pathway which may represent either cross-talk via the Notch pathway or novel actions of gamma secretase. These results require validation.

Based on the results with GSI-I, another gamma secretase inhibitor provided by Merck, MRK-003, was investigated in a murine pancreatic carcinoma xenograft model. Unfortunately the promising results seen with GSI-I were not reproduced. There may be a number of reasons for this. MRK-003 was identified as a weaker inhibitor of Notch activation than GSI-I. In addition, although some target tissue inhibition of HES-1 was seen, only a 50% knockdown was achieved. It may be that greater inhibition is required for

biological activity. In addition, this model is bound by the overall limitations of a murine xenograft model. It would, however, be premature to dismiss the potential of gamma secretase inhibition in pancreatic cancer. It is well known that effects seen in murine models do not always equate to those in clinical trials. To this end, the author has been involved in the development of a multicentre clinical trial of MK-0752 (a GSI with similar activity to MRK003), in patients with advanced pancreatic cancer, to address this issue. This trial has started recruiting and the results eagerly awaited. Gemcitabine is the current first-line chemotherapy for advanced pancreatic cancer. Once the tumour becomes refractory to this drug, very little in the way of second line treatment is available. It would be useful to know if GSIs possess any potential to overcome such resistance. The author has begun developing a gemcitabine-resistant pancreatic cell line to address this question. There appears to be sufficient evidence to maintain interest in the Notch pathway as a therapeutic target in pancreatic cancer even if the MK-0752 trial results prove negative. Different GSIs appear to have variable ability to inhibit activation of Notch signalling. Drug development of such inhibitors may yield novel, more biologically active agents. Recently there has been considerable interest in microRNAs (miR). These are conserved, short, non-coding mRNAs which modulate the expression of target genes by binding, with imperfect base paring, to target sites in the open reading frame or 3'-untranslated region of mRNAs (Bushati and Cohen, 2007), and can act in either an oncogenic or tumour suppressive capacity. Several microRNAs have been found to be upregulated in pancreatic cancer with potential diagnostic and prognostic value (Bloomston *et al*, 2007; Yu *et al*, 2010; Liu *et al*, 2011). In addition, several have been shown to negatively modulate the activity of the Notch pathway, particularly in cancer stem cells, including miR-1 (Kwon *et al*, 2005), miR-34 (Li *et al*, 2009), miR-199 (Garzia *et al*, 2009), and miR-200b (Wang *et al*, 2010d). Ji *et al* (2009) found miR-34 to be down-regulated in pancreatic adenocarcinoma. Restoration of miR-34

expression resulted in down-regulation of Notch-1 and -2, associated with inhibition of cell growth, invasion, and induction of apoptosis and G_2/M cell cycle arrest. These cells were also sensitised to chemotherapy and irradiation. miR-34 restoration also led to a 87% reduction in tumour stem cell population and inhibition of tumour growth *in vivo* (murine xenograft model). These data suggest that restoration of miR-34 may represent an attractive molecular therapeutic strategy for patients with pancreatic cancer via inhibiting cancer stem cells through direct modulation of the Notch pathway.

Following the presenilin/gamma secretase-dependent S3 proteolytic cleavage, the Notch-1 receptor has previously been found to undergo a S4 cleavage of the transmembrane domain, resulting in release of a peptide fragment into the extracellular fluid (Okochi *et al*, 2006). For the first time, the present study attempted to develop a method to detect this fragment in the plasma of patients with advanced pancreatic cancer and to investigate the potential as a diagnostic biomarker. Despite developing a method based on immunoprecipitation and sensitive mass spectrometry, the Notch-1 peptide fragment was not detected in plasma of patients with pancreatic cancer. Work is continuing in the author's department to optimise the technique to determine if this is a true finding or due to a lack of sensitivity. Since Notch-3 is activated in pancreatic cancer and associated with poor prognosis, it was hypothesised that an equivalent Notch-3 peptide fragment would be released into patients' plasma. Using a similar method to Notch-1, it was confirmed for the first time that this was the case. However the fragment was also detectable in healthy volunteers, as well as in patients with colorectal carcinoma. Despite this, the Notch-3 fragment was detected at a higher level in patients with pancreatic carcinoma than in age-matched controls. These data suggest that although the Notch-3 peptide fragment is not a specific biomarker for pancreatic carcinoma, it warrants further investigation and may be of use in a panel of biomarkers for diagnostic or

screening purposes. If so it should be possible to develop an ELISA assay. Future work is already underway in the department to expand the number of patient plasma samples in this series, and to include samples from patients with resectable pancreatic cancers and chronic pancreatitis. This will allow further evaluation of Notch-3 as a diagnostic marker, as well as examination of its relationship with prognosis and response to chemotherapy. In addition it will be incorporated into a panel with other novel biomarkers, including microRNAs. The aim of this will be to create a panel of biomarkers for diagnostic and prognostic purposes.

In summary, this thesis has demonstrated that the Notch pathway is activated in pancreatic cancer, and that activation of the Notch-3 pathway in particular is associated with poor survival following resection. It has also demonstrated initial promise of Notch-3 as a diagnostic biomarker and investigated Notch as a potential therapeutic target in these patients.

REFERENCES

Ali, S., Ahmad, A., Banerjee, S., Padhye, S., Dominiak, K., Schaffert, J.M., Wang, Z., Philip, P.A., and Sarkar, F.H. **(2010)**. "Gemcitabine sensitivity can be induced in pancreatic cancer cells through modulation of miR-200 and miR-21 expression by curcumin or its analogue CDF," *Cancer Res.* **70**(9), 3606-3617.

Almoguera, C., Shibata, D., Forrester, K., Martin, J., Arnheim, N., and Perucho, M. **(1988)**. "Most human carcinomas of the exocrine pancreas contain mutant c-K-ras genes," *Cell* **53**(4), 549-554.

Ansari, D., Rosendahl, A., Elebro, J., and Andersson, R. **(2011)**. "Systematic review of immunohistochemical biomarkers to identify prognostic subgroups of patients with pancreatic cancer," *Brit. J. Surg.* **98**, 1041-1055.

Aoki, K., Yoshida, T., Matsumoto, N., Ide, H., Sugimura, T., and Terada, M. **(1997)**. "Suppression of Ki-ras p21 levels leading to growth inhibition of pancreatic cancer cell lines with Ki-ras mutation but not those without Ki-ras mutation," *Mol. Carcinog.* **20**(2), 251-258.

Apelqvist, A., Li, H., Sommer, L., Beatus, P., Anderson, D.J., Honjo, T., Hrabe de Angelis, M., Lendahl, U., and Edlund, H. **(1999)**. "Notch signalling controls pancreatic cell differentiation," *Nature* **400**, 877-881.

Aprelikova, O., Xiong, Y., and Liu, E.T. **(1995)**. "Both p16 and p21 families of cyclin dependent kinase (CDK) inhibitors block the phosphorylation of cyclin-dependent kinases by the CDK-activating kinase," *J. Biol. Chem.* **270**, 18195-18197.

Artavanis-Tsakonas, S., Matsuno, K., and Fortini, M. **(1995)**. "Notch signalling," *Science* **268**, 225-232.

Artavanis-Tsakonas, S., Rand, M., and Lake, R. **(1999)**. "Notch signalling: cell fate control and signal integration in development," *Science* **284**, 770-776.

Aster, J.C., Xu, L., Karnell, F.G., Patriiub, V., Pui, J.C., and Pear, W.S. **(2000)**. "Essential roles for ankyrin repeat and transactivation domains in induction of T-cell leukemia by notch1," *Mol. Cell Biol.* **20**(20), 7505-7515.

Axelrod, J.D.., Matsuno, K., Artavanis-Tsakonas, S., and Perrimon, N. **(1996)**. "Interaction between Wingless and Notch signalling pathways mediated by dishevelled," *Science* **271**(5257), 1826-1832.

Ayad, N.G., Rankin, S., Murakami, M., Jebanathirajah, J., Gygi, S., and Kirschner, M.W. **(2003)**. "Tome-1, a trigger of mitotic entry, is degraded during G1 via the APC," *Cell* **113**(1), 101-113.

Bai, C., Richman, R., and Elledge, S.J. **(1994)**. "Human cyclin F," *EMBO J.* **13**(24), 6087-6098.

Baker, N. **(2000)**. "Notch signalling in the nervous system. Pieces still missing from the puzzle," *Bioessays* **22**, 264-273.

Barolo, S., Stone, T., Bang, A.G., and Posakony, J.W. **(2002)**. "Default repression and Notch signaling: Hairless acts as an adaptor to recruit the corepressors Groucho and dCtBP to Suppressor of Hairless," *Genes Dev.* **16**(15), 1964-1976.

Bartek, J., Bartkova, J., and Lukas, J. **(1997)**. "The retinoblastoma protein pathway in cell cycle control and cancer," *Exp. Cell. Res.* **237**, 1-6.

Bartel, D.P. **(2009)**. "MicroRNAs: target recognition and regulatory functions," *Cell* **136**(2), 215–233.

Bartsch, D.K., Kress, R., Sina-Frey, M., Grutzmann, R., Gerdes, B., Pilarsky, C., Heise, J.W., Schulte, K.M., Colombo-Benkmann, M., Schleicher, C., Witzigmann, H., Pridohl, O., Ghadimi, M.B., Messmann, H., Endlicher, E., Schneider, M., Ziegler, A., Schmiegel, W., Schafer, H., Rothmund, M., and Rieder, H. **(2004)**. "Prevalence of familial pancreatic cancer in Germany," *Int. J. Cancer* **110**(6), 902-906.

Beatus, P., Lundkvist, J., Oberg, C., and Lendahl, U. **(1999)**. "The Notch3 intracellular domain represses Notch1-mediated activation through Hairy/Enhancer of split (HES) promoters," *Development* **126,** 3925-3935.

Bellavia, D., Campese, A.F., Alesse, E., Vacca, A., Felli, M.P., Balestri, A., Stoppacciaro, A., Tiveron, C., Tatangelo, L., Giovarelli, M., Gaetano, C., Ruco, L., Hoffman, E.S., Hayday, A.C., Lendahl, U., Frati, L., Gulino, A., and Screpanti, I. **(2000)**. "Constitutive activation of NF-kappaB and T-cell leukemia/lymphoma in Notch3 transgenic mice," *EMBO J.* **19**(13), 3337-3348.

Bellavia, D., Checquolo, S., Campese, A.F., Felli, M.P., Gulino, A., and Screpanti, I. **(2008)**. "Notch3: from subtle structural differences to functional diversity," *Oncogene* **27**, 5092-5098.

Benassai, G., Mastrorilli, M., Quarto, G., Cappiello, A., Giani, U., Forestieri, P., Mazzeo, F. **(2000)**. "Factors influencing survival after resection for ductal adenocarcinoma of the head of the pancreas," *J. Surg. Oncol.* **73**(4), 212-218.

Benjamini, Y. and Hochberg, Y. **(1995)**. "Controlling the False Discovery Rate: a practical and powerful approach to multiple testing," *J. Royal. Stat. Soc.* **57**(1), 289-300.

Berdnik, K., Torok, T., Gonzalez-Gaitan, M., and Knoblich, J.A. **(2002)**. "The endocytic protein alpha-Adaptin is required for numb-mediated asymmetric cell division in Drosophila," *Dev. Cell* **3**(2), 221-231.

Bernstein, T., Caudy, A.A., Hammond, S.M., and Hannon, G.J. **(2001)**. "Role for a bidentate ribonuclease in the initiation step of RNA interference," *Nature* **409**, 363-366.

Bhatti, I., Peacock, O., Lloyd, G., Larvin, M., and Hall, R.I. **(2010)**. "Preoperative hematologic markers as independent predictors of prognosis in resected pancreatic ductal adenocarcinoma: neutrophil-lymphocyte versus platelet-lymphocyte ratio," *Am. J. Surg.* **200**(2), 197-203.

Biunno, I., Cattaneo, M., Orlandi, R., Canton, C., Biagiotti, L., Ferrero, S., Barberis, M., Pupa, S.M., Scarpa, A., and Menard, S. **(2006).** "SEL1L a multifaceted protein playing a role in tumor progression," *J. Cell Physiol.* **208**(1), 23-38.

Bland, C., Kimberly, P., and Rand, M. **(2003)**. "Notch-induced proteolysis and nuclear localization of the Delta ligand," *J Biol. Chem.* **278**(16), 13607-13610.

Blaumueller, C.M., Qi, H., Zagouras, P., and Artavanis-Tsakonas, S. **(1997)**. "Intracellular cleavage of Notch leads to a heterodimeric receptor on the plasma membrane," *Cell* **90**, 281-291.

Bloomston, M., Zervos, E.E., and Rosemurgy, A.S. 2nd **(2002)**. "Matrix metalloproteinases and their role in pancreatic cancer: a review of preclinical studies and clinical trials," *Ann. Surg. Oncol*. **9**(7), 688-674.

Bloomston, M., Frankel, W.L., Petrocca, F., Volinia, S., Alder, H., Hagan, J.P., Liu, C.G., Bhatt, D., Taccioli, C., and Croce, C.M. **(2007)**. "MicroRNA expression patterns to differentiate pancreatic adenocarcinoma from normal pancreas and chronic pancreatitis," *J.A.M.A.* **297**(17), 1901-1908.

Bonifacino, J.S. and Weissman, A.M. **(1998)**. "Ubiquitin and the control of protein fate in the secretory and endocytic pathways," *Ann. Rev. Cell. Dev. Biol.* **14**, 19-57.

Brou, C., Logeat, F., Gupta, N., Bessia, C., LeBail, O., Doedens, J.R., Cumano, A., Roux, P., Black, R.A., and Israel, A. **(2000)**. "A novel proteolytic cleavage involved in Notch signaling: the role of the disintegrin-metalloprotease TACE," *Mol. Cell.* **5**(2), 207-216.

Buchler, P., Gazdhar, A., Schubert, M., Giese, N., Reber, H.A., Hines, O.J., Giese, T., Ceyhan, G.O., Muller, M., Buchler, M.W., and Friess, H. **(2005)**. "The Notch signaling pathway is related to neurovascular progression of pancreatic cancer," *Ann. Surg.* **242**, 791-801.

Bunger, S., Laubert, T., Roblick, U.J., and Habermann, J.K. **(2011)**. "Serum biomarkers for improved diagnostic of pancreatic cancer: a current overview," *J. Cancer Res. Clin. Oncol.* **137**(3), 375-389.

Burris, H.A. 3rd., Moore, M.J., Andersen, J., Green, M.R., Rothenberg, M.L., Modiano, M.R., Cripps, M.C., Portenoy, R.K., Storniolo, A.M., Tarassoff, P., Nelson, R., Dorr, F.A., Stephens, C.D., and von Hoff, D.D. **(1997)**. "Improvements in survival and clinical benefit with gemcitabine as first-line therapy for patients with advanced pancreas cancer: a randomized trial," *J. Clin. Oncol.* **15**(6), 2403-2413.

Bush, G., di Sibio, G., Miyamoto, A., Denault, J.B., Leduc, R., and Weinmaster, G. **(2001)**. "Ligand-induced signalling in the absence of furin processing of Notch1," *Dev. Biol.* **229**(2), 494-502.

Bushati, N., and Cohen, S.M. **(2007)**. "MicroRNA functions," *Annu. Rev. Cell. Dev. Biol.* **23**, 175-205.

Callahan, J., Aster, J., Sklar, J., Kieff, E., and Robertson, E.S. **(2000)**. "Intracellular forms of human NOTCH1 interact at distinctly different levels with RBP-Jkappa in human B and T cells," *Leukemia* **14**(1), 84-92.

Callahan, R. and Egan, S. **(2004)**. "Notch signalling in mammary development and oncogenesis," *J. Mammary Gland Biol. Neoplasia* **9**, 145-163.

Campos, A.H., Wang, W., Pollman, M.J., and Gibbons G.H. **(2002)**. "Determinants of Notch-3 receptor expression and signalling in vascular smooth muscle cells: implications in cell-cycle regulation. *Circ. Res.* **91**, 999-1006.

Carlesso, N., Aster, J.C., Sklar, J., and Scadden, D.T. **(1999)**. "Notch1-induced delay of human hematopoietic progenitor cell differentiation in associated with altered cell cycle kinetics," *Blood*, **93**(3), 838-848.

Chan, S.M., Weng, A.P., Tibshirani, R., Aster, J.C., and Utz, P.J. **(2007)**. "Notch signals positively regulate activity of the mTOR pathway in T-cell acute lymphoblastic leukemia," *Blood* **110**, 278-286.

Chang, H.H., Lee, H., Hu, M.K., Tsao, P.N., Juan, H.F., Huang, M.C., Shih, Y.Y., Wang, B.J., Jeng, Y.M., Chang, C.L., Huang, S.F., Tsay, Y.G., Hseih, F.J., Lin, K.H., Hsu, W.M., and Liao, Y.F. **(2010)**. "Notch1 expression predicts an unfavourable prognosis and serves as a therapeutic target of patients with neuroblastoma," *Clin. Cancer Res.* **16**(17), 4411-4420.

Chano, T., Ikegawa, S., Kontani, K., Okabe, H., Baldini, N., and Saeki, Y. **(2002)**. "Identification of RB1CC1, a novel human gene that can induce RB1 in various human cells," *Oncogen*e **21**(8), 1295-1298.

Chapman, G., Liu, L., Sahlgren, C., Dahlqvist, C., and Lendahl, U. **(2006)**. "High levels of Notch signalling down-regulate Numb and Numblike," *J. Cell. Biol.* **175**(4), 535-540.

Chen, W.H., Horoszewicz, J.S., Leong, S.S., Shimano, T., Penetrante, R., Sanders, W.H., Berjian, R., Douglass, H.O., Martin, E.W., and Chu, T.M. **(1982)**. "Human pancreatic adenocarcinoma: in vitro and in vivo morphology of a new tumor line established from ascites," *In Vitro* **18**(1), 24-34.

Chen, Y., Shu, W., Chen, W., Wu, Q., Liu, H., and Cui, G. **(2007)**. "Curcumin, both histone deacetylase and p300/CBP-specific inhibitor represses the activity of nuclear factor kappa B and Notch1 in Raji cells," *Basic Clin. Pharmacol,Toxicol.* **101**(6), 427-433.

Chen, J., Kesari, S., Rooney, C., Strack, P.R., Chen, J., Shen, H., Wu, L., and Griffin, J.D. **(2010)**. "Inhibition of Notch signalling blocks growth of Glioblastoma cell lines and tumor neurospheres," *Genes Cancer* **1**(8), 822-835.

Cheng, P., Zlobin, A., Volgina, V., Gottipati, S., Osborne, B., Simel, E.J., Miele, L., and Gabrilovich, D.I. **(2001)**. "Notch-1 regulates NF-kappaB activity in hemopoietic progenitor cells," *J. Immunol.* **167**(8), 4458-4467.

Cheng, P., Nefedova, Y., Miele, L., Osborne, B.A., and Gabrilovich, D. **(2003)**. "Notch signalling is necessary but not sufficient for differentiation of dendritic cells," *Blood* **102**(12), 3980-3989.

Chi, Y., Huddleston, M.J., Zhang, X., Young, R.A., Annan, R.S., Carr, S.A., and Deshaies, R.J. **(2001)**. "Negative regulation of Gcn4 and Msn2 transcription factors by Srb10 cyclin-dependent kinase," *Genes Dev.* **15**(9), 1078-1092.

Chiaramonte, R., Calzavara, E., Balordi, F., Sabbadini, M., Capello, D., Gaidano, G., Serra, A., Comi, P., and Sherbet, G.V. **(2003)**. "Differential regulation of Notch signal transduction in leukaemia and lymphoma cells in culture," *J. Cell. Biochem.* **88**(3), 569-577.

Chiaramonte, R., Basile, A., Tassi, E., Calzavara, E., Cecchinato, V., Rossi, V., Biondi, A., and Comi, P. **(2005)**. "A wide role for NOTCH1 signalling in acute leukemia," *Cancer Lett.* **219**(1), 113-120.

Choi, J.H., Park, J.T., Davidson, B., Morin, P.J., Shih, L.M., Wang, T.L. **(2008)**. "Jagged-1 and Notch3 juxtacrine loop regulates ovarian tumor growth and adhesion," *Cancer Res.* **68**(14), 5716-5723.

Christensen, S., Kodoyianni, V., Bosenberg, M., Friedman, L., and Kimble, J. **(1996)**. "Lag-1, a gene required for lin-12 and glp-1 signaling in Caenorhabditis elegans, is homologous to human CBF1 and Drosophila Su(H)," *Development* **122**(5), 1373-1383.

Cohen, B., Shimizu, M., Izrailit, J., Ng, N.F., Buchman, Y., Pan, J.G., Dering, J., and Reediyk, M. **(2010)**. "Cyclin D1 in a direct target of JAG1-mediated Notch signalling in breast cancer," *Breast Cancer Res. Treat.* **123**(1), 113-124.

Conboy, I.M., Conboy, M.J., Smythe, G.M., and Rando, T.A. **(2003)**. "Notch-mediated restoration of regenerative potential to aged muscle," *Science* **302**, 1575-1577.

Coussens, L.M. and Werb, Z. **(2002)**. "Inflammation and cancer," *Nature* **420**(6917), 860-867.

Cress, R.D., Yin, D., Clarke, L., Bold, R., and Holly, E.A. **(2006)**. "Survival among patients with adenocarcinoma of the pancreas: a population-based study (United States)," *Cancer Causes Control* **17**(4), 403-409.

Cuevas, I.C., Slocum, A.L., Jun, P., Costello, J.F., Bollen, A.W., Riggins, G.L., McDermott, M.W., and Lal, A. **(2005)**. "Meningioma transcript profiles reveal deregulated Notch signalling pathway," *Cancer Res.* **65**(12), 5070-5075.

Cui, X.Y., Hu, Q.D., Tekaya, M., Shimoda, Y., Ang, B.T., Nie, D.Y., Sun, L., Hu, W.P., Karsak, M., Duka, T., Takeda, Y., Ou, L.Y., Dawa, G.S., Yu, F.G., Ahmed, S., Jin, L.H., Schachner, M., Watanabe, K., Arsenijevic, Y., and Xiao, Z.C. **(2004)**. "NB-3/Notch1 pathway via Deltex1 promotes neural progenitor differentiation into oligodendrocytes," *J. Biol. Chem.* **279**(24), 25858-25865.

Cullion, K., Draheim, K.M., Hermance, N., Tammam, J., Sharma, V.M., Ware, C., Nikov, G., Krishnamoorthy, V., Majumder, P.K., and Kelliher, M.A. **(2009)**. "Targeting the Notch1 and mTOR pathways in a mouse T-ALL model," *Blood* **113**(24), 6172-6181.

Curry, C.L., Reed, L.L., Golde, R.E., Miele, L., Nickoloff, B.J., and Foreman, K.E. **(2005)**. "Gamma secretase inhibitor blocks Notch activation and induces apoptosis in Kaposi's sarcoma tumor cells," *Oncogene* **24**, 6333-6344.

Curry, C.L., Reed, L.L., Broude, E., Golde, T.E., Miele, L., and Foreman, K.E. **(2007)**. "Notch inhibition in Kaposi's sarcoma tumor cells leads to mitotic catastrophe through nuclear factor-kappaB signalling," *Mol. Cancer Ther.* **6**(7), 1983-1992.

Dahlqvist, C., Blokzijl, A., Chapman, G., Falk, A., Dannaeus, K., Ibanez, C.F., and Lendahl, U. **(2003)**. "Function Notch signaling is required for BMP4-induced inhibition of myogenic differentiation," *Development* **130**(24), 6089-6099.

De Angelo, D.J., Stone, R.M., Silverman, L.B., Stock, W., Attar, E.C., Fearen, I., Dallob, A., Matthews, C., Stone, J., Freedman, S.J., and Aster, J. **(2006)**. "A phase I clinical trial of the notch inhibitor MK-0752 in patients with T-cell acute lymphoblastic leukemia/lymphoma (T-ALL) and other leukemias," *J. Clin. Oncol.* **24**(18S), 6585.

De Blandre, G., Lai, E., and Kintner, C. **(2001)**. "Xenopus neuralized is a ubiquitin ligase that interacts with XDelta1 and regulates Notch signalling," *Dev. Cell* **1**(6), 795-806.

De Hart, S., Heikens, M., and Tsai, S. **(2005)**. "Jagged2 promotes the development of natural killer cells and the establishment of functional natural killer cell lines," *Blood* **105**, 3521-3527.

De Hoffmann, E., and Stoobant, V. **(2007)**. "Mass spectrometry: principles and applications," Wiley Interscience, 3rd Edition.

De Keersmaecker, K., Lahortiga, I., Mentens, N., Folens, C., Van Neste, L., Bekaert, S., Vandenberghe, P., Odero, M.D., Marynen, P., and Cools, J. **(2008)**. "In vitro validation of gamma secretase inhibitors alone, or in combination with other anti-cancer drugs for the treatment of T-cell acute lymphoblastic leukemia," *Haematologica* **93**(4), 533-542.

De Strooper, B., Annaert, W., Cupers, P., Saftig, P., Craessaerts, K., Mumm, J.S., Schroeter, E.H., Schrijvers, V., Wolfe, M.S., Ray, W.J., Goate, A., and Kopan, R. **(1999)**. 2A

presenilin-1-dependent gamma-secretase-like protease mediates release of Notch intracellular domain," *Nature* **398**(6727), 518-522.

Dickson, B.C., Mulligan, A.M., Zhang, H., Lockwood, G., O'Malley, F.P., Egan, S.E., and Reedijk, M. **(2007)**. "High JAG1 mRNA and protein predict poor outcome in breast cancer," *Mod. Pathol.* **20**(6), 685-693.

Dievart, A., Beaulieu, N., and Jolicoeur, P. **(1999)**. "Involvement of Notch1 in the development of mouse mammary tumors," *Oncogene* **18**(44), 5973-5981.

Dite, P., Novotny, I., Precechtelova, M., Ruzicka, M., Zakova, A., and Hermanova, M. **(2010)**. "Incidence of pancreatic carcinoma in patients with chronic pancreatitis," *Hepatogastroenterol.* **57**, 957-967.

Doerfler, P., Shearman, M.S., and Perlmutter, R.M. **(2001)**. "Presenilin-dependent gamma secretase activity modulates thymocyte development," *Proc. Natl. Acad. Sci. U.S.A.* **98**(16), 9312-9317.

Donnem, T., Andersen, S., Al-Shibli, K., Al-Saad, S., Lill-Tove, B., and Bremnes, R.M. **(2010)**. "Prognostic impact of Notch ligands and receptors in nonsmall cell lung cancer," *Cancer* **116**(24), 5676-5685.

Donovan, J., Kordylewska, A., Jan, Y.N., and Utset, M.F. **(2002)**. "Tetralogy of fallot and other congenital heart defects in Hey2 mutant mice," *Curr. Biol.* **12**(18), 1605-1610.

Doucas, H., Mann, C.D., Sutton, C.D., Garcea, G., Neal, C.P., Berry, D.P., and Manson, M.M. **(2008)**. "Expression of nuclear Notch3 in pancreatic adenocarcinoma is associated with adverse clinical features, and correlates with the expression of STAT3 and phosphorylated Akt," *J. Surg. Oncol.* **97**, 63-68.

Duan, L., Yao, J., Wu, X., and Fan, M. **(2006)**. "Growth suppression induced by Notch1 activation involves Wnt-beta-catenin down-regulation in human tongue carcinoma cells," *Biol. Cell* **98**(8), 479-490.

Duffy, M.J., Sturgeon, C., Lamerz, R., Haglund, C., Holube, V.L., Klapdor, R., Nicolini, A., Topolcan, O., and Heinemann, V. **(2010)**. "Tumor markers in pancreatic cancer: a European Group on Tumor Makers (EGTM) status report," *Ann. Oncol.* **21**, 441-447.

Duncan, A.W., Rattis, F.M., Di Mascio, L.N., Congdon, K.L., Pazianos, G., Zhao, C., Yoon, K., Cook, J.M., Willert, K., Gaiano, N., and Reya, T. **(2005)**. "Integration of Notch and Wnt signalling in haematopoietic stem cell maintenance," *Nat. Immunol.* **6**(3), 314-322.

Edbauer, D., Winkler, E., Regula, J.T., Pesold, B., Steiner, H., and Haass, C. **(2003)**. "Reconstitution of gamma-secretase activity," *Nat. Cell. Biol.* **5**, 486-488.

Efferson, C.L., Winkelmann, C.T., Ware, C., Sullivan, T., Giampaoli, S., Tamman, J., Patel, S., Mesiti, G., Reilly, J.F., Gibson, R.E., Buser, C., Yeatman, T., Coppola, D., Winter, C., Clark, E.A., Draetta, G.F., Strack, P.R., and Majumder, P.K. **(2010)**. "Downregulation of Notch pathway by a gamma-secretase inhibitor attenuates AKT/mammalian target of rapamycin signalling and glucose uptake in an ERBB2 transgenic breast cancer model," *Cancer Res.* **70**(6), 2476-2484.

Elbashir, S.M., Lendeckel, W., and Tuschl, T. **(2001)**. "RNA interference is mediated by 21- and 22-nucleotide RNAs," *Genes Dev.* **15**, 188-200.

Ellisen, L.W., Bird, J., West, D.C., Soreng, A.L., Reynolds, T.C., Smith, S.D., and Sklar, J. **(1991)**. "TAN-1, the human homolog of the Drosophila notch gene, is broken by chromosomal translocations in T lymphoblastic neoplasms," *Cell* **66**(4), 649-661.

Fan, X., Mikolaenko, I., and Elhassan, I. **(2004)**. "Notch1 and notch2 have opposite effects on embryonal brain tumor growth," *Cancer Res.* **64**, 7787-7793.

Farnie, G., Clarke, R.B., Spence, K., Pinnock, N., Brennan, K., Anderson, N.G., and Bundred, N.J. **(2007)**. "Novel cell culture technique for primary ductal carcinoma in situ: role of Notch and epidermal growth factor receptor signalling pathways," *J. Nat. Cancer Inst.* **99**(8), 616-627.

Feldman, B., Hampton, T., and Cleary, M. **(2000)**. "A carboxy-terminal deletion mutant of Notch1 accelerates lymphoid oncogenesis in E2A-PBX1 transgenic mice," *Blood* **96**(5), 1906-1913.

Ferrone, C.R., Finkelstein, D.M., Thayer, S.P., Muzikansky, A., Fernandez-del-Castillo, C., and Warshaw, A.L. **(2006)**. "Perioperative CA19-9 levels can predict stage and survival in patients with resectable pancreatic adenocarcinoma," *J. Clin. Oncol.* **24**(18), 2897-2902.

Figueroa, D.J., Morris, J.A., Ma, L., Kandpal, G., Chen, E., Li, Y.M., and Austin, C.P. **(2002)**. "Presenilin-dependent gamma secretase activity modulates neurite outgrowth," *Neurobiol. Dis.* **9**(1), 49-60.

Fire, A., Xu, S., Montgomery, M.K., Kostas, S.A., Driver, S.E., and Mello, C.C. **(1998)**. Potent and specific genetic interference by double-strander RNA in Caenorhabditis elegans," *Nature* **391**, 806-811.

Fischer, A., Schumacher, N., Maier, M., Sendtner, M., and Gessler, M. **(2004)**. "The Notch target genes Hey1 and Hey2 are required for embryonic vascular development," *Genes Dev.* **18**(8), 901-911.

Fitzgerald, K., Harrington, A., and Leder, P. **(2000)**. "Ras pathway signals are required for notch-mediated oncogenesis," *Oncogene* **19**, 4191-4198.

Fleisher, A.S., Raman, R., Siemers, E.R., Becerra, L., Clark, C.M., Dean, R.A., Farlow, M.R., Galvin, J.E., Peskind, E.R., Quinn, J.F., Sherzai, A., Sowell, B.B., Aisen, P.S., and Thal, L.J. **(2008)**. "Phase 2 safety trial targeting amyloid beta production with a gamma-secretase inhibitor in Alzheimer disease," *Arch. Neurol.* **65**(8), 1031-1038.

Fortini, M. and Artavanis-Tsakonas, S. **(1994)**. "The suppressor of hairless protein participates in notch receptor signalling," *Cell* **79**(2), 273-282.

Fortini, M.E. **(2009)**. "Notch signalling: the core pathway and its posttranslational regulation," *Dev. Cell* **16**(5), 633-647.

Fre, S., Pallavi, S.K., Huyghe, M., Lae, M., Jannsen, K.P., Robine, S., Artavanis-Tsakonas, S., and Louvard, D. **(2009)**. "Notch and Wnt signals cooperatively control cell proliferation and tumorigenesis in the intestine," *Proc. Natl. Acad. Sci. USA.* **106**(15), 6309-6314.

Frise, E., Knoblich, J.A., Younger-Shepherd, S., Jan, L.Y., and Jan, Y.N. **(1996)**. "The Drosophila Numb protein inhibits signalling of the Notch receptor during cell-cell interation in sensory organ lineage," *Proc. Natl. Acad. Sci. U.S.A.* **93**(21), 11925-11932.

Fryer, C.J., Lamar, E., Turbachova, I., Kintner, C., and Jones, K.A. **(2002)**. "Mastermind mediates chromatin-specific transcription and turnover of the Notch enhancer complex," *Genes Dev.* **16**(11), 1397-1411.

Fryer, C.J., White, J.B., and Jones, K.A. **(2004)**. "Mastermind recruits CycC:CDK8 to phosphorylate the Notch ICD and coordinate activation with turnover," *Mol. Cell* **16**(4), 509-520.

Gallahan, D. and Callahan, R. **(1997)**. "The mouse mammary tumor associated gene INT3 is a unique member of the NOTCH gene family (NOTCH4)," *Oncogene* **14**(16), 1883-1890.

Garcea, G., Neal, C.P., Pattenden, C.J., Steward, W.P., and Berry, D.P. **(2005)**. "Molecular prognostic markers in pancreatic cancer: a systematic review," *Eur. J. Cancer* **41**(15), 2213-2236.

Garcea, G., Dennison, A.R., Ong, S.L., Pattenden, C.J., Neal, C.P., Sutton, C.D., Mann, C.D., and Berry, D.P. **(2007)**. "Tumour characteristics predictive of survival following resection for ductal adenocarcinoma of the head of pancreas," *Eur. J. Surg. Oncol.* **33**(7), 892-897.

Garcea, G., Dennison, A.R., Pattenden, C.J., Neal, C.P., Sutton, C.D., and Berry, D.P. **(2008)**. "Survival following curative resection for Pancreatic Ductal Adenocarcinoma. A systematic review of the literature," *J. Pancreas* **9**(2), 99-132.

Garcea, G., Ladwa, N., Neal, C.P., Metcalfe, M.S., Dennison, A.R., and Berry, D.P. **(2011)**. "Preoperative neutrophil-to-lymphocyte ratio (NLR) is associated with reduced disease-free survival following curative resection of pancreatic adenocarcinoma," *World. J. Surg.* **35**(4), 868-872.

Garzia, L., Andolfo, I., Cusanelli, E., Marino, N., Petrosino, G., De Martino, D., Esposito, V., Galeone, A., Navas, L., Esposito, S., Garqiulo, S., Fattet, S., Donofrio, V., Cinalli, G., Brunetti, A., Vecchio, L.D., Northcott, P.A., Delattre, O., Taylor, M.D., Iolascon, A., and Zollo, M. **(2009)**. "MicroRNA-199b-5p impairs cancer stem cells through negative regulation of HES1 in medulloblastoma," *PLoS One* **4**(3), e4998.

Gessler, M., Knobeloch, K.P., Helisch, A., Amann, K., Schumacher, N., Rohde, E., Fischer, A., and Leimeister, C. **(2002)**. "Mouse gridlock: no aortic coarctation of deficiency, but fatal cardiac defects in Hey2 -/- mice," *Curr. Biol.* **12**(18), 1601-1604.

Gil, J. and Esteban, M. **(2000)**. "Induction of apoptosis by the dsRNA-dependent protein kinase (PKR): mechanism of action," *Apoptosis* **5**(2), 107–114.

Giovannetti, E., Funel, N., Peters, G.J., Del Chiaro, M., Erozenci, L.A., Vasile, E., Leon, L.G., Pollina, L.E., Groen, A., Falcone, A., Danesi, R., Campani, D., Verheul, H.M., and Boggi, U. **(2010)**. "MicroRNA-21 in Pancreatic Cancer: Correlation with Clinical Outcome and Pharmacologic Aspects Underlying its role in the modulation of Gemcitabine activity," *Cancer Res.* **70**(11), 4528-4538.

Giovannini, C., Gramantieri, L., Chieco, P., Minguzzi, M., Lago, F., Pianetti, S., Ramazzotti, E., Marcu, K.B., and Bolondi, L. **(2009)**. "Selective ablation of Notch3 in HCC enhances doxorubicin's death promoting effect by a p53 dependent mechanism," *J. Hepatol.* **50**(5), 969-979.

Goldstein, A.M., Fraser, M.C., Struewing, J.P., Hussussian, C.J., Ranade, K., Zametkin, D.P., Fontaine, L.S., Organic, S.M., Dracopoli, N.C., Clark, W.H. *et al*. **(1995)**. "Increased

risk of pancreatic cancer in melanoma-prone kindreds with p16INK4 mutations," *N. Engl. J. Med.* **333**(15), 970-974.

Goonetilleke, K.S. and Siriwardena, A.K. **(2007)**. "Systematic review of carbohydrate antigen (CA 19-9) as a biochemical marker in the diagnosis of pancreatic cancer," *Eur. J. Surg. Oncol.* **33**(3), 266-270.

Gramantieri, L., Giovannini, C., Lanzi, A., Chieco, P., Ravaioli, M., Venturi, A., Grazi, G.L., and Bolondi, L. **(2007)**. "Aberrant Notch3 and Notch4 expression in human hepatocellular carcinoma," *Liver Int.* **27**(7), 997-1007.

Gray, G.E., Mann, R.S., Mitsiadis, E., Henrique, D., Carcangiu, M.L., Banks, A., Leiman, J., Ward, D., Ish-Horowitz, D., and Artavanis-Tsakonas, S. **(1999)**. "Human ligands of the Notch receptor," *Am. J. Pathol.* **154**(3), 785-794.

Greer, J.B. and Whitcomb, D.C. **(2009)**. "Inflammation and pancreatic cancer: an evidence-based review," *Curr. Opin. Pharmacol.* **9**(4), 411-418.

Grossman, S.R., Perez, M., Kung, A.L., Joseph, M., Mansur, C., Xiao, Z.X., Kumar, S., Howley, P.M., and Livingston, D.M. **(1998)**. "p300/MDM2 complexes participate in MDM2-mediated p53 degradation," *Mol. Cell* **2**(4), 405-415.

Guo, M., Jan, L., and Jan, Y. **(1996)**. "Control of daughter cell fates during asymmetric division: interaction of Numb and Notch," *Neuron.* **17**(1), 1-4.

Guo, D., Ye, J., Dai, J., Li, L., Chen, F., Ma, D., and Ji, C. **(2009)**. "Notch-1 regulates Akt signalling pathway and the expression of cell cycle regulatory proteins cyclin D1, CDK2, and p21 in T-ALL cell lines," *Leukaemia Res.* **33(5)**, 678-685.

Gupta-Rossi, N., Le Bail, O., Gonen, H., Brou, C., Logeat, F., Six, E., Ciehanover, A., and Israel, A. **(2001)**. "Functional interaction between SEL-10, an F-box protein, and the nuclear form of activated Notch1 receptor," *J. Biol. Chem.* **276**(37), 34371-34378.

Haass, C., and Steiner, H. **(2002)**. "Alhzeimers disease gamma-secretase: a complex story of GxGD-type presenilin proteases," *Trends Cell. Biol.* **12**(12), 556-562.

Haines, N. and Irvine, K.D. **(2003)**. "Glycosylation regulates Notch signalling," *Nat. Rev. Mol. Cell. Biol.* **4**(10), 786-797.

Hamilton, A.J. and Baulcombe, D.C. **(1999)**. "A species of small antisense RNA in posttranscriptional gene silencing in plants," *Science* **286**, 950-952.

Hanahan, D. and Weinberg, R.A. **(2011)**. "Hallmarks of cancer: the next generation," *Cell* **144**(5), 646-674.

Hanlon, L., Avila, J.L., Demarest, R.M., Troutman, S., Allen, M., Ratti, F., Rustgi, A.K., Stanger, B.Z., Radtke, F., Adsay, V., Long, F., Capobianco, A.J., and Kissil, J.L. **(2010)**. "Notch1 functions as a tumor suppressor in a model of K-ras-induced pancreatic ductal adenocarcinoma," *Cancer Res.* **70**(11), 4280-4286.

Hannon, G.J. **(2002)**. "RNA interference," *Nature* **418**(6894), 244–251.

Hannon, G.J. and Rossi, J.J. **(2004)**. "Unlocking the potential of the human genome with RNA interference," *Nature* **431**(7006), 371–378.

Harrison, H., Farnie, G., Howell, S.J., Rock, R.E., Stylianou, S., Brennan, K.R., Bundred, N.J., and Clarke, R.B. **(2010)**. "Regulation of breast cancer stem cell activity by signalling through the Notch4 receptor," *Cancer Res.* **70**(2), 709-718.

Haruki, N., Kawaguchi, K.S., Eichenberger, S., Massion, P.P., Olson, S., Gonzalez, A., Carbone, D.P., and Dang, T.P. **(2005)**. "Dominant-negative Notch3 receptor inhibits mitogen-activated protein kinase pathway and the growth of human lung cancers," *Cancer Res.* **65**(9), 3555-3561.

He, Y. and Pear, W. **(2003)**. "Notch signalling in B cells," *Semin. Cell. Dev. Biol.* **14**, 135-142.

Hess, V., Glimelius, B., Grawe, P., Dietrich, D., Bodoky, G., Ruhstaller, T., Bajetta, E., Saletti, P., Figer, A., Scheithauer, W., and Herrmann, R. **(2008)**. "CA 19-9 tumour-marker response to chemotherapy in patients with advanced pancreatic cancer enrolled in a randomised trial," *Lancet Oncol.* **9**(2), 132-138.

Hicks, C., Johnston, S.H., Di Sibio, G., Collazo, A., Vogt, T.F., and Weinmaster, G. **(2000)**. "Fringe differentially modulates Jagged1 and Delta1 signalling through Notch1 and Notch2," *Nat. Cell. Biol.* **2**(8), 515-520.

Ho, A. and Dowdy, S.F. **(2002)**. "Regulation of G(1) cell-cycle progression by oncogenes and tumor suppressor genes," *Curr. Opin. Genet. Dev.* **12**(1), 47-52.

Hoemann, C.D., Beaulieu, N., Girard, L., Rebai, N., and Jolicoeur, P. **(2000)**. "Two distinct Notch1 mutant alleles are involved in the induction of T-cell leukemia in c-myc transgenic mice," *Mol. Cell Biol.* **20**(11), 3831-3842.

Holcomb, B., Yip-Schneider, M., and Schmidt, C.M. **(2008)**. "The role of nuclear factor kappaB in pancreatic cancer and the clinical applications of targeted therapy," *Pancreas* **36**(3), 225-235.

Houde, C., Li, Y., Song, L., Barton, K., Zhang, Q., Godwin, J., Nand, S., Toor, A., Alkan, S., Smadja, N.V., Avet-Loiseau, H., Lima, C.S., Miele, L. and Coignet, L.J. **(2004)**. "Overexpression of the NOTCH ligand JAG2 in malignant plasma cells from multiple myeloma patients and cell lines," *Blood* **104**(12), 3697-3704.

Howells, L.M., Mitra, A., and Manson, M.M. **(2007)**. "Comparison of oxaliplatin- and curcumin-mediated antiproliferative effects in colorectal cell lines," *Int. J. Cancer* **121**, 175-183.

Hruban, R.H., Takaori, K., Klimstra, D.S., Adsay, N.V., Albores-Saavedra, J., Biankin, S.A., Compton, C., Fukushima, N., Furukawa, T., Goggins, M., Kato, Y.,Kloppel, G., Longnecker, D.S., Luttges, J., Maitra, A., Offerhaus, G.J., Shimizu, M., and Yonezawa, S. **(2004)**. "An illustrated consensus on the classification of the pancreatic intraepithelial neoplasia and intraductal papillary mucinous neoplasms," *Am. J. Surg. Pathol.* **28**(8), 977-987.

Hseih, J.J., Zhou, S., Chen, L., Young, D.B., and Hayward, S.D. **(1999)**. "CIR, a corepressor linking the DNA binding factor CBF1 to the histone deacetylase complex," *Proc. Natl. Acad. Sci. U.S.A.* **96**(1), 23-28.

Hu, Q.D., Ang, B.T., Karsak, M., Hu, W.P., Cui, X.Y., Duka, T., Takeda, Y., Chia, W., Sankar, N., Ng, Y.K., Ling, E.A., Maciag, T., Small, D., Trifonova, R., Kopan, R., Okano, H., Nakafuku, M., Chiba, S., Hirai, H., Aster, J.C., Schachner, M., Pallen, C.J., Watanabe, K., and Xiao, Z.C. **(2003)**. "F3/Contactin acts as a functional ligand for Notch during oligodendrocyte maturation," *Cell* **115**(2), 163-175.

Hubbard, E.J., Wu, G., Kitajewski, J., and Greenwald, I. **(1997)**. "sel-10, a negative regulator of lin-12 activity in Caenorhabditis elegans, encodes a member of the CDC4 family of proteins," *Genes Dev.* **11**(23), 3182-3193.

Hubmann, R., Schwarzmeier, J.D., Shehata, M., Hilgarth, M., Duechler, M., Dettke, M., and Berger, R. **(2002)**. "Notch2 is involved in the overexpression of CD23 in B-cell chronic lymphocytic leukemia," *Blood* **99**(10), 3742-3747.

Huppert, S.S., Le, A., Schroeter, E..H., Mumm, J.S., Saxena, M.T., Milner, L.A., and Kopan, R. **(2000)**. "Embryonic lethality in mice homozygous for a processing-deficient allele of Notch1," *Nature* **405**(6789), 966-970.

Huxley, R., Ansary-Moghaddam, A., de Gonzalez, A.B., Barzi, F., and Woodward M. **(2005)**. "Type-II diabetes and pancreatic cancer: a meta-analysis of 36 studies," *Brit. J. Cancer* **92**, 2076-2083.

Huynh, A.S., Abrahams, D.F., Torres, M.S., Baldwin, M.K., Gilles, R.J., and Morse, D.L. **(2011)**. "Development of an Orthotopic Human Pancreatic Cancer Xenograft model using Ultrasound guided injection of cells," *PLoS One* **6(5)**, e20330

Ikeuchi, T. and Sisodia, S.S. **(2002)**. "Cell-free generation of the notch1 intracellular domain (NICD) and APP-Ctfgamma: evidence for distinct intramembranous 'gamma-secretase' activities," *Neuromolecular Med.* **1**(1), 45-54.

Imatani, A. and Callahan, R. **(2000)**. "Identification of a novel NOTCH-4/INT-3 RNA species encoding an activated gene product in certain human tumor cell lines," *Oncogene* **19**(2), 223-231.

Iodice, S., Gandini, S., Maisonneuve, P., and Lowenfels, A.B. **(2008)**. "Tobacco and the risk of pancreatic cancer: a review and meta-analysis," *Langenbecks Arch. Surg.* **393**, 535-545.

Ishimura, N., Bronk, S.F., and Gores, G.J. **(2005)**. "Inducible nitric oxide synthase up-regulates Notch-1 in mouse cholangiocytes: implications for carcinogenesis," *Gastroenterology* **128**(5), 1354-1368.

Iso, T., Chung, G., Hamamori, Y., and Kedes, L. **(2002)**. "HERP1 is a cell type-specific primary target of Notch," *J. Biol. Chem.* **277**(8), 6598-6607.

Iso, T., Kedes, L., and Hamamori, Y. **(2003)**. "HES and HERP families: multiple effectors of the Notch signalling pathway," *J. Cell Physiol.* **194**(3), 237-255.

Itoh, M., Kim, C.H., Palardy, G., Oda, T., Jiang, Y.J., Maust, D., Yeo, S.Y., Lorick, K., Wright, G.J., Ariza-McNaughton, L., Weissman, A.M., Lewis, J., Chandrasekharappa,

S.C., and Chitnis, A.B. **(2003)**. "Mind bomb is a ubiquitin ligase that is essential for efficient activation of Notch signalling by Delta," *Dev. Cell.* **4**(1), 67-82.

Jackson, A.L., Bartz, S.R., Schelter, J., Kobayashi, S.V., Burchard, J., Mao, M., Li, B., Cavet, G., and Linsley, P.S. **(2003)**. "Expression profiling reveals off-target gene regulation by RNAi. Nat. Biotechnol," **21**(6), 635–637.

Jacobs, E.J., Chanocks, S.J., Fuchs, C.S., Lacroix, A., McWilliams, R.R>, Steplowski, E., Stolzenberg-Solomon, R.Z., Arslan, A.A., on behalf of the Pancreatic Cancer Cohort Consortium. **(2010)**. "Family history of cancer and risk of pancreatic cancer: a pooled analysis from the Pancreatic Cancer Cohort Consortium (PanScan)," *Int. J. Cancer* **127**(6), 1421-1428.

Jamieson, N.B., Flen, P., McMillan, D.C., McKay, C.J., Foulis, A.K., Carter, R., and Imrie, C.W. **(2005)**. "Systemic inflammatory response predicts outcome in patients undergoing resection for ductal adenocarcinoma head of pancreas," *Brit. J. Cancer* **92**, 21-23.

Jang, M.S., Miao, H., Carlesso, N., Shelly, L., Zlobin, A., Darack, N., Qin, J.Z., Nickoloff, B.J., and Miele, L. **(2004)**. "Notch-1 regulates cell death independently of differentiation in murine erythroleukemia cells through multiple apoptosis and cell cycle pathways," *J. Cell. Physiol.* **199**, 418-433.

Jarriault, S., Brou, C., Logeat, F., Schroeter, E.H., Kopan, R., and Israel, A. **(1995)**. "Signalling downstream of activated mammalian Notch," *Nature* **377**(6547), 355-358.

Jeffries, S. and Capobianco, A.J. **(2000)**. "Neoplastic transformation by Notch requires nuclear localization," *Mol. Cell Biol.* **20**(11), 3928-3941.

Jeffries, S., Robbins, D.J., and Capobianco, A.J. **(2002)**. "Characterisation of a high-molecular-weight Notch complex in the nucleus of Notch(ic)-transformed RKE cells and in a human T-cell leukemia cell line," *Mol. Cell Biol.* **22**(11), 3927-3941.

Jemal, A., Thomas, A., Murray, T., and Thun, M. **(2002)**. "Cancer statistics, 2002," *C.A. Cancer J. Clin.* **52(1)**, 23-47.

Jensen, J., Pedersen, E.E., Galante, P., Hald, J., Heller, R.S., Ishibashi, M., Kageyama, R., Guillemot, F., Serup, P., and Madsen, O.D. **(2000)**. "Control of endodermal endocrine development by Hes-1," *Nat. Genet.* **24**(1), 36-44.

Ji, Q., Hao, X., Zhang, M., Tang, W., Yang, M., Li, L., Xiang, D., Desano, J.T., Bommer, G.T., Fan, D., Fearon, E.R., Lawrence, T.S., and Xu, L. **(2009)**. "MicroRNA miR-34 inhibits human pancreatic cancer tumor-initiating cells," *PLoS One* **4**(8), e6818.

Jiao, L., Berrington de Gonzalez, A., Hartge, P., Pfeiffer, R.M., Park, Y., Freedman, D.M., Gail, M.H., Alavanja, M.C., Albanes, D., Beane-Freeman, L.E., Chow, W.H., Huang, W.Y., Hayes, R.B., Hoppin, J.A., Ji, B.T., Leitzmann, M.F., Linet, M.S., Meinhold, C.L., Shcairer, C., Schatzkin, A., Virtamo, J., Weinstein, S.J., Zheng, W., and Stolzenberg-Solomon, R.Z. **(2010)**. "Body mass index, effect modifiers, and risk of pancreatic cancer: a pooled study of seven prospective cohorts," *Cancer Causes Control* **21**(8), 1305-1314.

Jin, S., Tong, T., Fan, W., Fan, F., Antinore, M.J., Zhu, X., Mazzacurati, L., Li, X., Petrik, K.L., Rajasekaran, B., Wu., and Zhan, Q. **(2002)**. "GADD45-induced cell cycle G2-M arrest associates with altered subcellular distribution of cyclin B1 and is independent of p58 kinase activity," *Oncogene* **21**(57), 8696-8704.

Joshi, I., Minter, L.M., Telfer, J., Demarest, R.M., Capobianco, A.J., Aster, J.C., Sicinski, P., Fauq, A., Golde, T.E., and Osborne, B.A. **(2009)**. "Notch signalling mediates G1/S cell-cycle progression in T cells via cyclin D3 and its dependent kinases," *Blood* **113**(8), 1689-1698.

Joutel, A., Corpechot, C., Ducros, A., Vahedi, K., Chabriat, H., and Mouton, P. **(1996)**. "Notch3 mutation in CADASIL, a hereditary adult-onset condition causing stroke and dementia," *Nature* **383**, 707-710.

Ju, B.G., Solum, D., Song, E.J., Lee, K.J., Rose, D.W., Glass, C.D., and Rosenfeld, M.G. **(2004)**. "Activating the PARP-1 sensor component of the groucho/TLE1 corepressor complex mediates a CaMKinase IIdelta-dependent neurogenic gene activation pathway," *Cell* **119**(6), 815-829.

Jubb, A.M., Soilleux, E.J., Turley, H., Steers, G., Parker, A., Low, I., Blades, J., Li, J.L., Allen, P., Leek, R., Noguera-Troise, I., Gatter, K.C., Thurston, G., and Harris, A.L. **(2010)**. "Expression of vascular notch ligand delta-like 4 and inflammatory markers in breast cancer," *Am. J. Pathol.* **176**(4), 2019-2028

Jundt, F., Anagnostopoulos, I., Forster, R., Mathas, S., Stein, H., and Dorken, B. **(2002)**. "Activated Notch1 signalling promotes tumor cell proliferation and survival in Hodgkin and anaplastic large cell lymphoma," *Blood* **99**(9), 3398-3403.

Jundt, F., Probsting, K.S., Anagnostopoulos, I., Muehlinghaus, G., Chatterjee, M., Mathas, S.,Bargou, R.C., Manz, T., Stein, H., and Dorken, B. **(2004)**. "Jagged1-induced Notch signalling drives proliferation of multiple myeloma cells," *Blood* **103**(9), 3511-3515.

Jung, S.G., Kwon, Y.D., Song, J.A., Back, M.J., Lee, S.Y., Lee, C., Hwang, Y.Y., and An, H.J. **(2010)**. "Prognostic significance of Notch3 gene expression in ovarian serous carcinoma," *Cancer Sci.* **101**(9), 1977-1983.

Kamstrup, M.R., Gjerdrum, L.M., Biskup, E., Lauenborg, B.T., Ralfkiaer, E., Woetmann, A., Odum, N., and Gniadecki, R. **(2010)**. "Notch1 as a potential therapeutic target in cutaneous T-cell lymphoma," *Blood* **116**(14), 2504-2512.

Kang, J.H., Lee, D.H., Lee, J.S., Kim, H.J., Shin, J.W., Lee, Y.H., Lee, Y.S., Park, C.S., and Chung, I.Y. **(2005)**. "Eosinophilic differentiation is promoted by blockage of Notch signaling with a gamma-secretase inhibitor," *Eur. J. Immunol.* **35**(10), 2282-2990.

Kao, H.Y., Ordentlich, P., Koyano-Nakagawa, N., Tang, Z., Downes, M., Kinter, C.R., Evans, R.M., and Kadesch, T. **(1998)**. "A histone deacetylase corepressor complex regulates the Notch signal transduction pathway," *Genes Dev.* **12**(15), 2269-2277.

Kariko, K., Bhuyan, P., Capodici, J., and Weissman, D. **(2004)**. "Small interfering RNAs mediate sequence independent gene suppression and induce immune activation by signaling through toll-like receptor 3," *J. Immunol.* **172**(11), 6545–6549.

Karsan, A. **(2005)**. "The role of notch in modelling and maintaining the vasculature," *Can. J. Physiol. Pharmacol.* **83**, 14-23.

Kastrinos, F., Mukherjee, B., Tayob, N., Want, F., Sparr, J., Raymond, V.M., Bandipalliam, P., Stoffel, E.M., Gruber, S.B. and Syngal, S. **(2009)**. "Risk of pancreatic cancer in families with Lynch syndrome," *J.A.M.A.* **302**(16), 1790-1795.

Kawai-Kowase, K., and Owens, G.K. **(2007)**. "Multiple repressor pathways contribute to phenotypic switching of vascular smooth muscle cells," *Am. J. Physiol. Cell Physiol.* **292**, C59.

Kidd, S., Lieber, T., and Young, M. **(1998)**. "Ligand-induced cleavage and regulation of nuclear entry of Notch in Drosophila melanogaster embryos," *Genes Dev.* **12**(23), 3728-3740.

Killion, J.J., Radinsky, R., and Fidler, I.J. **(1999)**. "Orthotopic models are necessary to predict therapy of transplantable tumors in mice," *Cancer Metastasis Rev.* **17**(3), 279-284.

Kim, J., Kim, M., and Kim, K. **(2005)**. "Notch interferes with the scaffold function of JNK-interacting protein 1 to inhibit the JNK signalling pathway," *Proc. Natl. Acad. Sci. U.S.A.* **22**, 22.

Kimura, K., Satoh, K., Kanno, A., Hamada, S., Hirota, M., Endoh, M., Masamune, A., and Shimosegawa, T. **(2007)**. "Activation of Notch signaling in tumorigenesis of experimental pancreatic cancer induced by dimethylbenzanthracene in mice," *Cancer Sci.* **98**, 155-162.

Kindler, T., Cornejo, M.G., Scholl, C., Liu, J., Leeman, D.S., Haydu, J.E., Frohling, S., Lee, B.H., and Gilliland, D.G. **(2008)**. "K-RasG12D-induced T-cell lymphoblastic lymphoma/leukemias harbour Notch1 mutations and are sensitive to gamma-secretase inhibitors," *Blood* **112**(8), 3373-3382.

Koduru, S., Kumar, R., Srinivasan, S., Evers, M.B., and Damodaran, C. **(2010)**. "Notch-1 inhibition by Withaferin-A: a therapeutic target against colon carcinogenesis," *Mol. Cancer Ther.* **9**(1), 202-210.

Konishi, J., Kawaguchi, K.S., Vo, H., Haruki, N., Gonzalez, A., Carbone, D.P., and Dang, T.P. **(2007)**. "γ-secretase inhibitor prevents Notch3 activation and reduces proliferation in human lung cancers," *Cancer Res.* **67**(17), 8051-8057.

Konishi, J., Yi, F., Chen, X., Vo, H., Carbone, D.P., and Dang, T.P. **(2010)**. "Notch3 cooperates with the EGFR pathway to modulate apoptosis through the induction of Bim," *Oncogene* **29**(4), 589-596.

Koo, B.K., Lim, H.S., Song, R., Yoon, M.J., Yoon, K.J., Moon, J.S., Kim, Y.W., Dwon, M.C., Yoo, K.W., Kong, M.P., Lee, J., Chitnis, A.B., Kim, C.H., and Kong, Y.Y. **(2005)**. "Mind bomb 1 is essential for generating functional Notch ligands to activate Notch," *Development* **132**, 3459-3470.

Kordon, E.C., Smith, G.H., Callahan, R., and Gallahan, D. **(1995)**. "A novel non-mouse mammary tumor virus activation of the Int-3 gene in a spontaneous mouse mammary tumor," *J. Virol.* **69**(12), 8066-8069.

Krebs, L.T., Deftos, M.L., Bevan, M.J., and Gridley, T. **(2001)**. "The Nrarp gene encodes an ankyrin-repeat protein that is transcriptionally regulated by the notch signalling pathway," *Dev. Biol*. **238**(1), 110-119.

Krop, I.E., Kosh, M., Fearen, J., Savoie, J., Dallob, A., Matthews, C., Stone, J., Winer, E., Freedman, S.J., and Lorusso, P. **(2006)**. "Phase I pharmacokinetic (PK), and pharmacodynamic (PD) trial of the novel oral Notch inhibitor MK-0752 in patients with advanced breast cancer and other solid tumours," *J. Clin. Oncol.* **24**(18S), 10574.

Kuhlmann, K.F.D., de Castro, S.M.M., Wesseling, J.G., ten Kate, F.J.W., Offerhaus, G.J.A., Busch, O.R.C., van Gulik, T.M., Obertop, H., and Gouma, D.J. **(2004)**. "Surgical treatment of pancreatic adenocarcinoma: actual survival and prognostic factors in 343 patients," *Eur. J. Cancer* **40**, 549-558.

Kulik, G., Klippel, A., and Weber, M.J. **(1997)**. "Antiapoptotic signaling by the insulin-like growth factor I receptor, phosphatidylinositol 3-kinase, and Akt," *Mol. Cell. Biol.* **17**, 1595-1599

Kunnumakkara, A.B., Guha, S., Krishnan, S., Diagaradjane, P., Gelovani, A., and Aggarwal, B.B. **(2007)**. "Curcumin potentiates antitumor activity of gemcitabine in an orthotopic model of pancreatic cancer through suppression of proliferation, angiogenesis, and inhibition of nuclear factor-κB-related gene products," *Cancer Res.* **67**(7), 3853-3861.

Kuroda, K., Han, H., Tani, S., Tanigaki, K., Tun, T., Furukawa, T., Taniguchi, Y., Kurooka, H., Hamada, Y., Toyokuni, S., and Honjo, T. **(2003)**. "Regulation of marginal zone B cell development by MINT, a suppressor of Notch/RBP-J signalling pathway," *Immunity* **18**(2), 301-312.

Kwon, C., Han, Z., Olson, E.N., Srivastava, D. **(2005)**. "MicroRNA1 influences cardiac differentiation in Drosophila and regulates Notch signalling," *Proc. Natl. Acad. Sci. U.S.A.* **102**(52)

LaVoie, M. and Selkoe, D. **(2003)**. "The Notch ligands, Jagged and Delta, are sequentially processed by alpha-secretase and presenilin/gamma-secretase and release signaling fragments," *J. Biol. Chem.* **278**(36), 34427-34437.

Lai, E.C., Deblandre, G.A., Kitner, C., and Rubin, G.M. **(2001)**. "Drosophila neuralized is a ubiquitin ligase that promotes the internalization and degradation of delta," *Dev. Cell* **1**(6), 783-794.

Lamar, E., Deblandre, G., Wettstein, D., Gawantka, V., Pollet, N., Niehrs, C., and Kintner, C. **(2001)**. "Nrarp is a novel intracellular component of the Notch signalling pathway," *Genes Dev.* **15**(15), 1885-1899.

Lammert, E., Brown, J., and Melton, D. **(2000)**. "Notch gene expression during pancreatic organogenesis," *Mech. Dev.* **94**, 199-203.

Lan, K., Choudhuri, T., Murakami, M., Kuppers, D.A., and Robertson, E.S. **(2006)**. "Intracellular activated Notch1 is critical for proliferation of Kaposi's sarcoma-associated herpesvirus-associated B-lymphoma cell lines in vitro," *J. Virol.* **80**(13), 6411-6419.

Latchford, A., Greenhalf, W., Vitone, L.J., Neoptolemos, J.P., Lancaster, G.A., and Phillips, R.K. **(2006)**. "Peutz-Jeghers syndrome and screening for pancreatic cancer," *Brit. J. Surg.* **93**(12), 1446-1455.

Le, X.F., Vallian, S., Mu, Z.M., Hung, M.C., and Chang, K.S. **(1998)**. "Recombinant PML adenovirus suppresses growth and tumorigenicitiy of human breast cancer cells by inducing G1 cell cycle arrest and apoptosis," *Oncogene* **16**(14), 1839-1849.

Lee, S.Y., Kumano, K., Masuda, S., Hangaishi, A., Takita, J., Nakazaki, K., Kurokawa, M., Hayashi, Y., Ogawa, S., and Chiba, S. **(2005)**. "Mutations of the Notch1 gene in T-cell acute lymphoblastic leukemia: an analysis in adults and children," *Leukemia* **19**(10), 1841-1843.

Lee, C.W., Raskett, C.M., Prudovsky, I., and Altieri, D.C. **(2008)**. "Molecular dependence of estrogen receptor-negative breast cancer on a notch-survivin signalling axis," *Cancer Res.* **68**(13), 5273-5281.

Lei, L., Xu, A., Panin, V.M. and Irvine, K.D. **(2003)**. "An O-fucose site in the ligand binding domain inhibits Notch activation," *Development* **130**(26), 6411-6421.

Lewis, H.D., Leveridge, M., Strack, P.R., Haldon, C.D., O'Neil, J., Kim, H., Madin, A., Hannam, J.C., Look, A.T., Kohl, N., Draetta, G., Harrison, T., Kerby, J.A., Shearman, M.S., and Beher, D. **(2007)**. "Apoptosis in T cell acute lymphoblastic leukemia cells after cell cycle arrest induced by pharmacological inhibition of notch signalling," *Chem. Biol.* **14**(2), 209-219.

Li, Y.M., Lai, M.T., Xu, M., Huang, Q., DiMuxio-Mower, J., Sardana, M.K., Shi, X.P., Yin, K.C., Shafer, J.A., and Gardell, S.J. **(2000)**. "Presenilin 1 is linked with gamma-secretase activity in the detergent solubilized state," *Proc. Natl. Acad. Sci. U.S.A.* **97**(11), 6138-6143.

Li, D., Xie, K., Wolff, R., and Abbruzzese, J.L. **(2004)**. "Pancreatic cancer," *Lancet* **363**, 1049-1057.

Li, L., Braiteh, F.S., and Kurzrock, R. **(2005)**. "Liposome-encapsulated Curcumin. In vitro and in vivo effects on proliferation, apoptosis, signaling and angiogenesis," *Cancer* **104**, 1322-1331.

Li, Y., Guessous, F., Zhang, Y., Dipierro, C., Kefas, B., Johnson, E., Marcinkiewisz, L., Jiang, J., Yang, Y., Schmittgen, T.D., Lopes, B., Schiff, D., Purow, B., and Abounader, R. **(2009)**. "MicroRNA-34a inhibits glioblastoma growth by targeting multiple oncogenes," *Cancer Res.* **69**(19), 7569-7576.

Li, S., Francisco, A.B., Munroe, R.J., Schimenti, J.C., and Long, Q. **(2010)**. "SEL1L deficiency impairs growth and differentiation of pancreatic epithelial cells," *BMC Dev. Biol.* **10**, 19-32.

Lieber, M., Mazzetta, J., Nelson-Rees, W., Kaplan, M., and Todara, G. **(1975)**. "Establishment of a continuous tumor-cell line (panc-1) from a human carcinoma of the exocrine pancreas," *Int. J. Cancer* **15**(5), 741-747.

Lim, J.E., Chien, M.W., and Earle, C.C. **(2003)**. "Prognostic factors following curative resection for pancreatic adenocarcinoma: a population-based, linked database analysis of 396 patients," *Ann. Surg.* **237**(1), 74-85.

Lim, L. P., Lau, N. C., Garrett-Engele, P., Grimson, A., Schelter, J. M., Castle, J., Bartel, D. P., Linsley, P. S., and Johnson, J. M. **(2005)**. "Microarray analysis shows that some microRNAs downregulate large numbers of target mRNAs," *Nature* **433**, 769-773.

Lin, L., Mernaugh, R., Yi, F., Blum, D., Carbone, D.P., and Dang, T.P. **(2010)**. "Targeting specific regions of the Notch3 Ligand-binding domain induces apoptosis and inhibits tumor growth in Lung Cancer," *Cancer Res.* **70**, 632-638.

Lin, J.T., Chen, M.K., Yeh, K.T., Chang, C.S., Chang, T.H., Lin, C.Y., Wu, Y.C., Su, B.W., Lee, K.D., and Chang, P.J. **(2010a)**. "Associations of high levels of Jagged-1 and Notch-1 expression with poor prognosis in head and neck cancer," *Ann. Surg. Oncol.* **17**(11), 2976-2983.

Liptay, S., Weber, C.K., Ludwig, L., Wagner, M., Adler, G., and Schmid, R.M. **(2003)**. "Mitogenic and anti-apoptotic role of constitutive NF-kappaB/Rel activity in pancreatic cancer," *Int. J. Cancer* **105**, 735-746.

Liu, J., Gao, J., Du, Y., Li, Z., Ren, Y., Gu, J., Wang, X., Gong, Y., Wang, W., and Kong, X. **(2011)**. "Combination of plasma microRNAs with serum CA19-9 for early detection of pancreatic cancer," *Int. J. Cancer*, Epub.

Logeat, F., Bessia, C., Brou, C., LeBail, B., Jarriault, S., Seidah, N.G., and Israel, A. **(1998)**. "The Notch1 receptor is cleaved constitutively by a furin-like convertase," *Proc. Natl. Acad. Sci. U.S.A.* **95**(14), 8108-8112.

Lowenfels, A.B., Maisonneuve, P., DiMagno, E.P., Elitsur, Y., Gates, L.K. Jr., Perrault, J., and Whitcomb, D.C. **(1997)**. "Hereditary pancreatitis and the risk of pancreatic cancer: International Hereditary Pancreatitis Study Group," *J. Natl. Cancer Inst.* **89**(6), 442-446.

Lucenteforte, E., La Vecchia, C., Silverman, D., Petersen, G.M., Bracci, P.M. Ji, B.T., Bosetti, C., Li, D., Gallinger, S., Miller, A.B., Bueno-de-Mesquita, H.B., Talamini, T., Polesel, J., Ghadirian, P., Baghurst, P.A., Zatonski, W., Fontham, E., Bamlet, W.R., Holly, W.A., Gao, Y.T., Negri, E., Hassan, M., Cotterchio, M., Su, J., Maissoneuve, P., Boffetta, P., and Duell, E.J. **(2011)**. "Alcohol consumption and pancreatic cancer: a pooled analysis in the International Pancreatic Cancer Case-Control Consortium (PanC4)," *Ann. Oncol.* Epub.

Luo, D., Renault, V., and Rando, T. **(2005)**. "The regulation of Notch signalling in muscle stem cell activation and postnatal myogenesis," *Semin. Cell Dev. Biol.* **16**, 612-622.

Ma, S., Wan, T., and Chan, L. **(1999)**. "Cytogenetics and molecular genetics of childhood leukemia," *Hematol. Oncol.* **17**, 91-105.

MacKenzie, F., Duriez, P., Wong, F., Noseda, M., and Karsan, A. **(2004)**. "Notch4 inhibits endothelial apoptosis via RBP-Jkappa-dependent and –independent pathways," *J. Biol. Chem.* **279**(12), 11657-11663.

Maier, M.M. and Gessler, M. **(2000)**. "Comparative analysis of the human and mouse Hey1 promoter: Hey genes are new Notch target genes," *Biochem. Biophys. Res. Commun.* **275**, 652-600.

Mailard, I., Fang, T., and Pear, W. **(2005)**. "Regulation of lymphoid development, differentiation, and function by the Notch pathway," *Annu. Rev. Immunol.* **23**, 945-974.

Maithel, S.K., Maloney, S., Winston, C., Gonen, M., D'Angelica, M.I., Dematteo, R.P., Jarnagin, W.R., Brennan, M.F., and Allen, P.J. **(2008)**. "Preoperative CA 19-9 and the yield of staging laparoscopy in patients with radiographically resectable pancreatic adenocarcinoma," *Ann. Surg. Oncol.* **15**(12), 3512-3520.

Maitra, A., Kern, S.E., and Hruban, R.H. **(2006)**. "Molecular pathogenesis of pancreatic cancer," *Best Pract. Res. Clin. Gastroenterol.* **20**, 211-226.

Maitra, A. and Hruban, R.H. **(2008)**. "Pancreatic Cancer," *Annu. Rev. Pathol.* **3**, 157-188.

Major, M.L., Lepe, R., and Costa, R.H. **(2004)**. "Forkhead box M1B transcriptional activity requires binding of Cdk-cyclin complexes for phosphorylation-dependent recruitment of p300/CBP coactivators," *Mol. Cell. Biol.* **24**, 2649-2661.

Mann, C.D., Neal, C.P., Metcalfe, M.S., Pattenden, C.J., Dennison, A.R., and Berry, D.P. **(2007)**. "Clinical Risk Score predicts yield of staging laparoscopy in patients with colorectal liver metastases," *Brit. J. Surg.* **94**(7), 855-859.

Mann, C.D., Metcalfe, M.S., Neal, C.P., Rees, Y., Dennison, A.R., and Berry, D.P. **(2007a)**. "Role of ultrasound in the detection of resectable recurrence after hepatectomy for colorectal liver metastases," *Brit. J. Surg.* **94**(11), 1403-1407.

Mann, C.D., Metcalfe, M.S., and Nicholson, M.L. **(2009)**. "Normothermic perfusion of ischaemic porcine kidneys: an evaluation of ex vivo function and endothelin receptor antagonism," *J. Nephrol.* **22**(1), 144-151.

Marambaud, P., Shioi, J., Serban, G., Georgakopoulos, A., Sarner, S., Nagy, V., Baki, L., Wen, P., Efthimiopoulos, S., Shao, Z., Wisniewski, T., and Robakis, N.K. **(2002)**. "A presenilin-1/γ-secretase cleavage releases the E-cadherin intracellular domain and regulates disassembly of adherens junctions," *EMBO Journal* **21**, 1948-1956.

Martinez, J., Patkaniowska, A., Urlaub, H., Luhrmann, R., and Tuschl, T. **(2002)**. "Single-stranded antisense siRNAs guide target RNA cleavage in RNAi," *Cell* **110**(5), 563–574.

Martys-Zage, J.L., Kim, S.H., Berechil, B., Bingham, S.J., Chu, S., Sklar, J., Nye, J., and Sisodia, S.S. **(2000)**. "Requirement for presenilin 1 in facilitating Jagged-2-mediated endoproteolysis and signaling of notch 1," *J. Mol. Neurosci.* **15**(3), 189-204.

Masiero, M., Nardo, G., Indraccolo, S., and Favaro, E. **(2007)**. "RNA Interference: Implications for cancer treatment," *Mol. Aspects Med.* **28**, 143-164.

Massi, D., Tarantini, F., Franchi, A., Paglierani, M., Di Serio, C., Pellerito, S., Leoncini, G., Cirino, G., Geppetti, P., and Santucci, M. **(2006)**. "Evidence for differential expression of Notch receptors and their ligands in melanocytic nevi and cutaneous malignant melanoma," *Mod. Pathol.* **19**(2), 246-254.

Masuda, S., Kumano, K., and Shimizu, K. **(2005)**. "Notch1 oncoprotein antagonizes TGF-beta/Smad-mediated cell growth suppression via sequestration of coactivator p300," *Cancer Sci.* **96**, 274-282.

Masuya, M., Katayama, N., Hoshino, N., Nishikawa, H., Sakano, S., Araki, H., Mitani, H., Suzuki, H., Miyashita, H., Kobayashi, K., Nishii, K., Minami, N., and Shiku, H. **(2002)**. "The soluble Notch ligand, Jagged-1, inhibits proliferation of CD34+ macrophage progenitors," *Int. J. Hematol.* **75**(3), 269-276.

Matsuno, K., Diederich, R.J., Go, M.J., Blaumueller, C.M., and Artavanis-Tsakonas, S. **(1995)**. "Deltex acts as a positive regulator of Notch signalling through interactions with the Notch ankyrin repeats," *Development* **121**(8), 2633-2644.

Matsuno, K., Eastman, D., Mitsiades, T., Quinn, A.M., Carcanciu, M.L., Ordentlich, P., Kadesch, T., and Artavanis-Tsakonas, S. **(1998)**. "Human deltex is a conserved regulator of Notch signalling," *Nat. Genet.* **19**(1), 74-78.

Mazur, P.K., Einwachter, H., Lee, M., Sipos, B., Nakhai, H., Rad, R., Zimber-Strobl, U., Strobl, L.J., Radtke, F., Kloppel, G., Schmid, R.M., and Siveke, J.T. **(2010)**. "Notch2 is required for progression of pancreatic intraepithelial neoplasia and development of pancreatic ductal adenocarcinoma," *Proc. Natl. Acad. Sci. U.S.A.* **107**(30), 13438-13443.

McManus, M.T. and Sharp, P.A. **(2002)**. "Gene silencing in mammals by small interfering RNAs," *Nat. Rev. Genet.* **3**(10), 737–747.

Meng, X., Liu, J., and Shen, Z. **(2004)**. "Inhibition of G1 to S cell cycle progression by BCCIP beta," *Cell Cycle* **3**(3), 343-348.

Meng, X., Lu, H., and Shen, Z. **(2004a)**. "BCCIP functions through p53 to regulate the expression of p21Waf1/Cip1," *Cell Cycle* **3**(11), 1457-1462.

Michaud, D.S., Vrieling, A., Jiao, L., Mendelsohn, J.B., Steplowski, E., Lynch, S.M., Wactawski-Wende, J., Arslan, A.A., Bas bueno-de-Mesquita, H., Fuchs, C.S., Gross, M., Helzlsouer, K., Jacobs, E.J., Lacroix, A., Petersen, G., Zheng, W., Allen, N., Ammundadottir, L., Bergmann, M.M., Boffetta, P., Buring, J.E., Canzian, F., Chanock, S.J., Clavel-Chapelon, F., Clipp, S., Freiberg, M.S., Michael Graziano, J., Giovannucci,

E.L., Hankinson, S., Hartge, P., Hoover, R.N., Allan-Hubbell, F., Hunter, D.J., Hutchinson, A., Jacobs, K., Kooperberg, C., Kraft, P., Manier, J., Navarro, C., Peeters, P.H., Shu, X.O., Stevens, V., Thomas, G., Tionneland, A., Tobias, G.S., Trichopoulos, D., Tumino, R., Vineis, P., Virtamo, J., Wallace, R., Wolpin, B.M., Yu, K., Zeleniuch-Jacquotte, A., and Stolzenberg-Solomon, R.Z. **(2010)**. "Alcohol intake and pancreatic cancer: a pooled analysis from the pancreatic cancer cohort consortium (PanScan)," *Cancer Causes Control* **21**(8), 1213-1225.

Milner, L.A., Bigas, A., Kopan, R., Brasheim-Stgein, C., Bernstein, I.D., and Martin, D.I. **(1996)**. "Inhibition of granulocytic differentiation by mNotch1," *Proc. Natl. Acad. Sci. U.S.A.* **93**(23), 13014-13019.

Milner, L. and Bigas, A. **(1999)**. "Notch as a mediator of cell fate determination in hematopoiesis: evidence and speculation," *Blood* **93**, 2431-2448.

Mishra-Gorur, K., Rand, M.D., Perez-Villamil, B., and Artavanis-Tsakonas, S. **(2002)**. "Down-regulation of Delta by proteolytic processing," *J. Cell. Biol.* **159**(2), 313-324.

Miyamoto, S., and Rosenberg, D.W. **(2011)**. "Role of Notch signaling in colon homeostasis and carcinogenesis," *Cancer Sci.* Epub.

Miyamoto, Y., Maitra, A., Ghosh, B., Zechner, U., Argani, P., Iacobuzio-Donahue, C.A., Sriuranpong, V., Iso, T., Meszoely, I.M., Wolfe, M.S., Hruban, R.H., Ball, D.W., Schmid, R.M., and Leach, S.D. **(2003)**. "Notch mediates TGF alpha-induced changes in epithelial differentiation during pancreatic tumorigenesis," *Cancer Cell* **3**, 565-576.

Moloney, D.J., Panin, V.M., Johnston, S.H., Chen, J., Shao, L., Wilson, R., Wang, Y., Stanley, P., Irvine, K.D., Haltiwanger, R.S. and Vogt, T.F. **(2000)**. "Fringe is a glycosyltransferase that modifies Notch," *Nature* **406**(6794), 369-375.

Morgan, T.H. **(1917)**. "The theory of the gene," *Am. Nat.* **51**(609), 513-544.

Mullendore, M.E., Koorstra, J.B., Li, Y.M., Offerhaus, G.J., Fan, X., Henderson, C.M., Matsui, W., Eberhart, C.G., Maitra, A., and Feldmann, G. **(2009)**. "Ligand-dependent Notch signalling is involved in tumor initiation and tumor maintenance in pancreatic cancer," *Clin. Cancer Res.* **15**(7), 2291-2301.

Mumm, J. and Kopan, R. **(2000)**. "Notch signalling: from the outside in," *Dev. Biol.* **228**, 151-165.

Mumm, J.S., Schroeter, E.H., Saxena, M.T., Griesemer, A., Tian, X., Pan, D.J., Ray, W.J., and Kopan, R. **(2000)**. "A ligand-induced extracellular cleavage regulates gamma-secretase-like proteolytic activation of Notch1," *Mol. Cell.* **5**(2), 197-206.

Murata, K., Hattori, M., and Hirai, N. **(2005)**. "Hes1 directly controls cell proliferation through the transcriptional repression of p27Kip1," *Mol. Cell. Biol.* **25**, 4262-4271.

Murtaugh, L.C., Stranger, B.Z., Kwan, K.M., and Melton, D.A. **(2003)**. "Notch signaling controls multiple steps of pancreatic differentiation," *Proc. Natl. Acad. Sci. U.S.A.* **100**(25), 14920-14925.

Nagakawa, Y., Aoki, T., Kasuya, K., Tsuchida, A., and Koyanagi, Y. **(2002)**. "Histologic features of venous invasion, expression of vascular endothelial growth factor and matrix metalloproteinase-2 and matrix metalloproteinase-9, and the relation with liver metastasis in pancreatic cancer," *Pancreas* **24**, 169-178.

Nair, P., Somasundaram, K., and Krishna, S. **(2003)**. "Activated Notch1 inhibits p53-induced apoptosis and sustains transformation by human papillomavirus type 16 E6 and E7 oncogenes through a PI3K-PKB/Akt-dependent pathway," *J. Virol.* **77**(12), 7106-7112.

Nakaya, N., Hemish, J., Krasnov, P., Kim, S.Y., Stasiv, Y., Michurina, T., Herman, D., Davidoff, M.S., Middendorff, R., and Enikolopov, G. **(2007)**. "Noxin, a novel stress-induced gene involved in cell cycle and apoptosis," *Mol. Cell Biol.* **27**(15), 5430-5444.

Nam, Y., Weng, A.P., Aster, J.C., and Blacklow, S.C. **(2003)**. "Structural requirements for the assembly of the CSL intracellular Notch1 Mastermind-like 1 transcriptional activation complex," *J. Biol. Chem.* **278**(23), 21232-21239.

Nam, D.H., Jeon, H.M., Kim, S., Kim, M.H., Lee, Y.J., Lee, M.S., Kim, H., Joo, K.M., Lee, D.S., Price, J.E., Bang, S.I., and Park, W.Y. **(2008)**. "Activation of notch signalling in a xenograft model of brain metastasis," *Clin. Cancer Res.* **14**(13), 4059-4066.

Narlawar, R., Baumann, K., Schubenel, R., and Schmidt, B. **(2007)**. "Curcumin derivatives inhibit or modulated beta-amyloid precursor protein metabolism," *Neurodegen. Dis.* **4**(2-3), 88-93.

Neal, C.P., Mann, C.D., Garcea, G., Briggs, C.D., Dennison, A.R., and Berry, D.P. **(2011)**. "Perioperative systemic inflammation and infectious complications after resection of colorectal liver metastases," *Arch. Surg.* **146**(4), 471-478.

NCT00100152: A Notch Signaling Pathway Inhibitor for Patients With T-Cell Acute Lymphoblastic Leukemia/Lymphoma (ALL). *Clinical Trials, U.S. National Institute of Health.*

NCT00106145: A Notch Signalling Pathway Inhibitor for Patients With Advanced Breast Cancer. *Clinical Trials, U.S. National Institute of Health.*

NCT 00572182: MK0752 in Treating Young Patients With Recurrent or Refractory CNS Cancer. *Clinical Trials, U.S. National Institute of Health.*

NCT00645333: Phase I/II Study of MK-0752 Followed by Docetaxel in Advanced or Metastatic Breast Cancer. *Clinical Trials, U.S. National Institute of Health.*

NCT00756717: Study Of MK-0752 In Combination With Tamoxifen Or Letrozole to Treat Early Stage Breast Cancer. *Clinical Trials, U.S. National Institute of Health.*

Nefedova, Y., Sullivan, D.M., Bolick, S.C., Dalton, W.S., and Gabrilovich, D.I. **(2008)**. "Inhibition of Notch signalling induces apoptosis of myeloma cells and enhances sensitivity to chemotherapy,". *Blood* **111**(4), 2220-2229.

Nefedova, Y. and Gabrilovich, D. **(2008)**. "Mechanisms and clinical prospects of Notch inhibitors in the therapy of haematological malignancies," *Drug Resist. Updat.* **11**(6), 210-218.

Neoptolemos, J.P., Stocken, D.D., Dunn, J.A., Almond, J., Beger, H.G., Pederzoli, P., Bassi, C., Dervenis, C., Fernandez-Cruz, L., Lacaine, F., Buckels, J., Deakin, M., Adab, F.A., Sutton, R., Imrie, C., Ihse, I., Tihanyi, T., Olah, A., Pedrazzoli, S., Spooner, D., Kerr, D.J., Friess, H., and Buchler, M.W. for the members of the European Study Group for Pancreatic Cancer. **(2001)**. "Influence of resection margins on survival for patients with pancreatic cancer treated by adjuvant chemoradiation and/or chemotherapy in the ESPAC-1 randomized controlled trial," *Ann. Surg.* **234**(6), 758-768.

Nicholson, D.W. and Thornberry, N.A. **(1997)**. "Caspases: Killer proteases," *Trend Biochem. Sci.* **22**, 299-306.

Nickoloff, B.J., Qin, J.Z., Chaturvedi, V., Denning, M.F., Bonish, B., and Miele, L. **(2002)**. "Jagged-1 mediated activation of notch signalling induces complete maturation of human keratinocytes through NF-kappaB and PPARgamma," *Cell Death Diff.* **9**(8), 842-855.

Nicolas, M., Wolfer, A., and Raj, K. **(2003)**. "Notch1 functions as a tumor suppressor in mouse skin," *Nat. Genet.* **33**, 416-421.

Ning, L., Wentworth, L., Chen, H., and Weber, S.M. **(2009)**. "Down-regulation of Notch1 signaling inhibits tumor growth in human hepatocellular carcinoma," *Am. J. Transpl. Res.* **1**(4), 358-366.

Nofziger, D., Miyamoto, A., Lyons, K.M., and Weinmaster, G. **(1999)**. "Notch signalling imposes two distinct blocks in the differentiation of C2C12 myoblasts," *Development* **126**(8), 1689-1702.

Nykanen, A., Haley, B., and Zamore, P.D. **(2001)**. "ATP requirements and small interfering RNA structure in the RNA interference pathway," *Cell* **107**(3), 309–321.

O'Neil, J., Calvo, J., McKenna, K., Krishnamoorthy, V., Aster, J.C., Bassing, C.H., Alt, F.W., Kelliher, M., and Look, A.T. **(2006)**. "Activating Notch1 mutations in mouse models of T-ALL," *Blood* **107**(2), 781-785.

O'Neil, J., Grim, J., Strack, P., Rao, S., Tibbitts, D., Winter, C., Hardwick, J., Welcker, M., Meijerink, J.P., Pieters, R., Draetta, G., Sears, R., Clurman, B.E., and Look, A.T. **(2007)**. "FBW7 mutations in leukemic cells mediate NOTCH pathway activation and resistance to gamma-secretase inhibitors," *J. Exp. Med.* **204**(8), 1813-1824.

Oberg, C., Li, J., Pauley, A., Wolf, E., Gurney, M., and Lendahl, U. **(2001)**. "The Notch intracellular domain is ubiquitinated and negatively regulated by the mammalian Sel-10 homolog," *J. Biol. Chem.* **276**(38), 35847-35853.

Ohishi, K., Varnum-Finney, B., Flowers, D., Anasetti, C., Myerson, D., and Berstein, I.D. **(2000)**. "Monocytes express high amounts of Notch and undergo cytokine specific apoptosis following interaction with the Notch ligand, Delta-1," *Blood* **95**(9), 2847-2854.

Ohtsuka, T., Ishibashi, M., Gradwohl, G., Nakanishi, S., Guillemot, F., and Kageyama, R. **(1999)**. "Hes1 and Hes5 as notch effectors in mammalian neuronal differentiation," *EMBO J.* **18**(8), 2196-2207.

Oishi, K., Kamakura, S., Isazawa, Y., Yoshimatsu, T., Kuida, K., Nakafuku, M., Masuyama, N., and Gotoh, Y. **(2004)**. "Notch promotes survival of neural precursor cells via mechanisms distinct from those regulating neurogenesis," *Dev. Biol.* **276**(1), 172-184.

Okajima, T., Xu, A., and Irvine, K. **(2003)**. "Modulation of notch-ligand binding by protein O-fucosyltransferase 1 and fringe," *J. Biol. Chem.* **278**(43), 42340-42345.

Okochi, M., Steiner, H., Fukumori, A., Tanii, H., Tomita, T., Tanaka, T., Iwatsubo, T., Kubo, T., Takeda, M., and Haass, C. **(2002)**. "Presenilins mediate a dual intramembranous gamma-secretase cleavage of Notch-1," *EMBO J.* **21**(20), 5408-5416.

Okochi, M., Fukumori, A., Jiang, J., Itoh, N., Kimura, R., Steiner, H., Haass, C., Tagami, S., and Takeda, M. **(2006)**. "Secretion of the Notch-1 Aβ-like peptide during Notch signalling," *J. Biol. Chem.* **281**(12), 7890-7898.

Omerod, M.G. **(1990)**. "Flow Cytometry: A practical approach," *Oxford University Press.*

Omi, K., Tokunaga, K., and Hohjoh, H. **(2004)**. "Long-lasting RNAi activity in mammalian neurons," *FEBS Lett.* **558**(1–3), 89–95.

Ong, S.L., Garcea, G., Thomasset, S.C., Mann, C.D., Neal, C.P., Abu Amara, M., Dennison, A.R., and Berry, D.P. **(2008)**. "Surrogate markers of resectability in patients undergoing exploration of potentially resectable pancreatic adenocarcinoma," *J. Gastrointest. Surg.* **12**(6), 1068-1073.

Osipo, C., Patel, P., Rizzo, P., Clementz, A.G., Hao, L., Golde, T.E., and Miele, L. **(2008)**. "ErbB-2 inhibition activates Notch-1 and sensitizes breast cancer cells to a γ-secretase inhibitor," *Oncogene* **27**(37), 5019-5032.

Oswald, F., Liptay, S., Adler, G., and Schmid, R.M. **(1998)**. "NF-kappaB2 is a putative target of activated Notch-1 via RBP-Jkappa," *Mol. Cell. Biol.* **18**(4), 2077-2088.

Ozcelik, H, Schmocker, B., Di Nicola, N., Shi, X.H., Langer, B., Moore, M., Taylor, B.R., Narod, S.A., Darlington, G., Andrulis, I.L., Gallinger, S., and Redston, M. **(1997)**. "Germline BRCA2 6174delT mutations in Ashkenazi Jewish Pancreatic cancer patients," *Nat. Genet.* **16**(1), 17-18.

Park, J.T., Li, M., Nakayama, K., Mao, T.L., Davidson, B., Zhang, Z., Kurman, R.J., Eberhart, C.G., Shih, I.M., and Wang, T.L. **(2006)**. "Notch3 gene amplification in ovarian cancer," *Cancer Res.* **66**(12), 6312-6318.

Park, J.T., Shih, I.M., Wang, T.L. **(2008)**. "Identification of Pbx1, a potential oncogene, as a Notch3 target gene in ovarian cancer," *Cancer Res.* **68**(21), 8852-8860.

Park, J.P., Chen, X., Trope, C.G., Davidson, B., Shih, L.M., and Wang, T.L. **(2010)**. "Notch3 overexpression is related to the recurrence of ovarian cancer and confers resistance to carboplatin," *Am. J. Pathol.* **177**(3), 1087-1094.

Parks, A.L., Klueg, K.M., Stout, J.R., and Muskavitch, M.A. **(2000)**. "Ligand endocytosis drives receptor dissociation and activation in the Notch pathway," *Development* **127**(7), 1373-1385.

Parr, C., Watkins, G., and Jiang, W.G. **(2004)** "The possible correlation of Notch-1 and Notch-2 with clinical outcome and tumour clinicopathological parameters in human breast cancer," *Int. J. Mol. Med.* **14**(5), 779-786.

Pavlopoulos, E., Pitsouli, C., Klueg, K.M., Muskavitch, M.A., Moschonas, N.K., and Delidakis, C. **(2001)**. "Neuralized encodes a peripheral membrane protein involved in delta signaling and endocytosis," *Dev. Cell* **1**(6), 807-816.

Pear, W.S., Aster, J.C., Scott, M.L., Hasserjian, R.P., Soffer, B., Sklar, J., and Baltimore, D. **(1996)**. "Exclusive development of T cell neoplasms in mice transplanted with bone marrow expressing activated Notch alleles," *J. Exp. Med.* **183**(5), 2283-2291.

Pece, S., Serresi, M., Santolini, E., Capra, M., Hulleman, E., Galimberti, V., Zurrida, S., Maisonneuve, P., Viale, G., and Di Fiore, P.P. **(2004)**. "Loss of negative regulation by Numb over Notch is relevant to human breast carcinogenesis," *J. Cell. Biol.* **167**(2), 215-221.

Pellegata, N.S., Sessa, F., Renault, B., Bonato, M., Leone, B.E., Solcia, E., and Ranzani, G.N. **(1994)**. "K-ras and p53 gene mutations in pancreatic cancer: ductal and nonductal tumors progress through different genetic lesions," *Cancer Res.* **54**(6), 1556-1560.

Pierfelice, T.J., Schreck, K.C., Dang, L., Asnaghi, L., Gaiano, N., and Eberhart, C.G. **(2011)**. "Notch3 activation promotes invasive glioma formation in a tissue site-specific manner," *Cancer Res.* **71**(3), 1115-1125.

Pirot, P., van Grunsven, L.A., Marine, J.C., Huylebroeck, D., and Bellefroid, E.J. **(2004)**. "Direct regulation of the Nrarp gene promoter by the Notch signalling pathway," *Biochem. Biophys. Res. Commun.* ***3*22**(2), 526-534.

Plentz, R., Park, J.S., Rhim, A.D., Abravanel, D., Hezel, A.F., Sharma, S.V., Gurumurthy, S., Deshpande, V., Kenifiv, C., Settleman, J., Majumder, P.K., Stanger, B.Z., and Bardeesy, N. **(2009)**. "Inhibition of gamma secretase activity inhibits tumor progression in a mouse model of pancreatic ductal adenocarcinoma," *Gastroenterology* **136**(5), 1741-1719.

Purow, B.W., Haque, R.M., Noel, M.W., Su, Q., Burdick, M.J., Lee, J., Sundaresan, T., Pastorino, S., Park, J.L., Mikolaenko, I., Maric, D., Eberhart, C.G., and Fine, H.A. **(2005)**. "Expression of Notch-1 and its ligands, Delta-like-1 and Jagged-1, is critical for glioma cell survival and proliferation," *Cancer Res.* **65**(6), 2353-2363.

Qi, H., Rand, M.D., Wu, X., Sestan, N., Wang, W., Rakic, P., Xu, T., and Artavanis-Tsakonas, S. **(1999)**. "Processing of the notch ligand delta by the metalloprotease Kuzbanian," *Science* **283**(5398), 91-94.

Qi, R., An, H., Yu, U., Zhang, M., Liu, S., Xu, H., Guo, Z., Cheng, T., and Cao, X. **(2003)**. "Notch1 signalling inhibits growth of human hepatocellular carcinoma through induction of cell cycle arrest and apoptosis," *Cancer Res.* **63**(23), 8323-8329.

Qiu, L., Joazeiro, C., Fang, N., Wang, H.Y., Elly, C., Altman, Y., Fang, D., Hunter, T., and Liu, Y.C. **(2000)**. "Rocognisation and ubiquitination of Notch by Itch, a hect-type E3 ubiquitin ligase," *J. Biol. Chem.* **275**(46), 35734-35737.

Raafat, A., Zoltan-Jones, A., Strizzi, L., Bargo, S., Kimura, K., Salomon, D., and Callahan, R. **(2007)**. "Kit and PDGFR-alpha activities are necessary for Notch4/Int3-induced tumorigenesis," *Oncogene* **26**(5), 662-672.

Raafat, A., Lawson, S., Bargo, S., Klauzinska, M., Strizzi, L., Goldhar, A.S., Buono, K., Salomon, D., Vonderhaar, B.K., and Callahan, R. **(2009)**. "Rbpj conditional knockout reveals distinct functions of Notch4/Int3 in mammary gland development and tumorigenesis," *Oncogene* **28**, 219-230.

Radtke, F., Wilson, A., Stark, G., Bauer, M., van Meerwijk, J., MacDonald, H.R., and Aguet, M. **(1999)**. "Deficient T cell fate specification in mice with an induced inactivation of Notch1," *Immunity* **10**(5), 547-558.

Radtke, F., Wilson, A., Mancini, S.J.C., and MacDonald, H.R. **(2004)**. "Notch regulation of lymphocyte development and function," *Nat. Immunol.* **5**, 247-253.

Radtke, F., Schweisguth, F., and Pear, W. **(2005)**. "The Notch 'gospel', *EMBO Rep.* **6**(12), 1120-1125.

Rae, F.K., Stephenson, S.A., Nicol, D.L., and Clements, J.A. **(2000)**. "Novel association of a diverse range of genes with renal cell carcinoma as identified by differential display," *Int. J. Cancer* **88**(5), 726-732.

Raimondi, S., Lowenfels, A.B., Morselli-Labate, A.M., Maisonneuve, P., and Pezzilli, R. **(2010)**. "Pancreatic cancer in chronic pancreatitis: aetiology, incidence and early detection," *Best Pract. Res. Clin. Gastroenterol.* **24**(3), 349-358.

Rand, M.D., Grimm, L.M., Artavanis-Tsakonas, S., Patriub, V., Blacklow, S.C., Sklar, J., and Aster, J.C. **(2000)**. "Calcium depletion dissociates and activates heterodimeric notch receptors," *Mol. Cell. Biol.* **20**(5), 1825-1835.

Rand, T.A., Petersen, S., Du, F., and Wang, X. **(2005)**. "Argonaute2 cleaves the anti-guide strand of siRNA during RISC activation," *Cell* **123**(4), 621-629.

Rangarajan, A., Talora, C., and Okuyama, R. **(2001)**. "Notch signaling is a direct determinant of keratinocyte growth arrest and entry into differentiation," *EMBO J.* **20**, 3427-3436.

Raya, A., Koth, C.M., Buscher, D., Kawakami, Y., Itoh, T., Raya, R.M., Sternik, G., Tsai, H.J., Rodriguez-Esteban, C., and Izpisua-Belmonte, J.C. **(2003)**. "Activation of Notch signaling pathway precedes heart regeneration in zebrafish," *Proc. Natl. Acad. Sci. U.S.A.* **100**, 11889-11895.

Reedijk, M., Odocic, S., Chang, L., Zhang, H., Miller, N., McCready, D.R., Lockwood, G., and Egan, S.E. **(2005)**. "High level coexpression of JAG1 and NOTCH1 is observed in human breast cancer and is associated with poor overall survival," *Cancer Res.* **65**(18), 8530-8537.

Reedijk, M., Odorcic, S., Zhang, H., Chetty, R., Tennert, C., Dickson, B.C., Lockwood, G., Gallinger, S., and Egan, S.E. **(2008)**. "Activation of Notch signaling in human colon adenocarcinoma," *Int. J. Oncol.* **33**(6), 1223-1229.

Reedijk, M., Pinnaduwage, D., Dickson, B.C., Mulligan, A.M., Zhang, H., Bull, S.B., O'Malley, F.P., Egan, S.E., and Andrulis, I.L. **(2008a)**. "JAG1 expression is associated with a basal phenotype and recurrence in lymph node-negative breast cancer," *Breast Cancer Res. Treat.* **111**(3), 439-448.

Rizzo, P., Miao, H., D'Souza, G., Osipio, C., Song, L.L., Yun, J., Zhao, H., Mascarenhas, J., Wyatt, D., Anitco, G., Hao, L., Yao, K., Rajan, P., Hicks, C., Siziopikou, K., Selvaggi, S., Bashir, A., Bhandari, D., Marchese, A., Lendahl, U., Qin, J.Z., Tonetti, D.A., Albain, K., Nickoloff, B.J., and Miele, L. **(2008)**. "Cross-talk between notch and the estrogen receptor in breast cancer suggests novel therapeutic approaches," *Cancer Res.* **68**(13), 5226-5235.

Rodilla, V., Villanueva, A., Obrador-Hevia, A., Robert-Moreno, A., Fernandez-Majada, V., and Grilli, A. **(2009)**. "Jagged1 is the pathological link between Wnt and Notch pathways in colorectal cancer," *Proc. Natl. Acad. Sci. USA.* **106**, 6315.

Rohn, J.L., Lauring, A.S., Linenberger, M.L., and Overbaugh, J. **(1996)**. "Transduction of Notch2 in feline leukemia virus-induced lymphoma," *J. Virol*. **70**(11), 8071-8080.

Ronchini, C. and Capobianco, A. **(2001)**. "Induction of cyclin D1 and CDK2 activity by Notch(ic): implications for cell cycle disruption in transformation by Notch(ic)," *Mol. Cell. Biol.* **21**, 5925-5934.

Rooman, I., de Medts, N., Baeyens, L., Lardon, J., de Breuck, S., Heimberg, H., and Bouwens, L. **(2006)**. "Expression of the Notch signaling pathway and effect on exocrine cell proliferation in adult rat pancreas," *Am. J. Pathol.* **169**, 1206-1214.

Rosati, E., Sabatini, R., Rampino, G., Tabilio, A., Di Ianni, M., Fettucciari, K., Bartoli, A., Coaccioli, S., Screpanti, I., and Marconi, P. **(2009)**. "Constitutively activated Notch signalling is involved in survival and apoptosis resistance of B-CLL cells," *Blood* **113**(4), 856-865.

Ryther, R.C., Flynt, A.S., Phillips 3rd, J.A., and Patton, J.G. **(2005)**. "siRNA therapeutics: big potential from small RNAs," *Gene Ther*. **12**(1), 5–11.

Sabattini, E., Bisgaard, K., Ascani, S., Poggi, S., Piccioli, M., Ceccarelli, C., Pieri, F., Fraternali-Orcioni, G., and Pileri, S.A. **(1998)**. "The EnVision+ system: a new immunohistochemical method for diagnostics and research. Clinical comparison with the APAAP, ChemMate, CSA, LABC, and SABC techniques," *J. Clin. Pathol.* **51**, 506-511.

Sade, H., Krishna, S., and Sarin, A. **(2004)**. "The anti-apoptotic effect of Notch-1 requires p56Ick-dependent Akt/PKB-mediated signalling in T cells," *J. Biol. Chem.* **279**(4), 2937-2944.

Sakata, Y., Kamei, C.N., Nakagami, H., Bronson, R., Liao, J.K., and Chin, M.T. **(2002)**. "Ventricular septal defect and cardiomyopathy in mice lacking the transcription factor CHF1/Hey2," *Proc. Natl. Acad. Sci. U.S.A.* **99**(25), 16197-16202.

Sambandam, A., Maillard, I., Zediak, V.P., Xu, L., Gerstein, R.M., Aster, J.C., Pear, W.S., and Bhandoola, A. **(2005)**. "Notch signalling controls the generation and differentiation of early T lineage progenitors," *Nat. Immunol.* **6**(7), 663-670.

Santagata, S., Demichelis, F., Riva, A., Varambally, S., Hofer, M.D., Kutok, J.L., Kim, R., Tang, J., Montie, J.E., Chinnaiyan, A.M., Rubin, M.A. and Aster, J.C. **(2004)**. "JAGGED1 expression is associated with prostate cancer metastasis and recurrence," *Cancer Res.* **64**(19), 6854-6857.

Santibanez, M., Viogue, J., Alquacil, J., de la Hera, M.G., Moreno-Osset, E., Carrato, A., Porta, M., and Kauppinen, T. **(2010)**. "Occupational exposures and risk of pancreatic cancer," *Eur. J. Epidemiol.* **25**(10), 721-730.

Santolini, W., Puri, C., Salcini, A.E., Gagliani, M.C., Pelicci, P.G., Tacchetti, C., and Di Fiore, P.P. **(2000)**. "Numb is an endocytic protein," *J. Cell. Biol.* **151**(6), 1345-1352.

Sarmento, L.M., Huang, H., Limon, A., Gordon, W., Fernandes, J., Tavares, M.J., Miele, L., Cardoso, A.A., Classon, M., and Carlesso, N. **(2005)**. "Notch1 modulates timing of G1-S progression by inducing SKP2 transcription and p27 Kip1 degradation," *J. Exp. Med.* **202**(1), 157-168.

Sasamura, T., Sasaki, N., Miyashita, F., Nakao, S., Ishikawa, H.O., Ito, M., Kitagawa, M., Harigaya, K., Spana, E., Bilder, D., Perrimon, N., and Matsuno, K. **(2003)**. "Neurotic, a novel maternal neurogenic gene, encodes an O-fucosyltransferase that is essential for Notch-Delta interactions," *Development* **130**(20), 4785-4795.

Schroeter, E.H., Kisslinger, J.A., and Kopan, R. **(1998)**. Notch-1 signalling requires ligand-induced proteolytic release of intracellular domain," *Nature* **393**(6683), 382-386.

Schutte, M., Hruban, R.H., Geradts, J., Maynard, R., Hilgers, W., Rabindran, S.K., Moskaluk, C.A., Hahn, S.A., Schwarte-Waldhoff, I., Schmiegel, W., Baylin, S.B., Kern, S.E., and Herman, J.G. **(1997)**. "Abrogation of the Rb/p16 tumor-suppressive pathway in virtually all pancreatic carcinomas," *Cancer Res.* **57**(15), 3126-3130.

Sclabas, G.M., Uwagawa, T., Schmidt, C., Hess, K.R., Evans, D.B., Abbruzzese, J.L., and Chiao, P.J. **(2005)**. "Nuclear factor kappa B activation is a potential target for preventing pancreatic carcinoma by aspirin," *Cancer* **103**, 2485-2490.

Serafin, V., Persano, L., Moserle, L., Esposito, G., Ghisi, M., and Curtarello, M. **(2011)**. "Notch3 signaling promotes tumor growth in colorectal cancer," *J. Pathol.* **224**(4), 448-460.

Seugnet, L., Simpson, P., and Haenlin, M. **(1997)**. "Requirement for dynamin during Notch signaling in Drosophila neurogenesis," *Dev. Biol.* **192**(2), 585-598.

Shapiro, A.L. and Maizel, J.V. **(1969)**. "Molecular weight estimation of polypeptides by SDS-polyacrylamide gel electrophoresis: further data concerning resolving power and general considerations," *Anal. Biochem.* **29**, 505-514.

Sharma, V.M., Calvo, J.A., Draheim, K.M., Cunningham, L.A., Hermance, N., Beverly, L., Krishnamoorthy, V., Bhasin, M., Capobianco, A.J., and Kelliher, M.A. **(2006)**. "Notch1 contributes to mouse T-cell leukemia by directly inducing the expression of c-myc," *Mol.Cell Biol.***26**(21), 8022-8031.

Shearman, M.S., Beher, D., Clarke, E.E., Lewis, H.D., Harrison, T., Hunt, P., Nadin, A., Smith, A.L., Stevenson, G., and Castro, J.L. **(2000)**. "L-685,458, an asparyl protease transition state mimic, is a potent inhibitor of amyloid beta-protein precursor gamma secretase activity," *Biochemistry* **39**(30), 8698-8704.

Shelly, L.L., Fuchs, C., and Miele, L. **(1999)**. "Notch-1 inhibits apoptosis in murine erythroleukemia cells and is necessary for differentiation induced by hybrid polar compounds," *J. Cell. Biochem.* **73**(2), 164-175.

Shi, S.R., Key, M.E., and Kalra, K.L. **(1991)**. "Antigen retrieval in formalin-fixed, paraffin-embedded tissues: an enhancement method for immunohistochemical staining based on microwave oven heating of tissue sections," *J. Histochem. Cytochem.* **39**(6), 741-748.

Shi, T.P., Xu, H., Wei, J.F., Ai, X., Ma, X., Wang, B.J., Ju, Z.H., Zhang, G.X., Wang, C., Wu, Z.Q., and Zhang, X. **(2008)**. "Association of low expression of notch-1 and jagged-1 in human papillary bladder cancer and shorter survival," *J. Urol.* **180**(1), 361-366.

Shin, H.M., Minter, L.M., Cho, O.H., Gottipati, S., Faug, A.H., Golde, T.E., Sonenshein, G.E., and Osborne, B.A. **(2006)**. "Notch1 augments NF- κβ activity by facilitating its nuclear retention," *EMBO J.* **25**, 129-138.

Shou, J., Ross, S., Koeppen, H., de Sauvage, F.J., and Gao, W.Q. **(2001)**. "Dynamics of notch expression during murine prostate development and tumorigenesis," *Cancer Res.* **61**(19), 7291-7297.

Siemers, E.R., Quinn, J.F., Kaye, J., Farlow, M.R., Porsteinsson, A., Tariot, P., Zoulnouni, P., Galvin, J.E., Holtzman, D.M., Knopman, D.S., Satterwhite, J., Gonzales, C., Dean, R.A., and May, P.C. **(2006)**. "Effects of a gamma-secretase inhibitor in a randomized study of patients with Alzheimer disease," *Neurology* **66**(4), 602-604.

Siemers, E.R., Dean, R.A., Friedrich, S., Ferguson-Sells, L., Gonzales, C., Farlow, M.R., and May, P.C. **(2007)**. "Safety, tolerability, and effects on plasma and cerebrospinal fluid

amyloid-beta after inhibition of gamma-secretase," *Clin. Neuropharmacol.* **30**(6), 317-325.

Sledz, C.A., Holko, M., de Veer, M.J., Silverman, R.H., and Williams, B.R. **(2003)**. "Activation of the interferon system by short-interfering RNAs," *Nat. Cell Biol.* **5**(9), 834–839.

Small, D., Kovalenko, D., Kacer, D., Liaw, L., Landriscina, M., Di Serio, C., Prudovsky, I., and Maciag, T. **(2001)**. "Soluble Jagged1 represses the function of its transmembrane form to induce formation of the Src-dependent chord-like phenotype," *J. Biol. Chem.* **276**(34), 32022-32030.

Smith, G.H., Gallahan, D., Diella, F., Jhappan, C., Merlino, G., and Callahan, R. **(1995)**. "Constitutive expression of a truncated INT3 gene in mouse mammary epithelium impairs differentiation and functional development," *Cell Growth Differ.* **6**(5), 563-577.

Sohn, T.A., Yeo, C.J., Cameron, J.L., Koniaris, L., Kaushal, S., Abrams, R.A., Sauter, P.K., Coleman, J., Hruban, R.H., and Lillemoe, K.D. **(2000)**. "Resected adenocarcinoma of the pancreas – 616 patients: results, outcomes and prognostic indicators," *J. Gastrointest. Surg.* **4**(6), 567-579.

Song, E., Lee, S.K., Wang, J., Ince, N., Ouyang, N., Min, J., Chen, J., Shankar, P., and Lieberman, J. **(2003)**. "RNA interference targeting Fas protects mice from fulminant hepatitis," *Nat. Med.* **9**(3), 347–351.

Song, L.L., Peng, Y., Yun, J., Rizzo, P., Chaturvedi, V., Weijzen, S., Kast, W.M., Stone, P.J., Santos, L., Loredo, A., Lendahl, U., Sonenshein, G., Osborne, B., Qin, J.Z., Pannuti, A., Nickoloff, B.J., and Miele, L. **(2008)**. "Notch-1 associates with IKK alpha and regulates IKK activity in cervical cancer cells," *Oncogene* **27**(44), 5833-5844.

Soriano, J.V., Uyttendaele, H., Kitajewski, J., and Montesano, R. **(2000)**. "Expression of an activated Notch4(int-3) oncoprotein disrupts morphogenesis and induces an invasive phenotype in mammary epithelial cells in vitro," *Int. J. Cancer* **86**(5), 652-659.

Spana, E. and Doe, C. **(1996)**. "Numb antagonizes notch signalling to specify sibling neuron cell fates," *Neuron.* **17**(1), 21-26.

Sparey, T., Beher, D., Best, J., Biba, M., Castro, J.L., Clarke, E., Hannam, J., Harrison, T., Lewis, H., Madin, A., Shearman, M., Sohal, B., Tsou, N., Welch, C., and Wrigley, J.

(2005). "Cyclic sulfamide γ-secretase inhibitors," *Bioorg. Med. Chem. Lett.* **15**, 4212-4216.

Sriuranpong, V., Borges, M.W., Ravi, R.K., Arnold, D.R., Nelkin, B.D., Bavlin, S.B., and Ball, D.W. **(2001)**. "Notch signalling induces cell cycle arrest in small cell lung cancer cells," *Cancer Res.* **61**(7), 3200-3205.

Struhl, G. and Adachi, A. **(1998)**. "Nuclear access and action of notch in vivo," *Cell* **93**(4), 649-660.

Struhl, G. and Greenwald, I. **(1999)**. "Presenilin is required for activity and nuclear access of Notch in Drosophila," *Nature* **398**(6727), 522-525.

Stylianou, S., Clarke, R.B., and Brennan, K. **(2006)**. "Aberrant activation of notch signalling in human breast cancer," *Cancer Res.* **66**(3), 1517-1525.

Sumazaki, R., Shiojiri, N., Isoyama, S., Masu, M., Keino-Masu, K., Osawa, M., Nakauchi, H., Kageyama, R., and Matsui, A. **(2004)**. "Conversion of biliary system to pancreatic tissue in Hes1-deficient mice," *Nat. Genet.* **36**(1), 83-87.

Sun, Y., Lowther, W., Kato, K., Bianco, C., Kenney, N., Strizzi, L., Raafat, D., Hirota, M., Khan, N.I., Bargo, S., Jones, B., Salomon, D., and Callahan, R. **(2005)**. "Notch4 intracellular domain binding to Smad3 and inhibition of the TGF-β signalling," *Oncogene* **24**, 5365-5374.

Suwanjunee, S., Wongchana, W., and Palaga, T. **(2008)**. "Inhibition of gamma-secretase affects proliferation of leukemia and hepatoma cell lines through Notch signalling," *Anticancer Drugs* **19**(5), 477-486.

Suzuki, T., Aoki, D., Susumu, N., Udagawa, Y., and Nozawa, S. **(2000)**. "Imbalanced expression of TAN-1 and human Notch4 in endometrial cancers," *Int. J. Oncol.* **17**(6), 1131-1139.

Sweeney, C., Morrow, D., Birney, Y.A., Coyle, S., Hennessy, C., Scheller, C. **(2004)**. "Notch 1 and 3 receptor signalling modulates vascular smooth muscle cell growth, apoptosis, and migration via a CBF-1/RBP-Jk dependent pathway," *FASEBJ* **18**, 1421.

Sykes, D.B. and Kamps, M.P. **(2004)**. "E2a/Pbx1 induces the rapid proliferation of stem cell factor-dependent murine pro-T cells that cause acute T-lymphoid or myeloid leukemias in mice," *Mol. Cell. Biol.* **24**(3), 1256-1269.

Takasaki, H., Uchida, E., Tempero, M.A., Burnett, D.A., Metzgar, R.S., and Pour, P.M. **(1988)**. "Correllative study on expression of CA 19-9 and DU-PAN-2 in tumor tissue and serum of pancreatic cancer patients," *Cancer Res.* **48**, 1435-1438.

Talora, C., Sqroi, D.C., Crum, C.P., and Dotto, G.P. **(2002)**. "Specific down-modulation of Notch1 signalling in cervical cancer cells is required for sustained HPV-E6/E7 expression and late steps of malignant transformation," *Genes Dev.* **16**(17), 2252-2263.

Tammam, J., Ware, C., Efferson, C., O'Neil, J., Rao, S., Qu, X., Gorenstein, J., Angagaw, M., Kim, H., Kenific, C., Kunii, K., Leach, K.J., Nikov, G., Zhao, J., Dai, X., Hardwick, J., Scott, M., Winter, C., Bristow, L., Elbi, C., Reilly, J.F., Look, T., Draetta, G., van der Ploeg, L., Kohl, N.E., Strack, P.R. and Majumder, P.K. **(2009)**. "Down-regulation of the Notch pathway mediated by a gamma-secretase inhibitor induces anti-tumour effects in mouse models of T-cell leukaemia," *Br. J. Pharmacol.* **158**(5), 1183-1195.

Tan, M.H., Nowak, N.J., Loor, R., Ochi, H., Sandberg, A.A., Lopez, C., Pickren, J.W., Berjian, R., Douglass, H.O. Jr, and Chu, T.M. **(1986)**. "Characterization of a new primary human pancreatic tumor line," *Cancer Invest.* **4**(1), 15-23.

Tersmette, A.C., Petersen, G.M., Offerhaus, G.J., Falatko, F.C., Brune, K.A., Goggins, M., Rozenblum, E., Wilentz, R.E., Yeo, C.J., Cameron, J.L., Kern, S.E., and Hruban, R.H. **(2001)**. "Increased risk of incident pancreatic cancer among first-degree relatives of patients with familial pancreatic cancer," *Clin. Cancer Res.* **7**(3), 738-744.

Thelu, J., Rossio, P., and Favier, B. **(2002)**. "Notch signalling is linked to epidermal cell differentiation level in basal cell carcinoma, psoriasis and wound healing," *BMC Dermatol.* **2**, 7-12.

Thiebaut, A.C., Jiao, L., Silverman, D.T., Cross, A.J., Thompson, F.E., Subar, A.F., Hollenbeck, A.R., Schatzkin, A., and Stolzenberg-Solomon, R.Z. **(2009)**. "Dietary fatty acids and pancreatic cancer in the NIH-AARP diet and health study," *J. Natl. Cancer Inst.* **101**(14), 1001-1011.

Tian, G., Sobotka-Briner, C.D., Zysk, J., Liu, X., Birr, C., Sylvester, M.A., Edwards, P.D., Scott, C.D., and Greenberg, B.D. **(2002)**. "Linear Non-competitive inhibition of solubilized human gamma-secretase by pepstatin A methylester, L685458, sulfonamides, and benzodiazepines," *J. Biol. Chem.* **277**(35), 31499-31505.

Todha, S. and Nara, M. **(2001)**. "Expression of Notch1 and Jagged1 proteins in acute myeloid leukemia cells," *Blood* **103**(9), 3511-3515.

Tohda, S., Kogoshi, H., Murakami, N., Sakano, S., and Nara, N. **(2005)**. "Diverse effects of the Notch ligands Jagged1 and Delta1 on the growth and differentiation of primary acute myeloblastic leukemia cells," *Exp. Hematol.* **33**(50), 558-563.

Ueno, H., Kiyosawa, K., and Kaniwa, N. **(2007)**. "Pharmacogenomics of gemcitabine: can genetic studies lead to tailor-made therapy," *Br. J. Cancer* **97**, 145-151.

Vacca, A., Felli, M.P., Palermo, R., Di Mario, G., Calce, A., Di Giovine, M., Frati, L., Gulino, A., and Screpanti, I. **(2006)**. "Notch3 and pre-TCR interaction unveils distinct NF-κβ pathways in T-cell development and leukemia," *EMBO J*, **25**, 1000-1008.

Van Es, J.H., van Giyn, M.E., Ricco, O., vand den Born, M., Vooijs, M., Begthel, H., Cozijnsen, M., Robine, S., Winton, D.J., Radtke, G., and Clevers, H. **(2005)**. "Notch/gamma-secretase inhibition turns proliferative cells in intestinal crypts and adenomas into goblet cells," *Nature* **435**(7044), 959-963.

Van Heek, N.T., Meeker, A.K., Kern, S.E., Yeo, C.J., Lillemoe, K.D., Cameron, J.L., Offerhaus, G.J., Hicks, J.L., Wilentz, R.E., Goggins, M.G., De Marzo, A.M., Hruban, R.H., and Maitra, A. **(2002)**. "Telomere shortening is nearly universal in pancreatic intraepithelial neoplasia," *Am. J. Pathol.* **161**(5), 1541-1547.

Vandel, L. and Kouzarides, T. **(1999)**. "Residues phosphorylation by TFIIH are required for E2F-1 degradation during S-phase," *EMBO J.* **18**(15), 4280-4291.

Vardar, D., North, C.L., Sanchez-Irizarry, C., Aster, J.C., and Blacklow, S.C. **(2003)**. "Nuclear magnetic resonance structure of a prototype Lin12-Notch repeat module from human Notch1," *Biochemistry* **42**(23), 7061-7067.

Verdi, J.M., Schmandt, R., Bashirullah, A., Jacob, S., Salvino, R., Craig, C.G., Program, A.E., Lipshitz, H.D., and McGlade, C.J. **(1996)**. "Mammalian NUMB is an evolutionarily conserved signalling adapter protein that specifies cell fate," *Curr. Biol.* **6**(9), 1134-1145.

Vermes, I., Haanen, C., and Reutelingsperger, C. **(1995)**. "A novel assay for apoptosis based upon flow cytometric detection of phosphatidylserine on the cell-surface with use of fitc-labeled annexin-V," *Clin. Chem.* **41**, S91-S91.

Vis, A.N., Kranse, R., Nigg, A.L., and van der Dwast, T.H. **(2000)**. "Quantitative analysis of the decay of immunoreactivity in stored prostate needle biopsy sections," *Am. J. Clin. Pathol.* **113**, 369-373.

Wagner, M., Redaelli, C., Lietz, M., Seiler, C.A., Friess, H., and Buchler, M.W. **(2004)**. "Curative resection is the single most important factor determining outcome in patients with pancreatic adenocarcinoma," *Brit. J. Surg.* **91**(5), 586-594.

Wakamatsu, Y., Maynard, T.M., Jones, S.U., and Weston, J.A. **(1999)**. "NUMB localizes in the basal cortex of mitotic avian neuroepithelial cells and modulates neuronal differentiation by binding to NOTCH-1," *Neuron.* **23**(1), 71-81.

Wallberg, A.E., Pedersen, K., Lendahl, U., and Roeder, R.G. **(2002)**. "p300 and PCAF act cooperatively to mediate transcriptional activation from chromatin templates by notch intracellular domains in vitro," *Mol. Cell Biol.* **22**(22), 7812-7819.

Wang, S. and Barres, B. **(2000)**. "Up a notch: instructing gliogenesis," *Neuron.* **27**, 197-200.

Wang, J., Shelly, J., Miele, L., Boykins, R., Norcross, M.A., Guan, E. **(2001)**. "Human Notch-1 inhibits NF-kappaB activity in the nucleus through a direct interaction involving a novel domain," *J. Immunol.* **167**(1), 289-295.

Wang, Y., Shao, L., Shi, S., Harris, R.J., Spellman, M.W., Stanley, P., and Haltiwanger, R.S. **(2001a)**. "Modification of epidermal growth factor-like repeats with O-fucose. Molecular cloning and expression of a novel GDP-fucose protein O-fucosyltransferase," *J. Biol. Chem.* **276**(43), 40338-40345.

Wang, W., Prince, C.Z., Hu, X., Pollman, M.J. **(2003)**. "HRT1 modulates vascular smooth muscle cell proliferation and apoptosis," *Biochem. Biophys. Res. Commun.* **308**, 596.

Wang, Z., Zhang, Y., Banerfee, S., Li, Y., and Sarkar, F.H. **(2006)**. "Inhibition of nuclear factor κB activity by genistein is mediated via Notch-1 signaling pathway in pancreatic cancer cells," *Int. J. Cancer* **118**, 1930-1936.

Wang, Z., Zhang, Y., Li, Y., Banerjee, S., Liao, J., and Sarkar, F.H. **(2006a)**. "Down-regulation of Notch-1 contributes to cell growth inhibition and apoptosis in pancreatic cancer cells," *Mol. Cancer Ther.* **5**(3), 483-493.

Wang, Z., Banerfee, S., Li, Y., Rahman, K.M.W., Zhang, Y., and Sarkar, F.H. **(2006b)**. "Down-regulation of Notch-1 inhibits invasion by inactivation of nuclear factor-κB, vascular endothelial growth factor, and matrix metalloproteinase-9 in pancreatic cancer cells," *Cancer Res.* **66**(5), 2778-2784.

Wang, Z., Zhang, Y., Banerjee, S., Li, Y., and Sarkar, F.H. **(2006c)**. "Notch-1 down-regulation by curcumin is associated with the inhibition of cell growth and the induction of apoptosis in pancreatic cancer cells," *Cancer* **106**, 2503-2513.

Wang, Z., Sengupta, R., Banerjee, S., Li, Y., Zhang, Y., Rahman, K.M., Aboukameel, A., Mohammad, R., Majumdar, A.P., Abbruzzse, J.L., and Sarkar, F.H. **(2006d)**. "Epidermal growth factor receptor-related protein inhibits cell growth and invasion in pancreatic cancer," *Cancer Res.* **66**(15), 7653-7660.

Wang, Z., Kong, D., Banerjee, S., Li, Y., Adsay, N.V., Abbruzzese, J., and Sarkar, F.H. **(2007)**. "Down-regulation of platelet-derived growth factor-D inhibits cell growth and angiogenesis through inactivation of Notch-1 and nuclear factor-kappaB signalling," *Cancer Res.* **67**(23), 11377-11385.

Wang, Z., Banerjee, S., Kong, D., Li, Y., and Sarkar, F.H. **(2007a)**. "Down-regulation of Forkhead Box M1 Transcription factor leads to the inhibition of invasion and angiogenesis of pancreatic cancer cells," *Cancer Res.* **67**, 8293-8300.

Wang, L., Qin, H., Chen, B., Xin, X., Li, J., and Han, H. **(2007b)**. "Overexpression of active Notch1 induces cell growth arrest of HeLa cervical carcinoma cells," *Int. J. Gynecol. Cancer* **17**, 1283-1292.

Wang, T., Holt, C.M., Xu, .C, Ridley, C., and Baron, M. **(2007c)**. "Notch3 activation modulates cell growth behaviour and cross-talk to Wnt/TCF signalling pathway," *Cell. Signal.* **19**, 2458-2467.

Wang, Z., Desmoulin, S., Banerjee, S., Kong, D., Li, Y., Deraniyagala, R.L., Abbruzzese, J., and Sarkar, F.H. **(2008)**. "Synergistic effects of multiple natural products in pancreatic cancer cells," *Life Sci.* **83**(7-8), 293-300.

Wang, Z., Azmi, A.S., Ahmad, A., Banerjee, S., Wang, S., Sarkar, F.H., and Mohammad, R.M. **(2009)**. "TW-37, a small-molecule inhibitor of Bcl-2, inhibits cell growth and induces apoptosis in pancreatic cancer: involvement of Notch-1 signaling pathway," *Cancer Res.* **69**(7), 2757-2765.

Wang, M., Xue, L., Cao, Q., Lin, Y., Ding, Y., Yang, P., and Che, L. **(2009a)**. "Expression of Notch1, Jagged1 and beta-catenin and their clinicopathological significance in hepatocellular carcinoma," *Neoplasma* **56**(6), 533-541.

Wang, Z., Li, Y., Banerjee, S., Kong, D., Ahmad, A., Nogueira, V., Hay, N., and Sarkar, F.H. **(2010)**. "Down-regulation of Notch-1 and Jagged-1 inhibits prostate cancer cell growth

migration and invasion, and induces apoptosis via inactivation of Akt, mTOR and NFkappaB signalling pathways," *J. Cell. Biochem.* **109**(4), 726-736.

Wang, Z., Li, Y., Ahmad, A., Banerfee, S., Azmi, A.S., Kong, D., Wojewoda, C., Miele, L., and Sarkar, F.H. **(2010a)**. "Down-regulation of Notch-1 is associated with Akt and FoxM1 in inducing cell growth inhibition and apoptosis in prostate cancer cells," *J. Cell. Biochem.* **112**(1), 78-88.

Wang, M., Wang, J., Wang, L., Wu, L., and Xin, X. **(2010b)**. " Notch1 expression correlates with tumor differentiation status in ovarian carcinoma," *Med. Oncol.* **27**(4), 1329-1335.

Wang, X., Fu, Y., Chen, X., Ye, J., Lu, B., Ye, F., Lu, W., and Xie, X. **(2010c)**. "The expression of bHLH gene HES1 and HES5 in advanced ovarian serous adenocarcinomas and their prognostic significance: a retrospective clinical study," *J. Cancer Res. Clin. Oncol.* **136**(7), 989-996.

Wang, Z., Li, Y., Kong, D., Ahmad, A., Banergee, S., and Sarkar, F.H. **(2010d)**. "Crosstalk between miRNA and Notch signalling pathways in tumor development and progression," *Cancer Lett.* **292**(2), 141-148.

Watters, J.W., Cheng, C., Majumder, P.K., Wang, R., Yalavarthi, S., Meeske, C., Kong, L., Sun, W., Lin, J., Heyer, J., Ware, C., Winter, C., Reilly, J.F., Demuth, T., Clark, S., Chiu, M.I., Robinson, M.O., Kohl, N., and Kannan, K. **(2009)**. "De novo discovery of a gamma secretase inhibitor response signature using a novel in vivo breast tumor model," *Cancer Res.* **69**(23), 8949-8957.

Wei, J.S., Greer, B.T., Westermann, F., Steinberg, S.M., Son, C.G., Chen, Q.R., Whiteford, C.C., Bilke, S., Krasnselsky, A.L., Cenacchi, N., Catchpoole, D., Berthold, F., Schwab, M., and Khan, J. **(2004)**. "Prediction of clinical outcome using gene expression profiling and artificial neural networks for patients with neuroblastoma," *Cancer Res.* **64**(19), 6883-6891.

Weidemann, A., Eggert, S., Reinhard, F.B., Vogel, M., Paliga, K., Baier, G., Masters, C.L., Beyreuther, K., and Evin, G. **(2002)**. "A novel epsilon-cleavage within the transmembrane domain of the Alzheimer amyloid precursor protein demonstrates homology with Notch processing," *Biochemistry* **41**(8), 2825-2835.

Weijzen, S., Rizzo, P., Braid, M., Vaishnav, R., Jonkheer, S.M., Zlobin, A., Osborne, B.A., Gottipati, S., Aster, J.C., Hahn, W.C., Rudolf, M., Siziopikou, K., Kast, W.M., and Miele,

L. **(2002)**. "Activation of Notch-1 signalling maintains the neoplastic phenotype in human Ras-transformed cells," *Nat. Med.* **8**(9), 979-986.

Weng, A.P., Ferrando, A.A., Lee, W., Morris, J.P. 4th, Silverman, L.B., Sanchez-Irizarry, C., Blacklow, S.C., Look, A.T., and Aster, J.C. **(2004)**. "Activating mutations of Notch1 in human T cell acute lymphoblastic leukemia," *Science* **306**, 269-271.

Westerhout, E.M., Ooms, M., Vink, M., Das, A.T., and Berkhout, B. **(2005)**. "HIV-1 can escape from RNA interference by evolving an alternative structure in its RNA genome," *Nucleic Acids Res.* **33**(2), 796– 804.

Wharton, K.A., Johansen, K.M., Xu, T., and Artavanis-Tsakonas, S. **(1985)**. "Nucleotide sequence from the neurogenic locus notch implies a gene product that shares homology with proteins containing EGF-like repeats," *Cell* **43**, 567-581.

Whitcomb, D.C., Gorry, M.C., Preston, R.A., Furey, W., Sossenheimer, M.J., Ulrich, C.D., Martin, S.P., Gates, L.K. Jr., Amann, S.T., Toskes, P.P., Liddle, R., McGrath, K., Uomo, G., Post, J.C., and Ehrlich, G.D. **(1996)**. "Hereditary pancreatitis is caused by a mutation in the cationic trypsinogen gene," *Nat. Genet.* **14**(2), 141-145.

Wilentz, R.E., Iacobuzio-Donahue, C.A., Argani, P., McCarthy, D.M., Parsons, J.L., and Yeo, C.J. **(2000)**. "Loss of expression of Dpc4 in pancreatic intraepithelial neoplasia: evidence that DPC4 inactivation occurs late in neoplastic progression," *Cancer Res.* **60**, 2002-2006.

Wu, L., Aster, J.C., Blacklow, S.C., Lake, R., Artavanis-Tsakonas, S., and Griffin, J.D. **(2000)**. "MAML1, a human homologue of Drosophila mastermind, is a transcriptional co-activator for NOTCH receptors," *Nat. Genet.* **26**(4), 484-489.

Wu, G., Lyapina, S., Das, I., Li, J., Gurney, M., Pauley, A., Chui, I., Deshaies, R.J., and Kitajewski, J. **(2001)**. "SEL-10 is an inhibitor of notch signaling that targets notch for ubiquitin-mediated protein degradation," *Mol. Cell Biol.* **21**(21), 7403-7415.

Wu, L., Sun, T., Kobayashi, K., Gao, P., and Griffin, J.D. **(2002)**. "Identification of a family of mastermind-like transcriptional coactivators for mammalian notch receptors," *Mol. Cell Biol.* **22**(21), 7688-7700.

Wu, L. and Griffin, J. **(2004)**. "Modulation of Notch signalling by mastermind-like (MAML) transcriptional co-activators and their involvement in tumorigenesis," *Semin. Cancer Biol.* **14**, 348-356.

Wu, K., Xu, L., Zhang, L., Lin, Z., and Hou, J. **(2011)**. "High Jagged1 expression predicts poor outcome in clear cell renal cell carcinoma," *Jpn. J. Clin. Oncol.* **41**(3), 411-416.

Xiao, Y., Ye, Y., Zou, X., Jones, S., Yearsley, K., Shetuni, B., Tellez, J., and Barsky, S.H. **(2011)**. "The lymphovascular embolus of inflammatory breast cancer exhibits a Notch3 addiction," *Oncogene* **30**(3), 287-300.

Xie, R., Chung, J.Y., Ylaya, K., Williams, R.L., Guerrero, N., Nakatsuka, N., Badie, C., and Hewitt, S.M. **(2011)**. "Factors influencing the degradation of archival formalin-fixed paraffin-embedded tissue sections," *J Histochem. Cytochem.* **59**, 356-365.

Xiong, H.Q., Abbruzzese, J.L., Lin, E., Wang, L., Zheng, L., and Xie, K. **(2004)**. "NF-κB activity blockade impairs the angiogenic potential of human pancreatic cancer cells," *Int. J. Cancer* **108**, 181-188.

Yamada, T., Yamazaki, H. Yamane, T., Yoshino, M., Okuyama, H., Tsuneto, M., Kurino, T., Hayashi, S., and Sakano, S. **(2003)**. "Regulation of osteoclast development by Notch signalling directed to osteoclast precursors and through stromal cells," *Blood* **101**(6), 2227-2234.

Yamaguchi, N., Oyama, T., Ito, E., Satoh, H., Azuma, S., Hayashi, M., Shimizu, K., Honma, R., Yanagisawa, Y., Nishikawa, A., Kawamra, M., Imai, J., Ohwada, S., Tatsuta, K., Inoue, J., Semba, K., and Watanabe, S. **(2008)**. "Notch3 signaling pathway plays crucial roles in the proliferation of ErbB2-negative human Breast cancer cells," *Cancer Res.* **68**(6), 1881-1888.

Yamamoto, N., Yamamoto, S., Inagaki, F., Kawaichi, M., Fukamizu, A., Kishi, N., Matsuno, K., Nakamura, K., Weinmaster, G., Okano, H., and Nakafuku, M. **(2001)**. "Role of Deltex-1 as a transcriptional regulator downstream of the Notch receptor," *J. Biol. Chem.* **276**(48), 45031-45040.

Yao, J., Duan, L., Fan, M., and Wu, X. **(2007)**. "Gamma-secretase inhibitors exerts antitumor activity via down-regulation of Notch and Nuclear factor kappa B in human tongue carcinoma cells," *Oral Dis.* **13**(6), 555-563.

Yao, J., Duan, L., Fan, M., and Wu, X. **(2007a)**. "Notch1 induces cell cycle arrest and apoptosis in human cervical cancer cells: involvement of nuclear factor kappa B inhibition," *Int. J. Gynecol. Cancer.* **17**(2), 502-510.

Yasutomo, K., Doyle, C., Miele, L., Fuchs, C., and Germain, R.N. **(2000)**. "The duration of antigen receptor signalling determines CD4+ versus CD8+ T-cell lineage fate," *Nature* **404**(6777), 506-510.

Ye, Y, Lukinova, N., and Fortini, M.E. **(1999)**. "Neurogenic phenotypes and altered Notch processing in Drosophila Presenilin mutants," *Nature* **398**(6727), 525-529.

Yeasmin, S., Nakayama, K., Rahman, M.T., Rahman, M., Ishikawa, M., Iida, K., Otsuki, Y., Kobayashi, H., Nakayama, S., and Miyazaki, K. **(2010)**. "Expression of nuclear Notch3 in cervical squamous cell carcinomas and its association with adverse clinical outcomes," *Gynecol. Oncol.* **117**(3), 409-416.

Yee, A.S., Paulson, E.K., McDevitt, M.A., Rieger-Christ, K., Summerhayes, I., Berasi, S.P., Kim, J., Huang, C.Y., and Zhang, X. **(2004)**. "The HBP1 transcriptional repressor and the p38 MAP kinase: unlikely partners in G1 regulation and tumor suppression," *Gene* **336**(1), 1-13.

Yeh, E., Dermer, M., Commiso, C., Zhou, L., McGlade, C.J., and Boulianne, G.L. **(2001)**. "Neuralized functions as an E3 ubiquitin ligase during Drosophila development," *Curr. Biol.* **11**(21), 1675-1679.

Yeh, T.S., Wu, C.W., Hsu, K.W., Liao, W.J., Yang, M.C., Li, A.F.Y., Kuo, M.L., and Chi, C.W. **(2009)**. "The activated Notch1 signal pathway is associated with gastric cancer progression through cyclooxygenase-2," *Cancer Res.* **69**(12), 5039-5048.

Yoon, K. and Gaiano, N. **(2005)**. "Notch signalling in the mammalian central nervous system: insights from mouse mutants," *Nat. Neurosci.* **8**, 709-715.

Yu, J., Ohuchida, K., Mizumoto, K., Fujita, H., Nakata, K., and Tanaka, M. **(2010)**. "MicroRNA miR-17-5p is overexpressed in pancreatic cancer, associated with a poor prognosis, and involved in cancer cell proliferation and invasion," *Cancer Biol. Ther.* **10**(8), 748-757.

Yun, T.J. and Bevan, M.J. **(2003)**. "Notch-regulated ankyrin-repeat protein inhibits Notch1 signaling: multiple Notch1 signaling pathways involved in T cell development," *J. Immunol.* **170**(12), 5834-5841.

Yunis, A.A., Arimura, G.K., and Russin, D.J. **(1977)**. "Human pancreatic carcinoma (MIA PaCa-2) in continuous culture: sensitivity to asparaginase," *Int. J. Cancer* **19**(1), 128-135.

Zagouras, P., Stifani, S., Blaumueller, C.M., Carcangiu, M.L., and Artavanis-Tsakonas, S. **(1995)**. "Alterations in Notch signalling in neoplastic lesions of the human cervix," *Proc. Natl. Acad. Sci. U.S.A.* **92**(14), 6414-6418.

Zamore, P.D., Tuschl, T., Sharp, P.A., and Bartel, D.P. **(2000)**. "RNAi: double-stranded RNA directs the ATP-dependent cleavage of mRNA at 21 to 23 nucleotide intervals," *Cell* **101**, 25-33.

Zang, S., Ji, C.H., Qu, X., Dong, X., Ma, D., Ye, J., Ma, R., Dai, J., and Guo, D. **(2007)**. "A study on Notch signalling in human breast cancer," *Neoplasma* **54**(4), 304-310.

Zang, S., Chen, F., Dai, J., Guo, D., Tse, W., Ma, D., and Ji, C. **(2010)**. "RNAi-mediated knockdown of Notch-1 leads to cell growth inhibition and enhanced chemosensitivity in human breast cancer," *Oncol. Rep.* **23**(4), 898-899.

Zayzafoon, M., Abdulkadir, S.A., McDonald, J.M . **(2004)**. "Notch signaling and ERK activation are important for the osteomimetic properties of prostate cancer bone metastatic cell lines," *J. Biol. Chem.* **279**(5), 3662-3670.

Zhang, H., Ye, Y., Bai, Z., and Wang, S. **(2008)**. "The COX-2 selective inhibitor-independent COX-2 effect on colon carcinoma cells is associated with the Delta1/Notch1 pathway," *Dig. Dis. Sci.* **53**(8), 2195-2203.

Zhang, P., Yang, Y., Zweidler-McKay, P.A., and Hughes, D.P.M. **(2008a)**. "Critical role of Notch signaling in Osteosarcoma Invasion and Metastasis," *Clin. Cancer Res.* **14**(10), 2962-2969.

Zhang, K.J., Lu, Q.Y., Niu, X.Q., Zhang, P., Zhao, J.N., Wang, Z., Hu, J.S., Li, P., and Liu, W.L. **(2009)**. "Notch1 signaling inhibits growth of EC109 esophageal carcinoma cells through downmodulation of HPV18/E7 gene expression," *Acta. Pharmacol. Sin.* **30**(2), 153-158.

Zhang, P., Yang, Y., Nolo, R., Zweidler-McKay, P.A., and Hughes, D.P.M. **(2010)**. "Regulation of NOTCH signalling by reciprocal inhibition of HES1 and Deltex1 and its role in Osteosarcoma invasiveness," *Oncogene* **29**(20), 2916-2926.

Zhao, N., Guo, Y., Zhang, M., Lin, L., and Zheng, Z. **(2010)**. "Akt-mTOR signalling is involved in Notch-1-mediated glioma cell survival and proliferation," *Oncol. Rep.* **23**(5), 1443-1447.

Zhong, W., Feder, J.N., Jiang, M.M., Jan, L.Y., and Jan, Y.N. **(1996)**. "Asymmetric localization of a mammalian numb homolog during mouse cortical neurogenesis," *Neuron.* **17**(1), 43-53.

Zhou, S., Fujimuro, M., Hsieh, J.J., Chen, L., Miyamoto, A., Weinmaster, G., and Hayward, S.D. **(2000)**. "SKIP, a CBF1-associated protein, interacts with the ankyrin repeat domain of NotchIC to facilitate NotchIC function," *Mol. Cell Biol.* **20**(7), 2400-2410.

Zlobec, I., Terracciano, L., and Lugli, A. (**2007**). "Value of staining intensity in the interpretation of immunohistochemistry for tumor markers in colorectal cancer," *Virchows Arch.* **451**(4), 763-769.

Zhu, Q., Yao, J., Wani, G., Wani, M.A., and Wani, A.A. **(2001)**. "Mdm2 mutant defective in binding p300 promotes ubiquitination but not degradation of p53: evidence for the role of p300 in integrating ubiquitiation and proteolysis," *J. Biol. Chem.* **276**(32), 29695-29701.

APPENDIX

Copy of letter confirming ethical approval for this study

University Hospitals of Leicester NHS
NHS Trust

DIRECTORATE OF RESEARCH AND DEVELOPMENT
Director: Professor D Rowbotham
Business Manager: Dr N J Seare
Service Manager: Mr M Roberts

Co-ordinator: N Patel
Direct Dial: 0116 258 8246
Fax No: 0116 258 4226
email: natu.patel@uhl-tr.nhs.uk

Leicester General Hospital
Gwendolen Road
Leicester
LE5 4PW

Tel: 0116 249 0490
Fax: 0116 258 4666
Minicom: 0116 258 8188

24 February 2004

Ms Helena Doucas
Hepatobiliary Research Fellow
Department of Hepatobiliary Surgery
Leicester General Hospital
Gwendolen Road
Leicester
LE5 4PW

Dear Ms Doucas

RE: **UHL Ref. 9170** *[Please quote this number in all correspondence]*
Cell signalling in gastrointestinal tumours. Ethics Ref. 7176

We have now been notified by the Ethics Committee that this project has been given a favourable opinion by the Ethics Committee (please see the attached letter from the Ethics Committee).

Since all other aspects of your UHL R+D notification are complete, I now have pleasure in confirming full approval of the project on behalf of University Hospitals of Leicester NHS Trust, Leicester General Hospital Site.

This approval means that you are fully authorised to proceed with the project, using all the resources which you have declared in your notification form.

The project is also now covered by Trust Indemnity, except for those aspects already covered by external indemnity (e.g. ABPI in the case of most drug studies).

We will be requesting annual and final reports on the progress of this project, both on behalf of the Trust and on behalf of the Ethical Committee.

In the meantime, in order to keep our records up to date, could you please notify the Research Office if there are any significant changes to the start or end dates, protocol, funding or costs of the project.

I look forward to the opportunity of reading the published results of your study in due course.

Yours sincerely

Mr Michael Roberts
Service Manager for Research and Development